Université de Montréal

LES NEURONES SENSORIELS DIMINUENT L'IMMUNOSURVEILLANCE DU CANCER

Par

Mohammad Balood

Université de Montréal

Faculté de Médecine

These presentee en vue de l'obtention du grade de doctorat en Pharmacologie

January 2022

Université de Montréal

Faculté de médecine

Département de pharmacologie et physiologie

Cette thèse intitulée

LES NEURONES SENSORIELS DIMINUENT L'IMMUNOSURVEILLANCE DU CANCER

Présenté par

Mohammad Balood

A été évaluée par un jury composé de

Dr. Jean Francois Gauchat
Président-rapporteur

Dr. Sebastien Talbot
Directeur de recherche

Dr. Manu Rangachari
Codirecteur

Dr. Hélène Girouard
Membre du jury

Dr. Judith Mandl
Examinateur externe

Résumé

La diaphonie neuro-immune entre le système nerveux et le système immunitaire fait l'objet de nombreuses études, cependant, leurs fonctions modulatrices communes sont largement inconnues dans le cancer. Leurs relations réciproques composées de cytokines, de facteurs de croissance et de neuropeptides pourraient participer à la progression tumorale. Les peptides libérés par les nocicepteurs peuvent favoriser le chimiotactisme, la polarisation et l'activité du système immunitaire adaptatif. Les cellules T CD8 + acquièrent un phénotype épuisé pendant le cancer qui est défini comme une perte progressive de la fonction des cellules T caractérisées par une altération de la prolifération et la capacité de produire des cytokines telles que l'IFN-γ, l'IL-2 et le TNF-α, suivie d'une surexpression des inhibiteurs récepteurs telle que Tim-3, PD-1 et Lag-3. Étant donné que les neurones sensoriels sécrètent localement des neuropeptides, ces derniers modulent les activités des lymphocytes. Nous avons émis l'hypothèse que les neurones sensoriels sécrètent des neuropeptides entrainant l'épuisement des cellules T-CD8 + et, de cette manière, favorisent la croissance tumorale. Nous avons testé cette hypothèse en utilisant le modèle de mélanome murin B16F10. Nous avons constaté que les cellules cancéreuses de la peau de mélanome malin interagissent avec les neurones sensoriels en augmentant la croissance des neurites, la réactivité aux ligands nocifs et la libération de neuropeptides. À son tour, le CGRP, l'un de ces neuropeptides, augmente directement l'épuisement des cellules T CD8 + cytotoxiques, limitant leur capacité à éiminer les cellules de mélanome. L'ablation génétique des neurones sensoriels, leur désactivation temporaire locale par une technique pharmacologique et l'utilisation d'un antagoniste du récepteur CGRP ont démontré une diminution de l'épuisement des lymphocytes infiltrés dans la tumeur (TIL) et de la croissance tumorale. Inversement, un traitement avec du CGRP recombinant a restauré l'épuisement des lymphocytes T CD8 + chez des souris dépourvues de neurones sensoriels. En comparaison avec les lymphocytes T CD8 + de type sauvage, les lymphocytes T RAMP1$^{-/-}$ CD8 + ont été protégés contre l'épuisement lorsqu'ils ont été co-transplantés dans des souris déficientes en Rag1$^{-/-}$ portant une tumeur.

Mots-clés: Épuisement, RAMP1, Neuropeptides, Neurones sensoriel, CGRP,

Abstract

Crosstalk between the nervous system and the immune system has been the subject of many studies, however, their shared modulatory functions are largely unknown in cancer. Reciprocal interactions, carried out by cytokines, growth factors, and neuropeptides may contribute to tumor progression. Peptides released by nociceptors can promote the chemotaxis, polarization, and activity of the adaptive immune system. $CD8^+$ T cells gain an exhausted phenotype during cancer, which is defined as progressive loss of T cell function; this is characterized by an impaired ability to proliferate and produce cytokines such as IFN-γ, IL-2, and TNF-α, followed by overexpression of inhibitory receptors such as Tim-3, PD-1, and Lag-3. Given that nociceptors locally secrete neuropeptides that modulate lymphocyte activities, we hypothesized that sensory neurons may secrete neuropeptides that drive $CD8^+$ T cell exhaustion and promote tumor growth. We tested this hypothesis by using the mouse model of melanoma cancer and found that malignant melanoma skin cancer cells interacted with nociceptors to increase neurite outgrowth, responsiveness to noxious ligands, and neuropeptide release. In turn, Calcitonin gene-related peptide (CGRP), one such neuropeptide, directly increased the exhaustion of cytotoxic $CD8^+$ T cells and limited their capacity to eliminate melanoma cells. Genetic ablation of sensory neurons, local pharmacological silencing, and antagonism of the CGRP receptor, Receptor Activity Modifying Protein 1 (RAMP1) were all able to reduce tumor-infiltrating lymphocytes (TIL) exhaustion and tumor growth. Conversely, $CD8^+$ T cell exhaustion was rescued in sensory neuron-depleted mice treated with recombinant CGRP. Compared with wild-type cells, $RAMP1^{-/-}$ $CD8^+$ T cells were protected from undergoing exhaustion when co-transplanted into tumor-bearing $Rag1^{-/-}$ deficient mice.

Keywords: Exhaustion, RAMP1, Neuropeptide, Nociceptor, CGRP

Table of content

Liste of figures

Abbreviation

2B4: Cluster of Differentiation 244

ARG1: Arginase 1

Calcrl: calcitonin-receptor-like recepto

CAR: Chimeric antigen receptor

CCL17:C-C Motif Chemokine Ligand 17

CCL22:C-C Motif Chemokine Ligand 22

CCL24:C-C Motif Chemokine Ligand 24

CCL-5: C-C Motif Chemokine Ligand 5

CD: Cluster of differentiation

CEA : carcinoembryonic antigen

CGRP: Calcitonin Gene-Related Peptide

CNS: Central nervous system

CTLA-4: Cytotoxic T lymphocyte-associated antigen 4

CXCL-1: C-X-C Motif Chemokine Ligand 1

CXCL-10: (C-X-C motif) ligand 10

CXCL-19: (C-X-C motif) ligand 19

CXCL-2: C-X-C Motif Chemokine Ligand 2

DCs: dendritic cells

DMEM: Dulbecco/Vogt modified Eagle's minimal essential medium

DRG: Dorsal root ganglion neuron

DTA: Diphtheria toxin

ELISA: Enzyme-linked immunosorbent assay

EOMES: Eomesodermin

ERK : Extracellular signal-regulated kinases

FACS: Fluorescence-activated cell sorting

FAS-L: Fas Ligand

Foxp3: Forkhead box P3

GABA: G-aminobutyric acid

Gata3: GATA binding protein 3

GDNF: Glial cell line-derived neurotrophic factor

GM-CSF: Granulocyte macrophage colony-stimulating factor

GNZB: Granzyme B

GP-100: Glycoprotein 100

GPCRs: G-protein-coupled receptors

HNSCC: Head and neck squamous cell carcinoma

HSPCs : hematopoietic stem progenitor cells

ICIs: Immune checkpoint inhibitors

IDO : Indoleamine 2,3-dioxygenase

IFN-γ: Interferon-γ

Ig: Immunoglobulin

iDISCO: Immunolabeling-enabled imaging of solvent-cleared organs

IL: Interleukin

IL10 : Interleukin 10

IL2: Interleukin 2

ILC-2: Innate lymphoid cell

INOS: Inducible nitric oxide synthase

JAK3: Janus kinase 3

KO: Nock out

LAG-3 : Lymphocyte-activation gene 3

mAb: Monoclonal antibody

MART-1: Melanoma antigen recognized by T cells 1

MDSC: Myeloid-derived suppressor cells

MHC: Major histocompatibility complex

NaV1.8: Sodium voltage 1.8

NE : Norepinephrine

NFAT: nuclear factor of activated T cells

NFAT: Nuclear factor of activated T cells

NF-κB: Nuclear factor-κB

NGF: Nerve growth factor

NK cell: Natural killer cell

NKG2D: NK group 2 member D

NO : Nitric oxide

NPY: Neuropeptide Y

NR4A1: Nuclear Receptor Subfamily 4 Group A Member 1

OCSCC : Oral cavity squamous cell carcinoma

PD-1 : program cell death

PD-L1: Programmed death-ligand 1

PD-L2 : Programmed death-ligand 2

PGE2 : prostaglandin E2

PI3K: Phosphatidylinositide 3-kinase

Piezo : piezo type mechanosensitive ion channel component

PMA: phorbol 12-myristate 13-acetate

PNI: Perineural invasion

PNS: Peripheral nervous system

PNS: Peripheral Nervous System

RAG: recombination activating gene

Ramp1: receptor activity modifying protein 1

RAMP1: Receptor Activity Modifying Protein 1

ROS: reactive oxygen species

SLPI: Secretory Leukocyte Protease Inhibitor

SNAP-25: Synaptosomal-Associated Protein

SOM: Somatostatin

SP: Substance P

STAT5: Signal transducers and activators of transcription 5

TAFs: Tumor-associated fibroblasts

TAMs: Tumour Associated Macrophages

TANs: Tumor-associated neurons

T-bet: T-box expressed in T cells

TCR: T cell receptor

TFs: Transcription Factors

TGF-β: Transforming growth factor-β

Th1: T helper 1

Th17: T helper 17

Th2 cells: T helper type 2 cells

TIGIT: T cell immunoreceptor with Ig and ITIM domains

TIL: Tumor-infiltrating lymphocyte

Tim-3 : T cell immunoglobulin domain mucin domain-containing protein 3

TLR: Toll-like receptor

TME: Tumor microenvironment

TNF: tumor necrosis factor
TNFR: tumor necrosis factor receptor

TNF-α: Tumor necrosis factor-α

TOX: Thymocyte selection-associated HMG BOX

TRAIL: Tumor necrosis factor-related apoptosis-inducing ligand

Tregs: regulatory T cells

Trks: Tyrosine-receptor kinases

TRP: Transient receptor potential

TRPA1: TRP ankyrin subfamily, member 1

TRPV1: transient receptor potential vanilloid subfamily, member 1

VEGF: Vascular Endothelial Growth Factor

VIP: Vasoactive intestinal peptide

VPAC1: Vasoactive Intestinal Peptide receptor 1

XCL-1: X-C Motif Chemokine Ligand

Acknowledgment

Ph.D. is a long journey, and having a successful Ph.D. requires self-motivation, focus and enthusiasm towards the research work. We need to think of each day as an opportunity to improve, to be better and get closer to our goals. This is a lesson that I have learned over the last four years under the supervision of my director. Always saying thank you just does not seem to be enough to the supervisor, but I would like to give my warmest gratitude to Sebastien Talbot, my research director, for all of his support and help that he did for me to complete this journey. I would not have made it without the help that you gave me in the last four years for my work and my life. I hope that I can "pay forward" what you have done for me by helping other people. I am also grateful to thank my co-supervisor Dr. Manu Rangacheri at University Laval who accepted me first in 2017 as a Ph.D. student. He trained me very well and helped me to get familiar with the research environment in Canada. I also thank the jury members. Dr. Jean-Francois Gauchat, thank you for being the president of this jury. Dr. Helene Girouard and Dr. Judith N Mandl thank you for agreeing to be part of this committee. Your presence is an honor for me. I am grateful for the financial support that I received from UdeM and the Fonds de Recherche du Québec - Société et Culture (FRQS). Thank you to all the people who helped me during the last 4 years. I am very grateful to thank Maryam Ahmadi who always helped me in doing experiments. Thank you very much for your help. I want to truly thank Abdelilah Majdoubi who trained me for the flow cytometry and always assisted me with the experiments. I want to thank Ali Ahmadi, who always assisted me with my project. Thanks for everything you did Ali. You are an example of a persevering person. Many thanks to Tuany Eichwald for all the help and support that you have given me for my research project. I want to thank Katiane Roversi and Karine Roversi for sharing your expertise, your help, and your time. I also want to thank Theo Crosson and Jo Chiao Wang for the advice that you have shared during the last four years, It's an honor. Thank you to all those responsible for the platforms for their technical support. Thanks to Armelle, Annie, and Angelique for their collaboration on the flow cytometry. Thank you to Dr. Moutih Rafei for giving me access to his lab and his help with my project. Finally, to my wife, I would not have reached this success without her sincere encouragement, patience, and sacrifices. Thank you from the bottom of my heart.

Chapter 1 : Introduction

Cancer is a disease of uncontrollable cell growth. Malignant tumors are formed by cells that divide uncontrollably, spread and migrate through the body. Protecting the body against cancer requires an effective immune system response capable of recognizing and destroying transformed cells while avoiding damage to normal cells. Such immune responses require interaction between the two components of the immune system, namely innate and adaptive immunity. As the first line of defense, innate immunity recognizes transformed cells and responds accordingly, while adaptive immune responses are highly specific and critical for fighting cancer. However, adaptive immune responses are often ineffective without activation of the innate immune system. An important function in defense against cancer is the surveillance and identification of tumor antigens expressed by transformed cells.

The immune system encounters non-self-antigens daily and eliminates transformed cells. However, despite host immunity, transformed cells are able to grow and form malignant tissue in the host body. Established tumors develop different mechanisms in order to restrain anti-tumor immunity. For example, downregulation of expression of MHC molecules renders them unable to present tumor antigens to T cells, while secretion of immunosuppressive molecules in the tumor microenvironment inhibits T cell proliferation, and upregulation of expression of inhibitory ligands that bind to T cell receptors can inhibit T cell responses[1].

Protecting the body against foreign antigens requires both components of the immune system; however, new findings have recently shown that the nervous system can also detect foreign antigens and respond to them[2-8]. The peripheral nervous system includes sensory and motor neurons, which innervate all tissues and organs outside of the central nervous system and maintain homeostasis through the release of certain neurotransmitters and neuropeptides. Besides their function as regulators of tissue homeostasis, it has been demonstrated that nerves can innervate tumors and affect their growth, survival, and migration[9-11]. However, the mechanisms behind this role are still not fully known. It has been postulated that nerve fibers infiltrate tumors and release various neurotransmitters and growth factors into the neuro-neoplastic synapse, not only stimulating tumor cell growth but also modulating immune system responses. On the other hand, activation of cancer cells by these neuronal mediators results in the discharge of certain growth factors into the tumor microenvironment, which induces axonogenesis and suppresses anti-tumor immunity**.**

These data support the idea that neuro-neoplastic synapses play an important role in tumor progression and, furthermore, that these crosstalk mediators may constitute useful targets for boosting anti-tumor immunity[12-14]. In this project, we will investigate the mechanisms of cancer–sensory neuron interactions based on the hypothesis that sensory neurons suppress immune system responses through induction of T cell exhaustion in the tumor microenvironment. Furthermore, ablation of this subset of neurons boosts anti-tumor immunity, decreases tumor growth, and improves survival.

1.- Background

1.1.- Melanoma cancer

Melanoma is one of the most aggressive types of skin cancer that arise from specialized cells in the skin which are called melanocytes and their function is to generate skin pigment. Melanoma has a higher risk of spreading in comparison to other types of skin cancer, and the prevalence of melanoma has increased over the last several decades[15]. Factors that transform normal melanocytes into malignant melanocytes are a complex of genetic and environmental factors[16]. Dysregulated signaling pathways that are caused by genetic mutations promote melanoma cell proliferation, survival, and immune evasion. Around 50% of melanoma patients have BRAF mutations[17,18]. Some of the BRAF mutations such as V600, induce activation of mitogen-activated protein kinase (MAPK) pathway[18]. This signaling pathway is the key signaling in many malignancies such as melanoma that control cell growth and survival[19]. Melanoma is a hot tumor with a high tumor mutation burden that permits infiltration of immune cells and provides a suitable model for investigating the interaction of cancer cells with immune cells. During melanomagenesis, immune cells interact with tumor cells in order to prevent melanoma progression[20].

1.2- Immunosurveillance

The immune system has three major functions for the prevention of tumor growth: protection of the body from viruses that cause cancer, resolution of inflammation after eliminating infection, and destruction of tumor cells through the identification of tumor antigens expressed by tumor cells. The latter is considered cancer immunosurveillance, a process by which the immune system monitors the body to detect and destroy transformed cells. However, despite a functional immune system, tumor cells can still grow, migrate, and spread in the body due to

cancer immunoediting. Tumor immunoediting describes the process by which tumor cells escape from the immune system and continue their growth. It includes three phases: elimination, equilibrium, and escape[21]. The elimination phase involves the interaction of the adaptive and innate immune systems to detect and destroy all cancerous cells in the early phase of tumor growth when intrinsic tumor suppressors have failed. However, immune cells are sometimes unable to eliminate all the cancerous cells, a portion of which survive and enter the equilibrium phase. These less immunogenic cells continue to evolve and develop mechanisms to protect themselves against immune system attacks. The equilibrium phase results in the selection of tumor cells that are resistant to immune system attack and able to strongly suppress anti-tumor immunity, which leads to the escape phase. During this phase, anti-tumor immunity is no longer functional, and the tumor cells grow uncontrollably[22] **(Figure 1).**

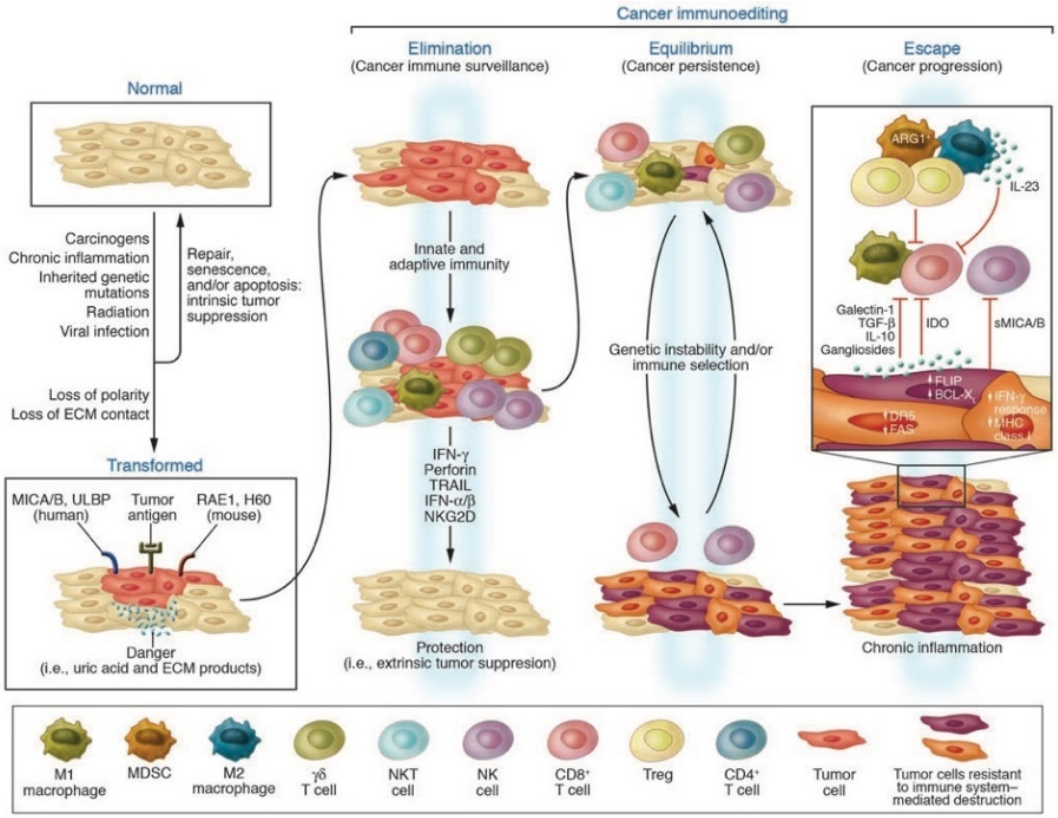

Figure 1.Tumor cells suppress the immune system response. The immune system detects and kills transformed cells when intrinsic tumor suppressors are failed (elimination phase). Cancer immunoediting is now considered to be a three-step process: elimination phase, when tumor cells are destroyed; equilibrium, when cancer cells evolve and develop suppressive mechanisms; and escape, when tumor cells become resistant to immune cells and grow progressively[23].

1.2.1- Cancer immunosurveillance in mouse

T cells are the key player in the elimination of tumor cells, however, in high tumor mutation burden such as melanoma, tumor cells go under immune evasion through releasing of immunosuppressive cytokines and upregulation of inhibitory ligands within the tumor microenvironment (TME)[24]. The theory that T cells mediates anti-tumor immunity through recognition of altered antigens evolved as cancer immunosurveillance hypothesis[25]. The basis of this theory is that tumor cells express tumor-specific antigens that are recognized by adaptive and innate immune cells and these cells eliminate malignant cells before they become clinically apparent. Recent studies provide several lines of evidence supporting that immunosurveillance has a fundamental role in the prevention of cancer development.

One of the key tools for studying immunosurveillance was the generation of immunodeficient mice. These mice are precious tools for studying the function of immune cells in cancer. It is well known that immunodeficient mice that do not have the main cellular component of the adaptive or innate immune system such as T, B, and natureal killer (NK) cells or mice that are deficient in the production of cytotoxic cytokines such as perforin[26-29], tumor necrosis factor-α (TNF-α) and interferon-γ (IFN-γ), are more susceptible for cancer development[27,30]. For example, mice that are deficient in the recombination activating gene 1 (RAG-1) or RAG-2 are not able to generate NK, T, and B cells[31,32]. Chemical induction of cancer such as sarcomas in RAG-$2^{-/-}$ mice caused tumor growth faster than wild-type controls[32] or sarcoma tumor formation in mice that do not have IFN-γ receptors was three-time more than wild-type control[32]. The same result for carcinogenesis was found in mice that do not have perforin[27]. Genetic ablation of T cell receptor (TCR) showed that T cells are crucial for tumor surveillance. The contribution of the αβ T cell in controlling tumor growth was found in the αβ T $cell^{-/-}$ (lacking the TCR β-chain). Fibrosarcoma growth in the αβ T $cell^{-/-}$ mice was faster than in control mice. These data showed that T cells are critical for preventing tumor development[33]. Stimulatory signals such as α-GalCer and interleukin IL-21 could increase the number of tumor

infiltrated NK cells, induce stronger antitumor activity by NK cells, and significantly decrease B16F10 metastasis[34]. By contrast, depletion of NK cells by antibodies, blocking the activation receptor NK group 2 member D (NKG2D)[35], or blocking tumor necrosis factor-related apoptosis-inducing ligand (TRAIL) on the surface of NK cells promoted tumor development in a mouse model of sarcoma[36].

1.2.2- Cancer immunosurveillance in human

There are several lines of evidence indicating that cancer immunosurveillance also exists in human. Transplanted patients who received immunosuppressive drugs[37-40], virally infected patients, or people with immunodeficiency showed a higher risk of cancer development[41-43]. For example, people who were virally infected with Epstein-Barr virus, human herpesvirus, AIDS, and human papilloma virus showed greater incidences of cancer[44]. The higher incidence of cancer in immunodeficient patients indicates the role of immune system in cancer immunosurveillance. In addition to epidemiological data, recent studies on cancer patients show that there is a positive correlation between the frequency of tumor infiltrated T cells (TILs) and better patient survival. This relationship has been observed in patients with melanoma[45,46], breast[47], bladder[48], colon[49,50] ,prostate[51], ovary[52], rectum[53], and for neuroblastoma[54].

If immunosurveillance exists in human, then we should see strong immune system responses in patients that are in the early phase of cancer development. There is some data in support of this theory. For instance, strong T cells responses have been observed in patients with monoclonal gammopathy which is a type of premalignancy[55], however, these responses are not found in patients with multiple myeloma[55], or another study showed that bone marrow of breast or pancreatic cancer patients contains antigen-specific $CD8^+$ T cells that have the ability to regress human tumors after transplantation into immunodeficient mice[56,57].

In summary, these findings in both human and mouse indicate that tumor cells are able to activate immune cells and trigger various immune system responses, but cancer cells still are able to find a mechanism to continue their growth. One of the possible mechanisms is that some of the tumor cells develop evasion mechanisms under the pressure of immune system known as immunoselection or they develop a specific immune-tolerance mechanism that inhibit immune system responses[58]. Altogether, these findings provide strong evidence for the existence of cancer immunosurveillance.

1.3- Adaptive immune responses in cancer

1.3.1- $CD8^+$ T cells

The adaptive immune system plays a critical role in cancer immunosurveillance. This system includes T and B lymphocytes[59-61]. $CD8^+$ T cells are responsible for the recognition and elimination of transformed and virally infected cells in the body in order to protect the host. Cytotoxic $CD8^+$ T cells are the primary cells that clear the body from malignancy. These cells develop in the thymus and then enter into the secondary lymphoid organs such as lymph nodes where dendritic cells (DCs) present antigens to them for the first time and prime them[62-64]. Naïve $CD8^+$ T cells require three signals in order to get activated and become effector cells. The first signal is mediated by the peptide-MHC I complex with the TCR-CD3 complex. The Second signal is a co-stimulatory signal that occurs by binding of CD28 on T cells to CD80/86 on the surface of antigen-presenting cells such as dendritic cells. The third is provided by cytokines that determine differentiation and expansion of $CD8^+$ T cells. Cytokines have a critical role in the generation of cytotoxic or memory T cells[64-66]. Naïve $CD8^+$ T cells after differentiation into cytotoxic lymphocytes (CTL) leave LN and migrate to the tumor or infected tissues where they encounter again with the antigens for the second time. This time virally infected cells or tumor cells present antigen to the CTL through the formation of synapse between TCR and peptide-MHC I on the target cells[64],

finally, CTLs kill target cells through different mechanisms including; releasing of cytotoxic granules such as perforin and granzyme B into the membrane of target cells[63,67], inducing apoptosis through CD95L that binds to CD95 on the target tissue, or by the production of IFN-γ and TNF-α[63].

1.3.2- CD4$^+$ T cell

CD4$^+$ T cells are another subset of adoptive immune cells that through releasing different cytokines modulate function of CD8$^+$, B, and innate immune cells. CD4$^+$ T cells recognize antigens that are presented on MHC II molecules expressed by DCs. CD4$^+$ cells after differentiation, are divided into T helper (Th1, Th2, Th17), and regulatory T (Treg) cells[68]. Depending on the type of antigens that are presented by DCs to naive CD4$^+$, DCs produce different cytokines that these cytokines along with TCR strength, and co-stimulatory signals determine differentiation of naive CD4$^+$ T cells to effector or Treg cells[68,69]. Th1 cells are the primary CD4$^+$ T cells that mediate anti-tumor immunity through different mechanisms including; providing help for cytotoxic CD8$^+$ T cells, secreting IFN-γ and TNF-α, and also inducing antibody responses. CD4$^+$ T cells secrete IL-2 which directly increases proliferation and activation of CD8$^+$ T cells in the tumor. Activated CD4$^+$ T cells express CD40 ligand (CD154) that bind to CD40[70-72] on DCs to induce and maintain pro-inflammatory DCs that generate type 1 immunity through secretion of IL-12 and expression of co-stimulatory ligands[73-76]. This intra-tumoral interaction of DCs with CD4$^+$ T cells causes tumor infiltrated naïve CD8$^+$ T cells to differentiate into cytotoxic CD8$^+$ T cells and increase antitumor immune responses[75,77-81]. Naïve CD4$^+$ T cells after activation and polarization to Th1 cells produce cytokines such as IFN-γ and TNF-α that induce tumor apoptosis[82-84]. Binding of CD40 ligand on T cells to CD40 on B cells induces production of specific antibodies against tumor by plasma cells[85].

1.3.3- B cell

B cells are another type of adaptive immune cell that can either suppress or promote tumor growth depending on their subtypes[86-88]. Through their ability to function as an antigen presenter, they induce an anti-tumor effect. This subset of B cells can provide a proliferation signal for tumor infiltrated T cells when DCs activity is slow and they are not able to present antigen to T cells in the tumor. B cells also provide proliferation and activation signals for $CD4^+$ T cells indicating that depletion of B cells in mouse impaired $CD4^+$ T cells clonal expansion. The proximity of tumor infiltrated $CD8^+$ T cells with B cells has been reported in ovarian cancer[89]. Activated B cells produce antibodies that can bind to tumor antigens and induce antibody-dependent cell-mediated (ADCC) by NK cells. On the other side, regulatory B cells are another subset of B cells that promote tumor growth through different mechanisms including secretion of immunosuppressive cytokines such as Transforming growth factor beta (TGF-β) and IL-10[90], suppression of T and NK cells through expression of Programmed death-ligand 1 (PD-L1)[91], and promote differentiation of $CD4^+$ T cells to Tregs[92].

1.4- Innate immune response in cancer

1.4.1- NK

However, most studies show that adaptive immunity including T cells has the most important role against tumors but there are also studies indicating that innate immune responses are also important in killing tumor cells. NK cells and type 1 macrophages (M1) are two subsets of innate immune cells that can directly interact with malignant cells and eliminate them.

NK cells are one group of innate immune cells that have been shown to play a critical role in cancer immunosurveillance and also boost adaptive immune responses in cancer[93,94]. NK cells

are the main killer of cancer cells that do not express major histocompatibility complex (MHC) molecules. They produce various cytokines such as IFN-γ, TNF-α, granulocyte-macrophage colony-stimulating factor (GM-CSF), and chemokines such as X-C Motif Chemokine Ligand 1 (XCL-1), and C-C Motif Chemokine Ligand 5 (CCL-5)[95-97] that shape adaptive and innate immune responses in TME. Interestingly, they eliminate transformed cells through different mechanisms including; secretion of cytotoxic granules such as perforin and granzymes that can directly lyse cancer cells[93], production of cytotoxic cytokines such as IFN-γ and TNF-α that induce apoptosis of tumor cells, and also antibody-dependent cell-mediated cytotoxicity (ADCC)[30].

However, expression of immunosuppressive factors such as TGF-β, indoleamine 2,3-dioxygenase (IDO) escape NK cells attack and inhibit antitumor immune functions[98,99]. Based on that NK cells do not need to recognize any specific antigen, rapidly kill cancer cells and produce proinflammatory cytokines to activate adaptive immune system, they can be an attractive option for cancer immunotherapy[94].

1.4.2- Macrophage

Tumour Associated Macrophages (TAMs) are divided into two types; Type 1 and Type 2. In the early stage of tumor development, infiltrated Type 1 macrophages (M1) in the tumor release pro-inflammatory cytokines, such as IFN-γ, IL-12, and TNF-α that promote differentiation of adaptive immune system and also through the secretion of chemokines such as CXCL-19 and CXCL-10 induce attraction of NK and $CD4^+$ T cells into the tumor. This type of Macrophages is also able to directly interact with cancer cells and kill them and has been associated with a good prognosis amongst cancer patients[100-103,104]. In contrast, in advanced tumors, high level of inflammation induces polarization of Type 1 macrophage to type 2 (M2) which has been correlated with tumor development[103,105-107]. This type of macrophage releases factors that induce Th2 differentiation, recruit Tregs through the secretion of chemokines such as CCL-17,

CCL-22, CCL-24, and induce angiogenesis through production of Vascular Endothelial Growth Factor (VEGF) and Epidermal Growth Factor (EGF)[105]. M2 macrophages decrease the cancer immunosurveillance by inhibiting anti-tumoral $CD8^+$ T cells responses through expression of PD-L1/PD-L2[108] and also by secreting immunosuppressive cytokines such as IL-10, TGF-β which prevent T cell activation[109-111].

1.5- T cell exhuastion

Activated $CD8^+$ T cells after infiltration into the tumor encounter tumor antigens and are primed for the second time. Priming of T cells with tumor antigens induces proliferation and upregulation of transcription factors and cytokines that generate cytotoxic lymphocytes in order to kill tumor cells[65,112,113]. However, prolonged stimulation of CTL with tumor antigens develops another fate which is known as Exhaustion[66,114].

Tumor infiltrated T cells (TILs) following infiltration into the tumor microenvironment, release cytotoxic granules that can directly lyse tumor cells or induce apoptosis. However, persistent stimulation of $CD8^+$ T cells by tumor antigens in the tumor microenvironment, together with secretion of immunosuppressive factors such as adenosine, lactate, and kynurenine by cancer cells[115] promotes effector $CD8^+$ T cells to reach a stage known as "Exhaustion". These exhausted $CD8^+$ T cells progressively lose their function, characterized by a gradual decline in the production of cytokines such as IL-2, TNF-α, and IFN-γ, and overexpression of inhibitory receptors such as program cell death (PD-1), T cell immunoglobulin domain mucin domain-containing protein 3 (Tim-3), cytotoxic T lymphocyte-associated antigen-4 (CTLA4), and lymphocyte-activation gene 3 (LAG-3)[116] **(Figure 2)**. These immune checkpoint receptors are able to block $CD8^+$ T cell activity upon binding to their ligands, e.g., PD-L1, on the surface of tumor cells[117].

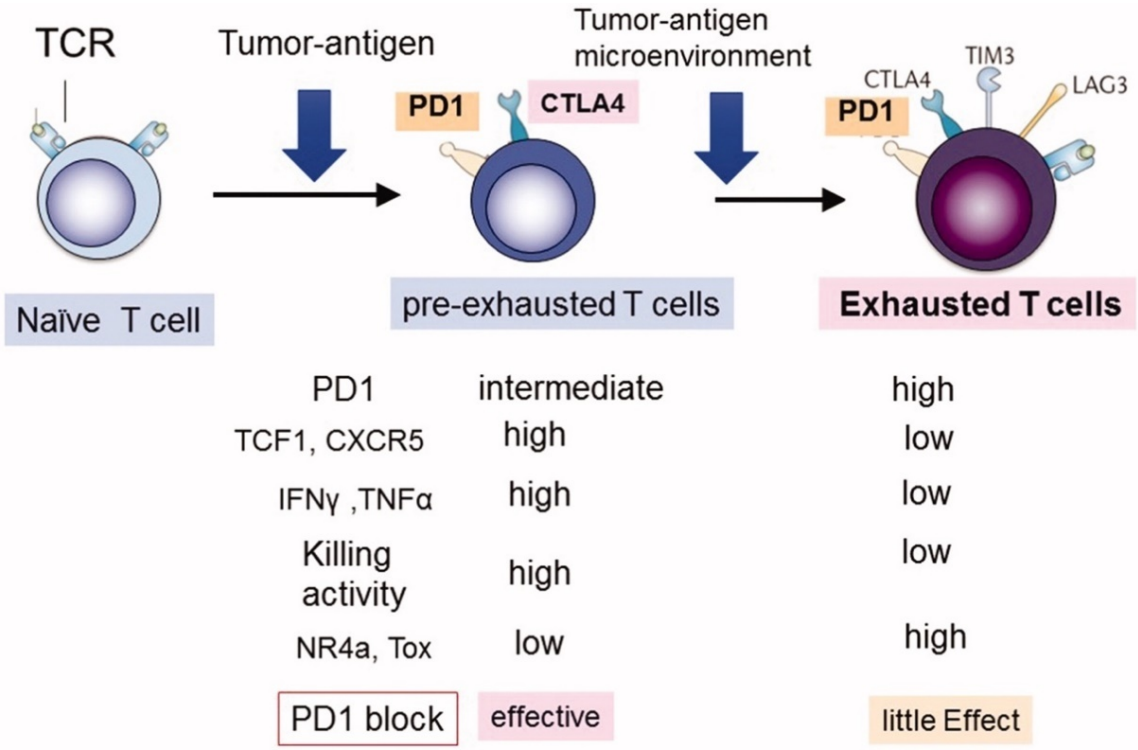

Figure 2. T cell exhaustion during the tumor progression. When encountering tumor antigens, naïve or activated T cells generate two types of tumor-infiltrating T cells (TILs): progenitor exhausted (or effector) T cells, which express low levels of PD1 and high levels of cytokines and respond to immune checkpoint blockade and terminal exhausted T cells, which overexpress immune checkpoint receptors such as PD1, Tim3, and Lag3, and do not respond to immune checkpoint blockade therapy[118].

1.5.1- TME contains factors that drive T cells exhaustion

Several pathways and factors in the TME mediate T cell exhaustion. These include inhibitory cells such as Regulatory T cells (Tregs), myeloid-derived suppressor cells (MDSC), Tumor-associated fibroblasts (TAFs), tumor-associated macrophages (TAM), Tumor-associated neurons (TANs), soluble molecules such as Adenosine, prostaglandin E2 (PGE2), Kynurenine, Reactive oxygen species (ROS), IL-10, and TGF-b, and also intrinsic regulatory factors such as transcription factors and inhibitory receptors that have been shown have an inhibitory effect on T cells. The interaction of T cells with these components of TME plays a critical role in impairing T cell function and driving T cell exhuastion[119] **(Figure 3)**.

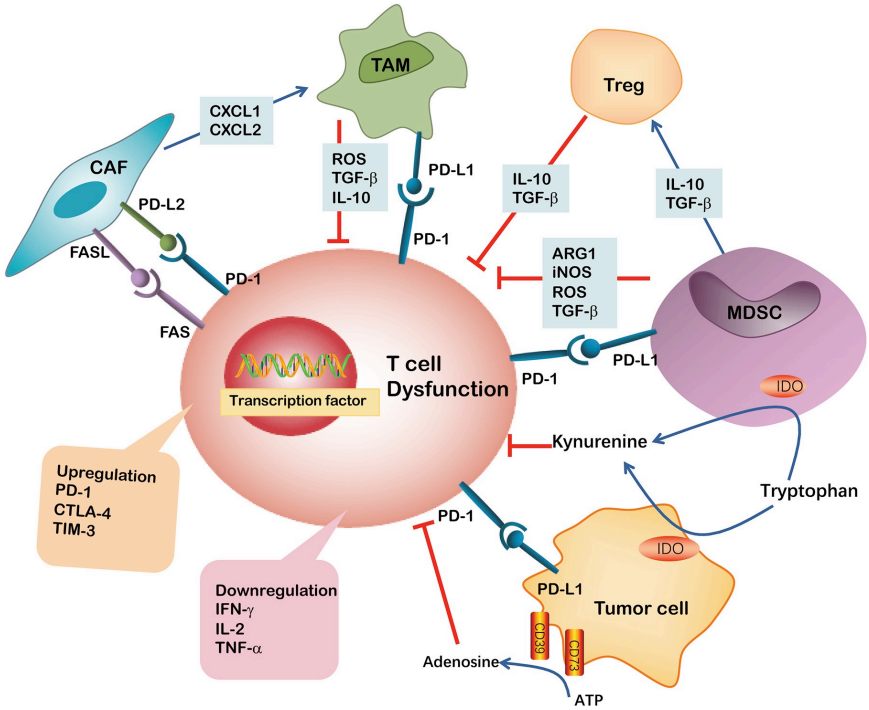

Figure3.Different cells and factors regulate CD8⁺ T cell exhaustion in TME. Secreted immunosuppressive molecules such as ARG1, iNOS, TGF-b, and IL-10 by MDSC, TAMs, and Treg inhibit T cell function. Kynurenine is another molecule that inhibits T cell proliferation and upregulates PD-1 expression. Upregulation of PD-L1 by MDSC and TAMs is another mechanism that drives CD8⁺ T cells exhaustion. Tumor cells generate adenosine that inhibits CD8⁺ T cell function. CAFs secrete CXCL-1 and CXCL-2 chemokines that drive polarization of M2 macrophages in TME and also express PD-L2 ligand that binds to PD-1 and inhibits CD8⁺ T cells function[120].

1.5.1.1- Myeloid drive suppressor cells (MDSc)

MDSCs are an immature and heterogamous population of myeloid cells that are recruited into the tumor during the cancer progression and are able to suppress immune system responses[121,122] by releasing toxic species such as ROS, nitric oxide (NO), and PGE2 [123]. For example, NO inhibits phosphorylation and activation of Janus Kinase 3 (JAK3) and Signal transducer and activator of transcription 5 (STAT5) transcription factors in $CD8^+$ T cells and inhibits their activity[124] or expression of arginase 1 (ARG-1) decreases CD3-chain synthesis[125]. MDSC produces high amounts of ROS in the tumor and ROS has been shown to drive $CD8^+$ T cells exhaustion and induce oxidative stress in T cells that cause T cell hyperresponsiveness[126]. Indoleamine dioxygenase (IDO) is one of the most important enzymes that is expressed by MDSC and catabolize tryptophan to an immunosuppressive molecule which is called kynurenine. This molecule has been shown to upregulate PD-1 expression on tumor-infiltrating $CD8^+$ T cells and inhibit clonal expansion of $CD8^+$ T cells[127].

1.5.1.2- Tumor associated macrophages (TAMs)

M2 macrophages are considered Tumor-associated macrophages (TAMs) that suppress anti-tumor immunity and promote tumor progression through different pathways[128,129]. They induce expression of PDL-1 in monocytes that upon binding to PD-1 on $CD8^+$ T cells can block activity of $CD8^+$ T cells, TAMs secret various immunosuppressive cytokines, and factors such as IL-10, TGF-β, and ROS that induce $CD8^+$ T cells exhaustion and dysfunction, and they directly inhibit $CD8^+$ T cell cytotoxicity through the depletion of amino acids such as L-arginine and tryptophan[129,130].

1.5.1.3- Tumor-associated fibroblasts (CAFs)

CAFs emerged as suppressive cells that promote tumor growth through recruiting and differentiation of myeloid cells. These cells release chemokines such as CXCL-1 and CXCL-2 that attract myeloid cells. In addition, CAFs also are able to polarize M1 macrophages to M2 macrophages[131]. However, new mechanisms have been attributed to CAFs indicating that CAFs can directly suppress tumor infiltrated $CD8^+$ T cells via upregulation of CD95 and PD-L1[132].

1.5.1.4- Soluble factors

Soluble factors that are released by TME components such as MDSCs, CAFs, and Tregs are crucial factors that can drive T cell exhaustion and inhibit T cell expansion and activation[123]. TGF-β is one of these immunosuppressive factors that are released by Tregs and M2 macrophages and promotes tumor progression by driving T cells exhaustion via upregulating expression of PD-1, TIM-3, and CTLA-4 in T cells and inhibiting Granzyme-B and IFN-γ production[133]. IL-10 is another factor that is secreted by cancer cell, TAMS, and $CD4^+$ Tregs[134] which suppresses $CD8^+$ activity[135].

1.5.1.5- Intrinsic regulators

1.5.1.5.1- Transcription factors (TFs)

It is well known now that TFs such as Nuclear Receptor Subfamily 4 Group A Member 1 (NR4A1), thymocyte selection-associated HMG BOX (TOX), Nuclear factor of activated T cells (NFAT), T-box expressed in T cells (T-bet), Basic Leucine Zipper ATF-Like Transcription Factor (BATF), Eomesodermin (EOMES), and B lymphocyte-induced maturation protein-1 (Blimp-1) regulate PD-1 expression and drive T cell exhaustion[136,137] **(Figure 4).** NR4A1 is highly expressed

in dysfunctional T cells and inhibit their proliferation. Deletion of this transcription factor significantly decreased expression of PD-1 and Tim-3 by $CD8^+$ T cells and enhanced their anti-tumor responses[137]. TOX is another transcription factor that has been reported to play a critical role in development of exhausted T cells during chronic infection[138]. Deletion of TOX prevented formation of exhausted $CD8^+$ T cells[139] and promoted anti-tumor effect of $CD8^+$ T cells[140]. Overexpression of T-bet was found to accelerate effector T cells toward the terminal differentiation[141] and high the level of Eomes expression was correlated with high level of PD-1 and other inhibitory receptors[142]. Expression of BATF in $CD8^+$ T cells was correlated with lower T cell proliferation and cytokine production during the HIV infection[143] and overexpression of Blimp-1 caused T cells dysfunctional during the chronic LCMV infection[143].

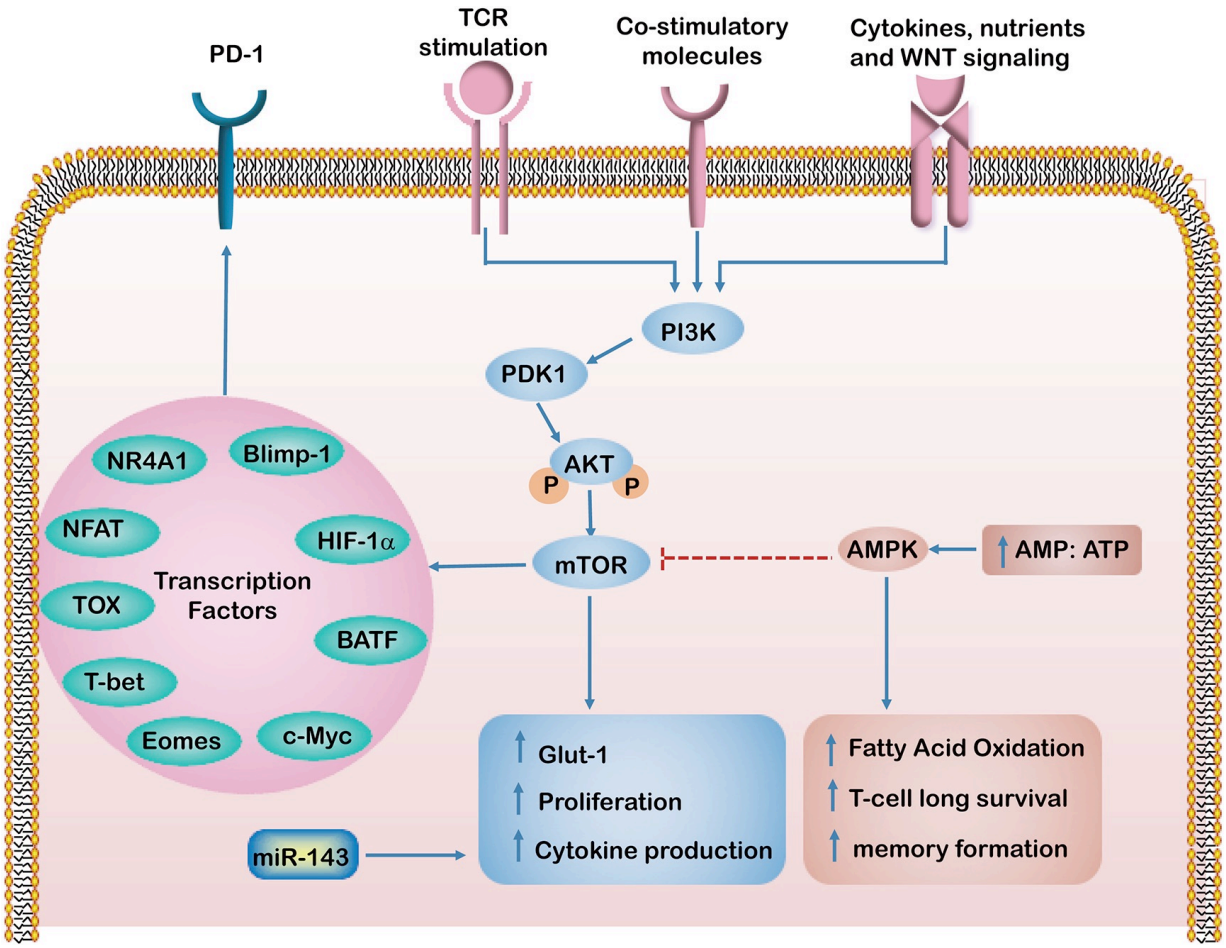

Figure 4.Transcription factors upregulate PD-1 expression on CD8^{+} T cell cells.TCR stimulation, cytokines, and co-stimulatory molecules activate PI3K/Akt/mTOR signaling pathways that have been implicated in regulation of transcription factors such as HIF-1a, NR4A1, TOX, Eomes, T-bet, Blimp-1, NFAT, and BATF. These transcription factors have been associated with T cell exhaustion[120].

1.5.1.6- Inhibitory receptors

Cytotoxic T-lymphocyte-associated protein 4 (CTLA-4)

CTLA-4 is an inhibitory receptor that is expressed on effector T cells after the TCR stimulation. Expression of CTLA-4 reaches the highest level 2-3 days after TCR stimulation in effector T cells[144,145]. CTLA-4 blocks CD28 co-stimulatory signaling through binding to CD80/86 on the surface of antigen-presenting cells (APCs) and in this way attenuates T cell activation[146,147]. Also, upregulation of CTLA-4 by APCs induces expression of indoleamine-2,3-dioxygenase by APCs that inhibit T cell proliferation[146].

Programmed cell death-1 PD-1 (PD-1)

PD-1 is the first immune checkpoint receptor that is expressed by activated T cells that upon binding to PD-L1 on the surface of tumor cells suppresses T cell activity and proliferation[148]. Overexpression of PD-1 on tumor infiltrated $CD8^+$ T cells has been associated with T cell dysfunction. PD-1 inhibits TCR signaling through dephosphorylation of key intermediates downstream of TCR [146]. Also, it has been shown that PD-1 can also downregulate co-stimulatory signaling by CD28[149]. However, there are many studies showings that expression of PD-1 alone is not associated with T cell exhaustion[148,150,151] and T cells gain exhausted phenotypes when they co-express several inhibitory receptors such as PD-1, Tim-3, Lag-3, TIGIT, CD160, and CD244[152-155]. For example, In vitro stimulation of OVA (257–264) specific TCR transgenic OT-I with OVA peptides showed that co-expression of several inhibitory receptors along with PD-1 generated $CD8^+$ T cells that had all characteristics of exhausted T cells[156,157].

T cell immunoreceptor with Ig and TIM domains (TIGIT)

TIGIT is an inhibitory receptor of the Ig superfamily that is expressed by T cells and inhibits adaptive and innate immune system responses[158-160]. It inhibits adaptive immune system through several mechanisms. Binding of this receptor to CD155 on DCs triggers a signaling pathway that induces secretion of IL-10 by DCs that inhibits T cells[161]. TIGIT also inhibits T cell proliferation and activation through attenuating TCR signalling[162-164]. This receptor is also expressed by NK cells and inhibits degranulation and cytokine production. Ligation of TIGIT on NK to CD155 on the surface of MDSC cells decreases cytotoxicity of NK cells by decreasing the phosphorylation of kinase such as extracellular signal-regulated kinases (ERK)[165]. TIGIT also competes with CD266 for binding to CD155[154].CD226 is a co-stimulatory receptor that expresses by $CD8^+$, NK, and $CD4^+$ T cells, triggers TCR signaling, and is involve in production of proinflammatory cytokines[166,167].

Lymphocyte activation gene 3 (LAG-3)

Lag-3 is expressed by $CD4^+$, $CD8^+$, and NK cells. This receptor plays an important role in inhibition of T cell activation and promotes differentiation of $CD4^+$T cells to Tregs[168]. MHC II, Galectin-3, and lymph node endothelial cell C-type lectin (LSECTIN) are ligands that bind to LAG-3[169-172]. However, the mechanism of action of LAG-3 is not very well known so far but several studies showed that LAG-3 upon binding to its ligand can inhibit signaling pathways downstream of TCR. This receptor prevents activation of transcription factor NFAT which plays a critical role in regulation of cytokine production and T cell proliferation. Inactivation of NFAT, decrease IL-2 production by T cells and also production of proinflammatory cytokines[169-171].

T cell immunoglobulin and mucin domain 3 (Tim-3)

Tim-3 is one of the main important inhibitory receptors that was initially identified on Th1 cells and was found that negatively regulate Th1 responses[173,174]. Later studies showed that Tim-3 is also expressed by other types of immune cells such as Treg cell[175], macrophage[176], dendritic cell[177,178], $CD8^+$ T cells, and natural killer (NK) cell[179]. Tim-3 is one of the last exhaustion markers

that upregulate in T cells after prolog exposure of T cells to tumor antigens. High expression of this receptor has been reported in highly exhausted $CD8^+$ T cells. Tim-3 binding to its ligand galectin-9 suppresses cytokine production and proliferation. Co-expression of Tim-3 and PD-1 on $CD8^+$ T cells in tumor has been associated with terminally exhausted $CD8^+$ T cells and blocking of these two inhibitory receptors together had a greater effect on T cell function restoration[153].

1.6- Cancer immunotherapy

1.6.1- CAR T cell

T cell therapy has been shown to be one of the most promising immunotherapies for the treatment of cancer such as blood cancer[180]. Recently, cancer immunotherapy using engineered T cells such as chimeric antigen receptor (CAR) T cell, T cell receptor (TCR) T cell, and immune checkpoint blockade have achieved substantial advances in treatment of cancer. However, the efficacy of CAR-T cells in controlling the growth of solid tumors has not been very successful, showing that TME has a negative effect on the function of CAR T cells[181-183]. Several studies showed that tumor cells markedly upregulated immunosuppressive molecules such as IL-10, TGF-β, and PD-L1 after infusion of CAR T cells[184,185] indicating that TME of solid tumors is able to suppress infiltrated CAR T cells. Besides that, CAR-T cells express high levels of exhaustion markers such as PD-1, Lag-3, Tim-3, and loss they functionality[185].

Generation of CAR-T cells that are resistant to exhaustion is a good strategy to improve CAR-T cell therapy for treatment of solid tumors. For example, one study showed that NR4A is a transcription factor that has a critical role in mediating CAR-T cell exhaustion and deletion of this transcription factor significantly decreased immune checkpoint receptors expression and increased anti-tumor immunity of CAR-T cells[186] . Another study showed that overexpression of C-Jun in CAR-T cells enhanced proliferation, functionality, and improved anti-tumor immunity of CAR-T cells in different subset of solid tumors[187].

1.6.2- Neoantigen T cell therapy

Neoantigens are new proteins that are expressed by cancer cells when a somatic mutation occurs in tumor DNA. These neoantigens are attractive targets for cancer immunotherapy[188]. Like CAR-T cells, engineered TCR can recognize neoantigens enabling them to attack tumor cells and it has been shown that it has a therapeutic potential for treatment of cancer. This approach of T cell therapy showed promising results in several types of cancer. For example, melanoma antigen recognized by T cells 1 (MART-1) or Glycoprotein 100 (gp-100) antigens are expressed by 80-95 % of melanoma patients, and targeting these antigens by TCR has been correlated with better patient survival and anti-tumor responses[189-192]. Another study showed that TCR targeting carcinoembryonic antigen (CEA) in colorectal cancer caused regression of tumor[193].

1.6.3- Immune checkpoint blockade

One of the main mechanisms of cancer evasion by tumor cells is expression of ligands that bind to inhibitory receptors on T cells to suppress them[194-196]. These proteins are known as immune checkpoints that have a very important role in prevention of self-tissue damage and development of autoimmune disease. One of the most promising and successful strategies for treatment of cancer is rescuing T cell exhaustion by using immune checkpoint inhibitors (ICIs)[149]. ICIs therapy has been approved by FDA for various types of cancer such as Melanoma[197], Lung cancer, and Hodgkin lymphoma and it has been correlated with improved patient survival. Targeting these inhibitory receptors such as PD-1, Tim-3, CTLA-4, LAG-3, and PDL-1 by monoclonal antibodies increased tumor infiltration of $CD8^+$ T cells and boosted anti-tumor immune responses. For example, Blockade of CTLA-4 decreased activity of $CD4^+$ Tregs, increased functionality of tumor infiltrated T cells and also priming of T cells in tumor draining lymph node[149] or PD-1/PDL-1 blocking increased activity of tumor infiltrated $CD8^+$ T cells. Combining CTLA-4 and PD-1 blocking significantly improved patient survival. However, using monoclonal antibodies against PD-1 and

CTLA-4 was correlated with good results in high tumor mutation burden such as melanoma and lung cancer, but results of using these Abs for treatment of cold tumors were not promising[198], also combination of these two Abs generated significant toxicities in recipient patients. This toxicity was associated with inflammatory disorders such as colitis and cutaneous inflammation[199,200]. Recent pre-clinical studies showed that targeting other inhibitory receptors such as Tim-3 or LAG-3 by mAb could provide a lower incidence of autoimmune side effects[149,201,202].

1.6.4- Targeting of inhibitory cells

One of the main obstacles for non-responder tumors to immune checkpoint blockades is secretion of immunosuppressive molecules by inhibitory cells such as MDSC and Tregs in the tumor microenvironment. Using pharmacological agents that block these immunosuppressive factors in combination with immune checkpoint blockades has been correlated with better immune responses in tumors with more complex immune landscape[149]. For example, in head and neck cancer depletion of MDSC in combination with immune checkpoint blockade caused regression of tumor [149]. Depletion of $CD4^+$ regulatory T cells can be another approach for cancer immunotherapy; however, this strategy would increase the chance of developing autoimmune disease[203,204].

1.6.5- Challenges and future directions of cancer immunotherapy

Targeting inhibitory receptors in order to improve anti-tumor immunity can break the normal tolerance mechanisms which are required for preventing the development of autoimmune disorders, therefore blocking these pathways can generate various side effects that can be difficult to control them[199,205,206]. Therefore, finding factors that are specifically upregulated in tumors and generation of pharmacological blockers for these factors would be a good strategy to decrease side effects of cancer immunotherapy[207].

1.7- Peripheral Nervous System (PNS)

1.7.1- Sensory neurons

The peripheral nervous system is the part of the nervous system outside of the brain and spinal cord that innervates peripheral tissues (e.g., gut, skin, lung, and other tissues); it is divided into somatic and autonomic nervous systems. The somatic nervous system includes two major types of neurons: sensory neurons (known as afferent neurons), which transfer information from the body to the brain and spinal cord, and motor neurons (also known as efferent neurons), which transmit signals from the brain and spinal cord to the periphery[208].

Sensory neurons include C and Aδ fibers, which are specialized for the detection of specific types of signals. Specialized sensory neurons that detect damaging stimuli, e.g., injury-related chemicals, extremes in temperature and pressures, toxins, and foreign antigens[209] are known as nociceptors. Nociceptors detect damaging stimuli through the expression of various types of ion channels such as Transient receptor potential cation channel (TRP), piezo type mechanosensitive ion channel component (Piezo), and acid-sensing ion channels (ASIC) channels. TRPV1 and TRPA1 are non-selective, ligand-gated cation channels of the TRP superfamily, which play important roles in pain and neurogenic inflammation through the activation of sensory nerves [210-212] **(Figure 5)**.

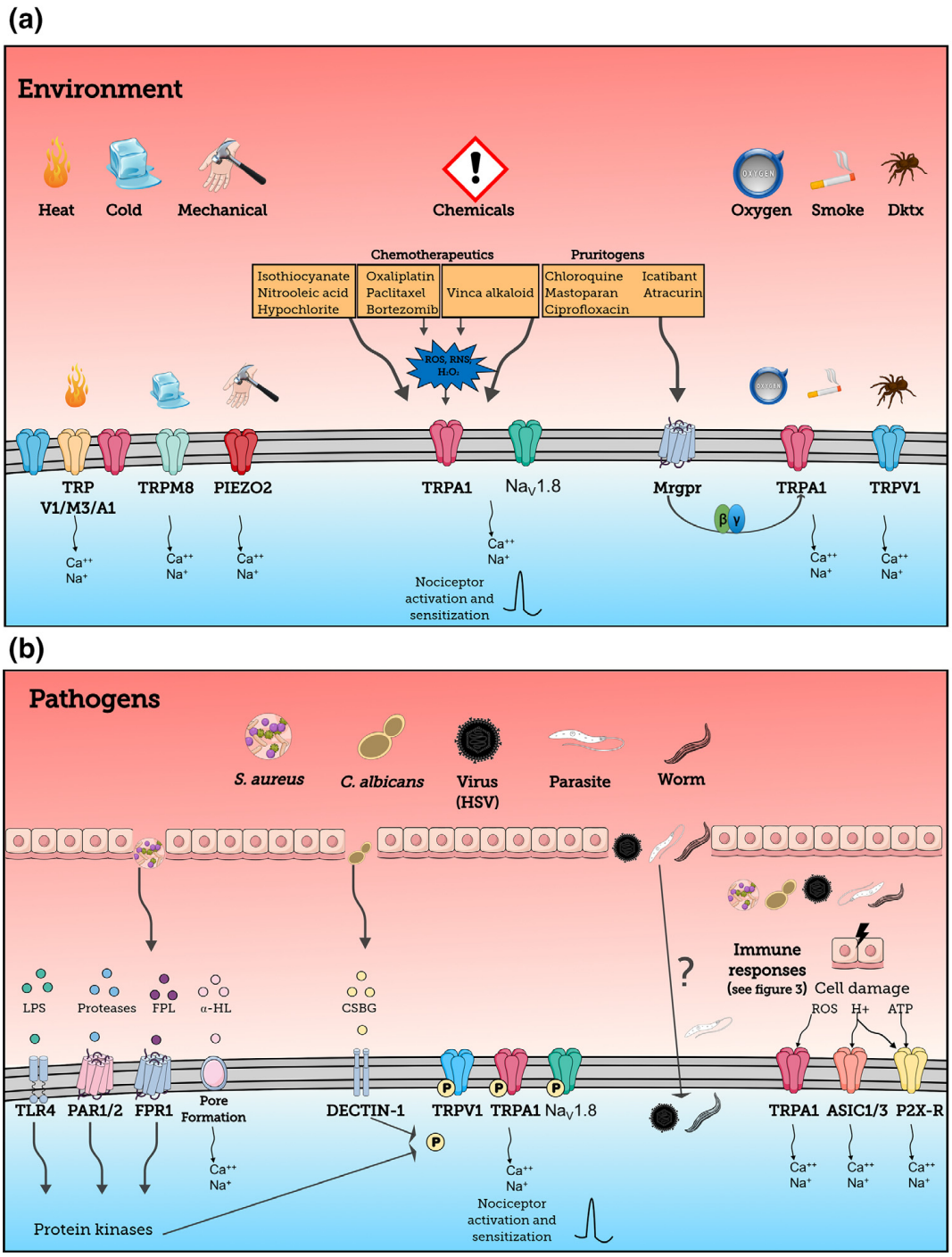

Figure 5. Expression of ion channels by sensory neurons. Nociceptor neurons express various types of ion channels such as TRP, Piezo, and ASIC channels, for the detection of noxious stimuli such as mechanical forces, temperature changes, and chemical agents. TRPV1 is well known for its roles in inflammation and pain sensation. Activation of these channels increase intracellular calcium signaling that leads to various physiological effects (a). Nociceptors also sense microbial antigens and toxins directly through the expression of pathogen-associated molecular pattern receptors such as TLRs and FPRs, which results in sensitization of sensory neurons (b) [213].

Transient receptor potential vanilloid 1 (TRPV1), expressed by sensory C and Aδ fibers and considered to be a pain sensor, is activated by a number of exogenous stimuli. These include heat, chemicals, and capsaicin (an ingredient in chili peppers)[214,215], as well as endogenous ligands such as ATP, H^+ ions, histamine, bradykinins, and prostaglandins, which are produced during tissue injury, inflammation, and tumor development [216-218]. Activation of the TRPV1 channel results in the influx of calcium and sodium into the sensory neurons, causing depolarization and subsequent release of pro-inflammatory neuropeptides, including calcitonin-gene-related peptides (CGRP) and substance P (SP), which can trigger neurogenic inflammation [219-223] **(Figure 6)**.

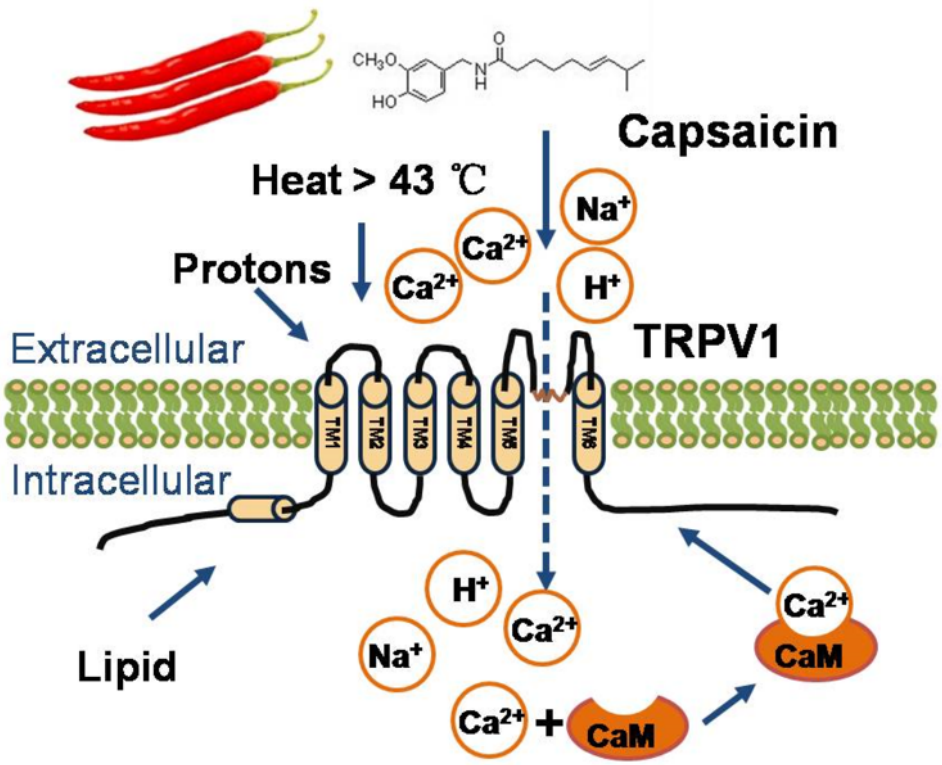

Figure 6.Structural and physiological characteristics of TRPV1.TRPV1 is a protein with six transmembrane regions. TRPV1 can be activated by capsaicin, heat, acidosis, and sensitized by NGF. Activation of TRPV1 induces influx of extracellular Ca^{2+} and Na^+ ions into cells, regulating the physiological functions of neurons [214,222].

1.7.2- Neurogenic inflammation

The idea that neurons are involved in the regulation of inflammation was first posited by Goltz (1874), who found that stimulation of the sciatic nerve induces vasodilation. Subsequently, Bayliss (1901) discovered that afferent neurons from the dorsal root ganglion (DRG) are the main players in this phenomenon[224]. Jancso and others showed that following stimulation of sensory neurons by noxious stimuli, the resulting action potential is transmitted into the central nervous system (CNS), initiating reflexes (withdrawal, scratching, expulsion) or sensations (pain, itch)[225]. When action potentials reach the CNS, signals are transmitted back to the peripheral axons, which increases the resting membrane potential of the neurons, activates voltage-gated calcium channels, and increases cytoplasmic calcium levels, inducing the rapid and local release of neuropeptides (SP and CGRP)[226-230]. These substances act locally on immune and vascular smooth muscle cells, inducing inflammation characterized by redness and warmth, swelling, and hypersensitivity. This phenomenon is termed “neurogenic inflammation”, that is, inflammatory symptoms that result from the release of substances from sensory nerves.

1.7.3- Interaction of pheripheral nervous system with immune system

The spleen and lymph nodes are innervated by the peripheral nervous system[231]. This nervous system secretes different hormones and neurotransmitters that directly modulate immune cell responses[7,232]. Immune cells also produce cytokines that affect the function of neurons[233]. Although this interaction is required for the maintenance of physiological homeostasis and defense against infection, it can also contribute to disease development.

1.7.4- Innervation of lymphoid organs

Several lines of evidence show that distribution and presence of nerve fibers in lymphoid organs indicate that there is a bidirectional communication between the peripheral nervous system (PNS) and lymphoid organs such as lymph nodes (LNs), spleen, and bone marrow. This crosstalk plays important role in the regulation of immune system responses in different pathophysiological context such as tissue injury, infection, and cancer[231,234-237]. The PNS include sympathetic, parasympathetic, and sensory neurons that after infiltration to the peripheral tissues innervate a particular zone in these tissues and their axonal terminal can be in close proximity to different residential cells. The precise mechanisms of how these interactions affect the function of immune cells are not fully known yet, however, it is thought that nerve fibers interact with immune cells through the local releasing of neuromodulators such as neuropeptides, neurotransmitters, and growth factors.

1.7.5- Innervation of spleen

One group of nerve fibers that enter the spleen is sympathetic neurons that are in close contact with the splenic artery[238-240]. These sympathetic neurons might interact with lymphocytes, macrophages, and DCs[241-243]. Recent studies using confocal microscopic and immunofluorescent staining showed that all parts of the spleen including nodules, lymphoid sheath, marginal zone, and red pulp are highly innervated with this type of nerves fibers and these neurons are in close contact with macrophages, lymphocytes (T, B), and dendritic cells (DCs). It is possible that neurotransmitters such as neuropeptide Y (NPY) and Vasoactive intestinal peptide, (VIP), and Norepinephrine that are released by sympathetic neurons can modulate function of the immune cells. However, there is a controversy regarding the presence of parasympathetic or cholinergic neurons in the spleen. Acetylcholine (ACh) was first isolated from the

spleen[236,240,244,245] but there are several studies failing in detection of cholinergic neurons[237,246,247]. The presence of sensory neurons in the white and red pulp of mouse spleen has been reported[248]. The majority of these afferent neurons are substance P $(SP)^+$ and $CGRP^+$ nerve fibers[249]. These nerves are in close proximity to the zone of macrophages, B, and T cells[250-252] and have been shown to modulate the function of these immune cells.

1.7.6- Innervation of the bone marrow

Recent studies confirm that nerve fibers enter the bone marrow and interact with the component of bone[253]. These nerves are autonomic and sensory fibers that are in close proximity with hematopoietic stem progenitor cells (HSPCs) and mature leukocytes[254-260]. Sympathetic neurons in the bone are divided into preganglionic and postganglionic neurons. Postganglionic nerve fibers are identified by expression of tyrosine hydroxylase (TH) and this subtype innervates the bone marrow and blood vessels[255]. These TH+ nerves are divided based on the expression of neurotransmitters. One group of them expresses NPY[255] and the other peptidergic neurons express VIP[256]. Another subset of autonomic nerves is parasympathetic nerves that innervate bone. These nerve fibers express choline acetyltransferase (ChAT) enzyme which is involved in production of acetylcholine[261,262]. Several recent studies showed that sensory neurons also innervate bone, sense bone marrow environment, and send the signal to the central nervous system. $CGRP^+$ and SP^+ nerve fibers are the main afferent fibers that innervate bone marrow, however, $CGRP^+$ fibers are more abundant[255].

1.7.7- Innervation of the LN

Several evidence shows both noradrenergic and peptidergic neurons innervate lymph nodes (LNs) and these nerves modulate the function of tissue-resident immune cells[263]. For instance, attenuation of inflammatory responses in mouse model of arthritis after local ablation of sensory neurons in the LN, showing a proinflammatory role for sensory neurons innervated LN[264,265] or systemic depletion of sensory neurons using a diphtheria toxin fragment A (DTA) showed that sensory neurons have an important role in the regulation of antigen trafficking to the LN[266]. A recent study using single-cell RNA sequencing and imaging showed that LNs are innervated with both sympathetic and sensory neurons. These Sensory neurons are heterogeneous and have a peptidergic identitiy[267]. It has been shown that cutaneous sensory neurons play an active role in development of psoriasis by inducing secretion of IL-23 by dermal dendritic cells and ablation of this subset of neurons significantly decreased inflammation[268]. These findings show that sensory neurons have a strong effect on the lymph nodes and systemic depletion of sensory neurons increased the number of lymphoid and myeloid in the LN[265].

1.8- Regulation of immune cells by neurotransmitters

1.8.1- Autonomic nervous system neurotransmitters

The anatomical connection between the nervous system with lymphoid tissues, and the expression of receptors for neuromodulators such as hormones and neuropeptides by immune cells, set the stage for studying the neuroimmune interaction. For example, activation of splenic sympathetic nerve fibers leads to release of neurotransmitters at the neuroimmune junction that modulates the function of immune cells in the spleen[269]. On the other side, cytokine production by immune cells also can activate sympathetic neurons[270-277].The molecular mechanism that how splenic sympathetic nerves modulate immune cell function has been extensively studied[278-284].

For example, Norepinephrine (NE) through alpha-adrenergic receptor (αARs) increase macrophage activity while beta receptors suppress macrophage activity[285-291]. T cells express beta-2 adrenergic receptors (β2Ars) and stimulation of these receptors has been shown that have a suppressive effect on T cells[280,292-297]. Stimulation of (β2Ars) on B cells increases cAMP that inhibits B cell proliferation and antibody production[292,298-301]. Stimulation of α1- and α2-ARs on NK cells increases cytotoxicity of NK cells[302] or stimulation of β2Ars on NK cells increases recruitment of these cells to the blood circulation[303].

The Vagus nerve includes afferent fibers [304,305] and sensory fibers that are thought to play a role in detection of peripheral antigens[306-308]. The presence of afferent fibers in the lymphoid organs and the production of Ach has been studied by several groups. It has been considered that lymphoid organs may be innervated by vagus nerve[309,310] or maybe not[245,246,311]. There is several evidence showing that stimulation of cholinergic nerves can modulate peripheral immune system responses. For example, it has been shown that ACh decreases proinflammatory cytokine production by macrophages[312] or stimulation of peripheral vagus nerve was correlated with reduction of TNF level in the serum and liver[312]. In addition, activation of the cholinergic nervous system in an animal model of inflammatory diseases such as arthritis, pancreatitis, and colitis significantly reduced disease symptoms[313-315].

NPY is another neurotransmitter that is released by sympathetic nerves and modulate the function of IgM^+ B cells and $CD169^+$ macrophages through different Y receptors such as (Y1, Y2, Y4, and Y5)[316]. Lack of Y1 receptors decreased number of B cells in the spleen and impaired IgG2a production by B cells[317]. VIP^+ nerves fibers have been shown in close proximity to T cells[318]. Vasoactive Intestinal Peptide receptor 1 (VPAC1) and VPAC2 receptors are expressed by macrophages, monocytes, dendritic cells, and lymphocytes following the activation[319]. This neuropeptide has been shown that has an inhibitory effect on immune cells by downregulating proinflammatory cytokines in T and macrophages[306,320]. It also generates antigen-specific regulatory T cells by activation of tolerogenic dendritic cells[306,321].

1.8.2- Sensory neuron neurotransmitters

Various bioactive neuropeptides that are released by sensory neuron fibers in the spleen, Lymph node, and bone marrow modulate the function of immune cells **(Figure 7)**. Substance P (SP) has been demonstrated that has a stimulatory effect on T lymphocyte and induce lymphocyte proliferation and production of cytokines such as IL-2, IL-4, and IFN-γ from T cells[305,314]. SP also activates macrophages and granulocytes and increases pro-inflammatory cytokines like TNF-a, IL-1β, IL-2, and IL-6 [322]. On the opposite, CGRP likely has an inhibitory effect on immune system responses. CGRP act through two receptors that express by a different subset of immune cells; receptor activity-modifying protein 1 (RAMP1), and calcitonin receptor-like receptor (CLR)[323,324] . CGRP has been shown that inhibit antigen presentation by Langerhans cells dendritic cells[323,325-327], suppress TNFα production by activated dendritic cells, and increase IL-10 production from these cells[324]. The same effect has been reported for the macrophage and neutrophils[307]. These findings show that these two neuropeptides have the opposite role in modulating the function of immune cells. CGRP signaling increases intracellular level of cAMP and activates protein kinase A (PKA). cAMP-PKA functions as an inhibitory pathway in immune cells and induces an anti-inflammatory response in order to prevent self-tissue damage[328]. $CGRP^{+}$ fibers have been shown to modulate hematopoietic stem cell mobilization to the circulating blood[329]. Altogether, these findings suggest that neuromodulators play an important role in the regulation of immune system responses, and it would be of interest to further explore how and what type of these mediators are involved in modulation of anti-tumor immune responses.

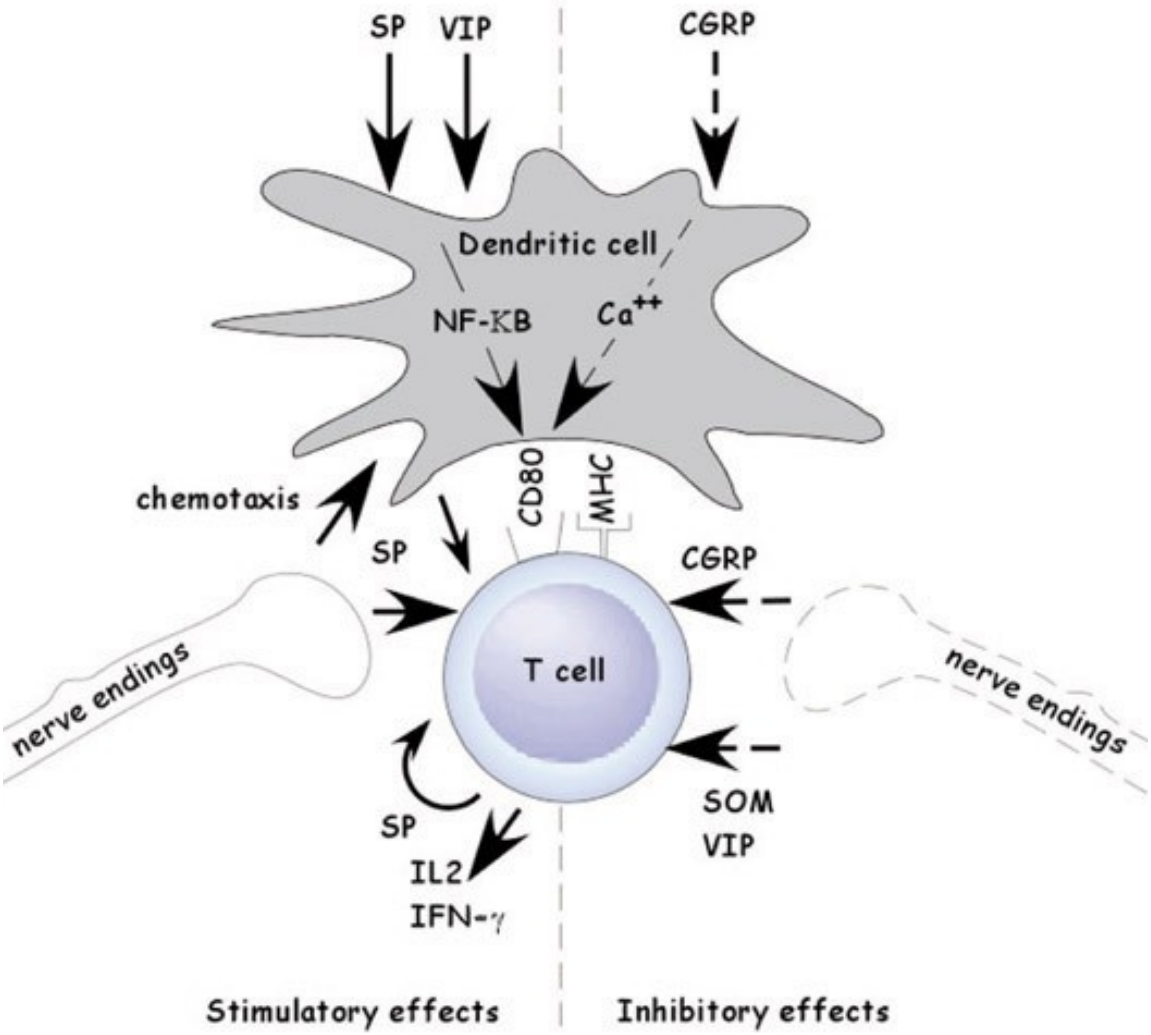

Figure 7.Impact of neuropeptides on dendritic cells and T cells. CGRP, VIP, and somatostatin have an inhibitory effect on T cells, abrogating their proliferation and activation, while substance P has a stimulatory effect on T cells. CGRP inhibits antigen presentation by dendritic cells, however, VIP and substance P have a stimulatory effect on dendritic cells. Solid arrows indicate stimulatory effects; broken arrows indicate inhibitory effects[330].

1.9- Nerve-cancer crosstalk

The role of nerves in cancer progression and dissemination has been confirmed by several recent studies. It has been shown that nerves can infiltrate into the tumor and communicate with components of TME. Nerve fibers interact directly with cancer cells and affect tumor cell proliferation and spreading, induce angiogenesis, and increase cancer chemoresistance. Intratumoral infiltration of nerves was found to be associated with cancer prognosis in patients and this association was observed in tumors that grow in highly innervated tissues such as skin, pancreas, head and neck, prostate, and colorectal cancers[331-339]. Analyzing patient's tumor samples revealed that there is a positive correlation between the nerve density with metastasis, morbidity, and mortality in different types of cacners[332,339-345]. Denervation was associated with reduced tumor growth[346]. Neuroactive factors secreted by nerves that are involved in tumor-nerve interaction can be classified into three groups: 1) neurotrophic factors such as nerve growth factor (NGF), brain-derived neurotrophic factor (BDNF), and other factors; 2) axon guidance molecules such as CCL-2, CX3CL-1, and Eph; 3)neurotransmitters such as Ach, epinephrine, norepinephrine, dopamine, etc[347].

1.9.1- Primary findings in nerve-cancer crosstalk

1.9.1.1- Tumor-drived factors induce axonogenesis

However, the mechanisms of axonogenesis in cancer have not been fully elucidated, but new findings provide compelling evidence that cancer cells release growth factors and vesicles that drive axonogenesis and neurogenesis**.** Axonogenesis or neurite outgrowths in cancer has been discovered for the first time in prostate cancer when Ayala et al found that there is a relationship between tumor growth and neurite outgrowths (increase in nerve density) in the tumor[338,348]. They discovered that axon-guided molecule semaphorin 4F (S4F) was overexpressed

by prostate cancer tumor cells when nerves and prostate cancer were co-cultured. Blocking of SF4 significantly decreased neurite outgrowths in a co-culture system. In addition to axonogenesis, Ayala et al demonstrated that cancer can drive neurogenesis. They found that neural progenitor cells migrate from the brain to the tumor region and metastatic tissues via bloodstream and differentiate into noradrenergic neurons **(Figure 8B).** In addition, they observed that number of neural stem cells in high-risk prostate cancer was higher in comparison to low risk. Depletion of these progenitor neural stem cells decreased tumor growth[349].

1.9.1.2- Neurogenic factors induce axonogenesis in cancer

Secretion of neurogenic factors either by tumor cells, tumor-associated cells, and nerves is another pathway that promotes axonogenesis in tumor. These factors such as nerve growth factor (NGF), Glial cell-derived neurotrophic factor (GDNF), Brain-derived neurotrophic factor (BDNF), and Neurturin are required for neuron survival, differentiation, and outgrowth (**Figure 8A)**. Binding of these growth factors to their receptors such as tyrosine-receptor kinases (Trks) TrkA, TrkB, TrkC, and p75 neurotrophin that are expressed by both nerve fibers and cancer cells stimulates prolifereation and survival of cancer and also drive neuron outgrotwh[350,351] (**Figure 9)**.

There are several pieces of evidence showing that cancer cells secrete these growth factors and induce axonogenesis in tumors. For instance, in a mouse model of prostate cancer overexpression of NGF by tumor stromal cells not only induced axonogenesis but also in a paracrine manner induced proliferation of tumor cells through tyrosine-receptor kinases (Trks) TrkA and TrkB that are expressed by tumor cells[352-354]. High level of NGF in gastric cancer increased enteric nerves[355,356]. High expression of NGF in breast cancer cells was correlated with a high density of nerve and tumor proliferation[357], and the same effect has been observed in melanoma[358]. BDNF is another neurotrophin that is released by adrenergic neurons and stimulates axonogenesis by activating TrK receptors[359-361]. This growth factor also induces angiogenesis and increased tumor cell proliferation[361] **(Figure 10)**. GDNF is highly expressed in human pancreatic ductal adenocarcinoma (PDAC) and was associated with neural invasion and

increased level of pain in patiens[362-364]. Overexpression of Neurturin and artemin in PDAC promoted tumor innervation[365] and was associated with tumor invasiveness[341,366-368]. These factors also have been implicated in tumor migration in several types of cacner[369,370]. For example, Netrin-1 has been considered as an oncogene that promoted gastric cancer cell migration along sensory dorsal root ganglia cells and sciatic nerve[371], or blocking of Slit2 expression in PADC reduced cancer cell metastasis and neural invasion[372].

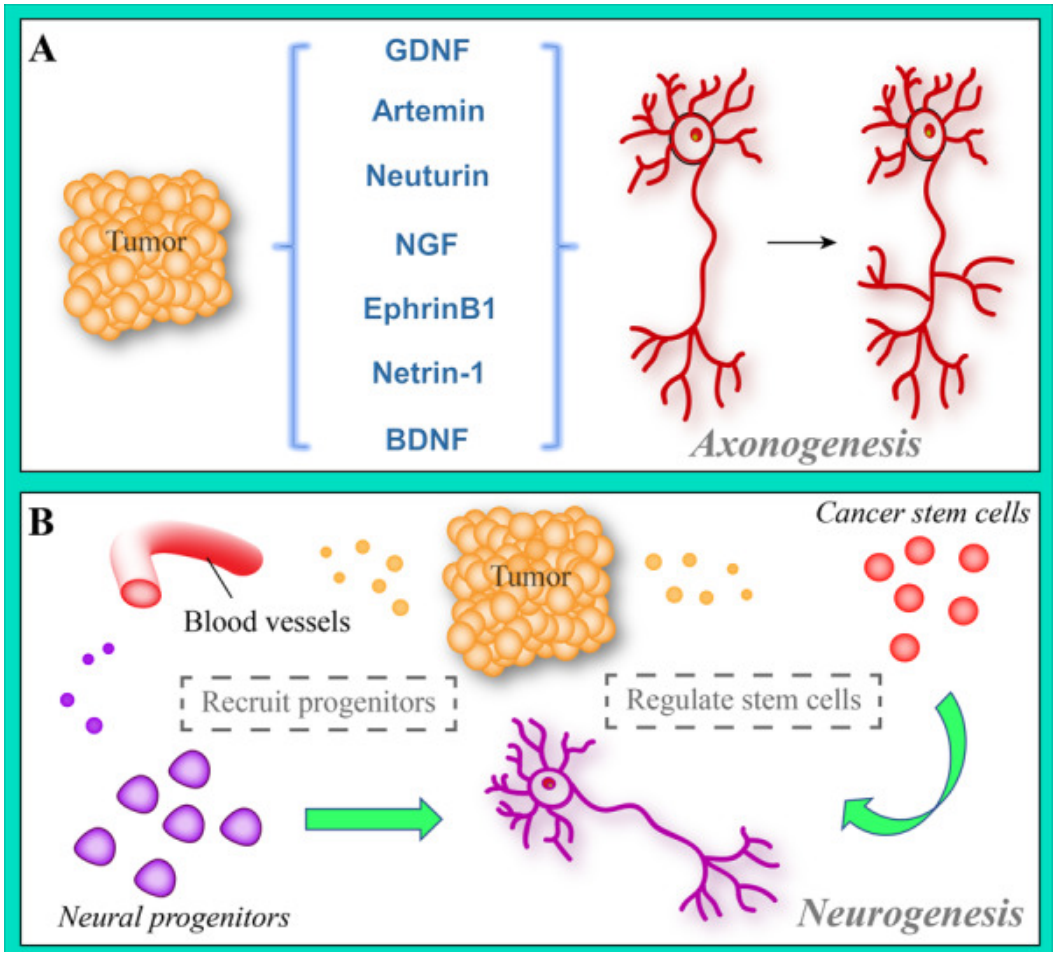

Figure 8. Neurogenesis and axonogenesis in TME. **A**. Neurogenic factors such as GDNF, BDNF, NGF, Artemin, Neuturin, EphrinB1, and Netrin-1 promote axonogenesis.**B.** Tumor cells induce migration of neural progenitor cells from the brain into the tumor tissue through the bloodstream. In addition, cancer generates new neurons from cancer stem cells in TME[373]**.**

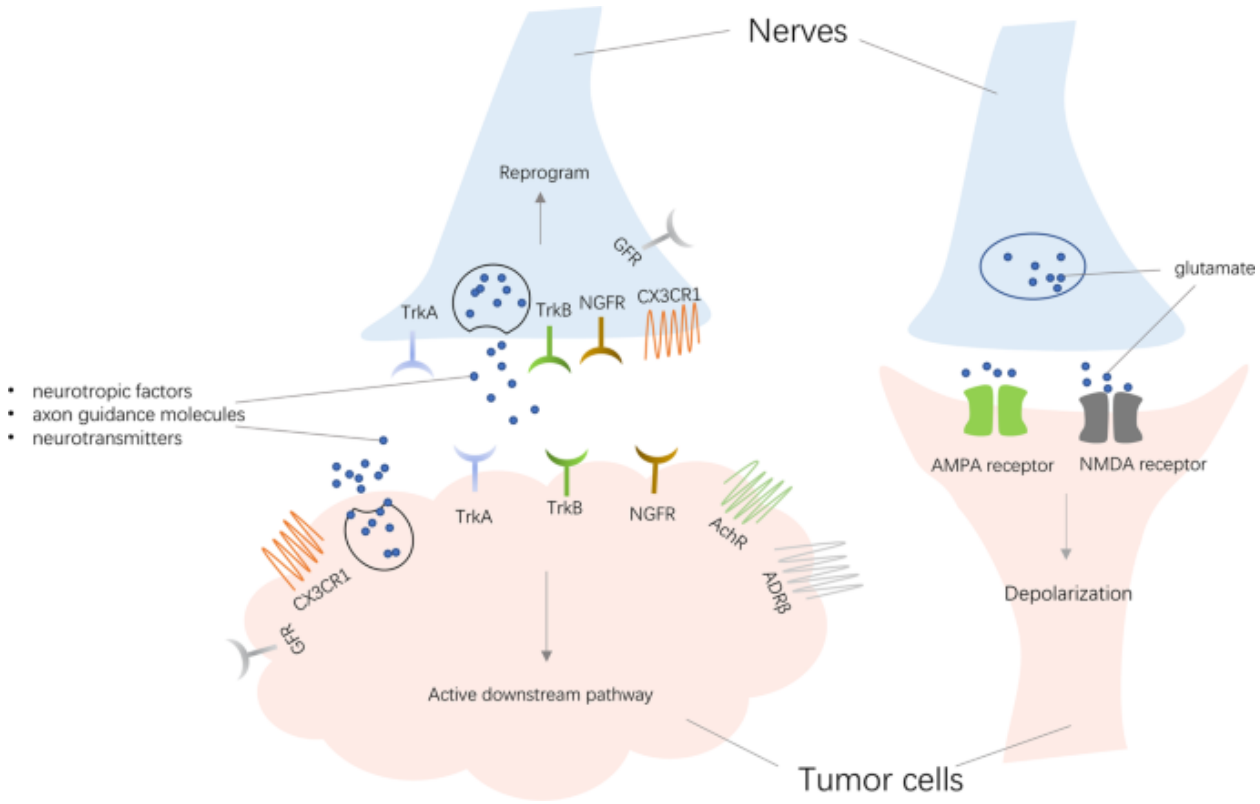

Figure 9.Neuromediators regulate tumor progression. Tumor cells and neurons release neurotransmitters, neurotrophic factors, and axon guidance molecules into the neuron-cancer synapse. These factors upon binding to their receptors induce neurogenesis and also promote tumor cell proliferation. In addition, these neurotransmitters also promote tumor progression by depolarization of cancer cells[374-377].

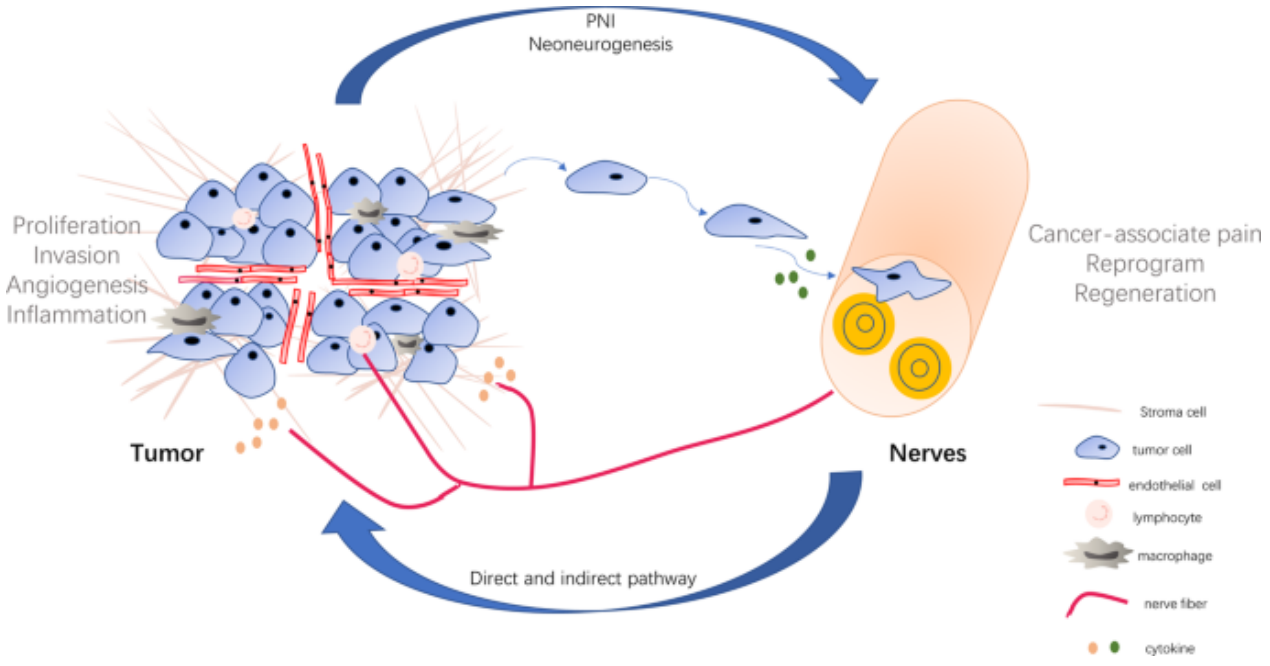

Figure 10.Nerve–cancer cross talk. Nerve secretes neurotrophic factors that promote tumor proliferation, invasion, and angiogenesis. On the other hand, migration of tumor cells into the nerves damages neurons and induces pain. In addition, cytokines produced by tumor cells induce nerve reprogramming and regeneration. PNI, perineural invasion[378].

1.9.1.3- Tumor cells stimulates neural reprogramming

Mauffrey et al, showed for the first time that tumor cells release extracellular vesicles (EVs) that can induce reprogramming of neurons. These small vesicles (30–150 nm) contain proteins, DNA, RNA, and lipids, which function as intracellular mediators and can be produced by tumor cells. It has been shown that stimulation of PC12 cells *in vitro* by exosomes derived either from tumor patients such as head and neck cancer or from murine oropharyngeal squamous cell carcinomas (OPSCC)[379] significantly increased neurite outgrowth in comparison to the control group[379]. Conversely, *in vivo*, inhibition of tumor-released exosomes decreased tumor innervation and growth[380]. Immunohistochemical staining of human and mouse samples also identified more

than 80% of tumor-innervating fibers as sensory fibers[379]. They found that Lack of miR-34a in vesicles that are driven from p53-knockout oral cavity squamous cell carcinoma (OCSCC) induces transcriptional reprogramming in tumor-associated sensory neurons and transdifferentiated them to adrenergic nerves, and promoted tumor growth in mouse model of (OCSCC)[381] **(Figure 11)**. This group found that[381] daily intratumoral injection of $p53^{WT}$ OCSCC EVs could suppress noradrenergic neurogenesis. This finding was similar to what has been found in head and neck cancerpatients[382].

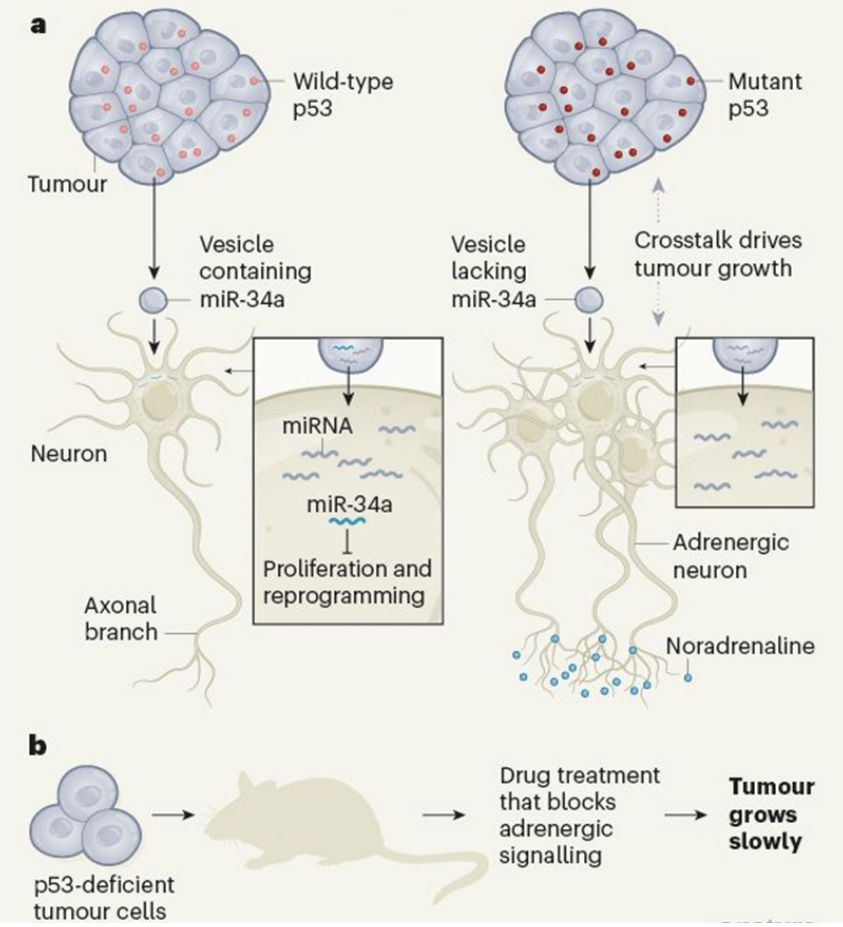

Figure 11. EVs released by tumor cells reprogram neurons. Lack of P53 expression by tumor cells changes the microRNA population within the exosomes. Loss of miR-34a expression by exosomes change existing sensory neurons to adrenergic neurons and promote tumor growth[381].

1.9.1.4- Tumor associated neurons suppress intratumoral immune Cells

Although the role of nerves in cancer still is in the early phase of research, several lines of evidence show that nerves play an important role in tumor progression either directly or indirectly through suppression of the immune system in the tumor microenvironment. Tumor-associated neurons (TANs) can interact with immune cells in TME and suppress anti-tumor immunity cells by different mechanisms **(Figure 12)**. For example, it has been discovered that tumor activated-sensory neurons release chemokines that recruit MDSC into the tumor microenvironment[383] or there is a correlation between the intensity of PDL-1 expression by sensory neurons and infiltration of T cells. It has been shown that higher intensity of PDL-1$^+$TANs was correlated with higher infiltration of regulatory T cells (Foxp3$^+$ T) and lower infiltration of cytotoxic CD8$^+$ T cells in human prostate cancer[383]. Secretion of GDNF by tumor infiltrated neurons upregulated expression of PDL-1 by head and neck squamous cell carcinoma (HNSCC) through JAK2-STAT1 signaling pathway[384].

Another study showed that there is a positive correlation between the density of sympathetic nerves and immune checkpoint receptor expression and a negative correlation between parasympathetic nerves with immune checkpoint receptor expression. Ablation of sympathetic nerves in mouse model of breast cancer decreased expression of PD-1 on both CD4$^+$ and CD8$^+$ T cells, increased expression of IFN-γ, and reduced infiltration of Treg. On the opposite, stimulation of parasympathetic neurons suppressed expression of PD-1 by tumor infiltrated CD4$^+$ and CD8$^+$ T cells and increased expression of IFN-γ. This effect has been observed in human breast cancer specimens also. There was a positive correlation between the density of TH$^+$ sympathetic nerves and expression of PD-1 by CD4$^+$ and CD8$^+$ T cells[385]. Depletion of CGRP$^+$ neurons in mouse model of oral cancer was correlated with slower tumor progression and higher infiltration of CD4$^+$ and CD8$^+$ T cells. However, CGRP did not impact the proliferation of cancer cells directly, but the expression of CGRP receptor RAMP1 was overexpressed in tumor infiltrated T cells which is indicating that CGRP can suppress the adaptive immune system function[386].

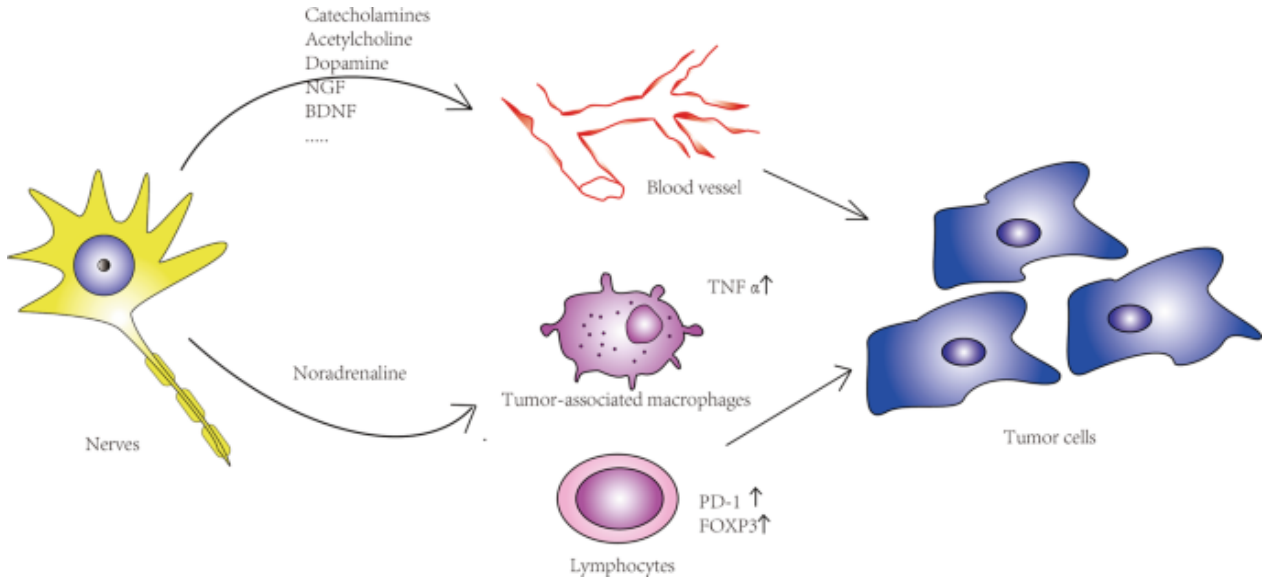

Figure 12. Nerve affect tumor cell growth through suppression of immune cells.Neuron–cancer communication results in the release of transmitters and neurotrophic factors by neurons, which induces angiogenesis, regulates tumor-associated macrophages, and modulates the expression of immune checkpoint receptors (PD-1, PD-L1, FOXP3) by lymphocytes, all of which promotes tumor progression[378].

1.9.1.5- Autonomic neurotransmitters promote tumor growth

Neurotransmitters in addition to modulating immune cells in the lymphoid tissues are also able to directly affect cancer development. Catecholamines and acetylcholine released by sympathetic and parasympathetic nerves can induce prostate tumor growth and metastasis. Stimulation of cancer cells by autonomic neurotransmitters induces cell growth. For instance, activation of β-adrenergic receptors increased tumor growth and metastasis in several cancers such as ovarican[387],pancreatic[388], and pulmonary[389]. Autonomic transmitters are also able to stimulate other components of TME such as endothelial and fibroblast cells[390].

The expression of neurotransmitter receptors by cancer cells and tumor-associated cells showed that these neurotransmitters mediate a pro-tumorigenic function through increasing tumor cell proliferation and angiogenesis. Noradrenaline and dopamine are two types of catecholamines that have the opposite effect on tumor angiogenesis. Noradrenaline upregulates expression of VEGF by macrophages and in this way stimulates tumor angiogenesis[391-393]. Deletion of β2-adrenergic and β3-adrenergic or depletion of sympathetic nerves in mouse model of prostate cancer reduced tumor angiogenesis[349,394] as well as growth and metastasis in lung and prostate cancer. On the contrary, dopamine inhibited signaling pathway by VEGF receptor and reduced tumor growth in mouse model of colon, ovarian, and gastric cancer [392,395,396].

1.9.1.6- Sensory neuron activity promote tumor progression

However, the exact mechanism of how sensory neurons promote tumor progression and metastasis still is not fully known but the role of sensory neurons in the initiation of neurogenic inflammation is very well documented. Neurogenic inflammation has been characterized as acute inflammatory response[397,398]. This response is required in normal physiology for clearance of pathogens and transformed cells[399,400]. However, besides triggering neurogenic inflammation, many studies show that prolonged activation of sensory neurons creates anti-inflammatory responses that function as a defense mechanism in order to prevent self-tissue damage and promote tissue repair[401,402]. Chronic inflammation has been characterized as a factor that promotes tumor growth and metastasis[403-406]. Therefore, activation of sensory neurons and consequently secretion of anti-inflammatory neuropeptides may induce tumor progression **(Figure 13)**. Recent studies showed that inhibition of sensory neuron activity has been associated with reduced tumor growth in several types of cancer such as peostate[407],gastric[408], basal cell carcinoma[409], and melanoma cacncer[374,410]. Similarly, chemical ablation of sensory neurons in mouse model of pancreatic and gastric cancer decreased tumor progression[411,412].

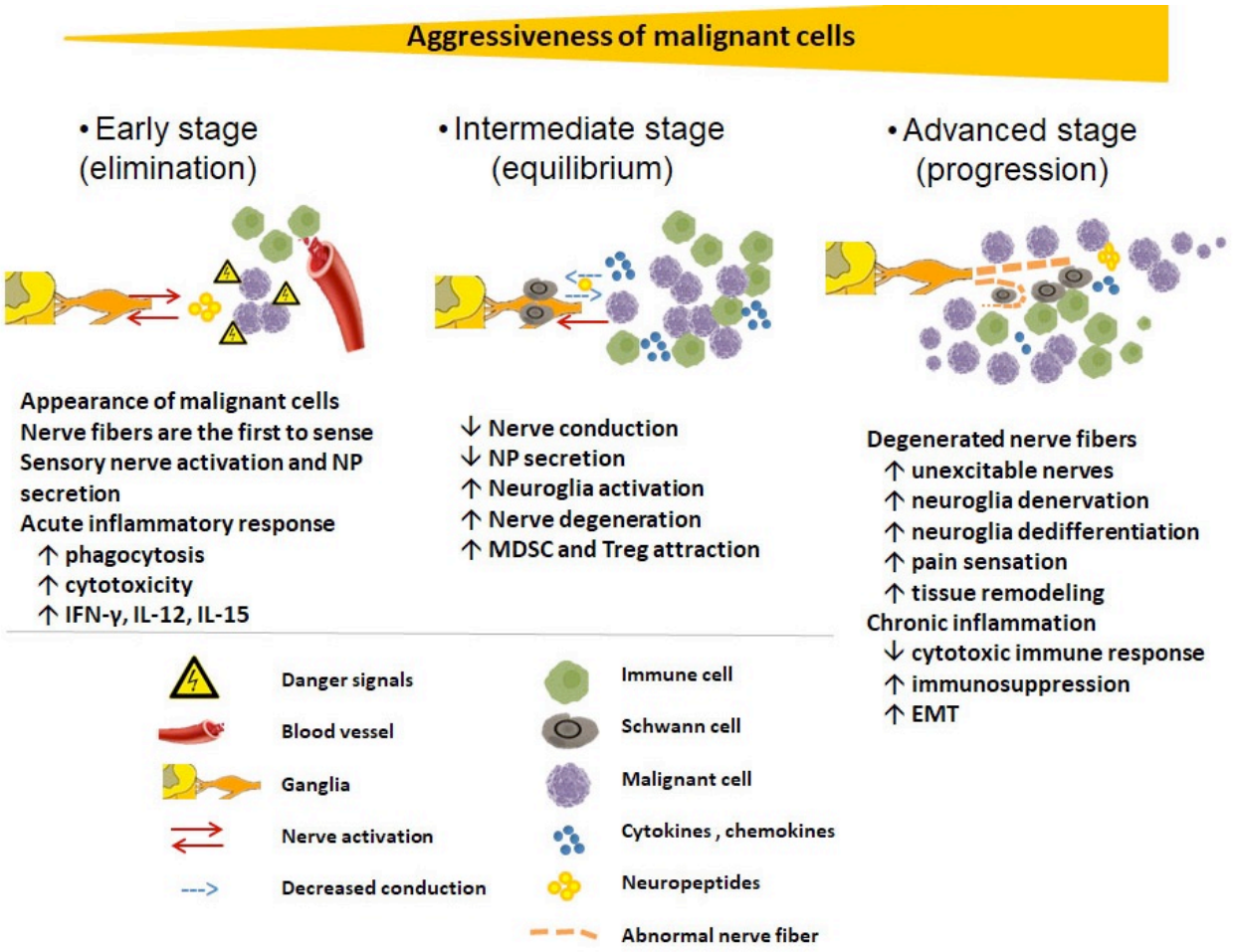

Figure 13. Hypothetical interaction of sensory neurons, immune cells, and tumor cells. During cancer immunoediting, tumor cells become more resistant to immune system destruction and become more aggressive. In addition, generation of new sensory fibers which have a tumorigenic characteristic promotes tumor progression. During the early stage of cancer development, sensory neurons through secretion of neuropeptides cooperate with the immune system to protect and defend the host by inducing an acute inflammatory response. In the intermediate phase, part of activated sensory neurons triggers anti-tumor immunity. In the late stage of tumor development, the formation of tumorigenic nerves enhances chronic inflammation, recruits suppressive cells such as MDSC, and increases metastasis[413].

Chaptere2 : Nociceptor neurons impair cancer immunosurveillance

Mohammad Balood [1,2,*], Maryam Ahmadi [1,*], Tuany Eichwald [1], Abdelilah Majdoubi [3], Karine Roversi [1], Ali Ahmadi [1], Katiane Roversi [1], Chris T. Lucido [4], Anthony Restaino [4], Siyi Huang [5], Lexiang Ji [5], Hongyue Dai [5], Chengyi J. Shu [5], Kai-Chih Huang [5], Elise Semerena [1], Sini C. Thomas [1], Hannah Merrison [6,7], Alexandre Parrin [6,7], Benjamin Doyle [6,7], Daniel W. Vermeer [4], Corey R. Seehus [6,7], Simmie L. Foster [8], Manu Rangachari [2], Jacques Thibodeau [3], Sonia Del Rincon [10], Ronny Drapkin [11], Moutih Rafei [1], Nader Ghasemlou [9], Paola D. Vermeer [4], Clifford J. Woolf [6,7], and Sebastien Talbot [1,#]

[1] Département de Pharmacologie et Physiologie, Université de Montréal, Montréal, Canada
[2] Département de Médecine Moléculaire, Faculté de Médecine, Université Laval, Québec, Canada
[3] Département de microbiologie, infectiologie et immunologie, Université de Montréal, Montréal, Canada[4] Sanford Research, Cancer Biology and Immunotherapy Sioux Falls, USA
[5] Cygnal Therapeutics, Cambridge, USA
[6] F.M. Kirby Neurobiology Center, Children's Hospital Boston, Boston, USA
[7] Department of Neurobiology, Harvard Medical School, Boston, USA
[8] Depression Clinical Research Program, Massachusetts General Hospital, Boston, USA
[9] Department of Anesthesiology and perioperative medicine, Queen's University. Kingston, Canada.
[10] Department of Oncology, McGill University, Montréal, Canada
[11] Penn Ovarian Cancer Research Center, University of Pennsylvania, Perelman School of Medicine, Philadelphia, USA
* Denotes equal contribution

Running title: Nociceptors decrease cancer immunosurveillance

Lead Contact:
Sebastien Talbot, PhD
Phone: 514-343-6111. Ext: 32787
Email: sebastien.talbot@umontreal.ca

Keywords. Nociceptor neurons, neuro-immunology, tumor innervation, melanoma, exhaustion, cytotoxic $CD8^+$ T-cells, CGRP, TRPV1, QX-314, Botox.

2.1- Abstract

Solid tumors are innervated by nerve fibers that arise from the autonomic and sensory peripheral nervous systems. In prostate cancer, doublecortin-expressing neural progenitors initiate autonomic adrenergic neurogenesis[349] which facilitates tumor development and dissemination[407] via an angiogenic switch that fuels cancer growth[414,415]. A loss of TP53 drives the reprogramming of tumor-innervating sensory nerves into adrenergic neurons in head and neck tumors, which promotes tumor growth[381]. The impact of tumor neo-innervation by pain-initiating sensory neurons remains unclear. Here, we show that melanoma cells interact with nociceptors, thereby increasing neurite outgrowth, responsiveness to noxious ligands, and neuropeptide release. In turn, CGRP, one such nociceptor-produced neuropeptide, directly increases exhaustion of cytotoxic $CD8^+$ T-cells ($PD1^+Lag3^+Tim3^+IFN\gamma^-$), thus limiting their capacity to eliminate melanoma. Genetic TRPV1 lineage ablation, local pharmacological silencing or blockade of neuropeptide release from tumor-innervating nociceptors, and the antagonism of the CGRP receptor RAMP1, all blunt tumor-infiltrating leukocyte exhaustion, and tumor growth, nearly tripling the survival rate of B16F10-inoculated mice. Inversely, $CD8^+$ T-cell exhaustion was rescued in sensory neuron depleted mice treated with recombinant CGRP. In comparison to wild-type $CD8^+$ T-cells, $RAMP1^{-/-}$ $CD8^+$ T-cells were protected against undergoing exhaustion when co-transplanted into tumor-bearing RAG1 deficient mice. Single-cell RNA sequencing of patient tumors revealed that intratumoral RAMP1-expressing $CD8^+$ T-cells are more exhausted than their RAMP1-negative counterparts. RAMP1 expression in intratumoral $CD8^+$ T-cells was also associated with resistance to immune checkpoint inhibitor treatment, while RAMP1 overexpression within the tumor correlated with a worse clinical prognosis. We conclude that reducing CGRP release from tumor-innervating nociceptors, by eliminating its immunomodulatory action on cytotoxic $CD8^+$ T-cells, constitutes a useful strategy to safeguard anti-tumor immunity.

2.2- Introduction

Cytotoxic T-cells express a variety of receptors, including PD-1 (*Programmed cell Death protein-1*), Lag-3 (*Lymphocyte activation gene-3*), and Tim-3 (*T-cell immunoglobulin and mucin domain-containing protein 3*)[202,416-418], which inhibit T-cell function after being activated by their cognate ligands. These checkpoint receptors ensure that immune responses to damage or infection are kept in check, preventing overly intense responses that might damage healthy cells[419]. Tumor cells express ligands for these immune checkpoints, which, when activated, block the cytolytic functions of T-cells, thereby favoring cancer cell survival[419-421]. Such neo-innervation is a prominent feature in cancer, which, together with the diverse actions of neuropeptides on immune cells [385,422-431], led us to explore whether local release of neuropeptides from activated nociceptors may favor cancer growth by suppressing immune surveillance.

Breast cancers show a hyper-sympathetic innervation but a decreased parasympathetic nerve density[385], whereas prostate cancers are infiltrated with cholinergic fibers and are surrounded by adrenergic fibers[407]. Although human malignant cells or immune cells do not express genes of neuronal origin (**Supp. Fig. 1A-C**), we observed a significant raise in their expression within melanoma patient's biopsies (**Supp. Fig. 1D**) [432-435]. Because these clinical data suggest increased melanoma innervation, we probed for the presence of nociceptor neurons by assessing $TRPV1^+$ (*Transient Receptor Potential cation channel subfamily Vanilloid 1*) cells in melanoma patients' biopsies. TRPV1 immunolabelling was increased ~2-fold in the tumor compared to adjacent healthy tissue; this feature was observed in each of the ten biopsies examined. Intra-tumoral TILs (*Tumor-Infiltrating Lymphocytes*) numbers correlated with increased TRPV1 immunolabelling (**Supp. Fig. 2;** R^2=0.63; $p<0.05$; *retrospective correlation analysis performed on patient's pathology report*). These data indicate that patients' melanomas are hyper-innervated by sensory neurons and that these neurons may impact intra-tumoral cell numbers.

To explore this further, we inoculated a GFP-expressing melanoma (B16F10-eGFP) cell line into $Na_V1.8^{cre}$::Td-tomato$^{fl/wt}$ mice and used a tissue-clearing approach known as iDISCO as a means to obtain a three-dimensional representation of the tumor innervation [267,436]. Twenty-two days after implantation, we found abundant $Na_V1.8^+$ nociceptor neurons around and within the tumor (**Fig. 1A**). Just as in the human biopsies (**Supp. Fig. 1A-B**), neither B16F10 cells nor mouse tumor-infiltrating immune cells express neuronal markers (i.e., $Na_V1.8$, TRPV1; **Supp. Fig. 3**) ascribing the $Na_V1.8$ signal to tumor-infiltrating nerves. We next used an *in vitro* co-culture approach to precisely quantify how the exposure to malignant cells would modulate nociceptor neuron morphology and neurite outgrowth and found that when co-cultured with B16F10-eGFP melanoma cells, fluorescently labeled (TRPV1^{cre}::Td-tomato$^{fl/wt}$) DRG nociceptor neurites extend towards the B16F10 cells (**Fig. 1B**). The average neurite length of nociceptor neurons increased (average neurite length; **Fig. 1C**) whereas the overall neuronal arborization/branching decreased (ramification index; **Fig. 1D**) when co-cultured with B16F10-eGFP cells. Cultured lumbar DRG nociceptors (L3-L5) harvested from tumor-inoculated mice (on d14) also extended longer neurites than their counterparts harvested from keratinocyte-injected mice (*not shown*). Taken together, these data indicate that nociceptor outgrowth is enhanced when in proximity to melanoma cells and that skin sensory neuron collaterals sprout directly into the tumor bed. Pathophysiologically, this phenomenon may be the neuronal equivalent of tumor angiogenesis.

Given that melanoma promotes axonogenesis leading to tumor innervation (**Fig. 1A; Supp. Fig. 2**), we next aimed to examine whether such physical proximity allow melanoma to modulate the sensitivity of the nociceptor. As nociceptor neurons detect signals from the local environment, we measured calcium flux changes in response to sub-threshold concentrations of capsaicin (an agonist of the heat-sensing TRPV1 channel), mustard oil (an agonist of the chemical sensing TRPA1 channel), and ATP (an agonist of the proton-sensing P2X3R channel). When nociceptors were cultured without melanoma cells, few responded to the ligands at the concentrations selected. However, the number of responsive neurons increased when co-cultured with B16F0 melanoma cells; this effect was made even more robust when exposed to the highly metastatic melanoma cell line B16F10 (**Fig. 1E**). Similarly, the amplitude of calcium flux responses to the

ligands was greater in lumbar DRG neurons (L3-L5) harvested ipsilateral to a fourteen-day tumor-inoculation in mice as compared to those harvested from non-tumorigenic keratinocyte-injected mice (**Fig. 1F**). Signals released from melanoma, therefore, heighten nociceptor sensitivity.

We next sought to test if such neuronal hypersensitivity would lead to increased release of immunomodulatory neuropeptides. As opposed to B16F10 cells alone, DRG neurons co-cultured with B16F10 cells ($5x10^4$ cells, 24h) actively release CGRP in the media (**Fig. 1G**). These data prompted us to test whether exposure to a melanoma alters the nociceptor neurons' transcriptome. To do so, naïve DRG neurons ($TRPV1^{cre}$::$QuASR2\text{-}eGFP^{fl/wt}$) were cultured alone or in combination with B16F10-mCherry-OVA. After 48h, $TRPV1^+$ nociceptors were harvested, FACS-purified and RNA-sequenced. Differentially expressed genes (DEG) were calculated and the neuropeptide gene *Calca* (encoding for CGRP), as well as the NGF receptor *Trka* were found to be overexpressed in cancer-exposed nociceptors (**Fig. 1H-J**). *Trka* overexpression may help drive melanoma-induced pain hypersensitivity, whereas CGRP (encoded by Calca), when released from activated nociceptors, may immunomodulate TILs.

To identify the mechanism through which melanoma sensitizes nociceptor neurons, we used a co-culture system designed to mimic the interactions at play in the melanoma microenvironment. T_{c1}-stimulated (*ex vivo* activated by CD3/CD28, IL-12 and anti-IL4 for 48h) OVA-specific cytotoxic $CD8^+$ T-cells (OT-1 mice), naïve DRG neurons ($TRPV1^{cre}$::$QuASR2\text{-}eGFP^{fl/wt}$), and B16F10-mCherry-OVA melanoma cancer cells were cultured alone or in combination. After 48h, the cells were harvested, FACS-purified and RNA sequenced. DEGs were calculated among the ten tested groups (**Fig. 2A-B**). Among others, we found that *Slpi* (*Secretory Leukocyte Protease Inhibitor*) was overexpressed in the melanoma cancer cells when co-cultured with either DRG neurons (~3.6-fold) or OVA-specific cytotoxic $CD8^+$ T-cells (~270-fold), and also when exposed to both populations (~150-fold; **Fig. 2A-B**). Basal *Slpi* levels in OVA-specific cytotoxic $CD8^+$ T-cells or in DRG neurons were minimal and were not impacted when cultured alone or with B16F10-mCherry-OVA melanoma cells (**Fig. 2B**). B16F10-mCherry-OVA cells, when co-cultured with naïve

DRG neurons and OVA-specific cytotoxic $CD8^+$ T-cells, increased SLPI secretion into the culture medium, an effect maximal after 48h (~200-fold; **Fig. 2C**).

In addition to protecting epithelial cells from serine protease activity, SLPI also enhances regeneration of transected retinal ganglion cell axons [437] and neural stem cell proliferation[438]. Although these data support SLPI activity on neurons, its role in nociception remains untested. To address this, we measured whether SLPI directly activates cultured DRG neurons using calcium microscopy. We found that SLPI (10 - 10000 pg/ml) activates ~20% of DRG neurons (**Fig. 2D-F**), including ~42% (n=261/n=614) of all capsaicin-responsive neurons (**Fig. 2E**). SLPI-responsive neurons are mostly small-sized neurons (**Fig. 2G-H**; mean area = 151µm^2), and ~90% of these SLPI-sensitive neurons also respond to capsaicin (**Fig. 2I**), which is compatible with them being nociceptors. Given that SLPI triggered calcium influx, we probed whether this is the mean by which B16F10 cells drive CGRP release from neurons (**Fig. 1G**). SLPI, when used at a concentration similar to one secreted by melanoma cells (**Fig. 2C**, 100 - 5000 pg/ml), prompted CGRP release from cultured naïve DRG neurons (**Fig. 2J**). Finally, we sought to test whether SLPI can drive pain hypersensitivity *in vivo*. When administered into the right hindpaw of naïve mice, SLPI (i.d.; 1µg/20µL) generated thermal hypersensitivity whereas saline had no impact (**Fig. 2K**).

Melanoma-secreted SLPI acts on nociceptors to trigger calcium influx, neuropeptide release and thermal hypersensitivity, which indicates that these sensory neurons detect, and react to, the presence of cancer cells. Whether such action affords the malignant cells a functional advantage over the host remains unknown. To assess this, we implanted B16F10-mCherry-OVA cells (i.d., 5×10^5 cells) into the hindpaw of 8-week-old male and female mice (n=75) and those with larger tumors showed a higher proportion of intra-tumoral $PD1^+Lag3^+Tim3^+$ $CD8^+$ T-cells and greater thermal pain hypersensitivity (*not shown*). Interestingly, heightened thermal pain sensitivity positively correlated (R^2=0.52, p<0.0001) with increased frequency in intra-tumoral $PD1^+Lag3^+Tim3^+$ CD8 T-cell (**Fig. 3A;** measured on day 13 post implantation).

The expression of adrenergic and cholinergic axon markers in tumors correlates with poor clinical outcome[407]. Gastric tumor denervation limits growth and vagotomized patients have lower mortality rates from intestinal cancer [407,408,429,439]. To investigate the nature of the three-way interaction between cancer–nociceptor–$CD8^+$ T-cells, we next used a syngeneic mouse model of triple-negative melanoma, which is an established model of immunosurveillance[419]. B16F10-mCherry-OVA cells were inoculated (i.d., 5×10^5 cells) into 8-week-old male and female nociceptor-ablated ($TRPV1^{cre}$::$DTA^{fl/wt}$) or intact mice (littermate control; $TRPV1^{wt}$::$DTA^{fl/wt}$). In both nociceptor-ablated males (n=50) and females (n=68), the median length of survival (*evaluated until day 22 and determined by reaching a volume of 1000mm^3 or other ethical endpoints*) increased by 2.5-fold ($p\leq0.0001$; 0.4 Mantel-Haenszel hazard ratio; **Fig. 3B**). In another set of mice analyzed sixteen days post tumor inoculation, we found that genetic ablation of nociceptors reduced tumor growth (~2.6-fold; **Fig 3C**) and increased the total number of tumor-infiltrating $CD8^+$ T-cells (**Fig. 3D**). It also increased the relative frequency of cytotoxic ($IFN\gamma^+$, $TNF\alpha^+$, $IL\text{-}2^+$, **Fig. 3E; Supp. Fig. 4A**) tumor-infiltrating $CD8^+$ T-cells while reducing the one of $PD1^+Lag3^+Tim3^+$ $CD8^+$ T-cells (~1.4-fold; **Fig. 3F; Supp. Fig. 4A**).

To this point, our data support nociceptor neurons as an upstream driver of intra-tumoral $PD1^+Lag3^+Tim3^+$ $CD8^+$ T-cells. To address whether this would be the case, we mapped out the kinetics of thermal pain hypersensitivity, increased frequency in intra-tumoral $PD1^+Lag3^+Tim3^+$ $CD8^+$ T-cells and tumor growth (left hindpaw, i.d., 2×10^5 B16F10-mCherry-OVA cells). When compared to their baseline threshold and to the one of sensory neuron ablated mice ($TRPV1^{cre}$::$DTA^{fl/wt}$; n=18), 8-weeks-old littermate control mice ($TRPV1^{wt}$::$DTA^{fl/wt}$; n=96) inoculated with B16F10-mCherry-OVA showed significant thermal hypersensitivity on day 7, an effect that peaks on day 21 (**Supp. Fig. 4B**). In these mice, intra-tumoral frequency of $PD1^+Lag3^+Tim3^+$ (**Supp. Fig. 4C**) or $IFN\gamma^+$ (**Supp. Fig. 4D**) $CD8^+$ T-cells is significantly increased 12 days post tumor inoculation and peaked on day 19. Finally, B16F10-mCherry-OVA tumor volume peaked on day 22 (**Supp. Fig. 4E**). Altogether these data showed that thermal hypersensitivity precede that of significant intra-tumoral $CD8^+$ T-cells exhaustion by ~5 days and that pain hypersensitivity developed prior to the tumor being measurable using a digital caliper (**Supp. Fig.**

4F). Consequently, the genetic elimination of pain-transmitting neurons shields melanoma-bearing mice from increasing the frequency of intra-tumoral $PD1^{+}Lag3^{+}Tim3^{+}$ $CD8^{+}$ T-cells and, in turn, delayed tumor growth (**Fig. 3B-E; Supp. Fig. 4A-F**).

Blocking the activity of immune checkpoint proteins releases a cancer cell-induced "brake" on the immune system, thereby increasing its ability to eliminate tumors[416-419]. Immune checkpoint inhibitors (ICI), including those targeting PDL1, improve clinical outcomes in patients with metastatic melanoma[418,440-442], however ICI efficacy varies drastically among patients, half of whom will not benefit[440]. We set out to assess whether the presence ($TRPV1^{wt}$::$DTA^{fl/wt}$) or absence ($TRPV1^{cre}$::$DTA^{fl/wt}$) of tumor-innervating nociceptor neurons would impact αPDL1 (i.p; days 7, 10, 13, 16) clinical responsiveness. αPDL1 was given either to mice whose tumor cells (B16F10-mCherry-OVA, i.d., 5×10^{5}) were inoculated on the same day, or to mice with established tumors (~$100mm^{3}$; achieved by inoculating $TRPV1^{cre}$::$DTA^{fl/wt}$ ~3 days before). Nociceptor ablation increased αPDL1-mediated tumor reduction (**Fig 3G**; **Supp. Fig 4G-H**) and also increased the infiltration of tumor-specific $CD8^{+}$ T-cell (**Supp. Fig 4I**).

To test whether the reduced tumor growth observed in the absence of nociceptor neurons depends on their action on immune cells, we compared the respective impacts of nociceptors on the growth of an immunogenic and a non-immunogenic isogenic melanoma model. YUMMER1.7 is a highly immunogenic derivative of the $Braf^{V600E}Cdkn2a^{-/-}Pten^{-/-}$ cell line modified by UV exposure, it represents a clinically relevant melanoma model[443]. As in the case of B16F10-OVA, ablation of nociceptors decreased tumor growth (~3.3 fold; measured twelve days post inoculation; **Fig. 3H**) and reduced the frequency in intra-tumoral $PD1^{+}Lag3^{+}Tim3^{+}$ CD8 T-cell while increasing their number and cytotoxic potential ($IFN\gamma^{+}$, $TNF\alpha^{+}$). In contrast, YUMM1.7 (the parental and non-immunogenic[444] counterpart of YUMMER1.7) showed similar tumor growth (**Supp. Fig. 4J**) and frequency of intra-tumoral $PD1^{+}Lag3^{+}Tim3^{+}$ CD8 T-cell in both the presence and absence of nociceptors (*not shown*).

Next, we assessed whether these differences were due to a nociceptor neurons' direct modulation of intra-tumoral T-cells and observed no major changes in tumor growth between nociceptor-intact and nociceptor-ablated mice upon systemic depletion of $CD8^+$ (**Fig. 3I**) or $CD3^+$ T-cells (**Supp. Fig. 4K**). While nociceptor neuron chemoablation with Resiniferatoxin (RTX) reduced tumor growth in B16F10-inoculated wild-type mice (**Fig. 3J**), we found that naïve OT-1 CD8 T-cells enhanced tumor shrinkage (**Fig. 3K**) while limiting the increased in the frequency of intra-tumoral $PD1^+Lag3^+Tim3^+$ CD8 T-cell (**Fig. 3L**) when transplanted in RTX-exposed $RAG1^{-/-}$ mice. To achieve this, we chemically depleted $TRPV1^+$ nociceptor neurons (RTX; s.c., 30, 70, 100 µg/kg) from $RAG1^{-/-}$ mice (devoid of B- and T-cells), inoculated B16F10-mCherry-OVA (i.d., 5×10^5 cells) six weeks post RTX and adoptively transferred these mice with naïve OVA-specific CD8 T cells (OT-1 mice; i.v., $1x10^6$ cells) when the tumor reached ~$500mm^3$ (**Fig. 3K-L).** These data imply that the slower tumor growth found in $TRPV1^{cre}$::$DTA^{fl/wt}$ and RTX-exposed mice depends on nociceptor-induced CD8 exhaustion.

Optogenetic activation of skin nociceptor neurons trigger the antidromic release of neuropeptides which mediate anticipatory immunity against microbes[445] and potentiate skin[446] and lung[447] immunity. Here, we used transdermal illumination (3.5 ms, 10Hz, 478nm, 60 mW, delivering ~2-6 mW/mm^2 to a 0.39 NA fiber placed 5-10 mm from the skin, for 20 min) to stimulate tumor-innervating $Na_V1.8^+$ Channelrhodopsin-expressing neurons ($Na_V1.8^{Cre}$::$ChR2^{fl/wt}$) in mice. In the case that exposure began when the tumor was either visible (~$20mm^3$) or well established (~$200mm^3$), we found that daily blue-light stimulation enhanced B16F10 tumor growth (**Supp. Fig. 4L**). This increased in tumor growth was also linked to enhance intra-tumoral CGRP levels, confirming the engagement of pain-transmitting neurons (**Supp. Fig. 4M**). Laser exposure had no effect on tumor growth in light-insensitive mice ($Na_V1.8^{wt}$::$ChR2^{fl/wt}$).

The neonatal/embryonic ablation of neuronal subsets may lead to compensatory changes. To circumvent this potential shortcoming, we silenced neurons using Botulinum neurotoxin A (BoNT/A), a neurotoxic protein produced by *Clostridium botulinum*, which acts by cleaving SNAP25[448]. BoNT/A causes a long-lasting (20 days) abolition of neurotransmitter release from

skin-innervating neurons[8]. BoNT/A reduces tumor growth in prostate cancer[407] and blocks nociceptor-mediated modulation of neutrophils during skin infection[8]. BoNT/A does not impact cultured B16F10 or $CD8^+$ T-cell function *in vitro* (**Supp. Fig. 5A-F**). When BoNT/A (25 pg/µL; 50µl; 5 i.d. sites) is administered one and three days prior to the B16F10-OVA cell inoculation, it reduced subsequent tumor growth and preserved intra-tumoral $CD8^+$ T-cells cytotoxic potential (**Supp. Fig. 5G-N;** as measured 18 days post inoculation). BoNT/A pre-treatment also reduced YUMMER1.7 tumor outgrowth (**Supp. Fig. 5O**), and enhanced αPDL1-mediated tumor regression (**Supp. Fig. 5P**). BoNT/A had limited efficacy when administered to mice with established tumors (~200mm^3; **Supp. Fig. 5G-N**) or to mice whose nociceptor neurons were genetically ablated ($TRPV1^{cre}$::$DTA^{fl/wt}$; **Supp. Fig. 5O**). These data hints that BoNT/A-mediated decrease tumor growth depends on the presence of active tumor-innervating nociceptor neurons

We next tested the anti-tumor efficacy of a proven nociceptor-selective silencing strategy[449]. This protocol uses large-pore ion channels (TRPV1) as cell-specific drug-entry ports to deliver QX-314, a charged and membrane-impermeable form of lidocaine, to block voltage-gated sodium (Na_V) channels. During inflammation, similar to what we observed in tumor microenvironments, these large pore ion channels open, allowing QX-314 to permeate the neurons, which results in a long-lasting electrical blockade[430]. While QX-314 did not impact cultured B16F10-mCherry-OVA cells or CD8 T-cell function *in vitro* (**Supp. Fig. 6A-F**), we confirm that it silences tumor-innervating nociceptors *in vivo*, as shown by reduced B16F10-induced CGRP release and pain hypersensitivity (**Supp. Fig. 6G-I**). We found that vehicle-exposed B16F10-mCherry-OVA -bearing mice succumb at a 2.7-fold higher rate ($p \leq 0.0001$) than QX-314-exposed mice (0.37 hazard ratio; **Supp. Fig. 6J**; *measured until day 19 and determined by reaching a volume of ~800mm^3 or other ethical endpoints*). QX-314-mediated sensory neurons silencing (0.3%; daily i.d. surrounding the tumor) reduced melanoma growth (~3-fold; **Supp. Fig. 6K-M;** *as observed seventeen days post tumor inoculation*) and limited intra-tumoral $CD8^+$ T-cell exhaustion (**Supp. Fig. 6R**). Nociceptor silencing also increased intra-tumor numbers of $CD8^+$ T-cells and preserved their cytotoxic potential ($IFN\gamma^+$, $TNF\alpha^+$) as well as proliferative capacity ($IL\text{-}2^+$; **Supp. Fig. 6N-Q**). Similar to what we observed in nociceptor-ablated mice ($TRPV1^{cre}$::$DTA^{fl/wt}$; **Fig. 3G**), silencing

tumor-innervating neurons with QX-314 enhanced αPDL1-mediated tumor regression (**Supp. Fig. 6S-T;** up to 5-fold). When administered to mice with an established B16F10-mCherry-OVA tumor (~200mm^3**; Supp. Fig. 6K-R**), QX-314 still reduced tumor growth and preserved CD8 T-cells anti-tumor capacity, thus supporting its potential use as a cancer therapeutic.

Tumor-specific sympathetic denervation downregulates expression of PDL1, PD1, and FOXP3 in tumor-infiltrating lymphocytes (TIL), whereas parasympathetic innervation has the opposite effects[385]. Thus, tumor-infiltrating lymphocytes exhaustion correlates with relative distance from sympathetic terminals[385]. Human (**Supp. Fig. 1B**) and mouse (**Supp. Fig. 3B**) cytotoxic CD8$^+$ T-cells express multiple neuropeptide receptors (≥10), including the CGRP receptor RAMP1. Given that nociceptors readily interact with CD8$^+$ T-cells in culture and that the neuropeptides they release block T_H1 immunity [7,8,450,451], we aimed to test whether these mediators drive CD8$^+$ T-cell expression of immune checkpoint receptors.

To do so, splenocyte-isolated CD8$^+$ T-cells were cultured under type 1 (T_{c1}) CD8$^+$ T-cell-stimulating conditions (*ex vivo* activated by CD3/CD28, IL-12, and anti-IL4) for two days and then were co-cultured with DRG neurons for an additional four days. We found that nociceptor stimulation with capsaicin increased the proportion of PD1$^+$Lag3$^+$Tim3$^+$ expressing CD8$^+$ T cells while it decreased the levels of IFNγ$^+$, TNFα$^+$, and IL2$^+$. Capsaicin had no measurable impact on CD8$^+$ T-cells in the absence of DRG neurons (**Supp. Fig. 7A-B**; measured after four days co-culture).

When Tc1-activated CD8$^+$ T-cells were exposed to fresh conditioned media (1:2 dilution) harvested from KCl (50 mM)-stimulated DRG neurons, it increased the proportion of PD1$^+$Lag3$^+$Tim3$^+$ cytotoxic CD8$^+$ T-cells and reduced those that are IFNγ$^+$ and TNFα$^+$ (**Supp. Fig. 7C-D**; measured after four days co-culture). These effects were prevented when the cytotoxic CD8$^+$ T-cells when challenged (1:2 dilution) with fresh KCl-induced conditioned media from BoNT/A-silenced neurons (100pg/200µL) or when co-exposed to the RAMP1 blocker $CGRP_{8-37}$ (2µg/mL **Supp. Fig. 7C-D**).

To confirm that nociceptor-released neuropeptides drive T-cells exhaustion we exposed Tc1-activated $CD8^+$ T-cells to CGRP. CGRP-treated $RAMP1^{wt}$ cells show increased exhaustion and limited cytotoxic potential. These effects were absent in CGRP-exposed CD8 T-cells harvested from CGRP receptor KO ($RAMP1^{-/-}$) mice (**Fig. 4A, Supp. Fig. 7E-F**).

We then probed whether nociceptor neuron-released neuropeptides blunt the anti-tumor responses of cytotoxic $CD8^+$ T-cells through exhaustion. OT1 cytotoxic T-cells induced robust apoptosis of cultured B16F10-mCherry-OVA cells ($annexinV^+7AAD^+$B16F10-mCherry-OVA; **Supp. Fig. 7G-I**). However, this B16F10-mCherry-OVA apoptosis was decreased when the T-cells were (i) co-cultured with DRG neurons-exposed to capsaicin; (ii) exposed to KCl-stimulated neuron-derived conditioned media or (iii) directly stimulated with CGRP (**Fig. 4B, Supp. Fig. 7G-I**). OT1 cytotoxic T-cells failed to eliminate cultured B16F10-mCherry-OVA when co-exposed to a RAMP1 blocker ($CGRP_{8-37}$; 2μg/mL) and neuron's conditioned media (KCl-induced; **Fig. 7H**). Along with earlier findings that CGRP blocks $CD8^+$ T-cell proliferation [452], our data suggest that via the CGRP-RAMP1 axis, nociceptors lead to the functional exhaustion of $CD8^+$ T-cells, as defined by simultaneous expression loss of cytotoxic molecules (i.e., IFNγ, TNFα) and proliferative capacity (i.e., IL-2), increased co-expression of several exhaustion markers ($PD1^+Lag3^+Tim3^+$) and a reduced capacity to eliminate malignant cells.

Nociceptor-produced neuropeptides reduce immunity against bacteria [451] and fungi [453], and promote cytotoxic $CD8^+$ T-cell exhaustion[422-425,427,431] (**Fig. 4A-B; Supp. Fig. 7**). Given that nociceptor-released CGRP is exacerbated when cultured with B16F10 cells (**Fig. 1G**) or exposed to SLPI (**Fig. 2J**), and that tumor-infiltrating nociceptor neurons overexpress Calca (**Fig. 1H-J**), we next sought to test whether intra-tumoral CGRP levels correlate with CD8 T-cell exhaustion. To do this we used $Na_V1.8^{cre}$ driver to ablate most mechano- and thermo-sensitive nociceptors with diphtheria toxin ($Na_V1.8^{cre}$::$DTA^{fl/wt}$) [430,451]. We found that when compared with littermate controls ($Na_V1.8^{wt}$::$DTA^{fl/wt}$), the ablation of $Na_V1.8^+$ sensory neurons preserve $CD8^+$ T-cells anti-tumor potential (**Supp. Fig. 8A-D;** as measured eleven days post inoculation). Moreover, intra-

tumoral CGRP levels in both groups of mice directly correlates with the proportion of intra-tumoral $PD1^{+}Lag3^{+}Tim3^{+}$ $CD8^{+}$ T-cells (**Fig. 4C**).

We then set out to rescue CGRP levels (rCGRP, daily intra-tumoral injection) in sensory neuron-ablated mice and measured the impact on tumor growth and TIL exhaustion. CGRP-treated sensory neuron-ablated mice ($TRPV1^{cre}$::$DTA^{fl/wt}$) showed similar tumor growth and $CD8^{+}$ T-cell exhaustion to that found in nociceptor intact mice (**Fig. 4D-E**; measured until day 11). Next, we treated tumor-bearing mice with the selective RAMP1 antagonist BIBN4096 (5 mg/kg, i.p.; once every two days). The latter was previously found to block neuro-immune interplay during microbe infections and rescues host anti-bacterial activity[7]. BIBN4096-exposed mice (0.37 hazard ratio; **Supp. Fig. 8E**; *measured until day 19 and determined by reaching a volume of ~800mm^3 or other ethical endpoints*) succumb at a rate 2.6-fold lower ($p \leq 0.04$) than vehicle-exposed B16F10-bearing mice. As measured on day 13, BIBN4096 (5 mg/kg, i.p.; *q.a.d.*) reduced B16F10 growth (~4.3-fold), tumor weight, and $CD8^{+}$ T-cell exhaustion (~1.3-fold**; Fig. 4F-G; Supp. Fig. 8F-K**). It is worth noting that BIBN4096 does not impact cultured B16F10 cells or $CD8^{+}$ T-cell function *in vitro*. Importantly, BIBN4096 anti-tumor property relies on the presence of intact nociceptor neurons as it showed no effect when administered to $TRPV1^{cre}$::$DTA^{fl/wt}$ ablated mice (**Supp. Fig. 8L-R**).

Finally, to address whether RAMP1 is the main driver of $CD8^{+}$ T-cell exhaustion we transplanted $RAG1^{-/-}$ mice with either $RAMP1^{-/-}$ or $RAMP1^{wt}$ $CD8^{+}$ T-cells (i.v.; $2.5x10^6$) or a 1:1 mixture of $RAMP1^{-/-}$ ($CD45.2^{+}$) and $RAMP1^{wt}$ ($CD45.1^{+}$). Although we retrieved similar numbers of CD8 T-cells across all three groups (**Supp. Fig. 8S**), limited B16F10-OVA tumor growth (**Fig. 4H**) was found in mice that received the $RAMP1^{-/-}$ $CD8^{+}$ T-cells – which are not responsive to CGRP. The relative proportion of intra-tumor $PD1^{+}Lag3^{+}Tim3^{+}$ $CD8^{+}$ T-cells was also lower in $RAMP1^{-/-}$-transplanted $RAG1^{-/-}$ mice (**Fig 4I**).

In $RAG1^{-/-}$ mice co-transplanted with RAMP1 expressing and non-expressing $CD8^{+}$ T-cells, we found that within the same tumor, the relative proportion of intra-tumor $PD1^{+}Lag3^{+}Tim3^{+}$

$CD8^+$ T-cells was lower in $RAMP1^{-/-}$ $CD8^+$ T-cells than in the $RAMP1^{wt}$ $CD8^+$ T-cells (**Fig 4J; Supp. Fig. 8T**). Next, we RNA-sequenced FACS-purified $RAMP1^{wt}$ and $RAMP1^{-/-}$ $CD8^+$ T-cells from these mice and confirmed that intra-tumoral $RAMP1^{-/-}$ $CD8^+$ T-cells express fewer exhaustion markers (*Pd1, Lag3, Tim3*) compared to their $RAMP1^{wt}$ counterparts (**Fig 4K**). The sequencing data also show that the pro-exhaustion transcription factors *Tox* and *Eomes* are elevated in intra-tumoral $RAMP1^{wt}$ CD8 T cells while the anti-exhaustion factor *Tbet* was reduced in the $RAMP1^{wt}$ $CD8^+$ T cells (**Fig 4K**). Overall, CGRP unresponsive $RAMP1^{-/-}$ $CD8^+$ T-cells are protected against undergoing nociceptor-induced exhaustion, thereby safeguarding their anti-tumor responses.

When compared with benign nevi, patient's melanomas display an overexpression of RAMP1 (**Supp. Fig. 1D**), which strongly correlates ($p \leq 0.05$; 459 patients) [454] with reduced patient' survival (1.8-fold hazard ratio**; Fig. 4L; Supp. Fig. 9A-L**). Whether RAMP1 does this by controlling intra-tumoral $CD8^+$ T-cell exhaustion is unknown. To answer this, we analyzed two independent unbiased single-cell RNA-sequencings of human melanomas[455,456], wherein we found that ~1% of tumor-infiltrating $CD8^+$ T-cells expressed RAMP1. The patients' melanoma-infiltrating $RAMP1^+$ $CD8^+$ T-cells overexpressed the immune checkpoint receptors *Pd1, Tim3, Lag3, Ctla4, Cd27;* this was coupled with a loss of the pro-proliferative cytokine *Il-2* (**Fig. 4M**; **Supp. Fig. 9M**). This analysis also revealed that tumor-infiltrating $CD8^+$ cells, when harvested from ICI resistant patients, substantially overexpress RAMP1 (~2.0-fold; **Supp. Fig. 9N-P**). This expression profile resembles the functional exhaustion of effector $CD8^+$ T-cells and confirms that the CGRP receptor RAMP1 controls patients' $CD8^+$ T-cell exhaustion and clinical response to ICI.

Altogether, genetic ablation of nociceptor neurons decreases B16F10 tumor growth by safeguarding $CD8^+$ T-cell from undergoing exhaustion, whereas exogenous administration of CGRP has the opposite effect. These actions are restricted to immunogenic tumors (B16F10-OVA, YUMMER1.7) and are not present in the absence of CD8 T-cells. Translationally, using the charged sodium channel blocker QX-314 to block tumor-innervating nociceptor release of CGRP, or blocking its receptor (RAMP1) with BIBN4096, decreases tumor growth and prevents $CD8^+$ T-cell exhaustion. Similar to the pre-clinical mouse modelling, our human data implies that nociceptor-

produced CGRP drives intra-tumoral $CD8^+$ T-cells exhaustion which, in turn, fuels cancer growth, blunts the response to ICI and worsens clinical prognosis. Tumor-innervating nociceptors therefore, act to dampen the immune response to melanoma via an upregulation of multiple immune checkpoint receptors on cytotoxic $CD8^+$ T-cells. Silencing these tumor-innervating sensory neurons can attenuate this immunomodulatory action of the nervous system on $CD8^+$ T-cells; thereby safeguarding the host anti-tumor immunity (**Supp. Fig. 10**), and providing new therapeutic opportunities by interrupting pro-cancerous neuroimmune links.

2.3- Author contributions

Mohammad Balood: Designed and performed the experiments, analyzed data, interpreted results, and wrote manuscript. Figures that were produce by mohammad include; Figure 14 (Graph A,H,I,J), Figure 15 (Graph A, B), Figure 16 (Graph A,B,C, D,E,G,F,I,J, K,L),Figure 17 (Graph A,B,C,D,E,H,I,J,K,L) Figure 21 (Graph A,B,C,D,E,F,G,H,I,J,K,L), Figure 24 (Graph A,B,C,D,E,F,G,H,I), Figure 25 (S,T).

Maryam Ahmadi. Performed the experiments and analyzed data. Figures that were produce by Maryam include, Figure 14(Graph B,C,D,E,F,G), Figure 16(Graph H), Figure 25 (Graph A, B,C,D,E,F,G,H,I,J,K,L,M,N,O,P,Q,R,S), Figure 17 (Graph F,G), Figure 22 (A,B,C,D,E,F,G,H,I, J,K,L,M), Figure 23 (Graph A,B,C,D,E,F,G,H,I,J,K,L,M,N,O,P,Q,R,S,T).

Tuany Eichwald. Performed the experiments and analyzed data. Graph that were generated by Tuany inculde, Figure 15 (Graph C, D, E, F, G, H, I, J, K), Figure 26 (Graph A, B, C, D, W, F, G, H, I, J, K, L, M, N, O, P), Figure 18 (Graph A, B, C, D), Figure 20 (A, B, C).

Paola Vermeer and Ronny Drapkin: Figure 19 (Graph A, B, C, D, E, F, G, H).

Abdelilah Majdoubi, Ali Ahmadi, Karine Roversi and Katiane Roversi assisted for doing experiments.

2.4- Results

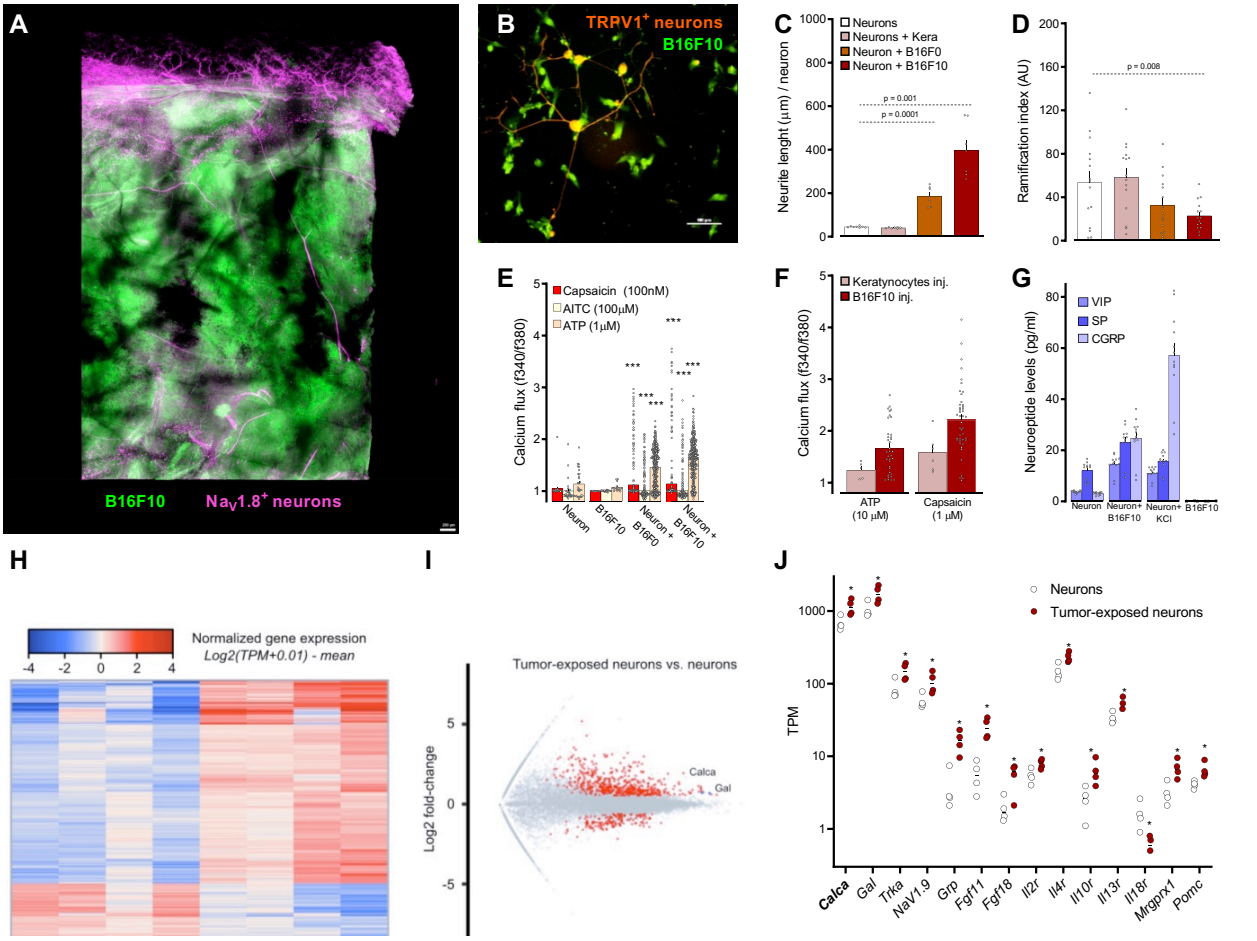

Figure 14.Melanoma sensitizes nociceptor neurons. **(A).** Nociceptor ($Na_V1.8^{cre}$::Td-$tomato^{fl/wt}$; magenta) reporter mice hindpaw were inoculated with B16F10-eGFP cancer cells (i.d.; 10^5 cells; green). Representative iDISCO image of $Na_V1.8^+$ nerve fibers (magenta) innervating B16F10-eGFP-inoculated mouse skin after 22 days (**A**).**(B-D)** When co-cultured with B16F10-eGFP cells, $TRPV1^+$ nociceptor (red; $TRPV1^{Cre}$::td-$tomato^{fl/wt}$; orange) neurons form neuro-neoplasic contacts (**B**), show longer neurites (**C**), and exhibit reduced arborization (**D**) than when cultured alone or with non-tumorigenic keratinocytes (**C-D**).**(E)** In co-culture, B16F0 or B16F10 cells sensitize the response of nociceptors to capsaicin (100nM), AITC (100µM), and ATP (1µM) as measured by calcium flux (**E**). Low concentration of the ligands induced minimal response in control neurons, whereas B16F10 cells show marginal sensitivity to ATP (**E**). **(F)** L3-L5 DRG neurons were harvested from mice 2-weeks after they were inoculated (left hindpaw; i.d.) with B16F10- or non-tumorigenic keratinocytes, cultured and calcium flux to ligands tested. Compared to keratinocytes, neurons from tumor-bearing mice were more sensitive to ATP (10 µM), and capsaicin (1 µM; **F**).**(G)** DRG neurons co-cultured with B16F10 cells release the neuropeptide CGRP (**G**). B16F10 cells alone do not release neuropeptides (**G**). **(H-J)** Naive DRG neurons

(TRPV1^{cre}::QuASR2-eGFP$^{fl/wt}$) were cultured alone or in combination with B16F10-mCherry-OVA. After 48h, the cells were harvested, FACS-purified, and RNA sequenced. Hierarchical clustering of sorted neuron DEG show distinct groups of transcripts enriched in TRPV1^{+} neuron vs cancer-exposed TRPV1^{+} neuron populations (**H**). Pairwise comparison of naive TRPV1^{+} neuron vs cancer-exposed TRPV1^{+} neuron populations showing differentially expressed transcripts as a volcano plot ($p<0.05$; **I**). Among others, *Calca* (gene encoding for CGRP) was overexpressed in TRPV1^{+} (FACS-purified eGFP-expressing cells) neurons when co-cultured with B16F10-mCherry-OVA (**H-J**).*Data are shown as representative images (**A-B**), mean ± S.E.M (**C-G**), heatmap of row Z-score (**H**), volcano plot (**I**) or scatter dot plot and median (**J**). N are as follows: **A-B**: n=4/groups, **C-D**: n=7-15/groups, **E**: n=10-12/group (total of 16-409 neurons), **F**: n=4/group (total of 5-44 neurons/groups), **G**: n=12/groups, **H-I**: n=4/groups. Experiments were independently repeated two (**A, F**) or three (**B-E, G**) times with similar results. Sequencing experiment was not repeated (**H-I**). P-values are shown in the figure and determined by one-way ANOVA post hoc Bonferroni (**C-E, G**) or unpaired Student's t-test (**F, J**). Na$_V$1.8^{+} nociceptors are labeled in magenta (**A**), TRPV1^{+} nociceptors are labeled in orange (**B**) and B16F10-eGFP cells are labeled in green (**A-B**). Scale bar = 200 µm (**A**) or 100 µm (**B**).*

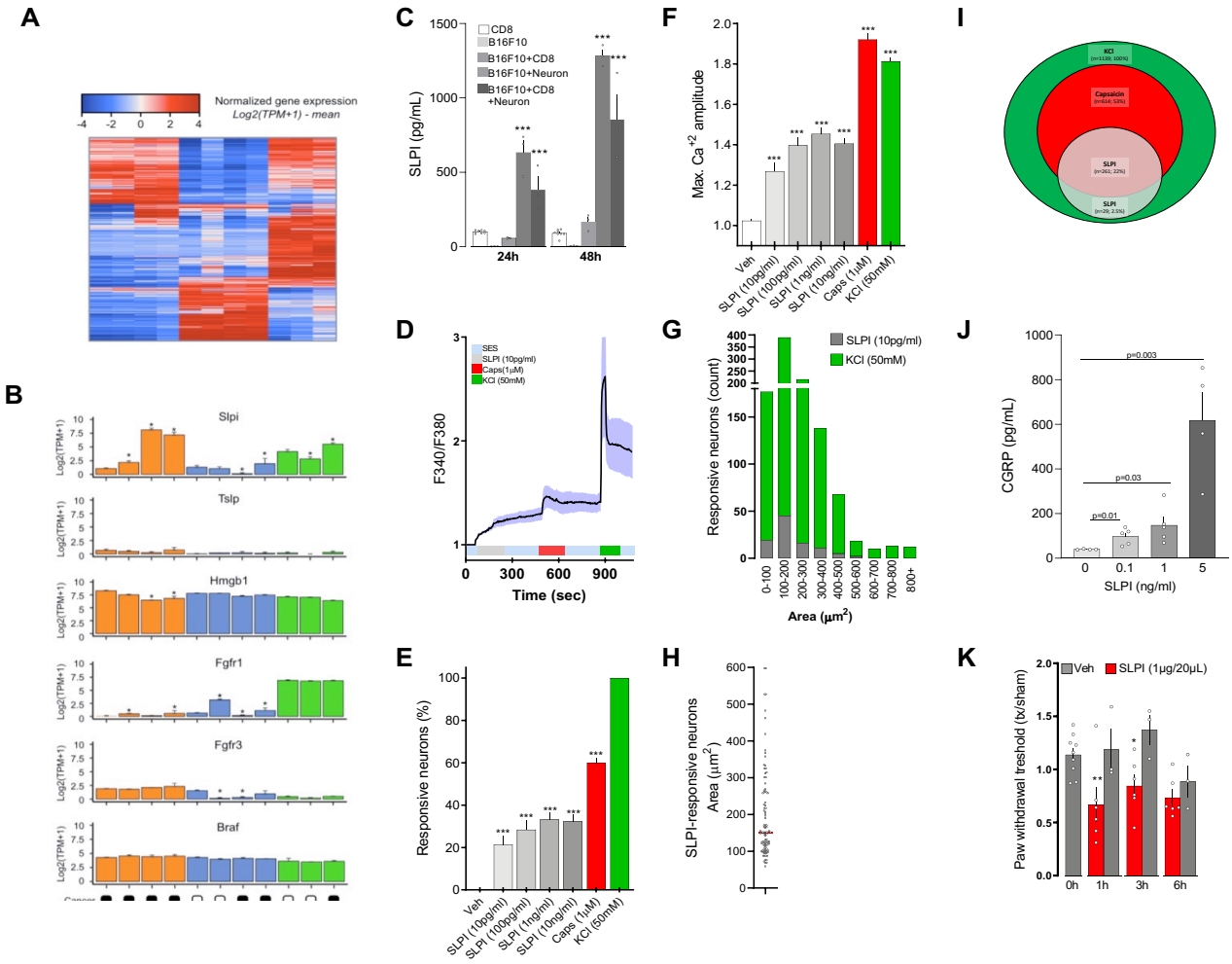

Figure 15.Cancer-secreted SLPI drives CGRP to release by nociceptor neurons. (A-B) Naive DRG neurons (TRPV1^{cre}::QuASR2-eGFP$^{fl/wt}$), B16F10-mCherry-OVA, and OVA-specific cytotoxic CD8^{+} T-cells were cultured alone or in combination. After 48h, the cells were harvested, FACS-purified, and RNA-sequenced. Hierarchical cluster analysis was performed using normalized gene expressions from protein-coding genes (**A**). Hierarchical clustering of sorted neuron molecular profiles depicts distinct groups of transcripts enriched in each group (**A**). Differentially expressed genes (DEG) were calculated, and SLPI (*Secretory Leukocyte Protease Inhibitor*) was found to be overexpressed in cancer cells when co-cultured with OVA-specific cytotoxic CD8^{+} T-cells, DRG neurons or both populations (**B**). **(C)** In the presence of protease inhibitors, B16F10-mCherry-OVA were cultured alone, with naive DRG neurons and/or with OVA-specific cytotoxic CD8^{+} T-cells. The culture supernatant was harvested after 24 or 48h, and SLPI secretion was measured by ELISA. We found increased SLPI secretion by B16F10-mCherry-OVA when co-cultured with naive DRG neurons and OVA-specific cytotoxic CD8^{+} T-cell, with a maximal effect after 48h (**C**). **D-I)** Using calcium microscopy, we then probed whether SLPI directly activates cultured DRG neurons. We found that SLPI (10pg/mL-10ng/mL) activated ~20% of DRG neurons (**D-F**). SLPI-responsive neurons are mostly small-sized neurons (**G-H;** mean area = 151µm^2) and largely capsaicin-responsive (**I;** ~42%). **(J)** Naive DRG neurons were cultured and stimulated with SLPI (0-5 ng/mL) for 3h. SLPI triggered CGRP release from cultured naive DRG neurons (**J**). **(K)** The right hindpaw of

naive mice was injected with saline or SLPI (i.d., 1µg/20µL), and the mice's noxious thermal nociceptive threshold was measured (0-6h). The ipsilateral paw injected with SLPI showed thermal hypersensitivity in contrast with the contralateral paw. Saline had no impact on the mice's thermal sensitivity (**K**). *Data are shown as heatmap (**A**) displaying normalized gene expression (Log$_2$(1+transcript per millions)-mean, mean ± S.D.(**B**), as mean ± S.E.M (**C-H; J-K**) or as a Venn Diagram (**I**). N are as follows: **A-B**: n=4/groups, **C**: n=3-8/groups, **D**: n=17/groups, **E**: n=8/groups, **F**: n=28-1139/groups, **G-I**: n=9-1139/groups, **J**: n=4-5/groups, **K**: n=3-9/groups. Experiments were independently repeated two (**J-K**) or three (**C-I**) times with similar results. Sequencing experiment was not repeated. (**A-B**). P-values are shown in the figure and determined by one-way ANOVA post hoc Bonferroni (**B, C, E, F**); or unpaired* Student's t-test (**J, K**).

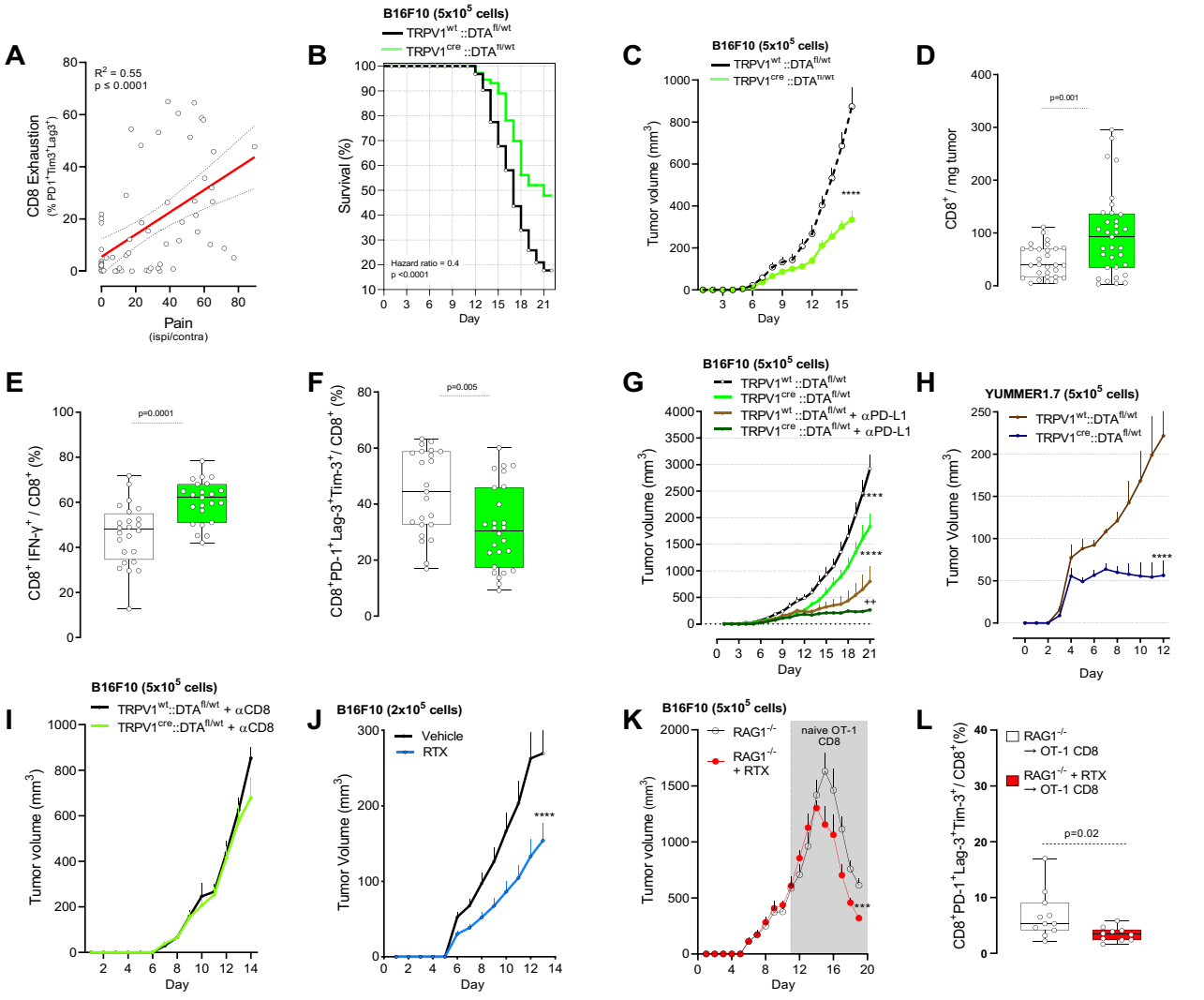

Figure 16.Genetic ablation of nociceptors safeguards anti-tumor immunity. **(A)** Orthotopic B16F10-mCherry-OVA (5x10^5 cells; i.d.) cells were injected into the left hindpaw of wild-type mice.

Thermal hypersensitivity was measured daily and intra-tumoral CD8 T-cells exhaustion was assessed on day 13. Thermal hypersensitivity positively correlated (R^2=0.52, p<0.0001) with CD8 T-cells exhaustion (**A**; as measured on day 13).**(B)** Orthotopic B16F10-mCherry-OVA ($5x10^5$ cells; i.d.) were inoculated into 8-week-old male and female sensory neurons intact or ablated mice. The median length of survival was increased by ~250% (**B;** *Mantel-Haenszel Hazard Ratio; measured on day 22*) in nociceptor ablated mice ($TRPV1^{Cre}$::$DTA^{fl/wt}$; **B**).**(C-F)** Sixteen days post tumor inoculation, sensory neuron ablated mice have reduced tumor growth (**C**), increased tumor infiltration of total (**D**) and $IFN\gamma^+$ $CD8^+$ T-cells (**E**); while the proportion of $PD1^+Lag3^+Tim3^+$ $CD8^+$ T-cells decreased (**F**).**(G)** Orthotopic B16F10-mCherry-OVA cells ($5x10^5$ cells; i.d.) were inoculated into 8-week-old male and female sensory neuron intact or ablated mice. The mice were treated with αPDL1 (6 mg/kg, i.p.; days 7, 10, 13, 16 post-tumor inoculation) or the isotype control (**G**). On day 21, αPDL1 potentiated the nociceptor ablation mediated reduction in B16F10-OVA tumor volume (**G**).**(H)** Sensory neurons ablation ($TRPV1^{Cre}$::$DTA^{fl/wt}$) decreased growth of YUMMER1.7 cells ($5x10^5$ cells; i.d.) an immunogenic version of a $Braf^{V600E}Cdkn2a^{-/-}Pten^{-/-}$ melanoma cell line (**H**; assessed until day 12).**(I)** The reduction in B16F10-mCherry-OVA ($5x10^5$ cells; i.d.) tumor growth observed in nociceptor ablated mice was absent following systemic CD8 depletion (**I,** assessed until day 14; αCD8, 200 μg/mice; i.p.; every 3 days).**(J-L)** To deplete their nociceptor neurons, wild-type (C57BL6; **J**) or $RAG1^{-/-}$ (**K-L**) mice were injected with Resiniferatoxin (RTX; s.c., 30, 70, 100 μg/kg) and were subsequently (28 days later) inoculated with B16F10-mCherry-OVA (**J**, $2x10^5$ cells;**K-L**, $5x10^5$ cells; i.d.). Wild-type RTX-injected mice showed reduced tumor growth when compared to vehicle-exposed mice (**J;** assessed until day 13). In $RAG1^{-/-}$, RTX-injected mice adoptively transferred with naive OVA-specific $CD8^+$ T-cells (i.v.,$1x10^6$ cells, when tumor reached ~$500mm^3$) showed reduced tumor growth (**K;** assessed until day 19) and exhaustion (**L**) compared to vehicle-exposed $RAG1^{-/-}$ mice. *Data are shown as linear regression analysis (**A**), Mantel-Cox regression analysis (**B**), mean ± S.E.M (**C, G-K**) or as box-and-whisker plots (running from minimal to maximal values) for which individual data points are given (**D-F; L**). N are as follows: **A**: n=61, **B**: n=67-75/groups, **C**: n=20-27/groups, **D-F**: n=29-33/groups, **G**: n=8-10/groups, **H**: n=8-11/groups, **I**: n=8-11/groups, **J**: n=10-11/groups, **K-L**: n=10-12/groups. Experiments were independently repeated two (**A, G-L**) or six (**B-F**) times with similar results. P-values are shown in the figure and determined by Simple Linear regression analysis (**A**), Mantel-Cox regression (**B**), two-way ANOVA posthoc Bonferroni (**C, G-K**); or unpaired Student's t-test (**D-F, L**).*

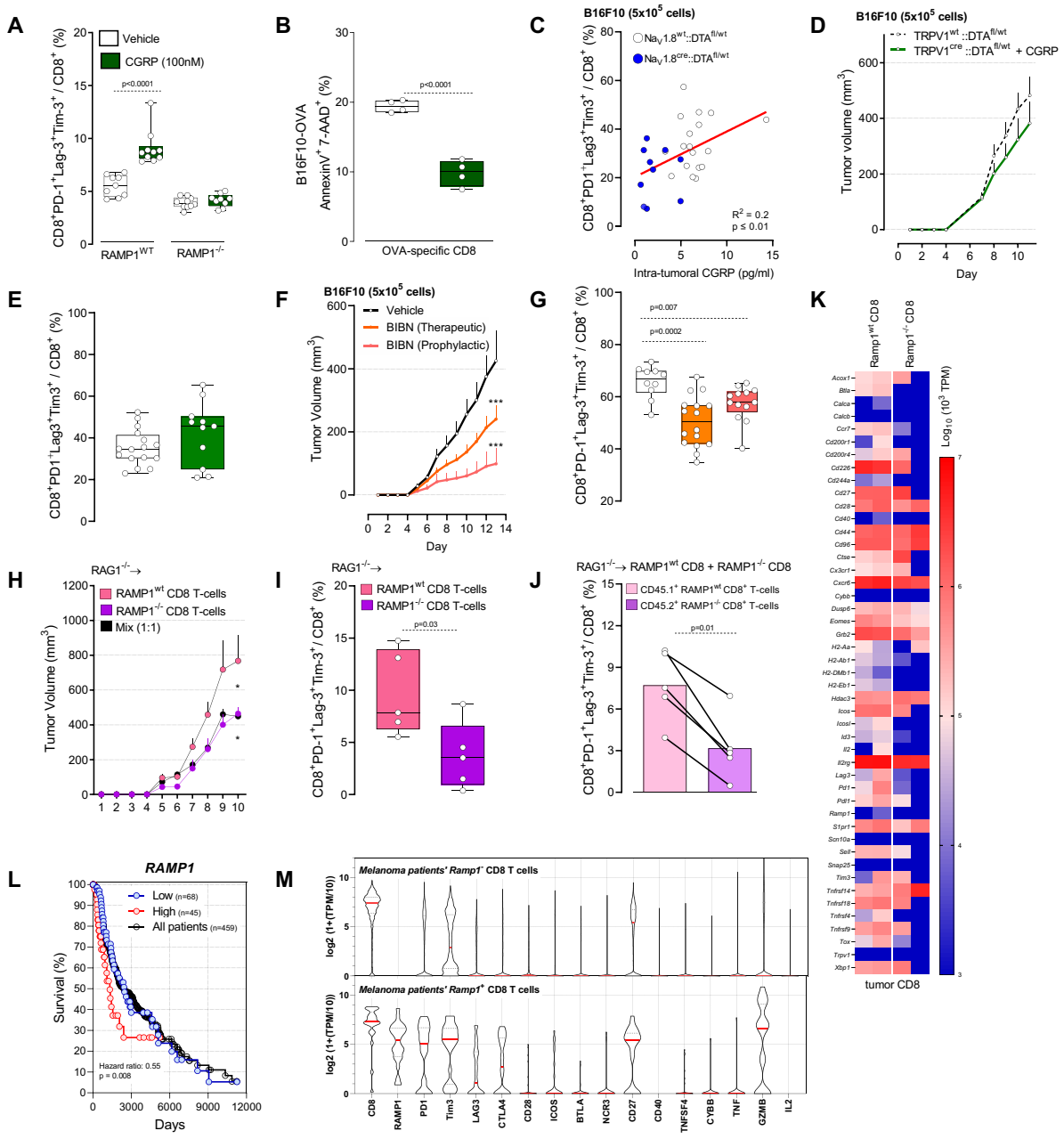

Figure 17.Nociceptor neuron-released CGRP controls CD8+ T-cells exhaustion. (A-B) Splenocytes-isolated CD8$^+$ T-cells from wild-type (**A**), naive OT-1 (**B**) and RAMP1$^{-/-}$ (**A-B**) mice were cultured under Tc1-stimulating conditions (*ex vivo* activated by CD3/CD28, IL-12 and anti-IL4) for 48h to generate cytotoxic CD8$^+$ T-cells (**A-B**). In the presence of IL-2 (10ng/ml) the cells were stimulated with CGRP (0.1 µM; challenged once every two days) for 96h. Wild-type cytotoxic CD8$^+$ T-cells showed an increased proportion of PD1$^+$Lag3$^+$Tim3$^+$ cells; this effect was absent when treating cytotoxic CD8$^+$ T-cells harvested from RAMP1$^{-/-}$ mice (**A**). Upon generating the cytotoxic CD8+ T-cells *in vitro*, B16F10-mCherry-OVA cancer cells were then co-cultured with or without

OT-1 cytotoxic $CD8^+$ T-cells ($4x10^5$ cells; **B**). B16F10-mCherry-OVA cell elimination by cytotoxic $CD8^+$ T-cells was reduced when the co-cultures were challenged with CGRP (0.1µM; once daily for two consecutive days; **B**).(**C**) Orthotopic B16F10-mCherry-OVA were injected into nociceptor intact ($NaV1.8^{wt}$::$DTA^{fl/wt}$) and ablated mice $NaV1.8^{Cre}$::$DTA^{fl/wt}$). On day 15, B16F10-mCherry-OVA ($5x10^5$ cells; i.d.)-tumor surrounding skin was harvested and capsaicin-induced CGRP release assessed by ELISA while intra-tumoral CD8 T-cell exhaustion (defined as $PD1^+Lag3^+Tim3^+$) was assessed by flow cytometry. Intra-tumoral CGRP levels positively correlate with the proportion of $PD1^+Lag3^+Tim3^+$ $CD8^+$ T-cells (**C**).(**D-E**) Orthotopic B16F10-mCherry-OVA cells ($5x10^5$ cells; i.d.) were inoculated into 8-week-old female sensory neuron intact or ablated mice. In nociceptor ablated mice, recombinant CGRP injection (100nM, i.d., once daily) rescues tumor growth (**D**; assessed until day 11) and intra-tumoral $CD8^+$ T-cells exhaustion (**E**; $PD1^+Lag3^+Tim3^+$).(**F-G**) Orthotopic B16F10-mCherry-OVA cells ($5x10^5$ cells; i.d.) were inoculated into 8-week-old male and female mice. Starting one day post inoculation (*defined as prophylactic*), the RAMP1 antagonist BIBN4096 (5mg/kg) was administered systemically (i.p.) once every two days (*q.a.d.*). In another group of mice, BIBN4096 (5mg/kg, i.p., *q.a.d.*) injections were started once the tumor reached a volume of ~$200mm^3$ (*defined as therapeutic*). Prophylactic or therapeutic BIBN4096 treatments decreased tumor growth (**F**) and reduced the proportion of intra-tumor $PD1^+Lag3^+Tim3^+$ $CD8^+$ T-cells (**G**, as measured thirteen days post tumor inoculation).(**H-K**) Naive splenocyte $CD8^+$ T-cells were FACS-purified from $RAMP1^{wt}$ ($CD45.1^+$) or $RAMP1^{-/-}$ ($CD45.2^+$) mice, expanded and stimulated (*CD3/CD28 + IL2*) *in vitro*. 8-week-old female $RAG1^{-/-}$ mice were transplanted (i.v., $2.5x10^6$ cells) with either activated $RAMP1^{-/-}$ or $RAMP1^{wt}$ $CD8^+$ T-cells or 1:1 mix of $5x10^6$ $RAMP1^{-/-}$ and $RAMP1^{wt}$ $CD8^+$ T-cells. One week post transplantation, the mice were inoculated with B16F10-mCherry-OVA cells ($5x10^5$ cells; i.d.). Ten days post B16F10 inoculation, we observed greater tumor growth (**H**) in $RAMP1^{WT}$ transplanted mice than in $RAMP1^{-/-}$ or $RAMP1^{wt}$ + $RAMP1^{-/-}$ co-transplanted mice. The relative proportion of intra-tumor $PD1^+Lag3^+Tim3^+$ $CD8^+$ T-cells was lower in $RAMP1^{-/-}$ transplanted mice (**I**). Within the same tumor, the relative proportion of intra-tumor $PD1^+Lag3^+Tim3^+$ $CD8^+$ T-cells was also lower in $RAMP1^{-/-}$ $CD8^+$ T-cells than in that found in $RAMP1^{wt}$ $CD8^+$ T-cells (**J**). On day ten, tumor and draining lymph node were harvested, and $RAMP1^{-/-}$ ($CD45.2^+$) and $RAMP1^{wt}$ ($CD45.1^+$) $CD8^+$ T-cells were FACS-purified and RNA sequenced (**K**). When compared with $RAMP1^{wt}$, $RAMP1^{-/-}$ $CD8^+$ T-cells showed reduced expression of the exhaustion markers *Ctla4, Havcr2 (Tim3), Lag3,* and *Pd1* as well as the pro-exhaustion transcription factors *Tox* and *Eomes*. In tumor-draining lymph nodes, the expression of exhaustion markers was similar across the two tested groups (**K**).(**L**) *In-silico* analysis of TCGA data [454] was used to correlate the survival rate of 459 melanoma patients with relative expression levels (determined by bulk RNA-sequencing) of RAMP1 found in their tumors (**L**). Kaplan-Meier curves show that increased RAMP1 expression (label as high; n=45 patients) in melanoma biopsy correlates with decreased patient survival ($p \leq 0.01$) in comparison to all patients or in patients found with low RAMP1 expression (label as low; n=68 patients; **L**).(**M**) In-silico analysis of single-cell RNA-sequencing of human melanoma [455] revealed that intratumoral RAMP1-expressing $CD8^+$ T-cells strongly overexpressed several immune checkpoint receptors (PD1, Tim3, Lag3, CTLA-4, CD28, ICOS, BTLA, CD27) in comparison to RAMP1-negative $CD8^+$ T-cells (**M**). *Data are shown as box-and-whisker plots (running from minimal to maximal values), for which individual data points are given (**A-B, E, G, I-J**), linear regression (**C**), mean ± S.E.M (**D, F, H**), heatmap displaying Log_{10} of 10^3 transcript per millions (**K**), survival plot (**L**) or violin plot (**M**). N*

are as follows: ***A****: n=9-10/groups,* ***B****: n=4/groups,* ***C****: n=10-18/groups,* ***D****: n=11-14/groups,* ***E****: n=11-16/groups,* ***F****: n=13-18/groups,* ***G-J****: n=5/groups,* ***K****: n=-23/groups,* ***L****: n=459,* ***M****: n=1712-1732/groups. E*xperiments were independently repeated two (**H-K**) or three (**A-G**) times with similar results. *P-values are shown in the figure and determined by unpaired Student's t-test (**A-B, E, G, I-J**), simple linear regression analysis (**C**), Mantel-Cox regression (**L**), and two-way ANOVA post-hoc Bonferroni (**D, F, H**).*

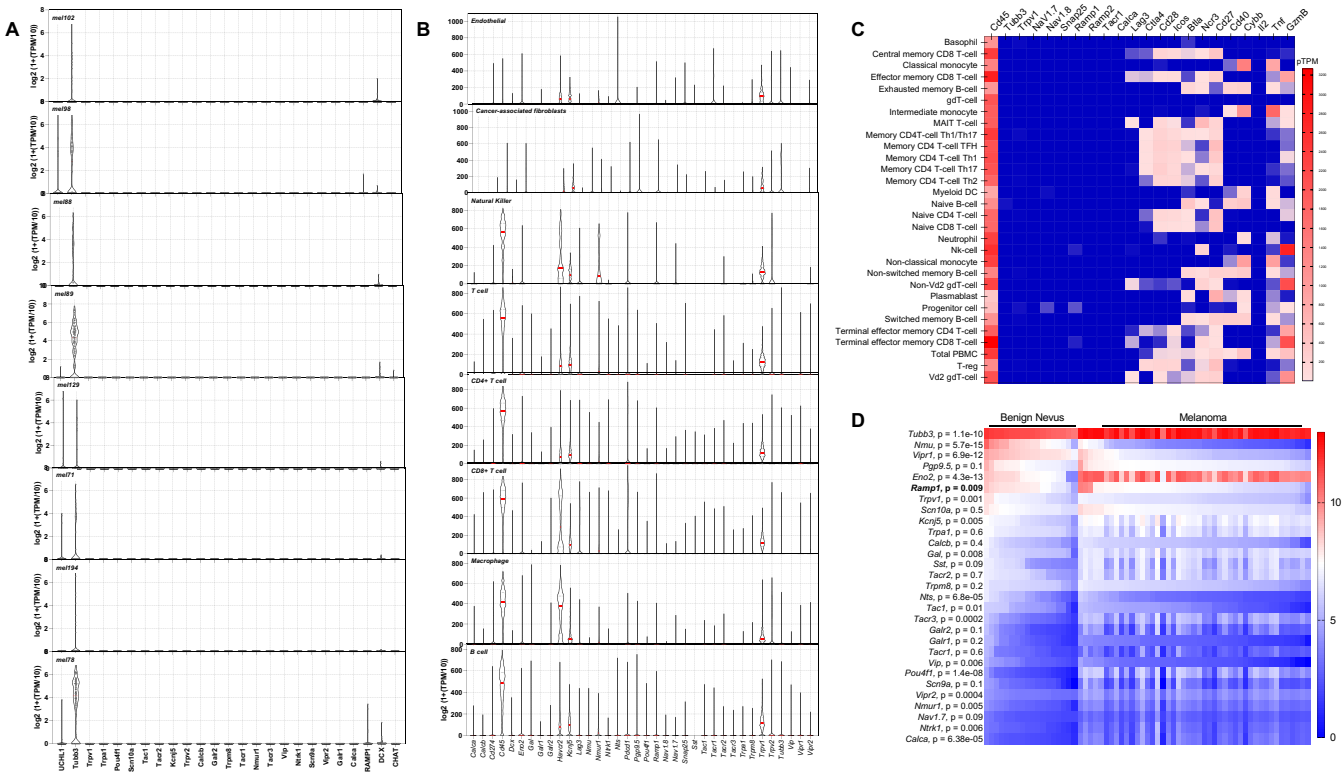

Figure 18.Nociceptor neuron-related transcripts are observed in patient melanoma biopsies but are not expressed by human immune cells or malignant cells. (**A-B**) *In-silico* analysis of single-cell RNA sequencing of human melanoma-infiltrating cells revealed no *Trpv1, Nav1.8* (Scn10a), *Snap25* (the molecular target of BoNT/A), *Calca* (gene encoding for CGRP) expression in malignant melanoma cells (defined as $CD90^{-}CD45^{-}$) from 10 different patients' biopsies (**A**). Similarly, cancer-associated fibroblasts, macrophage, endothelial, natural killer, T, and B cells do not express *Calca, Snap25, Trpv1* or *NaV1.8* channels (**B**). *Individual cell data are shown as a log_2 of 1 + (transcript per million / 10). Experimental details and cell clustering were defined in Jerby-Arnon et al.* [455]. ***A****: N=62-169/groups,* ***B****: N=92-1757/groups.* (**C**) *In-silico* analysis of human immune cells revealed their basal expression of *Cd45* and their absence of expression of *Calca, Snap25, Trpv1* and *$Na_V1.8$* channels. *Heatmaps show the read counts normalized to transcripts per million protein coding genes (pTPM) for each of the single-cell clusters. Experimental details and cell clustering were defined in Monaco et al.* [457] ***(C).***(**D**) Forty-five cutaneous melanomas and 18 benign melanocytic skin nevus biopsies transcriptomes were profiled using Affymetrix U133A microarrays[432]. In-silico analysis of this dataset revealed that cutaneous melanoma heightened expression levels of *Calca,*

Ramp1, Pouf4f1, Eno2, and *Tubb3*, as well as other neuronal-enriched genes (**D**). *Heatmap data are shown as log_2 (median centered intensity); unpaired Student's t-test; p-value shown in the figure. Experimental details were defined in Haqq et al. [432]. N=19-45/groups.*

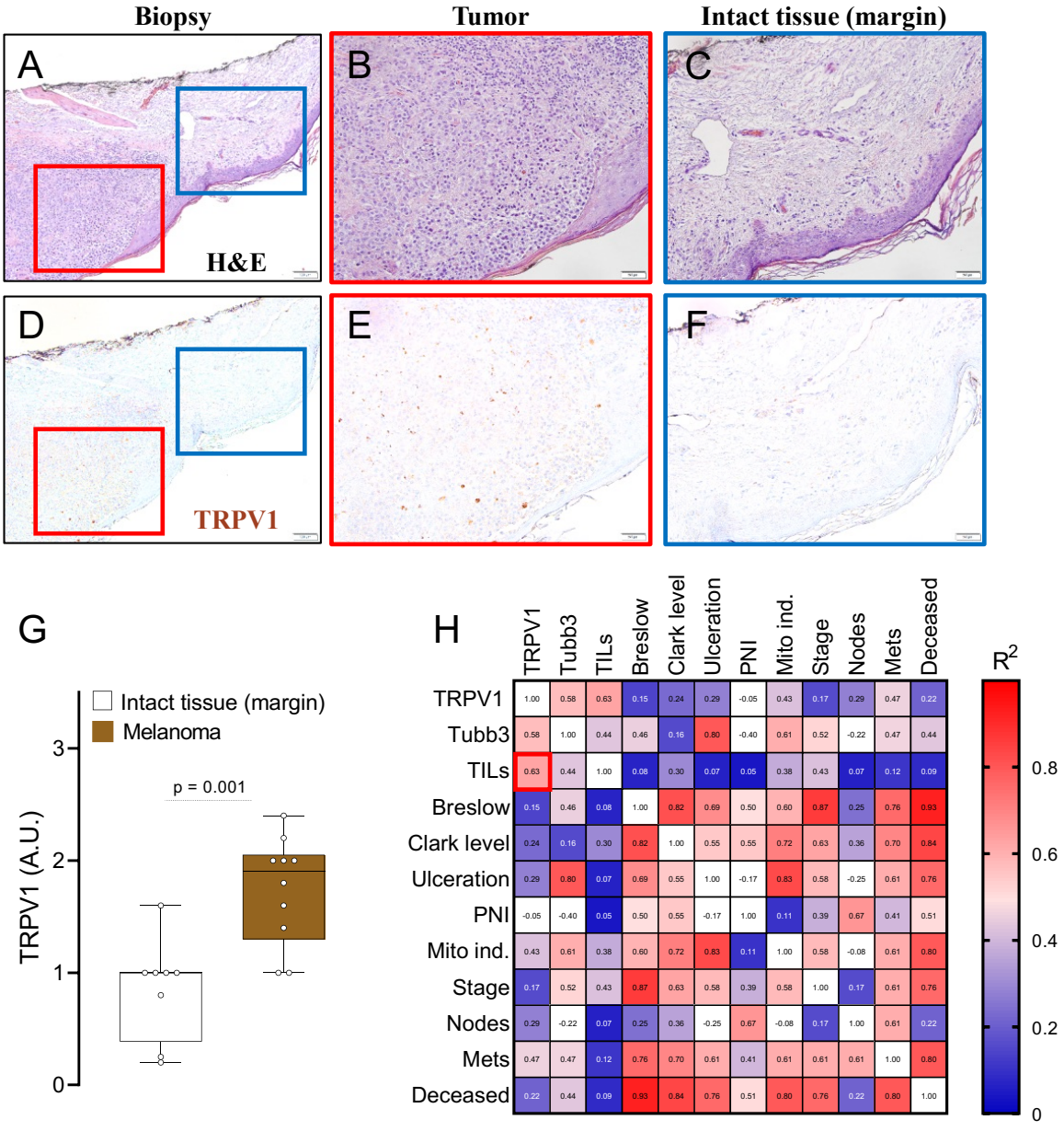

Figure 19. TRPV1+ neurons innervate patient melanomas.(A-H) Patients' melanoma sections were stained with hematoxylin eosin (A-F), and the presence of TRPV1 (D-F; brown) neurons was analyzed by immunohistochemistry. Increased levels of $TRPV1^+$ cells (G) were found in the tumor (delimited by red square; A-B, D-E) compared to healthy skin (delimited by blue square; A, C, D, F). Increased TRPV1 immunolabeling in tumor sections primarily correlated with enhanced levels

of tumor-infiltrating leukocytes (H) as scored from a retrospective correlation analysis performed on the patients' pathology reports (n=10 patients). *Data are shown as box-and-whisker plots (running from minimal to maximal values), for which individual data points are given (G) or as a heatmap (H) displaying Pearson's correlation (R^2). N are as follows: A-H: n=9-10/groups. Slides were scored blindly by two experienced medical pathologists. P-values are shown in the figure and determined by unpaired Student's t-test (G). Scale = 100µm (A, D), 50µm (B, C, E, F).*

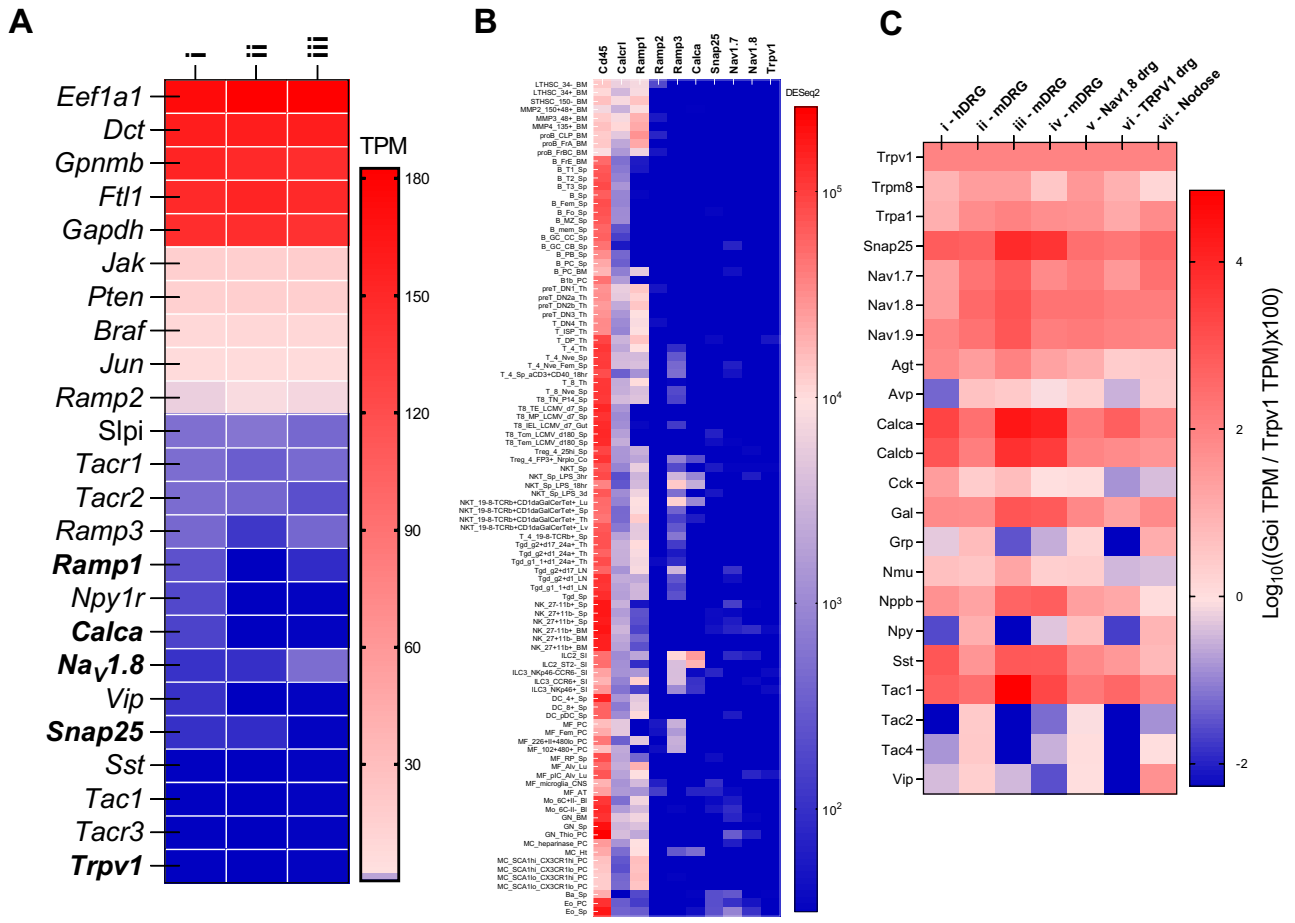

Figure 20.Trpv1, Nav1.8, Snap25, or Ramp1 are not expressed by B16F10 cancer cells or mouse immune cells. (**A**) *In-silico* analysis of three different B16F10 cells cultures (*labelled as i, ii, iii*) [458] revealed their basal expression of *Braf* and *Pten*. In contrast, B16F10 cells do not express *Trpv1 or Nav1.8* (necessary for QX-314 activity), *Snap25* (molecular target of BoNT/A), or *Ramp1* (molecular target of BIBN4096; **A**). *Heatmap data are shown as transcript per million (TPM) on a linear scale. Experimental details were defined in Castle et al.[458]. N=3/group* (**A**).(**B**) ImmGen RNA sequencing of leukocyte subpopulations [459] reveals their basal expression of *Cd45* and *Ramp1*. In contrast, immune cells do not express *Snap25, Trpv1,* or *Nav1.8* (**B**). *Heatmaps data are shown as DESeq$_2$ on a logarithmic scale (**B**).* (**C**) A meta-analysis of seven published nociceptor neuron expression profiling datasets [460] revealed the basal expression of sensory neuron markers (*Trpv1, Trpa1*) and neuropeptides (*Sp, Vip, Nmu, Calca*; **C**). *Expression across datasets was ratioed over Trpv1 and multiplied by 100. The log$_{10}$ of these values is presented as a heatmap. i) RNA sequencing of human lumbar neurons [461]; ii) microarrays of mouse FACS-*

sorted $Na_V1.8^+$ neurons [462]; iii) and iv) single-cell RNA sequencing of mouse lumbar neurons [463,464]; v) microarray profiling of mouse whole DRG [462]; vi) performed RNA sequencing of mouse $TRPV1^+$ neurons [465]; and vii) single-cell RNA sequencing of mouse vagal ganglia [466].

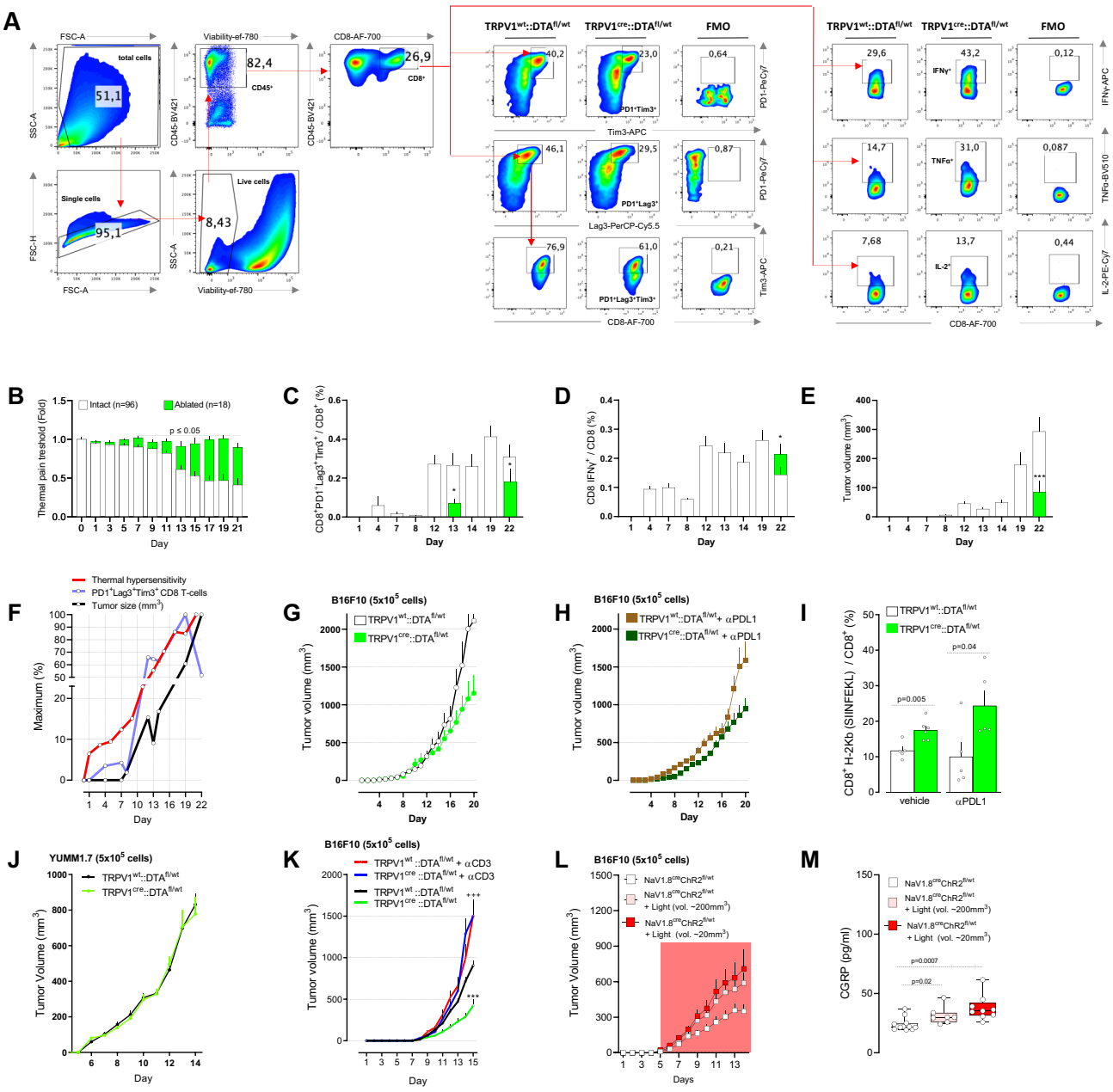

Figure 21.Nociceptor ablation prevents exhaustion of intra-tumoral CD8+ T cells. (A). Orthotopic B16F10-mCherry-OVA ($5x10^5$ cells; i.d.) cells were injected to nociceptor intact ($TRPV1^{wt}$::$DTA^{fl/wt}$) and ablated ($TRPV1^{Cre}$::$DTA^{fl/wt}$) mice. Fifteen days post-B16F10-mCherry-OVA cells inoculation ($5x10^5$ cells; i.d.), tumor-infiltrating $CD8^+$ T-cells were immunophenotyped. Representative flow cytometry panel are showed (**A**). (**B-F**) Orthotopic B16F10-mCherry-OVA ($2x10^5$ cells; i.d.) cells

were injected into the left hindpaw paw of nociceptor intact (n=96; TRPV1^{wt}::DTA$^{fl/wt}$) or ablated (n=18; TRPV1^{cre}::DTA$^{fl/wt}$) mice. When compared to their baseline threshold, littermate control mice showed significant thermal hypersensitivity on day 7, an effect that peaks on day 21 (**B**). In these mice, intra-tumoral frequency of PD1^{+}Lag3^{+}Tim3^{+} (**C**) and IFNγ^{+} (**D**) CD8^{+} T-cells increased 12 days post tumor inoculation, an effect that peaked on day 19. Finally, B16F10 tumor volume peaked on day 22 (**E**). When compared with littermate control mice, sensory neuron ablated mice inoculated with B16F10 cells showed no thermal pain hypersensitivity (**B**), reduced intra-tumoral frequency of PD1^{+}Lag3^{+}Tim3^{+} CD8^{+} T-cells (**C**) and tumor volume (**E**). In addition, nociceptor ablated mice have increased intra-tumoral frequency of IFNγ^{+} CD8^{+} T-cells (**D**). In littermate control mice, thermal pain hypersensitivity (day 7) precedes the increase in intra-tumoral frequency of PD1^{+}Lag3^{+}Tim3^{+} CD8^{+} T-cells (day 12), and significant tumor growth (day 12; **F**).(**G-I**) Orthotropic B16F10-mCherry-OVA cells (5x10^{5} cells, i.d.) were injected into a cohort of nociceptor neuron-ablated mice 3 days prior to the injection given to nociceptor intact mice. Mice from each group with similar tumor size (~85mm^{3}) were selected and exposed to αPDL1 (6 mg/kg, i.p.) once every 3 days for a total of 9 days. Twenty days post tumor inoculation, we found that αPDL1-reduced tumor growth was higher (~47%) in nociceptor-ablated mice than was observed in nociceptor-intact mice (~32%; **G-H**). In addition, nociceptor ablation increased the proportion of intra-tumoral tumor-specific (**I**; defined as H2KB^{+}) CD8^{+} T-cells. These differences were further enhanced by αPDL1 treatment (**G-I**). (**J**) The non-immunogenic YUMM1.7 cell line (5x10^{5} cells; i.d.; assessed until day 14) cells were injected to nociceptor intact (TRPV1^{wt}::DTA$^{fl/wt}$) and ablated mice (TRPV1^{Cre}::DTA$^{fl/wt}$). Nociceptor ablation had no impact on tumor growth (**J**). (**K**) Orthotopic B16F10-mCherry-OVA (5x10^{5} cells; i.d.) cells were injected to nociceptor intact (TRPV1^{wt}::DTA$^{fl/wt}$) and ablated mice (TRPV1^{Cre}::DTA$^{fl/wt}$). The reduction in B16F10-mCherry-OVA (1x10^{5} cells; i.d.) tumor growth observed in nociceptors ablated mice was absent following systemic CD3 depletion (**K,** assessed until day 15; αCD3, 200 µg/mice; i.p.; every 3 days).(**L-M**) Orthotopic B16F10-mCherry-OVA (5x10^{5} cells; i.d.) cells were injected to light sensitive mice (Na$_{V}$1.8^{Cre}::ChR2$^{fl/wt}$). As opposed to unstimulated mice, the optogenetic activation (3.5 ms, 10Hz, 478nm, 60 mW, giving approx. 2-6 mW/mm^{2} with a 0.39 NA fiber placed 5-10 mm from the skin, 20 min) of tumor-innervating nociceptor neurons, when started once B16F10 tumors were visible (~20mm^{3}) or well established (~200mm^{3}), resulted in enhanced tumor growth (**L**, as measured until day 14) and intra-tumoral CGRP release (**M**).*Data are shown as FACS plot (**A;** depict the gating strategy used in **figure 3 D-F**), mean ± S.E.M (**B-L**) or as box-and-whisker plots (running from minimal to maximal values) for which individual data points are given (**M**). N are as follows: **A**: n=20-25/groups, **B-F**: n=18-96/groups, **G-H**: n=4-14/groups, **I**: n=5-6/groups; **J**: n=6-13/groups, **K**: n=4-8/groups, **L-M**: n=8-12/groups. E*xperiments were independently repeated two (**B-M**) or ten (**A**) times with similar results*. P-values are shown in the figure and determined by unpaired Student's t-test (**B-E, I, M**), or two-way ANOVA post hoc Bonferroni (**G-H, J-L**).*

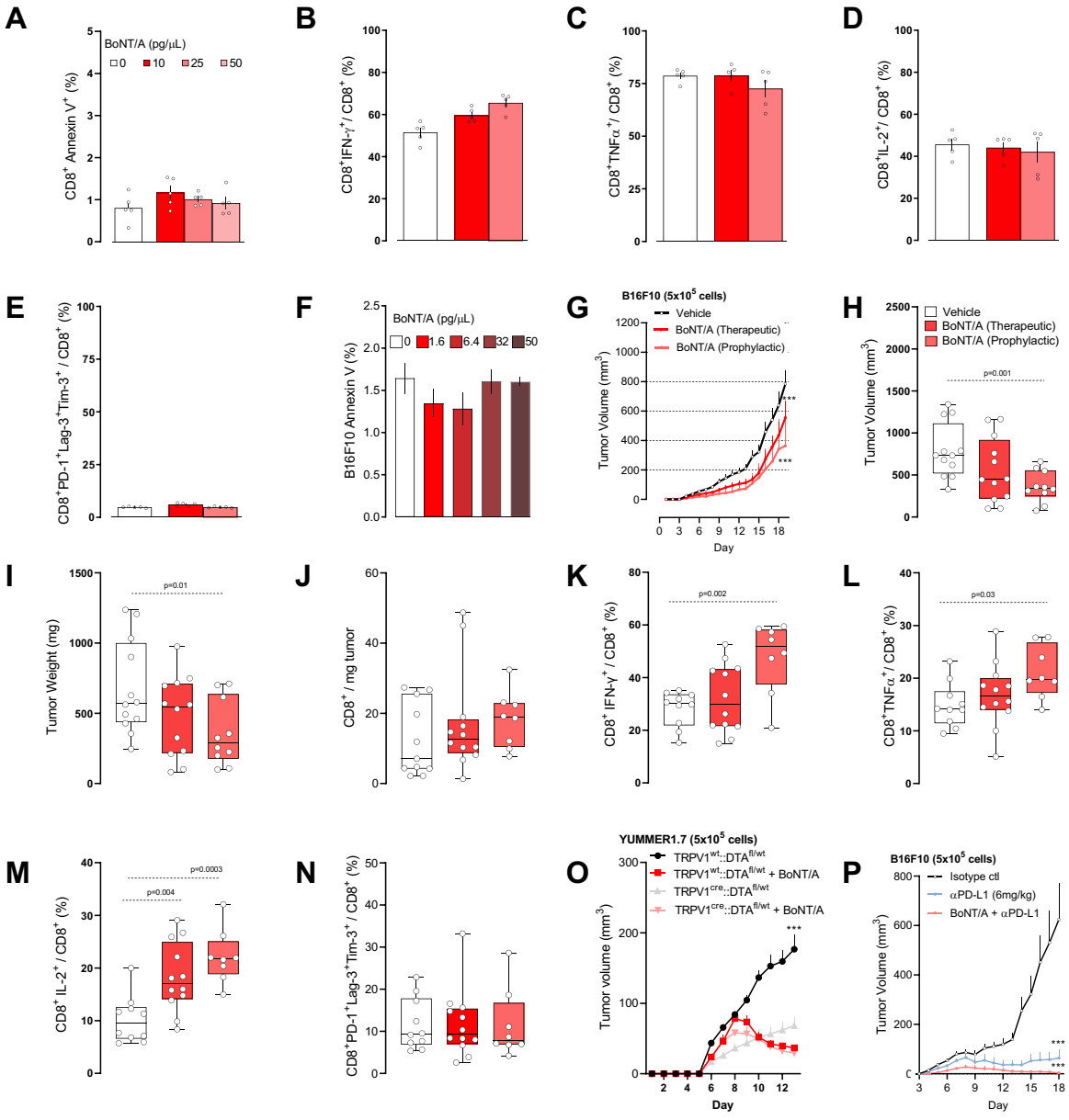

Figure 22.Botox silencing of B16F10-innervating neurons decreases tumor growth. (**A-E**) Splenocytes-isolated $CD8^+$ T-cells from naive C57BL6 mice were cultured under T_{c1}-stimulating conditions (*ex vivo* activated by CD3/CD28, IL-12, and anti-IL4) for 48h. The cells were then exposed to BoNT/A (10-50 pg/µL) for 24h; effects on apoptosis, exhaustion, and activation were measured by flow cytometry. When compared to vehicle-exposed cells, BoNT/A did not impact the survival (**A**) of cultured cytotoxic $CD8^+$ T-cells, nor their relative expression of $IFN\gamma^+$ (**B**), $TNF\alpha^+$ (**C**), $IL2^+$ (**D**) and $PD1^+Lag3^+Tim3^+$ (**E**). (**F**) B16F10 ($1x10^5$ cells) were cultured for 24h and subsequently exposed to BoNT/A (1.6-50 pg/µL) or its vehicle for an additional 24h. BoNT/A did not trigger B16F10 cells apoptosis, as measured by the mean fluorescence intensity of Annexin V (**F**). (**G-N**) One and three days prior to tumor inoculation (*defined as prophylactic*), the skin of 8-

week-old male and female mice was injected with BoNT/A (25 pg/µl; i.d.) or its vehicle. One day after the last injection, orthotopic B16F10-mCherry-OVA ($5x10^5$ cells; i.d.) were inoculated into the area pre-exposed to BoNT/A. In another group of mice, BoNT/A was administered (25 pg/µl; i.d.) one and three days after the tumor reached a volume of ~200mm3 *(defined as therapeutic*). The impact of neuron silencing on tumor size and tumor-infiltrating $CD8^+$ T-cell exhaustion was measured. Eighteen days post-tumor inoculation, we found that the tumor volume (**G, H**) and weight (**I**) were reduced in mice treated with BoNT/A (*Prophylactic group*). In parallel, we found that silencing tumor-innervating neurons increased the proportion of $IFN\gamma^+$ (**K**), $TNF\alpha^+$ (**L**), and $IL\text{-}2^+$ (**M**) $CD8^+$ T-cells. BoNT/A had no impact on the total number of intra-tumoral CD8 T cells (**J**) or the relative proportion of $PD1^+Lag3^+Tim3^+$ (**N**) $CD8^+$ T-cells. (**O**) One and three days prior to tumor inoculation, the skin of 8-week-old male and female sensory neuron-intact or ablated mice was injected with BoNT/A (25 pg/µl; i.d.) or its vehicle. One day following the last injection, orthotopic YUMMER1.7 cells ($5x10^5$ cells; i.d.) were inoculated into the area pre-exposed to BoNT/A. The effects of nociceptor neuron ablation on tumor size and volume were measured. Thirteen days post tumor inoculation, we found that the tumor growth was lower in mice treated with BoNT/A or in sensory neuron-ablated mice. BoNT/A had no additive effects when administered to sensory neuron-ablated mice (**O**).(**P**) One and three days prior to tumor inoculation, the skin of 8-week-old male and female mice was injected with BoNT/A (25 pg/µl; i.d.) or its vehicle. One day following the last injection, orthotopic B16F10-mCherry-OVA cells ($5x10^5$ cells; i.d.) were inoculated into the area pre-exposed to BoNT/A. On days 7, 10, and 13 post tumor inoculation, the mice were exposed to αPDL1 (6 mg/kg, i.p.) or its vehicle. Eighteen days post tumor inoculation, we found that neuron silencing using BoNT/A potentiated αPDL1-mediated tumor reduction (**P**). *Data are shown as mean ± S.E.M (**A-G, O-P**), as box-and-whisker plots (running from minimal to maximal values), for which individual data points are given (**H-N**). N are as follows: **A-E**: n=5/groups, **F**: n=3/groups, **G-I**: n=10-12/groups, **J-N**: n=8-12/groups, **O**: n=8-10/groups, **P**: n=7-8/groups. E*xperiments were independently repeated two (***A-F, O-P***) or four (***G-N***) times with similar results. *P-values are shown in the figure and determined by unpaired Student's t-test (**A-F**), two-way ANOVA post hoc Bonferroni (**G, O-P**) or one-way ANOVA posthoc Bonferonni (**H-N**).*

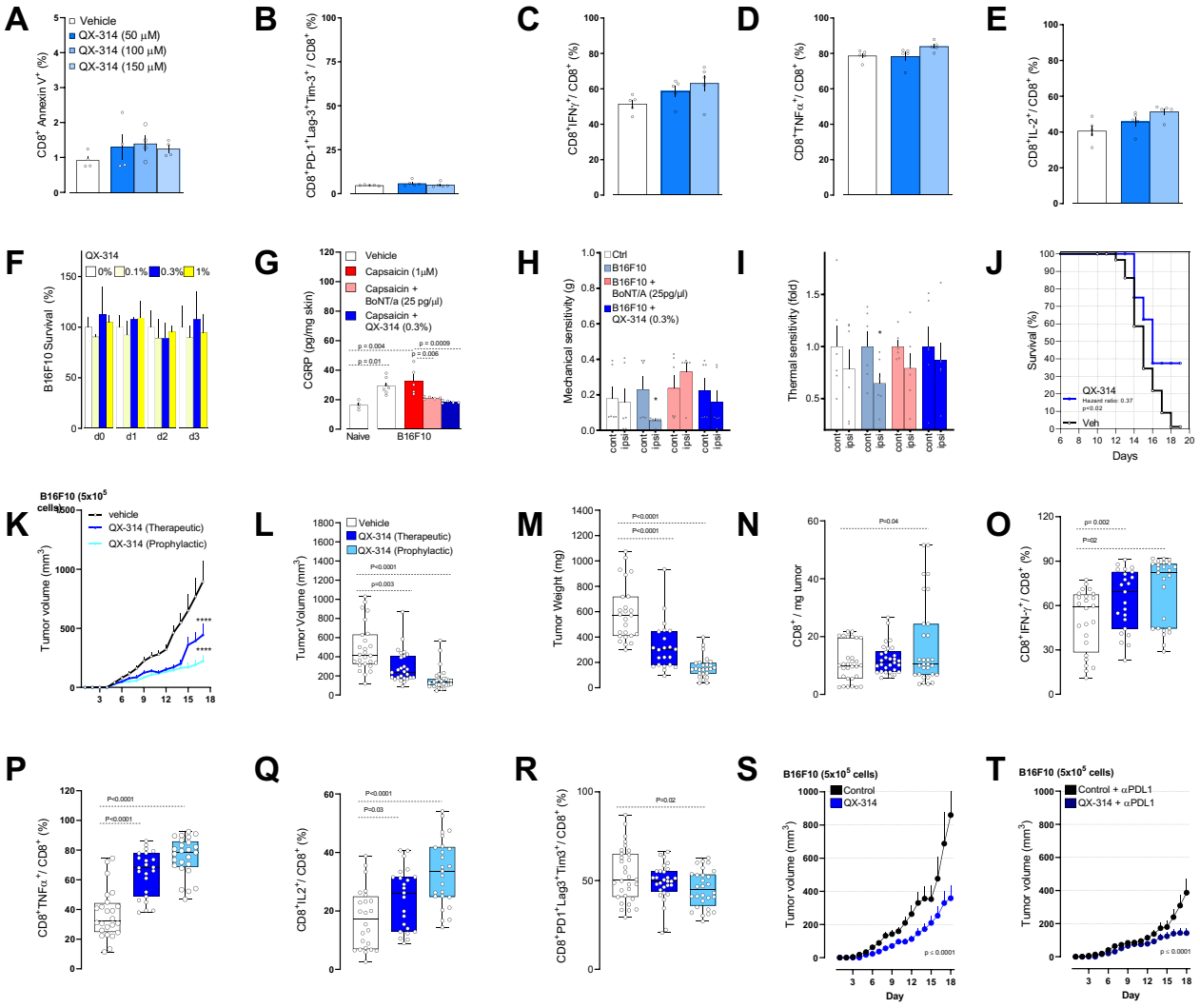

Figure 23.QX-314 silencing of B16F10-innervating neurons decreases tumor growth. (**A-E**) Splenocytes-isolated $CD8^+$ T-cells from naive C57BL6 mice were cultured under T_{c1}-stimulating conditions (*ex vivo* activated by CD3/CD28, IL-12, and anti-IL4) for 48h. The cells were then exposed to QX-314 (50-150 μM) for 24h, effects on apoptosis, exhaustion and activation were measured by flow cytometry. When compared to vehicle-exposed cells, QX-314 did not impact the survival of cultured cytotoxic $CD8^+$ T-cells (**A**), nor their relative expression of $PD1^+Lag3^+Tim3^+$ (**B**), $IFN\gamma^+$ (**C**), $TNF\alpha^+$ (**D**) and $IL\text{-}2^+$ (**E**).(**F**) B16F10 ($1x10^5$ cells) were cultured for 24h. The cells were then exposed or not to QX-314 (0.1-1%) for an additional 24-72h, and cell count was analyzed by bright-field microscopy. QX-314 did not impact B16F10 cells' survival, as measured by relative cell count changes (at each time point) in comparison to vehicle-exposed cells (**F**).(**G-I**) One and three days prior to tumor inoculation, 8-week-old male and female wild-type mice's right hind paws were injected with BoNT/A (25 pg/μl; i.d.) or its vehicle. On the following day, orthotopic B16F10 cells ($2x10^5$ cells; i.d.) were inoculated into the area pre-exposed to BoNT/A. Starting one day post

inoculation, QX-314 (0.3%) or its vehicle was administered (i.p.) once daily in another group of mice. The effects of sensory neuron silencing were tested on neuropeptide release (**G**), as well as mechanical (**H**) and thermal pain hypersensitivity (**I**). First, CGRP levels were increased in B16F10 tumor surrounding skin explant (assessed on day 15) in comparison to control skin; an effect further enhanced by capsaicin (1 µM; 3h) but was absent in skin pre-treated with BoNT/A (25 pg/µl) or QX-314 (0.3%; **G**). We also found that B16F10 injection induced mechanical (**H**) and thermal pain hypersensitivities (**I**) fourteen days post tumor inoculation. These effects were stopped by sensory neuron silencing with QX-314 or BoNT/A (**H-I**).(**J**) Orthotopic B16F10-mCherry-OVA cells ($5x10^5$ cells; i.d.) were inoculated into 8-week-old male and female mice. Starting one day post-inoculation, QX-314 (0.3%; i.d.; 5 sites) was injected once daily around the tumor. The impact of nociceptor neuron silencing on tumor size and tumor-infiltrating $CD8^+$ T-cell exhaustion was measured. We found that silencing tumor innervating neurons increased the mice's median length of survival (**J;** ~270% Mantel-Haenszel hazard ratio; measured on day 19).(**K-R**) Orthotopic B16F10-mCherry-OVA cells ($5x10^5$ cells; i.d.) were inoculated into 8-week-old male and female mice. Starting one day post-inoculation (*defined as prophylactic*), In other groups of mice, QX-314 daily injection started once the tumor reached a volume of ~200mm^3 (*defined as therapeutic*). As measured seventeen days post tumor inoculation, silencing tumor innervation also decreased tumor volume (**K, L**) and weight (**M**), as well as the relative proportion of $PD1^+Lag3^+Tim3^+$ (**R**) $CD8^+$ T-cells. QX-314 treatment also increased the total number of intra-tumoral $CD8^+$ T-cells (**N**), as well as relative proportion of $IFN\gamma^+$ (**O**), $TNF\alpha^+$ (**P**), and $IL\text{-}2^+$ (**Q**) $CD8^+$ T-cells. (**S-T**) Orthotropic B16F10-mCherry-OVA cells ($5x10^5$ cells, i.d.) were injected into mice treated with QX-314 (0.3%; i.d.) 2-3 days prior to being injected into vehicle-exposed mice. Mice from each group with similar tumor size (~100mm^3) were selected and exposed to αPDL1 (6 mg/kg, i.p.) once every 3 days for a total of 9 days. Sixteen days post tumor inoculation, we found that αPDL1-reduced tumor growth was higher (~61%) in nociceptor silenced mice than was observed in vehicle exposed mice (~49%; **S-T**). *Data are shown as mean ± S.E.M (**A-I; K; S-T**), Mantel-Cox regression analysis (**J**), as box-and-whisker plots (running from minimal to maximal values), for which individual data points are given (**L-R**). N are as follows: **A-E**: n=4-5/groups, **F**: n=3/groups, **G**: n=4-7/groups, **H-I**: n=6/groups, **J**: n=37-89/groups, **K-R**: n=14-31/groups, **S**: n=9-13/groups, **T**: n=12-18/groups. E*xperiments were independently repeated two **(A-I, S-T**) or four (**J-R**) times with similar results. *P-values are shown in the figure and determined by unpaired Student's t-test (**A-I**), Mantel-Cox regression (**J**), two-way ANOVA posthoc Bonferroni (**K, S-T**) or one-way ANOVA posthoc Bonferonni (**L-R**).*

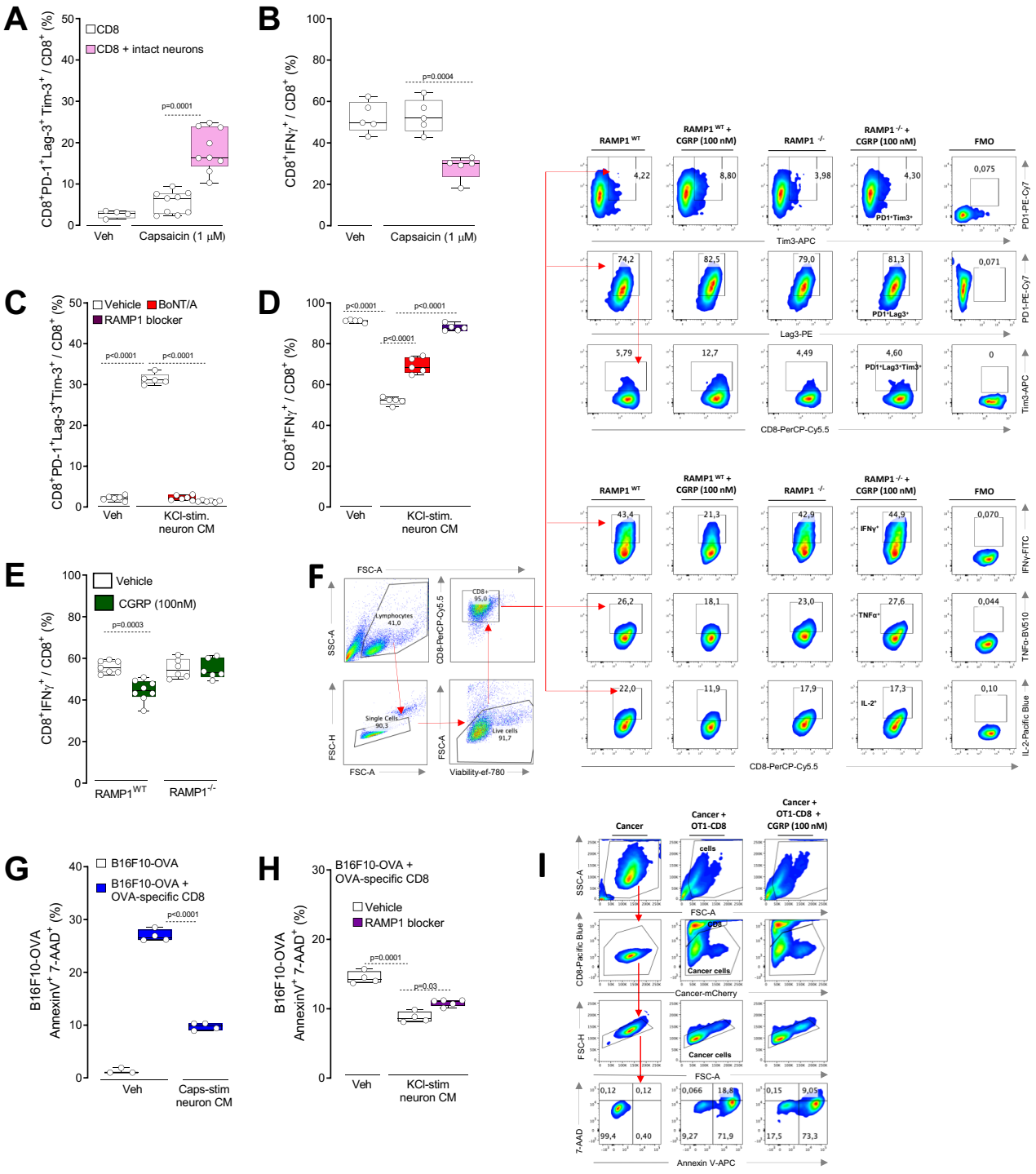

Figure 24.Nociceptor-released CGRP drives cytotoxic CD8+ T-cell exhaustion. **A-B**) Splenocytes-isolated $CD8^+$ T-cells were cultured under T_{c1}-stimulating condition (*ex vivo* activated by CD3/CD28, IL-12, and anti-IL4) for 48h. The cells were then cultured or not with wild-type DRG neurons and exposed to capsaicin (1µM, challenged once every two days) or its vehicle. As

measured after 4 days stimulation, capsaicin-stimulated intact neuron increased the proportion of $PD1^+Lag3^+Tim3^+$ (**A**) cytotoxic $CD8^+$ T-cells, while it decreased the one of $IFN\gamma^+$ (**B**). (**C-D**) Splenocytes-isolated $CD8^+$ T-cells were cultured under T_{c1}-stimulating conditions (*ex vivo* activated by CD3/CD28, IL-12, and anti-IL4) for 48h. In the presence of peptidase inhibitors (1µl/1000µl), naive DRG neurons were cultured in the presence of BoNT/A (100pg/200µl) or its vehicle for 24h. The cells were then washed, stimulated (30min) with KCl (50mM), and the conditioned media harvested. On alternate days for 4 days, the cytotoxic $CD8^+$ T-cells were exposed or not to a RAMP1 blocker ($CGRP_{8-37}$; 2µg/ml) and challenge (1:2 dilution) with fresh KCl-induced conditioned media from naive, or BoNT/A-silenced neurons. As measured after 4 days stimulation, KCl-stimulated neuron conditioned media increased the proportion of $PD1^+Lag3^+Tim3^+$ (**C**) cytotoxic $CD8^+$ T-cells, while it decreased the one of $IFN\gamma^+$ (**D**). Such effect was absent when cytotoxic $CD8^+$ T-cells were co-exposed to the RAMP1 blocker $CGRP_{8-37}$ or challenged with the neuron conditioned media harvested from BoNT/A-silenced neurons (**C-D**). (**E-F**) Splenocytes-isolated $CD8^+$ T-cells from wild-type and $RAMP1^{-/-}$ mice were cultured under T_{c1}-stimulating conditions (*ex vivo* activated by CD3/CD28, IL-12, and anti-IL4) for 48h. On alternate days for 4 days, the cytotoxic $CD8^+$ T-cells were exposed to CGRP (0.1µM) or its vehicle. As measured after 4 days stimulation, representative flow cytometry plots (n=3/group; **F**) show that CGRP decrease $RAMP1^{wt}$ cytotoxic $CD8^+$ T-cells expression of $IFN\gamma^+$ (**E, F**), $TNF\alpha^+$ (**F**), and $IL2^+$ (**F**) when exposed to CGRP. Inversely, CGRP increase the proportion of $PD1^+Lag3^+Tim3^+$ in $RAMP1^{wt}$ cytotoxic $CD8^+$ T-cells (**F**). $RAMP1^{-/-}$ cytotoxic $CD8^+$ T-cells were protected from the effect of CGRP (**E-F**).(**G-I**) Splenocytes-isolated $CD8^+$ T-cells from naive OT-1 mice were cultured under Tc1-stimulating conditions (*ex vivo* activated by CD3/CD28, IL-12, and anti-IL4) for 48h. B16F10-mCherry-OVA cells ($1x10^5$ cells) were then cultured with or without OT-1 cytotoxic $CD8^+$ T-cells ($4x10^5$ cells; **G-I**). Tc1-stimulated OT1-$CD8^+$ T-cells lead to B16F10-OVA cell apoptosis ($AnnexinV^+7AAD^+$; G, measured after 48h; **H-I**, measured after 24h). B16F10-mCherry-OVA cells elimination by cytotoxic $CD8^+$ T-cells was reduced when the co-cultures were challenged (1:2 dilution; once daily for two consecutive days) with fresh conditioned media harvested from capsaicin (1 µM)-stimulated naive DRG neurons (**G**; measured after 48h). Similarly, KCl (50mM)-stimulated naive DRG neurons conditioned media (1:2 dilution) reduced B16F10-mCherry-OVA apoptosis (**H**; measured after 24h). This effect was blunted when the cells were co-exposed to the RAMP1 blocker $CGRP_{8-37}$ (**H**; 2 µg/ml; measured after 24h). CGRP (0.1µM) challenges also reduced OT-1 cytotoxic $CD8^+$ T-cells elimination of B16F10-OVA cell (**I**; measured after 24h). *Data are shown as box-and-whisker plots (running from minimal to maximal values), for which individual data points are given (**A-E, G-H**), or representative FACS plot (**F, I**). N are as follows: **A-B**: n=4-9/groups, **B**: n=5/groups, **C-D**: n=5-6/groups, **E-F**: n=6-8/groups, **G**: n=3-4/groups, **H**: n=4-5/groups, **I**: n=4/groups. Experiments were repeated a minimum of three independent times with similar results. P-values are shown in the figure and determined by one-way ANOVA posthoc Bonferroni (**A-E, G-H**).*

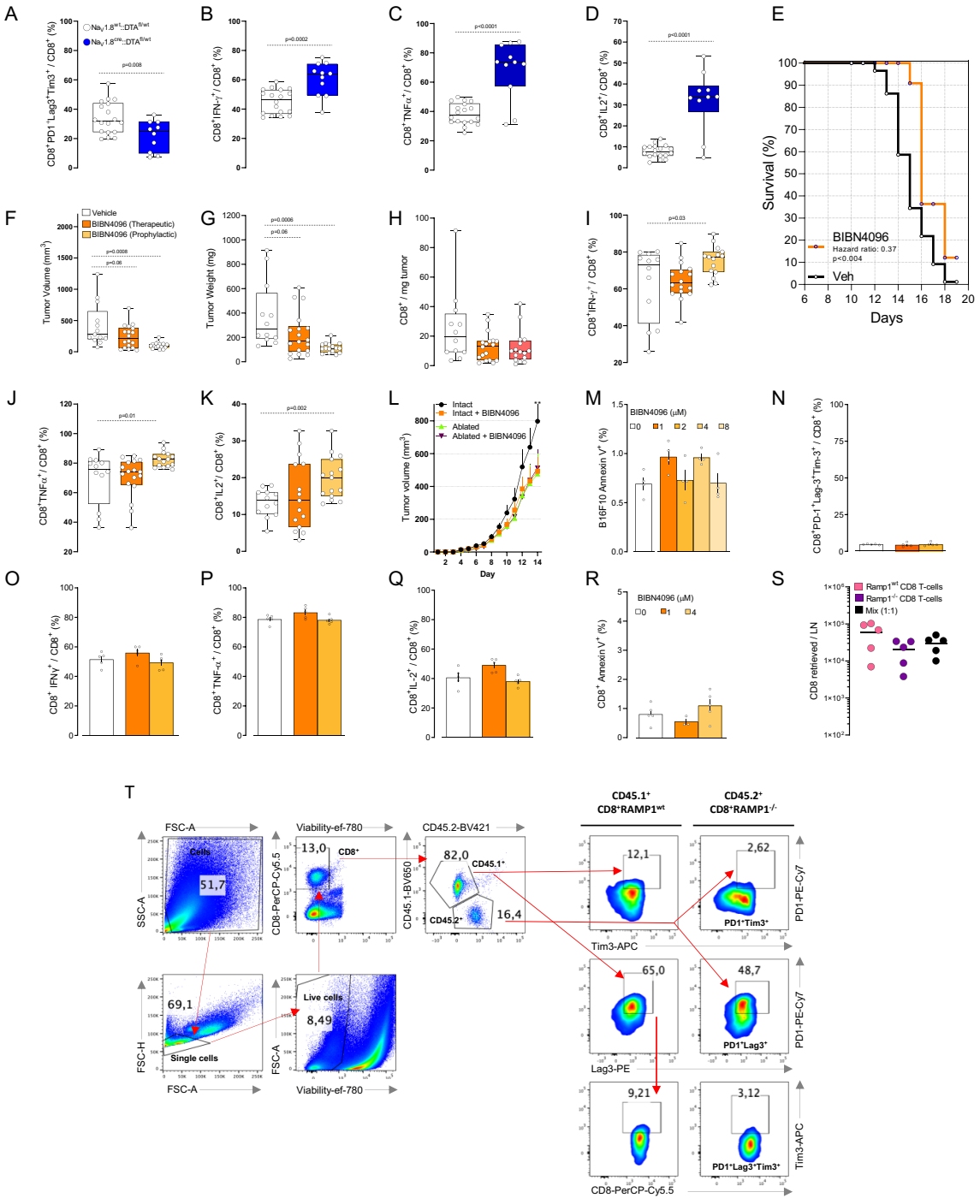

Figure 25.CGRP-RAMP1 axis controls intra-tumoral CD8+ T-cell exhaustion. (**A-D**) Orthotopic B16F10-mCherry-OVA (5x10^5 cells; i.d.) cells were injected to nociceptor intact (Na$_V$1.8^{wt}::DTA$^{fl/wt}$) and ablated mice (Na$_V$1.8^{Cre}::DTA$^{fl/wt}$). As measured fifteen days post inoculation, Na$_V$1.8$^+$ nociceptor-ablated animals had lower proportion of PD1$^+$Lag3$^+$Tim3$^+$ (**A**) CD8$^+$ T-cells, but

increased levels of IFNγ$^+$ (**B**), TNFα$^+$ (**C**), IL-2$^+$ (**D**) CD8$^+$ T-cells. (**E**) Orthotopic B16F10-mCherry-OVA cells (5x10^5 cells; i.d.) were inoculated into 8-week-old male and female mice. Starting one day post inoculation, the RAMP1 antagonist BIBN4096 (5mg/kg, i.p., q.a.d.) was administered systemically. We found that blocking the action of CGRP on RAMP1-expressing cells, increased the mice's median length of survival (**E**; ~270% Mantel–Haenszel hazard ratio; measured on day 19).(**F-K**) Orthotopic B16F10-mCherry-OVA cells (5x10^5 cells; i.d.) were inoculated into 8-week-old male and female mice. Starting one day post inoculation (*defined as prophylactic*), the RAMP1 antagonist BIBN4096 (5mg/kg, i.p., q.a.d.) was administered systemically. In another group of mice, BIBN4096 (5mg/kg, i.p., q.a.d.) injections were started once the tumor reached a volume of ~200mm^3 (*defined as therapeutic*). The impact of nociceptor neuron-silencing on tumor size and tumor infiltrating CD8$^+$ T-cell exhaustion was measured. As assessed thirteen days post tumor inoculation, BIBN4096 decreased tumor volume (**F**) and weight (**G**) but increased the relative proportion of IFNγ$^+$ (**I**), TNFα$^+$ (**J**), and IL-2$^+$ (**K**) CD8$^+$ T-cells. BIBN4096 had no impact on the number of intra-tumoral CD8$^+$ T-cells (**H**). When administered as therapeutic, BIBN4096 reduced tumor volume (**F**) and weight (**G**) but had limited impact on CD8$^+$ T-cells' cytotoxicity **(I-K**). (**L**) Orthotopic B16F10-mCherry-OVA cells (5x10^5 cells; i.d.) were inoculated into 8-week-old male and female sensory neuron-intact (TRPV1^{wt}::DTA$^{fl/wt}$) and ablated (TRPV1^{cre}::DTA$^{fl/wt}$) mice. Starting one day post inoculation, BIBN4096 (5 mg/kg) or its vehicle was administered (i.p.) on alternate days; effects on tumor volume were measured. Fourteen days post tumor inoculation, we found that tumor growth was reduced in sensory neuron-ablated mice and in BIBN4096-treated mice. BIBN4096 had no additive effect when given to sensory neuron-ablated mice (**L**). (**M-Q**) Splenocytes-isolated CD8$^+$ T-cells from naïve C57BL6 mice were cultured under Tc1-stimulating conditions (*ex vivo* activated by CD3/CD28, IL-12, and anti-IL4) for 48h. The cells were then exposed to BIBN4096 (1-4 μM) for 24h; effects on apoptosis, exhaustion and activation were measured by flow cytometry. When compared to vehicle-exposed cells, BIBN4096 did not impact the survival (**M**) of cultured cytotoxic CD8$^+$ T-cells, nor their relative expression of PD1$^+$Lag3$^+$Tim3$^+$ (**N**), IFNγ$^+$ (**O**), TNFα$^+$ (**P**), and IL2$^+$ (**Q**). (**R**) B16F10 cells (1x10^5 cells) were cultured for 24h. The cells were then exposed (or not) to BIBN4096 (1-4 μM) for an additional 24h; effects on apoptosis were measured by flow cytometry. BIBN4096 did not trigger B16F10 cells apoptosis, as measured by the mean fluorescence intensity of Annexin V (**R**). (**S-T**) Naive splenocyte CD8$^+$ T-cells were FACS-purified from RAMP1^{wt} (CD45.1$^+$) or RAMP1$^{-/-}$ (CD45.2$^+$) mice, expanded and stimulated (*CD3/CD28 + IL2*) *in vitro*. 8-week-old female RAG1$^{-/-}$ mice were transplanted (i.v., 2.5x10^6 cells) with either RAMP1$^{-/-}$ or RAMP1^{wt} CD8$^+$ T-cells or 1:1 mix of RAMP1$^{-/-}$ and RAMP1^{wt} CD8$^+$ T-cells. One week post transplantation, the mice were inoculated with B16F10-mCherry-OVA cells (5x10^5 cells; i.d.). Ten days post tumor inoculation, we retrieved a similar number of tumors draining lymph node CD8$^+$ T-cells across the three tested groups (**S**). Within the same tumor, intra-tumoral CD8$^+$ T-cell exhaustion was immunophenotyped by flow cytometry (*representative panel shown in **T***), which indicated that the relative proportion of PD1$^+$Lag3$^+$Tim3$^+$ CD8$^+$ T-cells was ~3-fold lower in RAMP1$^{-/-}$ CD8$^+$ T-cells than in RAMP1^{wt} CD8$^+$ T-cells (**T**).*Data are shown as mean ± S.E.M (**A–D; L–R**), Mantel-Cox regression analysis (**E**), as box-and-whisker plots (running from minimal to maximal values, for which individual data points are given (**F–K**), scatter dot plot (**S**) or as FACS plot (**T**). N are as follows **A–D**: n=10-18/groups, **E**: n=15–89/groups; **F-K**: n=12–18/groups, **L**: n=14/groups, **M**: n=4/groups, **N-R**: n=3-5/groups, **S**: n=5/groups. Experiments were independently repeated once (**S, T**), twice (**A–D, L–R**) or four (**E–K**) times with similar results. P-values are shown*

*in the figure and determined by unpaired Student's t-test (**A–D, M–S**), Mantel–Cox regression (**E**), by one-way ANOVA posthoc Bonferroni (**F-K**), or two-way ANOVA post-hoc Bonferroni (**L**).*

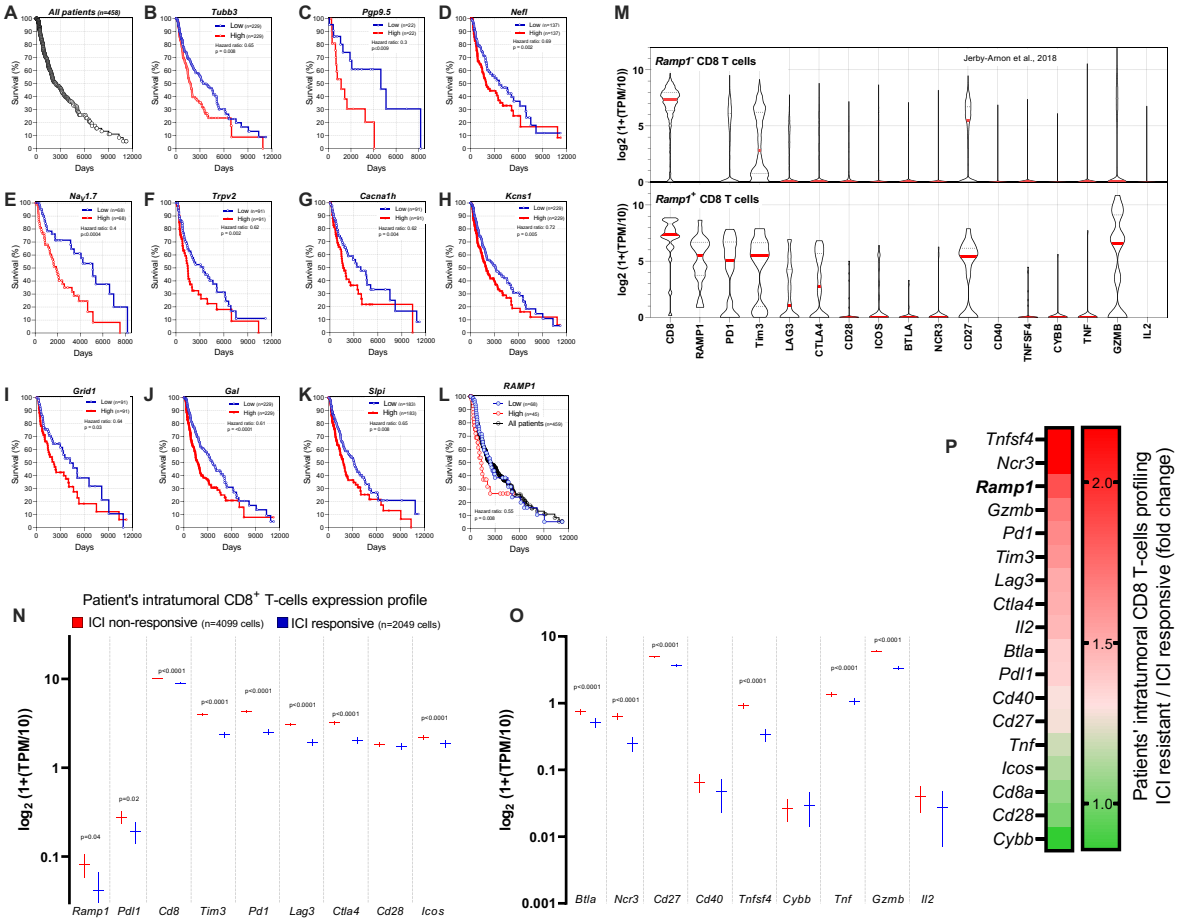

Figure 26. Ramp1 expression in patient melanoma-infiltrating T-cells correlates with worsened survival and poor responsiveness to ICI(**A-L**) *In-silico* analysis of Cancer Genome Atlas (TCGA)[454] data linked the survival rate among 459 melanoma patients with their relative expression levels of various genes of interest (determined by bulk RNA sequencing of tumor biopsy). Kaplan-Meier curves show the patients' survival after segregation in two groups defined by their low or high expression of a gene of interest. Increased gene expression (labelled as high; red curve) of *Tubb3* (**B**), *Pgp9.5* (**C**), *Na$_V$1.7* (**E**), *Slpi* (**K**) and *Ramp1* (**L**) in biopsy correlate with decreased patient survival (p≤0.05). The mantel-Haenszel hazard ratio and number of patients included in each analysis are shown in the figure. Experimental details were defined in Cancer Genome Atlas (TCGA)[454]. N=22-459/groups (**A-L**). (**M**) *In-silico* analysis of single-cell RNA sequencing of human melanoma-infiltrating T-cells revealed that *Ramp1*$^+$ T-cells downregulated *Il-2* expression and strongly overexpressed several immune checkpoint receptors (*Pd1, Tim3, Lag3, Ctla-4, Cd28, Icos, Btla, Cd27*) in comparison to *Ramp1*$^-$ T-cells. Individual cell data are shown as a log$_2$ of 1 + (transcript per million / 10). Experimental details and cell clustering were defined in *Jerby-Arnon et al.* [455]. N=25-1732/groups (**M**). (**N-P**) Based

on melanoma patients' clinical response to immune checkpoint blocker, Jerby-Arnon et al [455]. clustered patients into two groups, which they defined as immune checkpoint receptor-responsive or immune checkpoint receptor-resistant[455]. *In-silico* analysis of single-cell RNA sequencing of patients' biopsies revealed that tumor-infiltrating CD8+ T-cells from immune checkpoint receptor-resistant patients significantly overexpressed *Ramp1* (2.0-fold), *Pd1* (1.7-fold), *Lag3* (1.6-fold), *Ctla4* (1.6-fold), and *Tim3* (1.7-fold). Individual cell data are shown as a $\log_2$ of 1 + (transcript per million / 10). Experimental details and cell clustering were defined in *Tirosh et al.*[456] P-values are shown in the figure and determined by unpaired Student's t-test (**N-O**). N=2049-4099/groups (**N-P**).

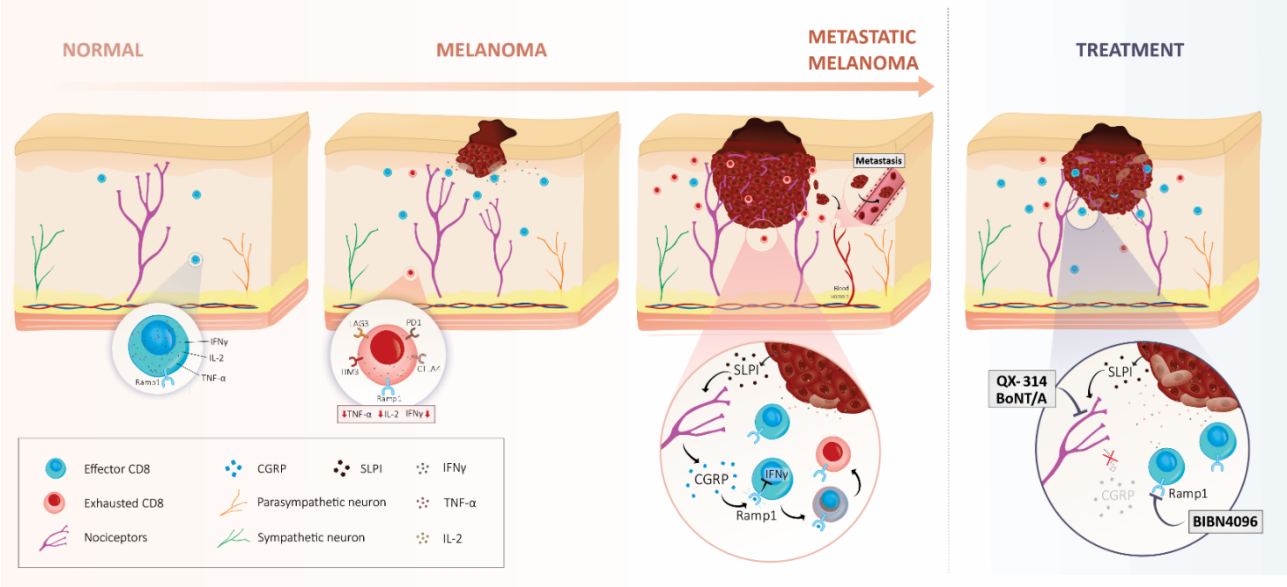

Figure 27.Melanoma-innervating nociceptors impair cancer immunosurveillance. Melanoma growth sets off anti-tumor immune responses, including the infiltration of effector CD8 T-cells and their subsequent release of cytotoxic cytokines (i.e., IFNγ, TNFα, Granzyme B). By acting on tissue-resident nociceptor neurons, melanoma-produced SLPI promotes pain hypersensitivity, tweaks the neurons' transcriptome, and drives neurite outgrowth. These effects culminate in dense melanoma innervation by nociceptors and abundant release of immunomodulatory neuropeptides. CGRP, one such peptide, acts on tumor-infiltrating effector $CD8^+$ T-cells that express the CGRP receptor RAMP1, increasing their expression of immune checkpoint receptors (i.e., PD1, LAG3, TIM3). Therefore, along with the immunosuppressive environment present in the tumor, nociceptor-produced CGRP leads to the functional exhaustion of tumor-infiltrating $CD8^+$ T-cells, which opens the door to unchecked proliferation of melanoma cells. Genetically ablating (i.e., $Na_V1.8$ or TRPV1 lineage) or pharmacologically silencing (i.e., QX-314, BoNT/A) nociceptor neurons as well as blocking the action of CGRP on RAMP1 using a selective antagonist (i.e., BIBN4096) prevents effector $CD8^+$ T-cells from undergoing exhaustion. Therefore, targeting melanoma-innervating nociceptor neurons constitutes a novel strategy to safeguard host anti-tumor immunity and stop tumor growth.

2.5- Material and methods

Supplementary methods.

Patients' biopsy. Melanoma biopsies were collected at Sanford Health, de-identified and classified by a board-certified pathologist. Sanford Health IRB company established that these samples were not considered human subjects research, and no IRB number was assigned. In brief, DERM103 patient sample classified as a malignant melanoma from the left posterior shoulder, MART-1 and HMB45 positive, melanocytic in nature (Elastic positive), and MIB-1 positive (increased proliferation). DERM107 patient sample classified as malignant melanoma, high mitotic index, invasive, stage pT2a, MART-1, SOX-10, P16, and HMB45 positive. DERM110 patient sample classified as malignant melanoma; high mitotic index, Clark's level IV, stage pT1b; the tumor appeared to be invading the epidermis with a fusion of malignant sheets of cells, strongly positive for SOX-10, MART-1, HMB45 with a moderate increase in proliferative index.

IHC Staining and Scoring. Patient melanoma skin biopsies were stained using a BenchMark XT slide staining system (Ventana Medical Systems). The Ventana iView DAB detection kit was used as the chromogen, and slides were counterstained with hematoxylin and anti-TRPV1 (Alomone Labs, ACC-030; 1:100). H&E staining followed standard procedures. TRPV1 IHC stained human samples were analyzed on an Olympus BX51 bright-field microscope. Sections were viewed under 20× magnification. Five random fields per sample for both tumor and adjacent normal tissue were analyzed and scored on a scale from 0-3. Scores were averaged. A score of 0 indicates no appreciated nerve fibres in the evaluated field; +1 indicates sparse nerve fibres; +2 indicates 5-20 nerve fibres; +3 indicates >20 nerve fibres.

Animals. The Institutional Animal Care and Use Committees of Boston Children's Hospital and the Université de Montréal (CDEA: #21046; #21047) approved all animal procedures. Mice were housed in standard environmental conditions (12h light/dark cycle; 23^{o}C; food and water ad libitum) at facilities accredited by the Association for Assessment and Accreditation of Laboratory Animal Care.

6-8-week-old C57BL6J (Jax, #000664); CD45.1^{+} C57BL6J (Jax, #002014), RAMP1$^{-/-}$ (Jax, #031560), RAG1$^{-/-}$ (Jax, #002216), OT-1 (Jax, #003831)[467], TRPV1^{cre} (Jax, #017769)[468], ChR2$^{fl/fl}$ (Jax, #012567)[469], td-tomato$^{fl/fl}$ (Jax, #007908)[470], DTA$^{fl/fl}$ (Jax, #009669)[471] or DTA$^{fl/fl}$ (Jax, #010527), QuASR2$^{fl/fl}$ (Jax, #028678)[472], mice were purchased from Jackson Laboratory. Na$_V$1.8^{cre} mice[473] were generously supplied by Professor Rohini Kuner (Heidelberg University) and Professor John Wood (UCL). Excluding CD45.1^{+} mice, all other lines were backcrossed >6 generations on C57BL6/J background (H2-Kb). It is worth noting that while the Capechi DTA$^{fl/fl}$ (Jax, #010527) was created on a mixed C57BL6J/129 background, both haplotypes are H2-Kb. These mice are therefore fully compatible to be transplanted with B16F10-derived cells (C57BL6/J background (H2-Kb)).

We used the cre/lox toolbox to engineer the various mice lines used (TRPV1^{cre}::DTA$^{fl/wt}$, TRPV1^{cre}::QuASR2$^{fl/wt}$, TRPV1^{cre}::Td-tomato$^{fl/wt}$, Na$_V$1.8^{cre}::DTA$^{fl/wt}$, Na$_V$1.8^{cre}::ChR2$^{fl/wt}$ and littermate control) by crossing male heterozygote Cre mice with female homozygous loxP mice.

All Cre driver lines used were viable and fertile, and abnormal phenotypes were not detected. Offspring were tail-clipped; tissue was used to assess the presence of transgene by standard PCR, as described by Jackson Laboratory. Offspring were used at 6-14 weeks of age.

QX-314. Starting one day post tumor inoculation (defined as prophylactic), QX-314 [449] (Tocris, #2313; 0.3%) was injected (i.d.) daily in 5 points around the tumor. In another group of mice, QX-314 daily injection started once the tumor reached a volume of ~200mm^3 (defined as therapeutic).

BoNT/A. Botulinum neurotoxin A [474] (List biological labs, #130B; 25 pg/µl) was injected (i.d.) three and one days prior to tumor inoculation (defined as prophylactic). BoNT/A (25 pg/µl; i.d.) was injected in 5 points around the tumor one and three days after the tumor reached a volume of ~200mm^3 (defined as therapeutic) in another group of C57BL/6 mice.

BIBN4096. Starting one day post tumor inoculation, BIBN4096 [45] (Tocris, #4561; 5mg/kg) was administered systemically (i.p.) on alternate days (*q.a.d.*) to 8-week-old male and female mice (*defined as prophylactic*). In another group of mice, BIBN4096 (5mg/kg) was administered systemically (i.p.) on alternate days (*q.a.d.*) once the tumor reached a volume of ~200mm^3 (*defined as therapeutic*).

Resiniferatoxin. RTX (Alomone labs, Cat #: R-400) was injected (s.c) in three dosages (30, 70, 100 µg/kg) into the right flank of ~3 weeks old RAG1$^{-/-}$ and C57BL/6 mice. Denervation was confirmed 28-days post-RTX by an absence of pain withdrawal reflex (paw flinching) when exposed to noxious heat (Hargreaves apparatus).

Cell lines. B16F0[475] (ATCC, #CRL-6322), B16F10[476] (ATCC, #CRL-6475), B16F10-mCherry-OVA[477] (Matthew F. Krummel, UCSF), B16F10-eGFP (Imanis, #CL053), YUMM1.7[444] (Marcus Bosenberg, Yale U), and non-tumorigenic keratinocytes (CellnTEC, #MPEK-BL6100) were cultured in complete Dulbecco's Modified Eagle's Medium high glucose (DMEM, Corning, #10-013-CV) supplemented with 10% fetal bovine serum FBS, Seradigm, #3100) and 1% penicillin/streptomycin (Corning, #MT-3001-Cl), and maintained at 37°C in a humidified incubator with 5% CO_2. YUMMER1.7[443] (Marcus Bosenberg, Yale U) cells were cultured in DMEM F12 (Gibco; #11320033) supplemented with 10% fetal bovine serum (Seradigm, #3100), 1% penicillin/streptomycin (Corning, #MT-3001-Cl) and MEM nonessential amino acids (Corning; #25-025Cl), and maintained at 37°C in a humidified incubator with 5% CO_2. The cell lines tested negative for mycoplasma.

Cancer inoculation and volume measurement. Cancer cells (5x10^5 cells) were resuspended in Phosphate Buffered Saline (PBS, Corning #21040CV) and injected to the mice's skin right flank (i.d., 150 µl) or hindpaw (i.d., 50 µl). Growth was assessed daily using a handheld digital caliper and tumor volume was determined by the formula $(L \times W2 \times 0.52)$[478], in which L = length and W = width.

Survival analysis. In dedicated groups of mice, orthotopic B16F10-mCherry-OVA (5x10^5 cells; i.d.) cells were administered to intact and nociceptor ablated mice and survival was measured until day 22 and determined by tumor reaching a volume ≥ 1000 mm^3 or pre-determined ethical endpoint (i.e, ulceration). In B16F10-mCherry-OVA inoculated mice treated with QX-314 or

BIBN4096, the survival was measured until day 19 and determined by tumor reaching a volume ≥ 800 mm^3 or predetermined ethical endpoint.

iDISCO imaging. Whole-mount immunohistochemistry of tumors was performed using an iDISCO protocol with methanol pre-treatment optimized for tumors[436]. Briefly, adult animals (8 weeks) were perfused with 25 mL of PBS (HyClone) and 25mL of 4% paraformaldehyde (Sigma) sequentially at room temperature (RT). Tumors were postfixed with 4% PFA for 6h at 4°C. For methanol pre-treatment, fixed tumors were washed sequentially in 50% methanol (in PBS) for 1 hr, 100% methanol for 1 hr, and then bleached in 5% H2O2 in 20% DMSO/methanol overnight at 4°C. Tumors were subsequently rehydrated in 100% methanol for 1hr twice, 20% DMSO/methanol for 1hr twice, 50% methanol in PBS for 1hr, PBS for 1 hr twice, and PBS/0.2% Triton X-100 for 1 hr twice at RT. Tumors were then left in PBS/0.2% Triton X-100/20% DMSO/0.3 M glycine (Sigma) overnight at RT and blocked in PBS/0.2% Triton X-100/10% DMSO/6% donkey serum (Jackson ImmunoResearch)/anti-CD16/CD32 (Fc block; Bio X cell) overnight at RT. Tumors were subsequently washed in PBS/0.2%

Tween-20/10 mg/mL heparin (Sigma) (PTwH), for 1h twice at RT before incubation with antibody mix (GFP (Aves Labs) at 1:500, mCherry (OriGene) at 1:500, in PTwH/5% DMSO/3% donkey serum/Fc block 1:100 for 4 days at RT. Tumors were extensively washed in PTwH at least 6 times over the course of 1 day at RT. Tumors were further incubated with a secondary panel of species-specific anti-IgG (H+L) Alexa Fluor 488 or 546-conjugated antibodies (Invitrogen or Jackson ImmunoResearch), all at 1:500, in PTwH/5% DMSO/3% donkey serum/Fc block 1:100 for 3 more days at RT. Tumors were washed in the same way as after primary antibody incubation for 1 day. Immunolabeled tumors were then processed for clearing, which included sequential incubation with 50% methanol for 1 hr at RT, 100% methanol for 1 hr three times at RT, and a mixture of 1 part benzyl alcohol (Sigma): 2 parts benzyl benzoates (Sigma) overnight at 4°C. For tdTomato and GFP immunolabeling, mCherry and GFP antibodies were preabsorbed against tumors from $tdTomato^-$ animals overnight at RT prior to use. Cleared whole mount tissues were imaged in BABB between two cover glasses using Olympus FV3000 confocal imaging system.

Tumor and tumor-draining lymph node digestion. Mice were euthanized when the tumor reached a volume of 800-1500 mm^3 [479,475,476]. Tumors and their draining lymph nodes (tdLN) were harvested. Tumors were enzymatically digested in DMEM + 5% FBS (Seradigm, #3100) + 2 mg/ml collagenase D (Sigma, #11088866001) + 1 mg/ml Collagenase IV (Sigma, #C5138-1G) + 40 ug/ml DNAse I (Sigma, #10104159001) under constant shaking (40 min, 37°C). The cell suspension was centrifuged at 400 g for 5 min. The pellet was resuspended in 70% Percoll gradient (GE Healthcare), overlaid with 40% Percoll, and centrifuged at 500g for 20 min at room temperature with acceleration and deceleration at 1. The cells were aspirated from the Percoll interface and passed through a 70-µm cell strainer. Tumor-draining lymph nodes were dissected in PBS + 5% FBS, mechanically dissociated using a plunger, strained (70µm), and washed with PBS.

Immunophenotyping. Single cells were resuspended in FACS buffer (PBS, 2% FCS, EDTA), Fc blocked (0.5 mg/ml, 15 min; BD Biosciences, #553141) and stained (15 min, RT) with ZombieAqua (BioLegend, #423102) or (15 min, 4°C) a Viability Dye eFluor 780 (eBioscience, #65-0865-14). The cells were than stained with either of anti-CD45-BV421 (1:100, BioLegend, #103134), anti-CD45.1-BV421 (1:100, BioLegend, #110732), anti-CD45.2-BV650 (1:100, BioLegend, #109836), anti-CD45-

Alexa Fluor 700 (1:100, BioLegend, #103128), anti-CD11b-APC/Cy7 (1:100, BioLegend, #101226), anti-CD8-AF700 (1:100, BioLegend, #100730), anti-CD8-BV421 (1:100, BioLegend, #100753), anti-CD8-PerCP/Cyanine5.5 (1:100, BioLegend, #100734), anti-CD8-Pacific Blue (1:100, BioLegend, #100725), anti-CD4-PerCP/Cyanine5.5 (1:100, BioLegend, #100540), anti-CD4-FITC (1:100, BioLegend, #100406), anti-PD-1-PE-Cy7 (1:100, BioLegend, #109110), anti-Lag3-PE (1:100, BioLegend, #125208), anti-Lag3-PerCP/Cyanine5.5 (1:100, BioLegend, #125212), anti-Tim-3-APC (1:100, BioLegend, #119706), and analyzed using a LSRFortessa or FACSCanto II (Becton Dickinson). Antigen specific $CD8^+$ T cells were stained with H-2Kb/OVA257-264 (NIH tetramer core facility) for 15 minutes at 37°C and were than stained with surface markers. Cytokines expression were analyzed after *in vitro* stimulation *(PMA/ionomycin; see Intracellular cytokine staining).*

Intracellular cytokine staining. Cells were stimulated (3h) with phorbol-12-myristate 13-acetate (PMA; 50 ng/ml, Sigma- Aldrich, #P1585), Ionomycin (1 µg/ml, Sigma-Aldrich, #I3909) and Golgi Stop (1:100, BD Biosciences, #554724). The cells were than fixed/permeabilized (1:100, BD Biosciences, #554714) and stained with anti-IFN-γ-APC (1:100, BioLegend, #505810), anti-IFN-γ-FITC (1:100, BioLegend, #505806), anti-TNFα-BV510 (1:100, BioLegend, #506339), anti-TNFα-BV5711 (1:100, BioLegend, #506349), anti-TNFα-PE (1:100, BioLegend, #506306), anti-IL2-Pecy7 (1:100, BioLegend, #503832), anti-IL-2-Pacific Blue (1:100, BioLegend, # 503820), anti-IL-2-BV510 (1:100, BioLegend, #503833), and analyzed using a LSR Fortessa or FACSCanto II (Becton Dickinson).

***In vivo* depletion of CD3 or CD8**. Anti-mouse CD3 (200 µg/mouse, Bio X Cell, #BE0001-1) or anti-mouse CD8 (200 µg/mouse, Bio X Cell, #BP0061) were injected (i.p.), 3 days prior to B16F10-mCherry-OVA inoculation (5×10^5 cells; i.d.) and continued every 3 days. Blood samples were taken twice weekly to confirm depletion, and tumor growth was measured daily.

***In vivo* CGRP injection**. TRPV1 ablated mice were injected (i.d.) once daily with recombinant CGRP (100nM) at 5 points around the tumor (treatment began once the tumor was visible), and tumor growth was measured daily by a handheld digital caliper. Mice were sacrificed, and tumor infiltrated $CD8^+$ cells exhaustion was immunophenotyped by flow cytometry using a LSRFortessa or FACSCanto II (Becton Dickinson).

αPDL1 treatment. Orthotopic B16F10-mCherry-OVA cells (5×10^5 cells; i.d.) were inoculated into 8-week-old male and female sensory neuron intact or ablated mice. On days 7-, 10-, 13-, and 16-days post-tumor inoculations, the mice were treated with αPD-$L1^{480}$ (Bio X Cell, #BE0101, 6 mg/kg; i.p.) or its vehicle. Twenty-one days post-tumor inoculation, the impact of αPDL1 was analyzed on tumor growth while TILs exhaustion was immunophenotyped using a LSRFortessa or FACSCanto II (Becton Dickinson).

αPDL1 treatment in mice with same size tumor. Orthotropic B16F10-mCherry-OVA cells (5×10^5 cells; i.d.) were injected into a cohort of nociceptor neuron-ablated mice 3 days prior to one given to nociceptor intact animals. Mice from each group with similar tumor size (~$85mm^3$) were selected and exposed to αPD-$L1^{480}$ (Bio X Cell, #BE0101, 6 mg/kg; i.p.) once every 3 days for a total of 9 days. The impact of αPDL1 treatment was analyzed on tumor growth until day 20.

Orthotropic B16F10-mCherry-OVA (5×10^5 cells; i.d.) were injected into mice treated with QX-314 (0.3%; i.d.) 2-3 days prior to being given to vehicle-exposed mice. Mice from each group with

similar tumor size (~100mm^3) were selected and exposed to αPD-L1 [31] (Bio X Cell, #BE0101, 6 mg/kg; i.p.) once every 3 days for a total of 9 days. Sixteen days post-tumor inoculation, the impact of αPDL1 was analyzed on tumor growth while TILs exhaustion was immunophenotyped using a LSRFortessa or FACSCanto II (Becton Dickinson).

Adoptive transfer of RAMP1^{wt} or RAMP1$^{-/-}$ CD8 T-cells. Total CD8$^+$ T-cells were isolated from the spleen of wild-type (CD45.1$^+$) or RAMP1$^{-/-}$ (CD45.2$^+$) mice, expanded and stimulated *in vitro* using a mouse T-cell Activation/Expansion Kit (Miltenyi cat #130-093-627). CD8$^+$ cells from RAMP1$^{-/-}$ and RAMP1^{wt} were injected separately or 1:1 mix through tail vein of RAG1$^{-/-}$ mice. One week after, the mice were inoculated with B16F10-mCherry-OVA cancer cells (5×10^5 cells; i.d.), and tumor growth was measured daily using a handheld digital caliper. On day 10, tumors were harvested and RAMP1$^{-/-}$ (CD45.2$^+$) and RAMP1^{wt} (CD45.1$^+$) CD8$^+$ T-cells were immunophenotyped using a FACSCanto II (Becton Dickinson) or FACS-purified using a FACSAria IIu cell sorter (Becton Dickinson).

RNA sequencing of adoptive transferred RAMP1^{wt} or RAMP1$^{-/-}$ CD8 T-cells. For FACS-purified cells, RAMP1$^{-/-}$ and RAMP1^{wt} CD8$^+$ T-cells RNA-seq libraries were constructed using KAPA Hyperprep RNA (1x75bp) following the manufacturer's instructions. Nextseq500 (0.5 Flowcell High Output; 200 M de fragments; 75 cycles Single-End read) sequencing was performed onsite at the IRIC (Institute for Research in Immunology and Cancer) genomic center. Sequences were trimmed for sequencing adapters and low quality 3' bases using Trimmomatic version 0.35 and aligned to the reference mouse genome version GRCm38 (gene annotation from Gencode version M23, based on Ensembl 98) using STAR v2.5.1b[481]. Gene expressions were obtained both as readcount directly from STAR as well as computed using RSEM in order to obtain normalized gene and transcript level expression, in TPM (Transcripts Per Kilobase Million) values, for these stranded RNA libraries. DESeq2 version 1.18.1[482] was then used to normalize gene readcounts. Individual cell data are shown as a $\log_{10}$ of (transcript per million x 1000). These data have been deposited in the National Center for Biotechnology Information (NCBI)'s Gene Expression Omnibus[483] (GSE205863).

Adoptive T-cell transfer in RTX-exposed mice. CD8$^+$ T-cells were isolated from OT-1 mice spleens and magnet-sorted (StemCell; #19858). Naïve CD8$^+$ T-cells (CD8$^+$CD44^{low}CD62L^{hi}) cells were than FACS-purified and injected (1x10^6 cells; i.v., tail vein) to vehicle- or RTX-exposed RAG1$^{-/-}$ mice.

Mechanical hypersensitivity. B16F10-mCherry-OVA (2×10^5 cells; i.d.) or non-cancerous keratinocytes (MPEK-BL6; (2×10^5 cells; i.d.) were inoculated intradermally in the mice's left hindpaw. On alternate days, mechanical sensitivity was evaluated using Von Frey filaments (Ugo Basile, #52-37450-275). To do so, the animals were placed in a test cage with a wire mesh floor and allowed to acclimatize (3 consecutive days; 1h/session). Von Frey filaments of increasing size (0.008-2 g) were applied to the plantar surface and response rate was evaluated using the up-down test paradigm.

Thermal hypersensitivity. B16F10-mCherry-OVA (2×10^5 cells; i.d.) or non-cancerous keratinocytes (MPEK-BL6; (2×10^5 cells; i.d.) were inoculated intradermally to the mice's left hindpaw. On alternate days, thermal sensitivity was evaluated using Hargreaves. To do so, the animals were placed in a Plexiglas box coupled to a heat source (Ugo Basile) and allowed to

acclimatize (3 consecutive days; 1h/session). Radiant heat (intensity: 48) was applied to the hindpaw and the time for withdrawal was measured.

Kinetics of pain and intra-tumoral CD8 T-cells exhaustion. We implanted B16F10-mCherry-OVA (2×10^5 cells; i.d.) in several groups of littermate control ($TRPV1^{wt}::DTA^{fl/wt}$; n=96) and nociceptor-ablated ($TRPV1^{cre}::DTA^{fl/wt}$; n=18) mice. We then evaluated the level of thermal hypersensitivity (daily), tumor size (handheld digital caliper), and intra-tumoral $CD8^+$ T cell exhaustion (flow cytometry) at the time of euthanasia (days 1, 4, 7, 8, 12, 13, 14, 19, 22). We processed these data by determining the percentage change of each data point to the maximal value obtained in the pain, exhaustion, size datasets, and then presented these data as percentages of the maximum (100%).

Optogenetic. Orthotopic B16F10-mCherry-OVA cells (5×10^5 cells; i.d.) were inoculated into the left flank of 8-week-old transgenic male mice expressing the light-sensitive protein Channelrhodopsin2 under the control of the $Na_V1.8$ promoter ($Na_V1.8^{cre}::ChR2^{fl/wt}$). Optogenetic stimulation (3.5 ms, 10Hz, 478nm, 60 mW, in a 0.39 NA fiber placed 5-10 mm from the skin, for 20 min) started either when the tumor was visible (~$20mm^3$; five days post inoculation) or when it reached a $200mm^3$ volume (eight days post inoculation) and lasted up to 14 days post tumor inoculation. The control mice ($Na_V1.8^{cre}::ChR2^{fl/wt}$) were not light-stimulated. Groups of littermate control ($Na_V1.8^{wt}::ChR2^{fl/wt}$) mice were light stimulated and show no response (not shown).

CGRP release from skin explant. Tumor-surrounding skin was harvested using 10 mm punch biopsies from nociceptor intact ($Na_V1.8^{wt}::DTA^{fl/wt}$), nociceptor ablated ($Na_V1.8^{Cre}::DTA^{fl/wt}$), light-sensitive nociceptor ($Na_V1.8^{cre}::ChR2^{fl/wt}$), or wild-type mice 3h following the exposure to vehicle (100 µl), QX-314 (0.3%, 100 µl) or BoNT/A (25 pg/µL, 100µl), The biopsies were transferred into 24-well plates and cultured in DMEM containing 1 µl/ml of protease inhibitor (Sigma, #P1860) and capsaicin (1 µM. Sigma, #M2028). After 30 min incubation (37°C), the supernatant was collected and CGRP release analyzed using a commercial ELISA[474] (Cayman Chemical, #589001).

Neuron culture. Mice were sacrificed, and dorsal root ganglia (DRG) were dissected out into DMEM medium (Corning, #10-013-CV), completed with 50U/mL penicillin and 50 µg/ml streptomycin (Corning, #MT-3001-Cl) and 10% FBS (Seradigm, #3100). Cells were then dissociated in HEPES buffered saline (Sigma, #51558) completed with 1 mg/mL collagenase IV (Sigma, #C0130) + 2.4 U/mL Dispase II (Sigma, #04942078001) and incubated for 80 min at 37°C. Ganglia were triturated with glass Pasteur pipettes of decreasing size in supplemented DMEM medium, then centrifuged over a 10% BSA gradient and plated on laminin (Sigma, #L2020) coated cell culture dishes. Cells were cultured with Neurobasal-A medium (Gibco, #21103-049) completed with 0.05 ng/µL NGF (Life Technologies, #13257-019), 0.002 ng/µL GDNF (PeproTech, #450-51-10), 0.01 mM AraC (Sigma, #C6645) and 200 mM L-Glutamine (VWR, #02-0131), and B-27 supplement (Gibco, #17504044).

Calcium imaging. L3-L5 DRG neurons were harvested and co-cultured with B16F10, B16F0, or MPEK-BL6 for 24-48h. The cells were then loaded with 5 mM Fura-2 AM (BioVision, #2243) in complete Neurobasal-A medium for 30 min at 37°C, washed in Standard Extracellular Solution (SES, 145 mM NaCl, 5 mM KCl, 2 mM $CaCl_2$, 1 mM $MgCl_2$, 10 mM glucose, 10 mM HEPES, pH 7.5),

and response to noxious ligands (100nM capsaicin; 100µM AITC; 1µM ATP) was analyzed at room temperature. Ligands were flowed (15s) directly onto neurons using perfusion barrels followed by buffer washout (105-sec minimum)[472]. Cells were illuminated by a UV light source (Xenon lamp, 75 watts, Nikon), 340 nm and 380 nm excitation alternated by an LEP MAC 5000 filter wheel (Spectra services), and fluorescence emission was captured by Cool SNAP ES camera (Princeton Instruments). 340/380 ratiometric images were processed, background corrected and analyzed (IPLab software; Scientific Analytics), and Microsoft Excel used for post hoc analyses. For SLPI, the DRG neurons were cultured for 24h and then loaded with 5 mM Fura-2 AM in complete Neurobasal-A medium for 45 min at 37°C, washed into SES, and response to noxious ligands (0-10ng/ml of mouse recombinant SLPI (LifeSpan BioSciences, #LS-G13637-10); 1µM capsaicin; 50 mM KCl) were analyzed at room temperature.

Immunofluorescence. $2x10^3$ DRG neurons were co-cultured with $2x10^4$ B16F10-mCherry-OVA for 24-48h. The cells were fixed (4% paraformaldehyde; 30 min), permeabilized (0.1 % Triton X-100, 20 min), and blocked (PBS, 0.1% Triton X-100, 5% BSA, 30 min). The cells were rinsed (PBS), stained, and mounted with vectashield containing DAPI (Vector Laboratories, #H-1000). Images were acquired using a Ti2 Nikon fluorescent microscope.

Neurite length, ramification index, and intersecting radii. $TRPV1^+$ nociceptors ($TRPV1^{cre}$::Td-$tomato^{fl/wt}$) were cultured alone ($2×10^3$ cells) or co-cultured ($2×10^4$ cells) with B16F10-GFP, B16F0, or non-tumorigenic keratinocytes (MPEK-BL6). After 48h, cells were fixed (see immunofluorescence section), and images were acquired using a Ti2 Nikon fluorescent microscope. $TRPV1^+$ (td-tomato) neurons' neurite length was measured using a neurite tracer macro in Image J developed by the Fournier lab[484], while the Schoenen ramification index (SRI) and the number of intersecting radii were measured by a Sholl analysis[485] macro in ImageJ.

$CD8^+$ T cell isolation. 6–8-week-old male and female mice were euthanized, spleen harvested in ice-cold PBS (5% FBS), and mechanically dissociated. The cells were strained (70 µm), RBC lysed (Life Technologies, #A1049201; 2 min), and counted using a hemocytometer. Total $CD8^+$ T-cells were magnet sorted (Stem cell, #19853A) and cultured (DMEM + FBS 10%, Pen/Strep 1% + non-essential amino acid (Corning, #25-025-Cl) + vitamin + β-mercaptoethanol (Gibco, #21985-023) + L-Glutamine (VWR, #02-0131) + sodium pyruvate (Corning, #25-000-Cl)). Cell purity was systematically confirmed after magnet sorting and the numbers of $CD8^+CD62L^{hi}$ immunophenotyped by flow cytometry. To generate cytotoxic T lymphocytes, $2x10^5$ $CD8^+$ T-cells were seeded and stimulated for 48h under T_{c1} inflammatory condition (2 µg/ml plate bounded αCD3/αCD28 (Bio X Cell, #BE00011, #BE00151) + 10 ng/ml rIL-12 (BioLegend, #577008) + 10 µg/ml of anti-IL-4 (Bio X Cell, #BE0045).

***In vitro* cytotoxic $CD8^+$ T-cell stimulation with neuron-conditioned media**. Naive or ablated DRG neurons were cultured (72h) in Neurobasal-A medium supplemented with 0.05 ng/µL NGF (Life Technologies, #13257-019) and 0.002 ng/µL GDNF (PeproTech, #450-51-10). After 48h, the neurobasal medium was removed, neurons were washed with PBS, and 200 µL/well of T-cell media supplemented with 1 µL/ml peptidase inhibitor (Sigma, #P1860) and, in certain cases, capsaicin (1µM) or KCl (50mM) was added to DRG neurons. The conditioned media or vehicle were collected after 30min and added to T_{c1} $CD8^+$ T-cells for another 96h. The $CD8^+$ T-cells expression of exhaustion markers (PD-1, Lag-3, Tim-3) and cytokine (IFN-γ, TNF-α, IL-2) were

analyzed by flow cytometry using a LSRFortessa or FACSCanto II (Becton Dickinson). Cytokines expression were analyzed after *in vitro* stimulation *(PMA/ionomycin; see Intracellular cytokine staining).*

***In vitro* cytotoxic CD8$^+$ T-cell stimulation with CGRP**. CD8$^+$ T-cells were isolated and stimulated under T_{c1} condition in 96 wells plate. After 48h, cells were treated with either CGRP (0.1 µM) or PBS in the presence of peptidase inhibitor (1 µM) for another 96h. Expression of PD-1, Lag-3, and Tim-3, as well as IFN-γ, TNF-α, and IL-2, was immunophenotyped by flow cytometry using a LSRFortessa or FACSCanto II (Becton Dickinson). Cytokines expression were analyzed after *in vitro* stimulation *(PMA/ionomycin; see Intracellular cytokine staining).*

***In vitro* DRG neuron silencing with Botox**. Naive DRG neurons (2×10^4) were seeded in a 96 well plate with neurobasal medium supplemented with NGF and GDNF. Neurons were pretreated with 50 pg/ml of BoNT/A for 24h. After 24 hours, the culture medium was removed, neurons were washed with PBS and 200 µl/well of T-cell media supplemented with 1 µl/ml peptidase inhibitor, and KCl (40 mM) was added to DRG neurons. The conditioned media or vehicle were collected after 30 min and added to T_{c1} CD8$^+$ T-cells for another 96h.

***In vitro* RAMP1 blockade**. αCGRP (Bioss, #bs-0791R), $CGRP_{8-37}$ (Tocris, #1169), and BIBN4096 (Tocris, #4561) were used in culture. CD8$^+$ T-cells were treated with BIBN4096 (4µM) 6h before being exposed to the neurons' conditioned media. For CGRP antagonists, the neurons' conditioned media were incubated for 1h with 2 µg/ml of αCGRP and 1 µg/ml of $CGRP_{8-37}$ before being added to the CD8$^+$ T-cells.

CD8$^+$ T-cell and DRG neurons co-culture. Naive DRG neurons (2×10^4) were seeded in a 96-well-plate with T-cell media (supplemented with 0.05 ng/µL NGF (Life Technologies, #13257-019), 0.002 ng/µL GDNF (PeproTech, #450-51-10). One day after, T_{c1} CD8$^+$ cells (1×10^5) were added to the neurons in the presence of IL-2 (BioLegend, #575408). In some instances, co-cultures were stimulated with either capsaicin (1 µM) or KCl (50mM). After 96h, the cells were collected by centrifugation (5 min at 1300 rpm), stained, and immunophenotyped by flow cytometry using a LSRFortessa or FACSCanto II (Becton Dickinson). Cytokines expression were analyzed after *in vitro* stimulation *(PMA/ionomycin; see Intracellular cytokine staining).*

RNA sequencing of CD8$^+$ T-cell and DRG neurons co-culture and data processing. 1×10^4 naive $TRPV1^{Cre}$::$QuASR2^{fl/wt}$ DRG neurons were co-cultured with 1×10^5 B16F10-mCherry-OVA overnight in T-cell media (supplemented with 0.05 ng/µL NGF (Life Technologies, #13257-019), 0.002 ng/µL GDNF (PeproTech, #450-51-10). After 48h, the cells were detached and TRPV1 neurons (CD45$^-$ eGFP$^+$), and OVA-specific CD8$^+$ T-cells (eGFP$^-$ CD45$^+$ CD3$^+$ CD8$^+$) were FACS-purified using a FACSAria IIu cell sorter (Becton Dickinson) and cell supernatant was collected for ELISAs. RNA-seq libraries were constructed using Illumina TruSeq Stranded RNA LT Kit (Illumina, San Diego, CA) following the manufacturer's instructions. Illumina sequencing was performed at the Fulgent Genetics (Temple City, CA). Reads were aligned to the Mouse mm10 reference genome using STAR v2.7[481]. Aligned reads were assigned to genic regions using featureCounts function from subread v1.6.4[486]. Gene expression levels were represented by TPM (Transcripts Per Kilobase Million). Hierarchical clustering was computed using heatmap.2 function (ward. D2 method) from gplots R package. Differential gene expression analysis was carried out by DeSeq2 v1.28.1[482].

These data have been deposited in the National Center for Biotechnology Information (NCBI)'s Gene Expression Omnibus[483] (GSE205865).

ELISA on CD8$^+$ T-cell and DRG neurons co-culture. SLPI (R&D Systems, #DY1735-05), TSLP (BioLegend, # 434104), and HMGB1 (Novus Biologicals, #NBP2-62767) levels were measured in the cells' supernatant (as described above) using commercial ELISA.

***In vitro* B16F10 cells apoptosis**. 2×10^4 naive TRPV1^{Cre}:QuASR2$^{fl/wt}$ DRG neurons were co-cultured with 1×10^5 B16F10-mCherry-OVA overnight in T-cell media (supplemented with 0.05 ng/µL NGF (Life Technologies, #13257-019), 0.002 ng/µL GDNF (PeproTech, #450-51-10). One day after, 4 $\times10^5$ stimulated OVA-specific CD8$^+$ T-cells under T_{c1} condition were added to the co-culture. After 48h, the cells were detached by trypsin (Gibco, #2062476) and collected by centrifugation (5 min at 1300 rpm), stained using anti-Annexin V, 7-AAD (BioLegend, #640930), and anti-CD8 for 20 minutes at 4^{o}C, and were immunophenotyped by flow cytometry using a FACSCanto II (Becton Dickinson). Cytokines expression were analyzed after *in vitro* stimulation *(PMA/ionomycin; see Intracellular cytokine staining).*

For neuron condition media, 4×10^5 stimulated OVA-specific CD8$^+$ T-cells were added to 1×10^5 B16F10-mCherry-OVA and treated with fresh condition media (1:2 dilution). After 48h, cells were stained using anti-Annexin V, 7-AAD (BioLegend, #640930), and anti-CD8 for 20 minutes at 4^{o}C, and were immunophenotyped by flow cytometry using a LSRfortessa or FACSCanto II (Becton Dickinson). For CGRP, 4×10^5 stimulated OVA-specific CD8$^+$ T-cells were added to 1×10^5 B16F10-mCherry-OVA and treated with CGRP (100nM). After 24h the cells were stained using anti-Annexin V, 7-AAD (BioLegend, #640930), and anti-CD8 for 20 minutes at 4^{o}C, and were immunophenotyped by flow cytometry using a LSRFortessa or FACSCanto II (Becton Dickinson). Cytokines expression were analyzed after *in vitro* stimulation *(PMA/ionomycin; see Intracellular cytokine staining).*

RNA sequencing of triple co-culture and data processing. 1×10^4 naive TRPV1^{Cre}:QuASR2$^{fl/wt}$ DRG neurons were co- cultured with 1×10^5 B16F10-mCherry-OVA overnight in T-cell media (supplemented with 0.05 ng/µL NGF (Life Technologies, #13257-019), 0.002 ng/µL GDNF (PeproTech, #450-51-10). One day after, 4 $\times10^5$ stimulated OVA-specific CD8$^+$ T-cells under T_{c1} condition were added to the co-culture. After 48h, the cells were detached and TRPV1 neurons (CD45$^-$ eGFP$^+$ mCherry$^-$), B16F10-mCherry-OVA (CD45$^-$ eGFP$^-$ mCherry$^+$), and OVA-specific CD8$^+$ T-cells (eGFP$^-$ mCherry-CD45$^+$ CD3$^+$ CD8$^+$) were FACS-purified using a FACSAria IIu cell sorter (Becton Dickinson). RNA-seq libraries were constructed using Illumina TruSeq Stranded RNA LT Kit (Illumina, San Diego, CA) following the manufacturer's instructions. Illumina sequencing was performed at the Fulgent Genetics (Temple City, CA). Reads were aligned to the Mouse mm10 reference genome using STAR v2.7[481]. Aligned reads were assigned to genic regions using featureCounts function from subread v1.6.4[486]. Gene expression levels were represented by TPM (Transcripts Per Kilobase Million). Hierarchical clustering was computed using heatmap.2 function (ward. D2 method) from gplots R package. Differential gene expression analysis was carried out by DeSeq2 v1.28.1[482]. These data have been deposited in the National Center for Biotechnology Information (NCBI)'s Gene Expression Omnibus[483] (GSE205864).

B16F10 survival. 1x10^5 B16F10 cells were cultured in 6-well-plate and challenged with BoNT/A (0-50 pg/µL) for 24h, QX-314 (0-1%) for 72h, BIBN4096 (1-4 µM) for 24h or their vehicle. B16F10 cell survival was assessed using anti-annexin V staining and measured by flow cytometry using a LSRFortessa or FACSCanto II (Becton Dickinson) or counted using a hemocytometer.

***In-silico* analysis of neuronal expression profile using RNA Sequencing and Microarray datasets**. Publicly available RNA Gene expression from seven datasets[487,488] were downloaded from the NCBI GEO portal. RNA Gene expression values of genes of interest were extracted. Expression values from single cell sequencing were averaged for all cells. To be able to compare expression from datasets that were generated using different techniques (scRNAseq, bulk RNAseq, microarrays) and normalization methods (TPM, RPKM, RMA, UMI), all genes of interest were ratioed over *Trpv1* expression, then multiplied by 100, and the Log_{10} of these values were plotted as a heatmap. *Kupari et al.,*[488] used single-cell RNA-sequencing of JNC neurons while *Usoskin et al.,*[489] and *Li et al.,*[490] used single-cell RNA-sequencing of lumbar neurons. *Chiu et al.,*[491] respectively measured gene expression by microarrays of whole and FACS-sorted NaV1.8$^+$ lumbar neurons. *Goswami et al.,*[487] performed RNA sequencing of TRPV1$^+$ lumbar neurons, whilst *Ray et al.,*[492] performed RNA-sequencing of human lumbar neurons.

***In-silico* analysis of melanoma patients' tumor expression profile using single-cell RNA sequencing**. Using the publicly available Broad Institute single-cell portal, we proceed to an in-silico analysis of single-cell RNA-sequencing of human melanoma biopsies. We assessed the gene profile of *Ramp1*-expressing and *Ramp1*-negative T cell in patients' tumor with metastatic melanoma[456]. Similarly, we assessed the genetic program of *Ramp1*-expressing and *Ramp1*-negative CD8$^+$ T-cells in patient with melanoma[455]. The latter dataset was also used to analyze the genetic profile of CD8$^+$ T-cells in patients responsive to immune checkpoint blocker or unresponsive to such treatment as well as the genetic profile of malignant melanoma cells (defined as CD90$^-$CD45$^-$) from 10 different patients' biopsies[455]. Individual cell data are shown as a log_2 of 1 + (transcript per million / 10). Experimental details and cell clustering were defined in *Tirosh et al.,*[456] and *Jerby-Arnon et al.,*[455].

***In-silico* analysis of human immune cells expression profile**. Publicly available RNA Gene expression from Monaco et al.,[457] was downloaded from the NCBI GEO portal. Read counts normalized to transcripts per million protein-coding genes (pTPM) values for genes of interest were extracted. Expression values from single cell sequencing were averaged for all cells. Experimental details and cell clustering were defined in *Monaco et al.,*[457].

***In-silico* analysis of cultured B16F10 cells expression profile**. Publicly available RNA Gene expression from Castle et al.,[458] was downloaded from the NCBI GEO portal. Read counts normalized to transcript per million (TPM) for genes of interest were extracted. Experimental details and cell clustering were defined in *Castle et al.,*[458].

***In-silico* analysis of mouse immune cells expression profile using the Immgen database**. Using the publicly available Immgen database we proceed to an in-silico analysis of RNA-sequencing data (DESeq2 data) of various mouse immune cells. As per Immgen protocol, RNA-sequencing reads were aligned to the mouse genome GENCODE GRCm38/mm10 primary assembly and gene annotations vM16 with STAR 2.5.4a. The ribosomal RNA gene annotations were removed from

general transfer format file. The gene-level quantification was calculated by featureCounts. Raw reads count tables were normalized by median of ratios method with DESeq2 package from Bioconductor and then converted to GCT and CLS format. Samples with less than 1 million uniquely mapped reads were automatically excluded from normalization. Experimental details were defined in *www.immgen.org/Protocols/ImmGenULI_RNAseq_methods.pdf*.

Oncomine. *In-silico* analysis of melanoma patient biopsy expression profile using BULK microarray sequencing. As described in Haqq et al., samples from forty-five cutaneous melanomas and 18 benign melanocytic skin nevus biopsies (~5-20µm) were harvested, amplified and transcriptome profiled using Affymetrix U133A microarrays. Data were downloaded from oncomine database (www.oncomine.org) as $\log_2$ (median centered intensity) and gene of interest were displayed as heatmaps. Experimental details and cell clustering were defined in *Haqq et al.,*[432].

Melanoma patient survival analysis. OncoLnc (www.oncolnc.org) contains survival data for 8,647 patients from 21 cancer studies performed by The Cancer Genome Atlas (TCGA)[454]. Using OncoLnc we assess transcript expression of a user defined list of 333 neuronal-enriched genes (neuronal membrane proteins, neural stem cell markers, transcription factors, ion channel receptors, and neuropeptides) in 459 skin cancer (SKCM) tumor biopsies from the Cancer Genome Atlas (TCGA) database. Of these genes, 206 were expressed, and 108 were selected based on their negative Cox coefficient value, indicating a link between lower gene expression and improved patient survival. Kaplan-Meier curves show the patients' survival after segregation in two groups defined by their low or high expression of a gene of interest. Details of patients can be found in the Cancer Genome Atlas[454] and computational analysis were defined by *Anaya et al., 2016* (*doi.org/10.7717/peerj-cs.67*).

Data availability statement. The datasets generated and/or analyzed during the current study are available at www.talbotlab.com/new-page (Password: Nature) of from the corresponding author on reasonable request. The RNA sequencing datasets have been deposited in the National Center for Biotechnology Information's Gene Expression Omnibus (#GSE205863, #GSE205864, #GSE205865).

Statistics. Data expressed as mean ± S.E.M. Statistical significance determined by Mantel-Cox regression (survival curve), one-way or two-way ANOVA for multiple comparisons and two-tail unpaired Student t-test for single variable comparison. P-values less than 0.05 were considered significant. Numbers of animals are defined in figures.

Chaptere 3 : Discussion

The major contribution of this study was to demonstrate the role of tumor-associated sensory neurons in the progression of cancer, which was achieved by the utilization of *in vitro* and *in vivo* models of melanoma cancer. To better understand the mechanism of action of sensory neurons, two major questions need to be answered : which mediators and neuronal genes are involved when tumor cells and tumor-associated neurons interact in the tumor microenvironment, and what is their impact on anti-tumor immunity? To answer these two questions, we performed several *in vitro* experiments, including transcriptomic analysis, tissue staining, tumor–neuron co-culture, and several *in vivo* experiments. The findings of this study opened several avenues of investigation in the field of cancer research. The following paragraphs will discuss our findings, as well as future research that can further cancer research.

3.1- Tumor cells interact with sensory neurons

A growing body of evidence indicates that tumor cells are innervated and innervation supports cancer progression[349,493,494], it has also been shown that neurogenesis (number of neurons) and axonogenesis (neural sprouting in the tumor microenvironment) play a significant role in tumorigenesis[338,349,495]. However, there is contradictory evidence regarding the infiltration of nerve fibers within the tumor[496-498]. Some studies indicate the presence and infiltration of nerve fibers within the tumor, while other reports indicate that nerves are only visible surrounding the tumor or are absent altogether.

One possibility for this contradiction is the variability in types of cancer or stages of tumor development that have been used for staining of the nerve fibers. In this study, iDISCO imaging of $NaV1.8^{+}$ nerve fibers revealed melanoma-infiltrating sensory nerve fibers, and we found that these intra-tumoral sensory neurons contributed to tumor progression **(Figure 14)**. We also carried out an *in vitro* study of DRG neurons with melanoma tumor cells as an approach to study

the interaction of DRG neurons with tumor cells. Several studies have revealed that there is bidirectional communication between tumor cells and DRG neurons, which can influence neurite extension by neurons and the migratory potential of tumor cells through nerves. Semaphorin S4F produced by prostate cancer cells has been shown to induce axonogenesis [348]. In our study, we found that *in vitro* co-culture of DRG neurons with melanoma tumor cells (B16F0 or B16F10) increased neurite outgrowth and upregulated the expression of several neuropeptides secreted by DRG neurons. In addition, the number of neurons responsive to capsaicin, ATP, and mustard oil was significantly increased in presence of melanoma tumor cells. Interestingly, our *in vivo* data also showed that DRG neurons isolated from melanoma-bearing mice showed greater responses to ligands than neurons harvested from tumor-free mice **(Figure 14)**. These results suggested sensitization of these sensory neurons by tumor cells and showed that there is reciprocal communication between DRG neurons and tumor cells. In addition, it is possible that tumor cells may have a systemic effect on the peripheral nervous system.

3.2- Tumor cells sensitize sensory neurons

As a component of the tumor stroma, nerves promote tumor growth, invasion, and metastasis[376].Reciprocal communication between cancer and nerves occurs through factors released by both tumor cells and nerve fibers. Tumor cells release neurotrophic factors, which induce axonogenesis to innervate the growing tumor cells[360], while nerve fibers release neuropeptides and neurotransmitters, which stimulate tumor cell proliferation and survival. Many of these factors, such as glutamate, γ-aminobutyric acid (GABA), noradrenaline or acetylcholine, NGF, and GDNF have already been well studied. Our RNA sequencing data showed that sensitization of DRG neurons by cancer cells resulted in overexpression of a number of genes by DRG neurons, including neuropeptides such as CGRP and galanin, cytokines such as IL-4, IL-10, IL-13, and growth factors such as fibroblast growth factors **(Figuer 14).** On the other hand, we also found that, when co-cultured with DRG neurons, melanoma tumor cells overexpressed a factor known as Secretory Leukocyte Protease Inhibitor (SLPI), which was able to sensitize sensory

neurons. We confirmed this data by measuring the concentration of SLPI in the supernatant obtained from DRG neurons co-cultured with B16F10 cancer cells. We also observed that exposing DRG neurons to SLPI triggered CGRP release and induced calcium flux, supporting the idea that secretion of SLPI by cancer cells is able to sensitize tumor-associated sensory neurons (**Figure 15**).

3.3- Sensitization of tumor-associated neurons induce pain

Cancer-related pain is a common symptom of cancer affecting approximately 66% of patients[499]. Cancer-related pain involves both neuropathic and nociceptive components[500]. Under normal conditions, nociceptor neurons generate pain as a protective mechanism when they are stimulated by a noxious stimulus, in order to prevent tissue injury[501]. Invasion of tumor cells into the nerves, inflammatory mediators, and tumor-induced acidosis in the tumor microenvironment sensitize nociceptive neurons in an abnormal way, resulting in the induction of pain[502-504]. In this study, we found that SLPI increased the excitability of sensory neurons when injected intradermally into the mouse, implicating SLPI as an active nociceptive agent in cancer pain (**Figure 15**). Constant signaling by SLPI in the tumor microenvironment could favor long-term activation of tumor-associated sensory neurons, along with increased levels of neuropeptides. In addition, we found a correlation between pain score and tumor size. We observed that mice with bigger tumors showed higher pain scores in comparison to mice with medium or small tumors. One possible mechanism underlying this difference could be the lower number of infiltrated sensory neurons in smaller tumors, as well as lower levels of inflammatory mediators in the tumor microenvironment. Our results also imply that SLPI could be relevant to the mechanism of pain sensation in cancer patients

Cancer patients can suffer from pain during disease progression and bone metastasis [505]. Tumor cells release inflammatory mediators that induce injury and irritation around the site; however, in most cases, pain associated with bone metastasis is not caused by tissue damage alone, indicating that it has a neuropathic nature[506-510]. The activation of nociceptor neurons in cancer patients by nociceptive mediators can generate pain that reduces their quality of life,

leading to reduced survival. The current study identified SLPI as a mediator that was released by cancer cells and activated sensory neurons. It was also shown, in cancer patients, that lower expression of SLPI was correlated with better survival (**Figure 26**). Therefore, blocking SLPI could be another target for alleviating pain in cancer patients and improving their quality of life. The autocrine or paracrine involvement of neuropeptides or their receptors in promoting tumor metastasis and proliferation indicates that there are amplification loops between sensory nociceptors and cancer cells.

3.4- DRG neurons drive $CD8^+$ T cells exhaustion

The above findings prompted us to investigate the *in vitro* and *in vivo* effects of DRG neurons on the function of the immune system, in particular cytotoxic $CD8^+$ T cells. Effector $CD8^+$ T cells play a crucial role in anti-tumor immunity. In cancer, a high level of T cell exhaustion has been correlated with faster tumor progression. Thus, our *in vitro* results showed that either co-culture of $CD8^+$ T cells with neurons or exposure of $CD8^+$ T cells to supernatant obtained from stimulated neurons accelerated $CD8^+$ T cell exhaustion. Given that neuron supernatant contains various neuropeptides, we tested the effect of individual neuropeptides CGRP, substance P, and galanin on $CD8^+$ T cells. Interestingly, we found that CGRP is the main driver of $CD8^+$ T cell exhaustion, while galanin also partially induced $CD8^+$ T cell exhaustion, and substance P had no effect **(Figure 24**). CGRP has previously been shown to inhibit T cell proliferation through inhibiting IL-2 production by T cells[511]. In this study, we found that $CD8^+$ T cells upregulated CGRP receptor (RAMP1) when they were in direct contact with DRG neurons. Given that CGRP drives $CD8^+$ T cell exhaustion, it is possible that on binding to its receptor, CGRP inhibits IL-2 production by $CD8^+$ T cells through upregulation of immune checkpoint proteins such as PD1. We also found that $CD8^+$ T cells exposed to neuron supernatant or CGRP were less efficient at eliminating B16F10 cancer cells, confirming that neuropeptides secreted by DRG neurons are able to dampen anti-tumor immunity **(Figure 24).**

Although these *in vitro* and *in vivo* experiments were useful for testing neuron–immune and neuron–cancer interactions, it was necessary to investigate the effectiveness of these interactions in a mouse model of cancer, i.e., by examining the effect of ablation or silencing of tumor sensory neurons on immune system responses and control of tumor growth. It was hoped that such investigations would provide a novel insight into the mechanism of tumorigenesis.

3.5- Tumor-associated sensory neurons promote cancer progression

Tumor-associated nerves play an important role in tumor progression and dissemination. However, the role of tumor-associated sensory neurons in this context remains unknown. We found that DRG neuron-derived neuropeptides reduced cancer cell elimination by cytotoxic $CD8^+$ T cells and induced $CD8^+$ T exhaustion **(Figure 16)**. Therefore, it is possible that sensory neurons can suppress anti-tumor immunity through the modulation of immune checkpoint receptor expression by $CD8^+$ T cells. $CD8^+$ T cells are one of the most abundant types of immune cells in tumors, where they play an important role in destroying tumor cells[33,512-518]. Our findings showed that genetic ablation of sensory neurons reduced tumor growth and promoted anti-tumor immunity. Infiltrated $CD8^+$ T cells produced more cytokines and expressed lower level of immune checkpoint receptors, indicating that they were less exhausted. More activated $CD8^+$ T cells correlated with less tumor growth.

Therefore, considering our findings, we concluded that a high level of inflammatory mediators in the tumor can activate tumor-associated sensory neurons and that activated sensory neurons release various neuropeptides that inhibit the infiltration and activation of $CD8^+$ T cells in tumors. As genetic ablation of sensory neurons has the potential to generate indirect side effects and lead to compensatory mechanisms, we also carried out experiments to locally silence tumor-innervated sensory neurons using botulinum toxin A and a membrane-impermeable form

of lidocaine, (QX-314). We found that both approaches decreased tumor growth and reduced $CD8^+$ T cell exhaustion **(Figure 22,23).**

Knowing that neuropeptides can modulate immune responses, we decided to study intra-tumoral neuropeptide signaling in order to uncover possible mechanisms that may be involved in neural suppression of anti-tumor immunity during tumor progression. CGRP has more than one effect on immune responses and affects both immune and non-immune cells. For example, CGRP has been shown to promote inflammation in asthma through upregulation of IL-5 production by ILCs[519] or enhancement of IL-10 production by macrophages[520].

CGRP also inhibits T cell function through upregulating inhibitory genes such as Pdcd1, Tnfrsf18, Entpd1, Lilbr4, Tnfrsf9, and Icos in T cells[198]. To investigate whether *in vivo* release of neuropeptides by neurons promotes $CD8^+$ T cell exhaustion, we pharmacologically blocked neuropeptide signaling. Expression of multiple neuropeptide receptors, including RAMP1, by $CD8^+$ T cells suggests that CGRP may mediate immune suppressive function in tumors. Therefore, we blocked CGRP-RAMP1 signaling using the pharmacological blocking reagent BIBN4096. Our results showed that inhibiting CGRP-RAMP1 signaling significantly reduced tumor growth and $CD8^+$ T cell exhaustion. We confirmed this data using *in vivo* adoptive transfer of $RAMP1^{-/-}$ or $RAMP1^{wt}$ $CD8^+$ T cells to $Rag1^{-/-}$ mice, which lack T and B cells **(Figure 17)**. Using an alternative method, we also found that daily intertumoral injection of CGRP in mice ablated for sensory neurons resulted in similar rates of tumor growth and T cell exhaustion as in nociceptor-intact mice **(Figure 17)**. These data supported the idea that secretion of neuropeptides by sensory neurons is one of the mechanisms by which sensory neuron suppress immune system responses in tumors.

3.6- Melanoma patient biopsies are innervated by TRPV1$^+$ sensory neurons

We found that melanoma patient samples were innervated by TRPV1$^+$ neurons, while staining for TRPV1 was almost two-fold higher in tumors in comparison to healthy adjacent tissue, indicating a higher level of innervation in tumor tissue **(Figure 19)**. Given that we have shown that these sensory neurons are important for controlling tumor growth *in vivo*, specific targeting of these neurons represents an opportunity for clinical intervention. For example, we showed that TRPV1$^+$ neuron function was increased in melanoma tumors, dampening anti-tumor immunity and promoting tumor cell growth. Therefore, inhibiting TRPV1$^+$ neuron function, in combination with other cancer therapeutics, such as immune checkpoint blockers and chemotherapeutic agents, could enhance the efficacy of treatments.

3.7- Neuropeptide-induced modulation of carcinogenesis in human

Several studies have indicated that infiltration of sensory neurons into a tumor can drive tumor-cell proliferation and immune-cell suppression through the local secretion of neurotransmitters and growth factors. These findings have been associated with poor clinical outcomes, metastasis, and reduced patient survival[332,360,521,522]. Neuro-inflammatory neuropeptides including substance P (SP), calcitonin gene-related peptide (CGRP), and neurokinin A (NKA) have been implicated in autocrine or paracrine stimulation of several cancers[523-528]. Increased expression of their receptors on cancer cells was associated with the migration and proliferation of cancer cells. For example, NK1R and NK2R are receptors for SP, which has been shown to promote the migration and aggressiveness of human metastatic breast-cancer cell lines. By contrast, neuropeptide Y1 (NPY1) receptor expression in patients with breast cancer was correlated with the inhibition of tumor-cell proliferation[529].

However, CGRP, after binding to receptor-activity modifying protein 1 (RAMP1) and calcitonin receptor-like receptor (CALCRL), did not have an impact on human breast-cancer cell lines[530], whereas transcriptomic analysis of melanoma biopsies showed that upregulation of neuronal genes, such as calcitonin gene-related polypeptide-alpha (*CALCA*), class III β-tubulin (*TUBB3*), and *RAMP1*, was associated with reduced patient survival **(Figure 26).**

Discovering that neuropeptides acting as growth factors can drive the proliferation of tumor cells in a paracrine or autocrine manner[531] or the overexpression of neuropeptide receptors by human cancers as a factor for prognosis and progression of disease, suggested novel possibilities for translational research. Ttargeting these neuropeptides or their receptors with antibodies, antagonists, or selective inhibitors is not sufficient for the elimination of tumor cells. However, strategies that can block the secretion or biological effects of many neuropeptides can provide an effective approach for treating cancers in which they play a role as a growth factor.

In the current study, different approaches such as silencing by the intracellular sodium-channel blocker QX-314 and botulinum toxin (Botox), genetic ablation, and blocking CGRP receptor by pharmacological blockers were found to decrease tumor growth and boost immune-system responses.

3.8- Neuro-immunotherapy as a theracpeutic approch for cancer

Identifying the mechanism by which nerves suppress immune-system function in the tumor microenvironment (TME) can boost anti-tumor immunity and improve patient survival. Several studies have shown that T cells and other immune cells express receptors for various types of neurotransmitters and neuropeptide including CGRP receptors, dopamine receptors[532-535], glutamate receptors[536-539]acetylcholine receptors[540,541] γ-aminobutyric acid (GABA) receptors[542,543] and vasoactive intestinal peptide (VIP) receptors[544]. Secretion of these neurotransmitters from the nerve endings in the vicinity of immune cells in tumor tissues can affect the function of immune cells cells[545,546] . For example, RNA sequencing of human melanoma-infiltrating T cells showed that expression of RAMP1 by cytotoxic T cells ($CD8^+$ cells) was correlated with a higher expression of immune-checkpoint receptors and lower cytokine production in comparison with $RAMP1^{-/-}$ T cells **(Figure 26)**. These data indicate that the release of CGRP by tumor-associated sensory neurons could drive T-cell exhaustion in patients.

Cancer immunotherapy using immune-checkpoint blockers such as anti-programmed cell death-1 (anti-PD1) or anti-programmed cell death ligand-1 (anti-PDL-1), or adoptive T-cell therapies such as chimeric antigen receptor (CAR) T cells, has revolutionized treatment for several cancers[547,548]. However, it remains necessary to search for the mechanisms that increase the expression of immune-checkpoint receptors in order to improve therapeutic strategies. The present study investigated whether neuropeptides such as CGRP or galanin could drive $CD8^+$ T-cell exhaustion and suppress anti-tumor immunity; to this end, we examined whether blocking these neuropeptides in combination with immune-checkpoint blockers could boost anti-tumor immunity. We found that either local silencing of neurons by QX-314 or Botox, or genetic ablation of sensory neurons in combination with anti-PDL-1, could significantly increase $CD8^+$ T-cell responses, reduce $CD8^+$ T-cell exhaustion, and decrease tumor growth **(Figure 16,21)**.

Consistent with previous findings, our results indicated that direct communication between neurons and either cancer or T cells through neurotransmitters or neuropeptides facilitated tumor progression; therefore, blocking this direct communication by QX-314 or Botox could be beneficial for patients and could be translated into therapeutic approaches.

We proposed that a combination of immunotherapy with neuropeptide blockers, which has been called 'neuro-immunotherapy'[549] could be an effective strategy to improve T-cell adoptive or immune-checkpoint therapy by enhancing T-cell function, proliferation, and migration in the TME. This novel combination may increase survival and improve the quality of life of cancer patients. We hypothesized that this could be achievable based on several sources of evidence such as the ability of neuropeptides to drive T-cell exhaustion and to function as growth factors for tumor cells, involving the generation of neurogenic inflammation and angiogenesis.

3.9- Limitations of the study

Patient samples

One of the limitations of our study was related to access to patient samples. Examining innervation at different stage of tumor progression in different types of cancer would be extremely informative, however, obtaining fresh cancer tissue from clinicians was difficult. Generation of mouse with conditional knockout of CGRP gene in sensory neurons

In this study we showed that CGRP is the key neuropeptide released by DRG neurons to dampen anti-tumor immunity. Although we used pharmacological blockers to inhibit CGRP signaling, it would be extremely useful to confirm these data using mice that are genetically knocked out for secretion of CGRP by sensory neurons. Unfortunately, this strain of mouse was not available.

3.10- Future Directions

The role of nerves in cancer is becoming a hot topic in cancer research. Discovering the role of tumor-infiltrated nerves could assist in uncovering unknown mechanisms used by cancerous cells for progression and migration. Neuronal activity has been correlated with tumor progression in several types of cancers, including prostate, stomach, and colon cancer; however, the mechanism of function of these nerves is still not well understood. So far, our knowledge of mechanism is related to downstream signaling from neurotransmitters and growth factors, which has been shown to be involved in cancer progression and tumor cell division.

There remains much to be discovered about the modulatory role of nerves in the immune system in the context of cancer. Our findings of the suppressive effect of intertumoral neuropeptides on $CD8^+$ T cells in the tumor milieu indicate that there is a strong link between tumor-associated sensory neurons and adaptive immune system function. Knowing that sensory neurons have many different subsets with different functions, the identification of aberrant neurons within the tumor microenvironment could increase our knowledge of the role of nerves in anti-tumor immunity. Given that ablation of sensory neurons would have adverse effects on cancer patients, another strategy would be to perform single cell transcriptomics on tumor-associated sensory neurons in mice in order to identify novel drug targets (a project currently underway in the Talbot Lab). The effect of tumor cells on neurogenesis has been shown by several groups using multiple mouse models of cancer. Since neurons use electrical stimulation as a means of communication within the body, it would be interesting to investigate whether melanoma tumor cells are able to induce electrical stimulation of neurons, and whether this electrical stimulation affects tumor growth.

Several neuropeptides, such as bradykinin (BK), CGRP, and NPY, have been demonstrated to regulate angiogenesis. BK is a neuropeptide that, through binding to the B2 receptor in the endothelial cells, increases capillary permeability and also upregulates the expression of vascular

endothelial growth factor (VEGF) in stromal fibroblasts to promote angiogenesis[550]. CGRP enhances tube formation by endothelial cells and also increases the expression of VEGF in the tumor stroma[551]. NPY has been shown to stimulate endothelial cell migration, proliferation, and differentiation, and also to increase the release of VEGF[552]. However, in this study, we did not investigate the angiogenesis directly, but it would be highly interesting to see if ablation or silencing of sensory neurons by Botox or QX-314 can reduce angiogenesis.

There are several studies indicating that injection of Botox was correlated with improvement. For example, it has been shown that intradermal injection of Botox inhibited scars by reducing the expression of VEGF and angiogenesis[553] or another study showed that intramuscular injection of Botox could reduce expression of VEGF, CD31, and other proteoglycans that are involved in angiogenesis[554]. Also, it has been described that injection of Botox could reduce tumor volume in patients with prostate cancer[555].

However, there is a confliction regarding the inhibitory effect of Botox on angiogenesis. Some studies showed that Botox treatment might increase expression of VEGF and induce protection against ischemia[553]. These findings suggested that investigating the effect of Botox on angiogenesis during the cancer progression can help us to understand weather Botox provides a therapeutic advantage for treatment of cancer.

The role of sensory neurons in affecting the function of the innate immune system also merits investigation. For instance, one group of immune cells whose role in pain has been highlighted is macrophages[556,557]. Macrophage's release neurotrophins, which can stimulate sensory neurons and enhance pain. M2 macrophages induce regeneration of nerves and neurite outgrowth through secretion of VEGF and Semaphorin 4D, respectively[558-560]. Given that macrophages express multiple neuropeptide receptors, it would be interesting to examine whether ablation of sensory neurons affects the function and phenotype of tumor-associated macrophages.

3.11- Conclusion

In conclusion, the signaling of neurons to the immune system has a major impact on the outcome of tumor growth. During the course of studying novel aspects of the somatosensory neuronal control of host immune defense, we found that neurons may form active synapses with cancer cells or cytotoxic T-cells. After stimulation by cancer cells, these neurons release neuropeptides, which bind to receptors on cytotoxic $CD8^+$ T cells and induce overexpression of immune checkpoint receptors. In turn, this dampens the anti-tumor activity of the T cells. It appears that in order to prevent overly intense immune responses, nociceptor neurons can initiate a local retro-control feedback loop to reduce cytotoxic T-cell activity.

Overall, by expressing certain ligands and controlling the expression of immune checkpoint receptors, sensory neurons emerged as inhibitors of host anti-tumor activity. To test the way in which sensory neurons affect tumor development, we ablated or silenced tumor-associated sensory neurons. Our approach revealed that inhibition of sensory neurons decreased tumor growth and enhanced anti-tumor immunity.

4.- Bibliography

1 Spurrell, E. L. & Lockley, M. Adaptive immunity in cancer immunology and therapeutics. *Ecancermedicalscience* 8, 441, doi:10.3332/ecancer.2014.441 (2014).

2 Diogenes, A., Ferraz, C. C., Akopian, A. N., Henry, M. A. & Hargreaves, K. M. LPS sensitizes TRPV1 via activation of TLR4 in trigeminal sensory neurons. *J Dent Res* 90, 759-764, doi:10.1177/0022034511400225 (2011).

3 Lim, J. Y., Choi, S. I., Choi, G. & Hwang, S. W. Atypical sensors for direct and rapid neuronal detection of bacterial pathogens. *Mol Brain* 9, 26, doi:10.1186/s13041-016-0202-x (2016).

4 Akira, S., Uematsu, S. & Takeuchi, O. Pathogen recognition and innate immunity. *Cell* 124, 783-801, doi:10.1016/j.cell.2006.02.015 (2006).

5 Chiu, I. M., Pinho-Ribeiro, F. A. & Woolf, C. J. Pain and infection: pathogen detection by nociceptors. *Pain* 157, 1192-1193, doi:10.1097/j.pain.0000000000000559 (2016).

6 Blake, K. J. *et al.* Staphylococcus aureus produces pain through pore-forming toxins and neuronal TRPV1 that is silenced by QX-314. *Nat Commun* 9, 37, doi:10.1038/s41467-017-02448-6 (2018).

7 Baral, P. *et al.* Nociceptor sensory neurons suppress neutrophil and gammadelta T cell responses in bacterial lung infections and lethal pneumonia. *Nat Med* 24, 417-426, doi:10.1038/nm.4501 (2018).

8 Pinho-Ribeiro, F. A. *et al.* Blocking Neuronal Signaling to Immune Cells Treats Streptococcal Invasive Infection. *Cell* 173, 1083-1097 e1022, doi:10.1016/j.cell.2018.04.006 (2018).

9 Zhu, Z. *et al.* Nerve growth factor and enhancement of proliferation, invasion, and tumorigenicity of pancreatic cancer cells. *Mol Carcinog* 35, 138-147, doi:10.1002/mc.10083 (2002).

10 Sloan, E. K. *et al.* The sympathetic nervous system induces a metastatic switch in primary breast cancer. *Cancer Res* 70, 7042-7052, doi:10.1158/0008-5472.CAN-10-0522 (2010).

11 Sung, S. Y., Hsieh, C. L., Wu, D., Chung, L. W. & Johnstone, P. A. Tumor microenvironment promotes cancer progression, metastasis, and therapeutic resistance. *Curr Probl Cancer* 31, 36-100, doi:10.1016/j.currproblcancer.2006.12.002 (2007).

12 Renz, B. W. *et al.* Cholinergic Signaling via Muscarinic Receptors Directly and Indirectly Suppresses Pancreatic Tumorigenesis and Cancer Stemness. *Cancer Discov* 8, 1458-1473, doi:10.1158/2159-8290.CD-18-0046 (2018).

13 Rosas-Ballina, M. *et al.* Acetylcholine-synthesizing T cells relay neural signals in a vagus nerve circuit. *Science* 334, 98-101, doi:10.1126/science.1209985 (2011).

14 Wong, C. H., Jenne, C. N., Lee, W. Y., Leger, C. & Kubes, P. Functional innervation of hepatic iNKT cells is immunosuppressive following stroke. *Science* 334, 101-105, doi:10.1126/science.1210301 (2011).

15 Ferlay, J. *et al.* Cancer incidence and mortality worldwide: sources, methods and major patterns in GLOBOCAN 2012. *Int J Cancer* 136, E359-386, doi:10.1002/ijc.29210 (2015).

16 Bandarchi, B., Jabbari, C. A., Vedadi, A. & Navab, R. Molecular biology of normal melanocytes and melanoma cells. *J Clin Pathol* 66, 644-648, doi:10.1136/jclinpath-2013-201471 (2013).

17 Brose, M. S. *et al.* BRAF and RAS mutations in human lung cancer and melanoma. *Cancer Res* 62, 6997-7000 (2002).
18 Davies, H. *et al.* Mutations of the BRAF gene in human cancer. *Nature* 417, 949-954, doi:10.1038/nature00766 (2002).
19 Omholt, K., Platz, A., Kanter, L., Ringborg, U. & Hansson, J. NRAS and BRAF mutations arise early during melanoma pathogenesis and are preserved throughout tumor progression. *Clin Cancer Res* 9, 6483-6488 (2003).
20 Bhatia, A. & Kumar, Y. Cancer-immune equilibrium: questions unanswered. *Cancer Microenviron* 4, 209-217, doi:10.1007/s12307-011-0065-8 (2011).
21 Mittal, D., Gubin, M. M., Schreiber, R. D. & Smyth, M. J. New insights into cancer immunoediting and its three component phases--elimination, equilibrium and escape. *Curr Opin Immunol* 27, 16-25, doi:10.1016/j.coi.2014.01.004 (2014).
22 Swann, J. B. & Smyth, M. J. Immune surveillance of tumors. *J Clin Invest* 117, 1137-1146, doi:10.1172/JCI31405 (2007).
23 Smyth, M. J., Dunn, G. P. & Schreiber, R. D. Cancer immunosurveillance and immunoediting: the roles of immunity in suppressing tumor development and shaping tumor immunogenicity. *Adv Immunol* 90, 1-50, doi:10.1016/S0065-2776(06)90001-7 (2006).
24 Whiteside, T. L. The tumor microenvironment and its role in promoting tumor growth. *Oncogene* 27, 5904-5912, doi:10.1038/onc.2008.271 (2008).
25 Dunn, G. P., Old, L. J. & Schreiber, R. D. The immunobiology of cancer immunosurveillance and immunoediting. *Immunity* 21, 137-148, doi:10.1016/j.immuni.2004.07.017 (2004).
26 Russell, J. H. & Ley, T. J. Lymphocyte-mediated cytotoxicity. *Annu Rev Immunol* 20, 323-370, doi:10.1146/annurev.immunol.20.100201.131730 (2002).
27 Street, S. E., Cretney, E. & Smyth, M. J. Perforin and interferon-gamma activities independently control tumor initiation, growth, and metastasis. *Blood* 97, 192-197, doi:10.1182/blood.v97.1.192 (2001).
28 van den Broek, M. E. *et al.* Decreased tumor surveillance in perforin-deficient mice. *J Exp Med* 184, 1781-1790, doi:10.1084/jem.184.5.1781 (1996).
29 Smyth, M. J. *et al.* Differential tumor surveillance by natural killer (NK) and NKT cells. *J Exp Med* 191, 661-668, doi:10.1084/jem.191.4.661 (2000).
30 Kaplan, D. H. *et al.* Demonstration of an interferon gamma-dependent tumor surveillance system in immunocompetent mice. *Proc Natl Acad Sci U S A* 95, 7556-7561, doi:10.1073/pnas.95.13.7556 (1998).
31 Shinkai, Y. *et al.* RAG-2-deficient mice lack mature lymphocytes owing to inability to initiate V(D)J rearrangement. *Cell* 68, 855-867, doi:10.1016/0092-8674(92)90029-c (1992).
32 Shankaran, V. *et al.* IFNgamma and lymphocytes prevent primary tumour development and shape tumour immunogenicity. *Nature* 410, 1107-1111, doi:10.1038/35074122 (2001).
33 Girardi, M. *et al.* Regulation of cutaneous malignancy by gammadelta T cells. *Science* 294, 605-609, doi:10.1126/science.1063916 (2001).
34 Smyth, M. J. *et al.* Sequential activation of NKT cells and NK cells provides effective innate immunotherapy of cancer. *J Exp Med* 201, 1973-1985, doi:10.1084/jem.20042280 (2005).

35 Raulet, D. H. Roles of the NKG2D immunoreceptor and its ligands. *Nat Rev Immunol* 3, 781-790, doi:10.1038/nri1199 (2003).
36 Takeda, K. *et al.* Critical role for tumor necrosis factor-related apoptosis-inducing ligand in immune surveillance against tumor development. *J Exp Med* 195, 161-169, doi:10.1084/jem.20011171 (2002).
37 Sheil, A. G. Cancer after transplantation. *World J Surg* 10, 389-396, doi:10.1007/BF01655298 (1986).
38 Penn, I. Malignant melanoma in organ allograft recipients. *Transplantation* 61, 274-278, doi:10.1097/00007890-199601270-00019 (1996).
39 Penn, I. Sarcomas in organ allograft recipients. *Transplantation* 60, 1485-1491, doi:10.1097/00007890-199560120-00020 (1995).
40 Pham, S. M. *et al.* Solid tumors after heart transplantation: lethality of lung cancer. *Ann Thorac Surg* 60, 1623-1626, doi:10.1016/0003-4975(95)00120-4 (1995).
41 Gatti, R. A. & Good, R. A. Occurrence of malignancy in immunodeficiency diseases. A literature review. *Cancer* 28, 89-98, doi:10.1002/1097-0142(197107)28:1<89::aid-cncr2820280117>3.0.co;2-q (1971).
42 Penn, I. Posttransplant malignancies. *Transplant Proc* 31, 1260-1262, doi:10.1016/s0041-1345(98)01987-3 (1999).
43 Sheil, A. G. Organ transplantation and malignancy: inevitable linkage. *Transplant Proc* 34, 2436-2437, doi:10.1016/s0041-1345(02)03169-x (2002).
44 Boshoff, C. & Weiss, R. AIDS-related malignancies. *Nat Rev Cancer* 2, 373-382, doi:10.1038/nrc797 (2002).
45 Clark, W. H., Jr. *et al.* Model predicting survival in stage I melanoma based on tumor progression. *J Natl Cancer Inst* 81, 1893-1904, doi:10.1093/jnci/81.24.1893 (1989).
46 Clemente, C. G. *et al.* Prognostic value of tumor infiltrating lymphocytes in the vertical growth phase of primary cutaneous melanoma. *Cancer* 77, 1303-1310, doi:10.1002/(SICI)1097-0142(19960401)77:7<1303::AID-CNCR12>3.0.CO;2-5 (1996).
47 Rilke, F. *et al.* Prognostic significance of HER-2/neu expression in breast cancer and its relationship to other prognostic factors. *Int J Cancer* 49, 44-49, doi:10.1002/ijc.2910490109 (1991).
48 Lipponen, P. K., Eskelinen, M. J., Jauhiainen, K., Harju, E. & Terho, R. Tumour infiltrating lymphocytes as an independent prognostic factor in transitional cell bladder cancer. *Eur J Cancer* 29A, 69-75, doi:10.1016/0959-8049(93)90579-5 (1992).
49 Nacopoulou, L., Azaris, P., Papacharalampous, N. & Davaris, P. Prognostic significance of histologic host response in cancer of the large bowel. *Cancer* 47, 930-936, doi:10.1002/1097-0142(19810301)47:5<930::aid-cncr2820470519>3.0.co;2-1 (1981).
50 Naito, Y. *et al.* CD8+ T cells infiltrated within cancer cell nests as a prognostic factor in human colorectal cancer. *Cancer Res* 58, 3491-3494 (1998).
51 Epstein, N. A. & Fatti, L. P. Prostatic carcinoma: some morphological features affecting prognosis. *Cancer* 37, 2455-2465, doi:10.1002/1097-0142(197605)37:5<2455::aid-cncr2820370539>3.0.co;2-v (1976).
52 Deligdisch, L., Jacobs, A. J. & Cohen, C. J. Histologic correlates of virulence in ovarian adenocarcinoma. II. Morphologic correlates of host response. *Am J Obstet Gynecol* 144, 885-889, doi:10.1016/0002-9378(82)90178-8 (1982).

53 Jass, J. R. Lymphocytic infiltration and survival in rectal cancer. *J Clin Pathol* 39, 585-589, doi:10.1136/jcp.39.6.585 (1986).
54 Palma, L., Di Lorenzo, N. & Guidetti, B. Lymphocytic infiltrates in primary glioblastomas and recidivous gliomas. Incidence, fate, and relevance to prognosis in 228 operated cases. *J Neurosurg* 49, 854-861, doi:10.3171/jns.1978.49.6.0854 (1978).
55 Dhodapkar, M. V., Krasovsky, J., Osman, K. & Geller, M. D. Vigorous premalignancy-specific effector T cell response in the bone marrow of patients with monoclonal gammopathy. *J Exp Med* 198, 1753-1757, doi:10.1084/jem.20031030 (2003).
56 Beckhove, P. *et al.* Specifically activated memory T cell subsets from cancer patients recognize and reject xenotransplanted autologous tumors. *J Clin Invest* 114, 67-76, doi:10.1172/JCI20278 (2004).
57 Schmitz-Winnenthal, F. H. *et al.* High frequencies of functional tumor-reactive T cells in bone marrow and blood of pancreatic cancer patients. *Cancer Res* 65, 10079-10087, doi:10.1158/0008-5472.CAN-05-1098 (2005).
58 Willimsky, G. & Blankenstein, T. Sporadic immunogenic tumours avoid destruction by inducing T-cell tolerance. *Nature* 437, 141-146, doi:10.1038/nature03954 (2005).
59 Chaplin, D. D. Overview of the immune response. *J Allergy Clin Immunol* 125, S3-23, doi:10.1016/j.jaci.2009.12.980 (2010).
60 Bonilla, F. A. & Oettgen, H. C. Adaptive immunity. *J Allergy Clin Immunol* 125, S33-40, doi:10.1016/j.jaci.2009.09.017 (2010).
61 Parkin, J. & Cohen, B. An overview of the immune system. *Lancet* 357, 1777-1789, doi:10.1016/S0140-6736(00)04904-7 (2001).
62 Takahama, Y. Journey through the thymus: stromal guides for T-cell development and selection. *Nat Rev Immunol* 6, 127-135, doi:10.1038/nri1781 (2006).
63 Janicki, C. N., Jenkinson, S. R., Williams, N. A. & Morgan, D. J. Loss of CTL function among high-avidity tumor-specific CD8+ T cells following tumor infiltration. *Cancer Res* 68, 2993-3000, doi:10.1158/0008-5472.CAN-07-5008 (2008).
64 Raveney, B. J. & Morgan, D. J. Dynamic control of self-specific CD8+ T cell responses via a combination of signals mediated by dendritic cells. *J Immunol* 179, 2870-2879, doi:10.4049/jimmunol.179.5.2870 (2007).
65 Kaech, S. M. & Wherry, E. J. Heterogeneity and cell-fate decisions in effector and memory CD8+ T cell differentiation during viral infection. *Immunity* 27, 393-405, doi:10.1016/j.immuni.2007.08.007 (2007).
66 Kaech, S. M. & Cui, W. Transcriptional control of effector and memory CD8+ T cell differentiation. *Nat Rev Immunol* 12, 749-761, doi:10.1038/nri3307 (2012).
67 Griffiths, G. M., Tsun, A. & Stinchcombe, J. C. The immunological synapse: a focal point for endocytosis and exocytosis. *J Cell Biol* 189, 399-406, doi:10.1083/jcb.201002027 (2010).
68 Sallusto, F. Heterogeneity of Human CD4(+) T Cells Against Microbes. *Annu Rev Immunol* 34, 317-334, doi:10.1146/annurev-immunol-032414-112056 (2016).
69 DuPage, M. & Bluestone, J. A. Harnessing the plasticity of CD4(+) T cells to treat immune-mediated disease. *Nat Rev Immunol* 16, 149-163, doi:10.1038/nri.2015.18 (2016).
70 Schoenberger, S. P., Toes, R. E., van der Voort, E. I., Offringa, R. & Melief, C. J. T-cell help for cytotoxic T lymphocytes is mediated by CD40-CD40L interactions. *Nature* 393, 480-483, doi:10.1038/31002 (1998).

71 Bennett, S. R. *et al.* Help for cytotoxic-T-cell responses is mediated by CD40 signalling. *Nature* 393, 478-480, doi:10.1038/30996 (1998).
72 Hawiger, D. *et al.* Dendritic cells induce peripheral T cell unresponsiveness under steady state conditions in vivo. *J Exp Med* 194, 769-779, doi:10.1084/jem.194.6.769 (2001).
73 Hor, J. L. *et al.* Spatiotemporally Distinct Interactions with Dendritic Cell Subsets Facilitates CD4+ and CD8+ T Cell Activation to Localized Viral Infection. *Immunity* 43, 554-565, doi:10.1016/j.immuni.2015.07.020 (2015).
74 Laidlaw, B. J., Craft, J. E. & Kaech, S. M. The multifaceted role of CD4(+) T cells in CD8(+) T cell memory. *Nat Rev Immunol* 16, 102-111, doi:10.1038/nri.2015.10 (2016).
75 Smith, C. M. *et al.* Cognate CD4(+) T cell licensing of dendritic cells in CD8(+) T cell immunity. *Nat Immunol* 5, 1143-1148, doi:10.1038/ni1129 (2004).
76 Borst, J., Ahrends, T., Babala, N., Melief, C. J. M. & Kastenmuller, W. CD4(+) T cell help in cancer immunology and immunotherapy. *Nat Rev Immunol* 18, 635-647, doi:10.1038/s41577-018-0044-0 (2018).
77 Ahrends, T. *et al.* CD4(+) T Cell Help Confers a Cytotoxic T Cell Effector Program Including Coinhibitory Receptor Downregulation and Increased Tissue Invasiveness. *Immunity* 47, 848-861 e845, doi:10.1016/j.immuni.2017.10.009 (2017).
78 Curtsinger, J. M., Johnson, C. M. & Mescher, M. F. CD8 T cell clonal expansion and development of effector function require prolonged exposure to antigen, costimulation, and signal 3 cytokine. *J Immunol* 171, 5165-5171, doi:10.4049/jimmunol.171.10.5165 (2003).
79 Church, S. E., Jensen, S. M., Antony, P. A., Restifo, N. P. & Fox, B. A. Tumor-specific CD4+ T cells maintain effector and memory tumor-specific CD8+ T cells. *Eur J Immunol* 44, 69-79, doi:10.1002/eji.201343718 (2014).
80 Janssen, E. M. *et al.* CD4+ T cells are required for secondary expansion and memory in CD8+ T lymphocytes. *Nature* 421, 852-856, doi:10.1038/nature01441 (2003).
81 Ramsburg, E. A., Publicover, J. M., Coppock, D. & Rose, J. K. Requirement for CD4 T cell help in maintenance of memory CD8 T cell responses is epitope dependent. *J Immunol* 178, 6350-6358, doi:10.4049/jimmunol.178.10.6350 (2007).
82 Quezada, S. A. *et al.* Tumor-reactive CD4(+) T cells develop cytotoxic activity and eradicate large established melanoma after transfer into lymphopenic hosts. *J Exp Med* 207, 637-650, doi:10.1084/jem.20091918 (2010).
83 Xie, Y. *et al.* Naive tumor-specific CD4(+) T cells differentiated in vivo eradicate established melanoma. *J Exp Med* 207, 651-667, doi:10.1084/jem.20091921 (2010).
84 Takeuchi, A. *et al.* CRTAM determines the CD4+ cytotoxic T lymphocyte lineage. *J Exp Med* 213, 123-138, doi:10.1084/jem.20150519 (2016).
85 Gnjatic, S. *et al.* Survey of naturally occurring CD4+ T cell responses against NY-ESO-1 in cancer patients: correlation with antibody responses. *Proc Natl Acad Sci U S A* 100, 8862-8867, doi:10.1073/pnas.1133324100 (2003).
86 Sarvaria, A., Madrigal, J. A. & Saudemont, A. B cell regulation in cancer and anti-tumor immunity. *Cell Mol Immunol* 14, 662-674, doi:10.1038/cmi.2017.35 (2017).
87 Tsou, P., Katayama, H., Ostrin, E. J. & Hanash, S. M. The Emerging Role of B Cells in Tumor Immunity. *Cancer Res* 76, 5597-5601, doi:10.1158/0008-5472.CAN-16-0431 (2016).

88 Yuen, G. J., Demissie, E. & Pillai, S. B lymphocytes and cancer: a love-hate relationship. *Trends Cancer* 2, 747-757, doi:10.1016/j.trecan.2016.10.010 (2016).
89 Nielsen, J. S. *et al.* CD20+ tumor-infiltrating lymphocytes have an atypical CD27- memory phenotype and together with CD8+ T cells promote favorable prognosis in ovarian cancer. *Clin Cancer Res* 18, 3281-3292, doi:10.1158/1078-0432.CCR-12-0234 (2012).
90 Mizoguchi, A., Mizoguchi, E., Takedatsu, H., Blumberg, R. S. & Bhan, A. K. Chronic intestinal inflammatory condition generates IL-10-producing regulatory B cell subset characterized by CD1d upregulation. *Immunity* 16, 219-230, doi:10.1016/s1074-7613(02)00274-1 (2002).
91 Khan, A. R. *et al.* PD-L1hi B cells are critical regulators of humoral immunity. *Nat Commun* 6, 5997, doi:10.1038/ncomms6997 (2015).
92 Olkhanud, P. B. *et al.* Tumor-evoked regulatory B cells promote breast cancer metastasis by converting resting CD4(+) T cells to T-regulatory cells. *Cancer Res* 71, 3505-3515, doi:10.1158/0008-5472.CAN-10-4316 (2011).
93 Paul, S., Kulkarni, N., Shilpi & Lal, G. Intratumoral natural killer cells show reduced effector and cytolytic properties and control the differentiation of effector Th1 cells. *Oncoimmunology* 5, e1235106, doi:10.1080/2162402X.2016.1235106 (2016).
94 Sconocchia, G. *et al.* NK cells and T cells cooperate during the clinical course of colorectal cancer. *Oncoimmunology* 3, e952197, doi:10.4161/21624011.2014.952197 (2014).
95 Bluman, E. M., Bartynski, K. J., Avalos, B. R. & Caligiuri, M. A. Human natural killer cells produce abundant macrophage inflammatory protein-1 alpha in response to monocyte-derived cytokines. *J Clin Invest* 97, 2722-2727, doi:10.1172/JCI118726 (1996).
96 Roda, J. M. *et al.* Natural killer cells produce T cell-recruiting chemokines in response to antibody-coated tumor cells. *Cancer Res* 66, 517-526, doi:10.1158/0008-5472.CAN-05-2429 (2006).
97 Fauriat, C., Long, E. O., Ljunggren, H. G. & Bryceson, Y. T. Regulation of human NK-cell cytokine and chemokine production by target cell recognition. *Blood* 115, 2167-2176, doi:10.1182/blood-2009-08-238469 (2010).
98 Baginska, J. *et al.* The critical role of the tumor microenvironment in shaping natural killer cell-mediated anti-tumor immunity. *Front Immunol* 4, 490, doi:10.3389/fimmu.2013.00490 (2013).
99 Pietra, G. *et al.* Melanoma cells inhibit natural killer cell function by modulating the expression of activating receptors and cytolytic activity. *Cancer Res* 72, 1407-1415, doi:10.1158/0008-5472.CAN-11-2544 (2012).
100 Grivennikov, S. I., Greten, F. R. & Karin, M. Immunity, inflammation, and cancer. *Cell* 140, 883-899, doi:10.1016/j.cell.2010.01.025 (2010).
101 Karin, M. Nuclear factor-kappaB in cancer development and progression. *Nature* 441, 431-436, doi:10.1038/nature04870 (2006).
102 Nagaraj, S. & Gabrilovich, D. I. Myeloid-derived suppressor cells in human cancer. *Cancer J* 16, 348-353, doi:10.1097/PPO.0b013e3181eb3358 (2010).
103 Yang, L. *et al.* Abrogation of TGF beta signaling in mammary carcinomas recruits Gr-1+CD11b+ myeloid cells that promote metastasis. *Cancer Cell* 13, 23-35, doi:10.1016/j.ccr.2007.12.004 (2008).

104 Krausgruber, T. *et al.* IRF5 promotes inflammatory macrophage polarization and TH1-TH17 responses. *Nat Immunol* 12, 231-238, doi:10.1038/ni.1990 (2011).
105 Biswas, S. K. & Mantovani, A. Macrophage plasticity and interaction with lymphocyte subsets: cancer as a paradigm. *Nat Immunol* 11, 889-896, doi:10.1038/ni.1937 (2010).
106 Gabrilovich, D. I. & Nagaraj, S. Myeloid-derived suppressor cells as regulators of the immune system. *Nat Rev Immunol* 9, 162-174, doi:10.1038/nri2506 (2009).
107 Movahedi, K. *et al.* Different tumor microenvironments contain functionally distinct subsets of macrophages derived from Ly6C(high) monocytes. *Cancer Res* 70, 5728-5739, doi:10.1158/0008-5472.CAN-09-4672 (2010).
108 Kuang, D. M. *et al.* Activated monocytes in peritumoral stroma of hepatocellular carcinoma foster immune privilege and disease progression through PD-L1. *J Exp Med* 206, 1327-1337, doi:10.1084/jem.20082173 (2009).
109 Aras, S. & Zaidi, M. R. TAMeless traitors: macrophages in cancer progression and metastasis. *Br J Cancer* 117, 1583-1591, doi:10.1038/bjc.2017.356 (2017).
110 Shimizu, K., Iyoda, T., Okada, M., Yamasaki, S. & Fujii, S. I. Immune suppression and reversal of the suppressive tumor microenvironment. *Int Immunol* 30, 445-454, doi:10.1093/intimm/dxy042 (2018).
111 Ruffell, B. *et al.* Macrophage IL-10 blocks CD8+ T cell-dependent responses to chemotherapy by suppressing IL-12 expression in intratumoral dendritic cells. *Cancer Cell* 26, 623-637, doi:10.1016/j.ccell.2014.09.006 (2014).
112 Tran, T. T. P. *et al.* Humoral immune response to adenovirus induce tolerogenic bystander dendritic cells that promote generation of regulatory T cells. *PLoS Pathog* 14, e1007127, doi:10.1371/journal.ppat.1007127 (2018).
113 Wherry, E. J. *et al.* Molecular signature of CD8+ T cell exhaustion during chronic viral infection. *Immunity* 27, 670-684, doi:10.1016/j.immuni.2007.09.006 (2007).
114 Schietinger, A. & Greenberg, P. D. Tolerance and exhaustion: defining mechanisms of T cell dysfunction. *Trends Immunol* 35, 51-60, doi:10.1016/j.it.2013.10.001 (2014).
115 Li, J. *et al.* CD39/CD73 upregulation on myeloid-derived suppressor cells via TGF-beta-mTOR-HIF-1 signaling in patients with non-small cell lung cancer. *Oncoimmunology* 6, e1320011, doi:10.1080/2162402X.2017.1320011 (2017).
116 Xia, A., Zhang, Y., Xu, J., Yin, T. & Lu, X. J. T Cell Dysfunction in Cancer Immunity and Immunotherapy. *Front Immunol* 10, 1719, doi:10.3389/fimmu.2019.01719 (2019).
117 Wherry, E. J. T cell exhaustion. *Nat Immunol* 12, 492-499, doi:10.1038/ni.2035 (2011).
118 Ando, M., Ito, M., Srirat, T., Kondo, T. & Yoshimura, A. Memory T cell, exhaustion, and tumor immunity. *Immunol Med* 43, 1-9, doi:10.1080/25785826.2019.1698261 (2020).
119 Maimela, N. R., Liu, S. & Zhang, Y. Fates of CD8+ T cells in Tumor Microenvironment. *Comput Struct Biotechnol J* 17, 1-13, doi:10.1016/j.csbj.2018.11.004 (2019).
120 Zhang, Z. *et al.* T Cell Dysfunction and Exhaustion in Cancer. *Front Cell Dev Biol* 8, 17, doi:10.3389/fcell.2020.00017 (2020).
121 Ostrand-Rosenberg, S. & Fenselau, C. Myeloid-Derived Suppressor Cells: Immune-Suppressive Cells That Impair Antitumor Immunity and Are Sculpted by Their Environment. *J Immunol* 200, 422-431, doi:10.4049/jimmunol.1701019 (2018).

122 Li, L. *et al.* Metformin-Induced Reduction of CD39 and CD73 Blocks Myeloid-Derived Suppressor Cell Activity in Patients with Ovarian Cancer. *Cancer Res* 78, 1779-1791, doi:10.1158/0008-5472.CAN-17-2460 (2018).
123 Chen, J. *et al.* Suppression of T cells by myeloid-derived suppressor cells in cancer. *Hum Immunol* 78, 113-119, doi:10.1016/j.humimm.2016.12.001 (2017).
124 Wu, A. A., Drake, V., Huang, H. S., Chiu, S. & Zheng, L. Reprogramming the tumor microenvironment: tumor-induced immunosuppressive factors paralyze T cells. *Oncoimmunology* 4, e1016700, doi:10.1080/2162402X.2015.1016700 (2015).
125 Rodriguez, P. C. *et al.* Regulation of T cell receptor CD3zeta chain expression by L-arginine. *J Biol Chem* 277, 21123-21129, doi:10.1074/jbc.M110675200 (2002).
126 Chen, X., Song, M., Zhang, B. & Zhang, Y. Reactive Oxygen Species Regulate T Cell Immune Response in the Tumor Microenvironment. *Oxid Med Cell Longev* 2016, 1580967, doi:10.1155/2016/1580967 (2016).
127 Wu, D. & Zhu, Y. Role of kynurenine in promoting the generation of exhausted CD8(+) T cells in colorectal cancer. *Am J Transl Res* 13, 1535-1547 (2021).
128 Liu, S. *et al.* Molecular and clinical characterization of CD163 expression via large-scale analysis in glioma. *Oncoimmunology* 8, 1601478, doi:10.1080/2162402X.2019.1601478 (2019).
129 Yang, L. & Zhang, Y. Tumor-associated macrophages: from basic research to clinical application. *J Hematol Oncol* 10, 58, doi:10.1186/s13045-017-0430-2 (2017).
130 Jiang, Y., Li, Y. & Zhu, B. T-cell exhaustion in the tumor microenvironment. *Cell Death Dis* 6, e1792, doi:10.1038/cddis.2015.162 (2015).
131 Zhen, Z. *et al.* Protein Nanocage Mediated Fibroblast-Activation Protein Targeted Photoimmunotherapy To Enhance Cytotoxic T Cell Infiltration and Tumor Control. *Nano Lett* 17, 862-869, doi:10.1021/acs.nanolett.6b04150 (2017).
132 Lakins, M. A., Ghorani, E., Munir, H., Martins, C. P. & Shields, J. D. Cancer-associated fibroblasts induce antigen-specific deletion of CD8 (+) T Cells to protect tumour cells. *Nat Commun* 9, 948, doi:10.1038/s41467-018-03347-0 (2018).
133 Wang, D. *et al.* Macrophage-derived CCL22 promotes an immunosuppressive tumor microenvironment via IL-8 in malignant pleural effusion. *Cancer Lett* 452, 244-253, doi:10.1016/j.canlet.2019.03.040 (2019).
134 Landskron, G., De la Fuente, M., Thuwajit, P., Thuwajit, C. & Hermoso, M. A. Chronic inflammation and cytokines in the tumor microenvironment. *J Immunol Res* 2014, 149185, doi:10.1155/2014/149185 (2014).
135 Li, L., Ma, Y. & Xu, Y. Follicular regulatory T cells infiltrated the ovarian carcinoma and resulted in CD8 T cell dysfunction dependent on IL-10 pathway. *Int Immunopharmacol* 68, 81-87, doi:10.1016/j.intimp.2018.12.051 (2019).
136 Wang, C., Singer, M. & Anderson, A. C. Molecular Dissection of CD8(+) T-Cell Dysfunction. *Trends Immunol* 38, 567-576, doi:10.1016/j.it.2017.05.008 (2017).
137 Liu, X. *et al.* Genome-wide analysis identifies NR4A1 as a key mediator of T cell dysfunction. *Nature* 567, 525-529, doi:10.1038/s41586-019-0979-8 (2019).
138 Alfei, F. *et al.* TOX reinforces the phenotype and longevity of exhausted T cells in chronic viral infection. *Nature* 571, 265-269, doi:10.1038/s41586-019-1326-9 (2019).

139 Khan, O. *et al.* TOX transcriptionally and epigenetically programs CD8(+) T cell exhaustion. *Nature* 571, 211-218, doi:10.1038/s41586-019-1325-x (2019).
140 Wang, X. *et al.* TOX promotes the exhaustion of antitumor CD8(+) T cells by preventing PD1 degradation in hepatocellular carcinoma. *J Hepatol* 71, 731-741, doi:10.1016/j.jhep.2019.05.015 (2019).
141 Chang, J. T., Wherry, E. J. & Goldrath, A. W. Molecular regulation of effector and memory T cell differentiation. *Nat Immunol* 15, 1104-1115, doi:10.1038/ni.3031 (2014).
142 Li, J., He, Y., Hao, J., Ni, L. & Dong, C. High Levels of Eomes Promote Exhaustion of Anti-tumor CD8(+) T Cells. *Front Immunol* 9, 2981, doi:10.3389/fimmu.2018.02981 (2018).
143 Quigley, M. *et al.* Transcriptional analysis of HIV-specific CD8+ T cells shows that PD-1 inhibits T cell function by upregulating BATF. *Nat Med* 16, 1147-1151, doi:10.1038/nm.2232 (2010).
144 Walunas, T. L. *et al.* CTLA-4 can function as a negative regulator of T cell activation. *Immunity* 1, 405-413, doi:10.1016/1074-7613(94)90071-x (1994).
145 Brunner, M. C. *et al.* CTLA-4-Mediated inhibition of early events of T cell proliferation. *J Immunol* 162, 5813-5820 (1999).
146 Murakami, N. & Riella, L. V. Co-inhibitory pathways and their importance in immune regulation. *Transplantation* 98, 3-14, doi:10.1097/TP.0000000000000169 (2014).
147 Buchbinder, E. I. & Desai, A. CTLA-4 and PD-1 Pathways: Similarities, Differences, and Implications of Their Inhibition. *Am J Clin Oncol* 39, 98-106, doi:10.1097/COC.0000000000000239 (2016).
148 Ambler, R. *et al.* PD-1 suppresses the maintenance of cell couples between cytotoxic T cells and target tumor cells within the tumor. *Sci Signal* 13, doi:10.1126/scisignal.aau4518 (2020).
149 Galon, J. & Bruni, D. Approaches to treat immune hot, altered and cold tumours with combination immunotherapies. *Nat Rev Drug Discov* 18, 197-218, doi:10.1038/s41573-018-0007-y (2019).
150 Wherry, E. J. & Kurachi, M. Molecular and cellular insights into T cell exhaustion. *Nat Rev Immunol* 15, 486-499, doi:10.1038/nri3862 (2015).
151 Sakuishi, K. *et al.* Targeting Tim-3 and PD-1 pathways to reverse T cell exhaustion and restore anti-tumor immunity. *J Exp Med* 207, 2187-2194, doi:10.1084/jem.20100643 (2010).
152 Attanasio, J. & Wherry, E. J. Costimulatory and Coinhibitory Receptor Pathways in Infectious Disease. *Immunity* 44, 1052-1068, doi:10.1016/j.immuni.2016.04.022 (2016).
153 Jin, H. T. *et al.* Cooperation of Tim-3 and PD-1 in CD8 T-cell exhaustion during chronic viral infection. *Proc Natl Acad Sci U S A* 107, 14733-14738, doi:10.1073/pnas.1009731107 (2010).
154 Johnston, R. J. *et al.* The immunoreceptor TIGIT regulates antitumor and antiviral CD8(+) T cell effector function. *Cancer Cell* 26, 923-937, doi:10.1016/j.ccell.2014.10.018 (2014).
155 Blackburn, S. D. *et al.* Coregulation of CD8+ T cell exhaustion by multiple inhibitory receptors during chronic viral infection. *Nat Immunol* 10, 29-37, doi:10.1038/ni.1679 (2009).

156 Zhao, M. *et al.* Rapid in vitro generation of bona fide exhausted CD8+ T cells is accompanied by Tcf7 promotor methylation. *PLoS Pathog* 16, e1008555, doi:10.1371/journal.ppat.1008555 (2020).
157 Parry, R. V. *et al.* CTLA-4 and PD-1 receptors inhibit T-cell activation by distinct mechanisms. *Mol Cell Biol* 25, 9543-9553, doi:10.1128/MCB.25.21.9543-9553.2005 (2005).
158 Hellmann, M. D. *et al.* Nivolumab plus Ipilimumab in Advanced Non-Small-Cell Lung Cancer. *N Engl J Med* 381, 2020-2031, doi:10.1056/NEJMoa1910231 (2019).
159 Boles, K. S. *et al.* A novel molecular interaction for the adhesion of follicular CD4 T cells to follicular DC. *Eur J Immunol* 39, 695-703, doi:10.1002/eji.200839116 (2009).
160 Stanietsky, N. *et al.* The interaction of TIGIT with PVR and PVRL2 inhibits human NK cell cytotoxicity. *Proc Natl Acad Sci U S A* 106, 17858-17863, doi:10.1073/pnas.0903474106 (2009).
161 Yu, X. *et al.* The surface protein TIGIT suppresses T cell activation by promoting the generation of mature immunoregulatory dendritic cells. *Nat Immunol* 10, 48-57, doi:10.1038/ni.1674 (2009).
162 Levin, S. D. *et al.* Vstm3 is a member of the CD28 family and an important modulator of T-cell function. *Eur J Immunol* 41, 902-915, doi:10.1002/eji.201041136 (2011).
163 Joller, N. *et al.* Cutting edge: TIGIT has T cell-intrinsic inhibitory functions. *J Immunol* 186, 1338-1342, doi:10.4049/jimmunol.1003081 (2011).
164 Lozano, E., Dominguez-Villar, M., Kuchroo, V. & Hafler, D. A. The TIGIT/CD226 axis regulates human T cell function. *J Immunol* 188, 3869-3875, doi:10.4049/jimmunol.1103627 (2012).
165 Sarhan, D. *et al.* Adaptive NK Cells with Low TIGIT Expression Are Inherently Resistant to Myeloid-Derived Suppressor Cells. *Cancer Res* 76, 5696-5706, doi:10.1158/0008-5472.CAN-16-0839 (2016).
166 Shibuya, A. *et al.* DNAM-1, a novel adhesion molecule involved in the cytolytic function of T lymphocytes. *Immunity* 4, 573-581, doi:10.1016/s1074-7613(00)70060-4 (1996).
167 Kojima, H. *et al.* CD226 mediates platelet and megakaryocytic cell adhesion to vascular endothelial cells. *J Biol Chem* 278, 36748-36753, doi:10.1074/jbc.M300702200 (2003).
168 Durham, N. M. *et al.* Lymphocyte Activation Gene 3 (LAG-3) modulates the ability of CD4 T-cells to be suppressed in vivo. *PLoS One* 9, e109080, doi:10.1371/journal.pone.0109080 (2014).
169 Xu, F. *et al.* LSECtin expressed on melanoma cells promotes tumor progression by inhibiting antitumor T-cell responses. *Cancer Res* 74, 3418-3428, doi:10.1158/0008-5472.CAN-13-2690 (2014).
170 Wang, J. *et al.* Fibrinogen-like Protein 1 Is a Major Immune Inhibitory Ligand of LAG-3. *Cell* 176, 334-347 e312, doi:10.1016/j.cell.2018.11.010 (2019).
171 Mao, X. *et al.* Pathological alpha-synuclein transmission initiated by binding lymphocyte-activation gene 3. *Science* 353, doi:10.1126/science.aah3374 (2016).
172 Baixeras, E. *et al.* Characterization of the lymphocyte activation gene 3-encoded protein. A new ligand for human leukocyte antigen class II antigens. *J Exp Med* 176, 327-337, doi:10.1084/jem.176.2.327 (1992).

173 Monney, L. *et al.* Th1-specific cell surface protein Tim-3 regulates macrophage activation and severity of an autoimmune disease. *Nature* 415, 536-541, doi:10.1038/415536a (2002).
174 Sanchez-Fueyo, A. *et al.* Tim-3 inhibits T helper type 1-mediated auto- and alloimmune responses and promotes immunological tolerance. *Nat Immunol* 4, 1093-1101, doi:10.1038/ni987 (2003).
175 Gupta, S. *et al.* Allograft rejection is restrained by short-lived TIM-3+PD-1+Foxp3+ Tregs. *J Clin Invest* 122, 2395-2404, doi:10.1172/JCI45138 (2012).
176 Ocana-Guzman, R., Torre-Bouscoulet, L. & Sada-Ovalle, I. TIM-3 Regulates Distinct Functions in Macrophages. *Front Immunol* 7, 229, doi:10.3389/fimmu.2016.00229 (2016).
177 Anderson, A. C. *et al.* Promotion of tissue inflammation by the immune receptor Tim-3 expressed on innate immune cells. *Science* 318, 1141-1143, doi:10.1126/science.1148536 (2007).
178 Nakayama, M. *et al.* Tim-3 mediates phagocytosis of apoptotic cells and cross-presentation. *Blood* 113, 3821-3830, doi:10.1182/blood-2008-10-185884 (2009).
179 Ju, Y. *et al.* T cell immunoglobulin- and mucin-domain-containing molecule-3 (Tim-3) mediates natural killer cell suppression in chronic hepatitis B. *J Hepatol* 52, 322-329, doi:10.1016/j.jhep.2009.12.005 (2010).
180 Maude, S. L. *et al.* Chimeric antigen receptor T cells for sustained remissions in leukemia. *N Engl J Med* 371, 1507-1517, doi:10.1056/NEJMoa1407222 (2014).
181 Yu, S. *et al.* Chimeric antigen receptor T cells: a novel therapy for solid tumors. *J Hematol Oncol* 10, 78, doi:10.1186/s13045-017-0444-9 (2017).
182 Li, J. *et al.* Chimeric antigen receptor T cell (CAR-T) immunotherapy for solid tumors: lessons learned and strategies for moving forward. *J Hematol Oncol* 11, 22, doi:10.1186/s13045-018-0568-6 (2018).
183 Yan, Z. X. *et al.* Clinical Efficacy and Tumor Microenvironment Influence in a Dose-Escalation Study of Anti-CD19 Chimeric Antigen Receptor T Cells in Refractory B-Cell Non-Hodgkin's Lymphoma. *Clin Cancer Res* 25, 6995-7003, doi:10.1158/1078-0432.CCR-19-0101 (2019).
184 O'Rourke, D. M. *et al.* A single dose of peripherally infused EGFRvIII-directed CAR T cells mediates antigen loss and induces adaptive resistance in patients with recurrent glioblastoma. *Sci Transl Med* 9, doi:10.1126/scitranslmed.aaa0984 (2017).
185 Lim, W. A. & June, C. H. The Principles of Engineering Immune Cells to Treat Cancer. *Cell* 168, 724-740, doi:10.1016/j.cell.2017.01.016 (2017).
186 Chen, J. *et al.* NR4A transcription factors limit CAR T cell function in solid tumours. *Nature* 567, 530-534, doi:10.1038/s41586-019-0985-x (2019).
187 Lynn, R. C. *et al.* c-Jun overexpression in CAR T cells induces exhaustion resistance. *Nature* 576, 293-300, doi:10.1038/s41586-019-1805-z (2019).
188 Chu, Y., Liu, Q., Wei, J. & Liu, B. Personalized cancer neoantigen vaccines come of age. *Theranostics* 8, 4238-4246, doi:10.7150/thno.24387 (2018).
189 Chen, Y. T. *et al.* Serological analysis of Melan-A(MART-1), a melanocyte-specific protein homogeneously expressed in human melanomas. *Proc Natl Acad Sci U S A* 93, 5915-5919, doi:10.1073/pnas.93.12.5915 (1996).

190 Barrow, C. *et al.* Tumor antigen expression in melanoma varies according to antigen and stage. *Clin Cancer Res* 12, 764-771, doi:10.1158/1078-0432.CCR-05-1544 (2006).
191 Morgan, R. A. *et al.* Cancer regression in patients after transfer of genetically engineered lymphocytes. *Science* 314, 126-129, doi:10.1126/science.1129003 (2006).
192 Johnson, L. A. *et al.* Gene therapy with human and mouse T-cell receptors mediates cancer regression and targets normal tissues expressing cognate antigen. *Blood* 114, 535-546, doi:10.1182/blood-2009-03-211714 (2009).
193 Hammarstrom, S. The carcinoembryonic antigen (CEA) family: structures, suggested functions and expression in normal and malignant tissues. *Semin Cancer Biol* 9, 67-81, doi:10.1006/scbi.1998.0119 (1999).
194 Jenkins, R. W., Barbie, D. A. & Flaherty, K. T. Mechanisms of resistance to immune checkpoint inhibitors. *Br J Cancer* 118, 9-16, doi:10.1038/bjc.2017.434 (2018).
195 Das, S. & Johnson, D. B. Immune-related adverse events and anti-tumor efficacy of immune checkpoint inhibitors. *J Immunother Cancer* 7, 306, doi:10.1186/s40425-019-0805-8 (2019).
196 Perazella, M. A. & Shirali, A. C. Immune checkpoint inhibitor nephrotoxicity: what do we know and what should we do? *Kidney Int* 97, 62-74, doi:10.1016/j.kint.2019.07.022 (2020).
197 Hodi, F. S. *et al.* Nivolumab plus ipilimumab or nivolumab alone versus ipilimumab alone in advanced melanoma (CheckMate 067): 4-year outcomes of a multicentre, randomised, phase 3 trial. *Lancet Oncol* 19, 1480-1492, doi:10.1016/S1470-2045(18)30700-9 (2018).
198 Chihara, N. *et al.* Induction and transcriptional regulation of the co-inhibitory gene module in T cells. *Nature* 558, 454-459, doi:10.1038/s41586-018-0206-z (2018).
199 Weber, J. S. *et al.* Sequential administration of nivolumab and ipilimumab with a planned switch in patients with advanced melanoma (CheckMate 064): an open-label, randomised, phase 2 trial. *Lancet Oncol* 17, 943-955, doi:10.1016/S1470-2045(16)30126-7 (2016).
200 Mehta, G. U. *et al.* Outcomes of Adoptive Cell Transfer With Tumor-infiltrating Lymphocytes for Metastatic Melanoma Patients With and Without Brain Metastases. *J Immunother* 41, 241-247, doi:10.1097/CJI.0000000000000223 (2018).
201 Zhou, Q. *et al.* Coexpression of Tim-3 and PD-1 identifies a CD8+ T-cell exhaustion phenotype in mice with disseminated acute myelogenous leukemia. *Blood* 117, 4501-4510, doi:10.1182/blood-2010-10-310425 (2011).
202 Das, M., Zhu, C. & Kuchroo, V. K. Tim-3 and its role in regulating anti-tumor immunity. *Immunol Rev* 276, 97-111, doi:10.1111/imr.12520 (2017).
203 Colbeck, E. J. *et al.* Treg Depletion Licenses T Cell-Driven HEV Neogenesis and Promotes Tumor Destruction. *Cancer Immunol Res* 5, 1005-1015, doi:10.1158/2326-6066.CIR-17-0131 (2017).
204 Andrews, L. P., Marciscano, A. E., Drake, C. G. & Vignali, D. A. LAG3 (CD223) as a cancer immunotherapy target. *Immunol Rev* 276, 80-96, doi:10.1111/imr.12519 (2017).
205 Schadendorf, D. *et al.* Health-related quality of life results from the phase III CheckMate 067 study. *Eur J Cancer* 82, 80-91, doi:10.1016/j.ejca.2017.05.031 (2017).
206 Weber, J. S. *et al.* Nivolumab versus chemotherapy in patients with advanced melanoma who progressed after anti-CTLA-4 treatment (CheckMate 037): a randomised, controlled,

open-label, phase 3 trial. *Lancet Oncol* 16, 375-384, doi:10.1016/S1470-2045(15)70076-8 (2015).

207 Chen, D. S. & Mellman, I. Oncology meets immunology: the cancer-immunity cycle. *Immunity* 39, 1-10, doi:10.1016/j.immuni.2013.07.012 (2013).

208 Goldstein, B. Anatomy of the peripheral nervous system. *Phys Med Rehabil Clin N Am* 12, 207-236 (2001).

209 Yam, M. F. *et al.* General Pathways of Pain Sensation and the Major Neurotransmitters Involved in Pain Regulation. *Int J Mol Sci* 19, doi:10.3390/ijms19082164 (2018).

210 Bevan, S. & Andersson, D. A. TRP channel antagonists for pain--opportunities beyond TRPV1. *Curr Opin Investig Drugs* 10, 655-663 (2009).

211 Fernandes, E. S. *et al.* A distinct role for transient receptor potential ankyrin 1, in addition to transient receptor potential vanilloid 1, in tumor necrosis factor alpha-induced inflammatory hyperalgesia and Freund's complete adjuvant-induced monarthritis. *Arthritis Rheum* 63, 819-829, doi:10.1002/art.30150 (2011).

212 Geppetti, P., Nassini, R., Materazzi, S. & Benemei, S. The concept of neurogenic inflammation. *BJU Int* 101 Suppl 3, 2-6, doi:10.1111/j.1464-410X.2008.07493.x (2008).

213 Crosson, T. *et al.* Profiling of how nociceptor neurons detect danger - new and old foes. *J Intern Med* 286, 268-289, doi:10.1111/joim.12957 (2019).

214 Szallasi, A., Cortright, D. N., Blum, C. A. & Eid, S. R. The vanilloid receptor TRPV1: 10 years from channel cloning to antagonist proof-of-concept. *Nat Rev Drug Discov* 6, 357-372, doi:10.1038/nrd2280 (2007).

215 Li, L. *et al.* Transient receptor potential vanilloid 1 activation by dietary capsaicin promotes urinary sodium excretion by inhibiting epithelial sodium channel alpha subunit-mediated sodium reabsorption. *Hypertension* 64, 397-404, doi:10.1161/HYPERTENSIONAHA.114.03105 (2014).

216 Tominaga, M., Wada, M. & Masu, M. Potentiation of capsaicin receptor activity by metabotropic ATP receptors as a possible mechanism for ATP-evoked pain and hyperalgesia. *Proc Natl Acad Sci U S A* 98, 6951-6956, doi:10.1073/pnas.111025298 (2001).

217 Zhang, H. *et al.* Neurokinin-1 receptor enhances TRPV1 activity in primary sensory neurons via PKCepsilon: a novel pathway for heat hyperalgesia. *J Neurosci* 27, 12067-12077, doi:10.1523/JNEUROSCI.0496-07.2007 (2007).

218 Moriyama, T. *et al.* Sensitization of TRPV1 by EP1 and IP reveals peripheral nociceptive mechanism of prostaglandins. *Mol Pain* 1, 3, doi:10.1186/1744-8069-1-3 (2005).

219 Caterina, M. J. *et al.* The capsaicin receptor: a heat-activated ion channel in the pain pathway. *Nature* 389, 816-824, doi:10.1038/39807 (1997).

220 Huang, W., Wang, H., Galligan, J. J. & Wang, D. H. Transient receptor potential vanilloid subtype 1 channel mediated neuropeptide secretion and depressor effects: role of endoplasmic reticulum associated Ca2+ release receptors in rat dorsal root ganglion neurons. *J Hypertens* 26, 1966-1975, doi:10.1097/HJH.0b013e328309eff9 (2008).

221 Gazzieri, D. *et al.* Substance P released by TRPV1-expressing neurons produces reactive oxygen species that mediate ethanol-induced gastric injury. *Free Radic Biol Med* 43, 581-589, doi:10.1016/j.freeradbiomed.2007.05.018 (2007).

222 Chen, J. *et al.* Activation of TRPV1 channel by dietary capsaicin improves visceral fat remodeling through connexin43-mediated Ca2+ influx. *Cardiovasc Diabetol* 14, 22, doi:10.1186/s12933-015-0183-6 (2015).
223 Tsuji, F. & Aono, H. Role of transient receptor potential vanilloid 1 in inflammation and autoimmune diseases. *Pharmaceuticals (Basel)* 5, 837-852, doi:10.3390/ph5080837 (2012).
224 Chiu, I. M., von Hehn, C. A. & Woolf, C. J. Neurogenic inflammation and the peripheral nervous system in host defense and immunopathology. *Nat Neurosci* 15, 1063-1067, doi:10.1038/nn.3144 (2012).
225 Talbot, S., Foster, S. L. & Woolf, C. J. Neuroimmunity: Physiology and Pathology. *Annu Rev Immunol* 34, 421-447, doi:10.1146/annurev-immunol-041015-055340 (2016).
226 Sauer, S. K., Reeh, P. W. & Bove, G. M. Noxious heat-induced CGRP release from rat sciatic nerve axons in vitro. *Eur J Neurosci* 14, 1203-1208, doi:10.1046/j.0953-816x.2001.01741.x (2001).
227 Edvinsson, L., Ekman, R., Jansen, I., McCulloch, J. & Uddman, R. Calcitonin gene-related peptide and cerebral blood vessels: distribution and vasomotor effects. *J Cereb Blood Flow Metab* 7, 720-728, doi:10.1038/jcbfm.1987.126 (1987).
228 McCormack, D. G., Mak, J. C., Coupe, M. O. & Barnes, P. J. Calcitonin gene-related peptide vasodilation of human pulmonary vessels. *J Appl Physiol (1985)* 67, 1265-1270, doi:10.1152/jappl.1989.67.3.1265 (1989).
229 Saria, A. Substance P in sensory nerve fibres contributes to the development of oedema in the rat hind paw after thermal injury. *Br J Pharmacol* 82, 217-222, doi:10.1111/j.1476-5381.1984.tb16461.x (1984).
230 Fryer, A. D. *et al.* Neuronal eotaxin and the effects of CCR3 antagonist on airway hyperreactivity and M2 receptor dysfunction. *J Clin Invest* 116, 228-236, doi:10.1172/JCI25423 (2006).
231 Kenney, M. J. & Ganta, C. K. Autonomic nervous system and immune system interactions. *Compr Physiol* 4, 1177-1200, doi:10.1002/cphy.c130051 (2014).
232 Klose, C. S. N. *et al.* The neuropeptide neuromedin U stimulates innate lymphoid cells and type 2 inflammation. *Nature* 549, 282-286, doi:10.1038/nature23676 (2017).
233 Kabata, H. & Artis, D. Neuro-immune crosstalk and allergic inflammation. *J Clin Invest* 129, 1475-1482, doi:10.1172/JCI124609 (2019).
234 Gabanyi, I. *et al.* Neuro-immune Interactions Drive Tissue Programming in Intestinal Macrophages. *Cell* 164, 378-391, doi:10.1016/j.cell.2015.12.023 (2016).
235 Yoo, B. B. & Mazmanian, S. K. The Enteric Network: Interactions between the Immune and Nervous Systems of the Gut. *Immunity* 46, 910-926, doi:10.1016/j.immuni.2017.05.011 (2017).
236 Nance, D. M. & Sanders, V. M. Autonomic innervation and regulation of the immune system (1987-2007). *Brain Behav Immun* 21, 736-745, doi:10.1016/j.bbi.2007.03.008 (2007).
237 Gautron, L. *et al.* Neuronal and nonneuronal cholinergic structures in the mouse gastrointestinal tract and spleen. *J Comp Neurol* 521, 3741-3767, doi:10.1002/cne.23376 (2013).

238 Felten, D. L., Ackerman, K. D., Wiegand, S. J. & Felten, S. Y. Noradrenergic sympathetic innervation of the spleen: I. Nerve fibers associate with lymphocytes and macrophages in specific compartments of the splenic white pulp. *J Neurosci Res* 18, 28-36, 118-121, doi:10.1002/jnr.490180107 (1987).
239 Anagnostou, V. K. *et al.* Ontogeny of intrinsic innervation in the human thymus and spleen. *J Histochem Cytochem* 55, 813-820, doi:10.1369/jhc.6A7168.2007 (2007).
240 Murray, K. *et al.* Neuroanatomy of the spleen: Mapping the relationship between sympathetic neurons and lymphocytes. *PLoS One* 12, e0182416, doi:10.1371/journal.pone.0182416 (2017).
241 Bassi, G. S. *et al.* Anatomical and clinical implications of vagal modulation of the spleen. *Neurosci Biobehav Rev* 112, 363-373, doi:10.1016/j.neubiorev.2020.02.011 (2020).
242 Lori, A., Perrotta, M., Lembo, G. & Carnevale, D. The Spleen: A Hub Connecting Nervous and Immune Systems in Cardiovascular and Metabolic Diseases. *Int J Mol Sci* 18, doi:10.3390/ijms18061216 (2017).
243 Noble, B. T., Brennan, F. H. & Popovich, P. G. The spleen as a neuroimmune interface after spinal cord injury. *J Neuroimmunol* 321, 1-11, doi:10.1016/j.jneuroim.2018.05.007 (2018).
244 Jung, W. C., Levesque, J. P. & Ruitenberg, M. J. It takes nerve to fight back: The significance of neural innervation of the bone marrow and spleen for immune function. *Semin Cell Dev Biol* 61, 60-70, doi:10.1016/j.semcdb.2016.08.010 (2017).
245 Bratton, B. O. *et al.* Neural regulation of inflammation: no neural connection from the vagus to splenic sympathetic neurons. *Exp Physiol* 97, 1180-1185, doi:10.1113/expphysiol.2011.061531 (2012).
246 Bellinger, D. L., Lorton, D., Hamill, R. W., Felten, S. Y. & Felten, D. L. Acetylcholinesterase staining and choline acetyltransferase activity in the young adult rat spleen: lack of evidence for cholinergic innervation. *Brain Behav Immun* 7, 191-204, doi:10.1006/brbi.1993.1021 (1993).
247 Martelli, D., McKinley, M. J. & McAllen, R. M. The cholinergic anti-inflammatory pathway: a critical review. *Auton Neurosci* 182, 65-69, doi:10.1016/j.autneu.2013.12.007 (2014).
248 Elfvin, L. G., Aldskogius, H. & Johansson, J. Splenic primary sensory afferents in the guinea pig demonstrated with anterogradely transported wheat-germ agglutinin conjugated to horseradish peroxidase. *Cell Tissue Res* 269, 229-234, doi:10.1007/BF00319613 (1992).
249 Lundberg, J. M., Anggard, A., Pernow, J. & Hokfelt, T. Neuropeptide Y-, substance P- and VIP-immunoreactive nerves in cat spleen in relation to autonomic vascular and volume control. *Cell Tissue Res* 239, 9-18, doi:10.1007/BF00214896 (1985).
250 Mignini, F., Streccioni, V. & Amenta, F. Autonomic innervation of immune organs and neuroimmune modulation. *Auton Autacoid Pharmacol* 23, 1-25, doi:10.1046/j.1474-8673.2003.00280.x (2003).
251 Lorton, D., Bellinger, D. L., Felten, S. Y. & Felten, D. L. Substance P innervation of spleen in rats: nerve fibers associate with lymphocytes and macrophages in specific compartments of the spleen. *Brain Behav Immun* 5, 29-40, doi:10.1016/0889-1591(91)90005-u (1991).
252 Stevens-Felten, S. Y. & Bellinger, D. L. Noradrenergic and peptidergic innervation of lymphoid organs. *Chem Immunol* 69, 99-131, doi:10.1159/000058655 (1997).
253 Calvo, W. The innervation of the bone marrow in laboratory animals. *Am J Anat* 123, 315-328, doi:10.1002/aja.1001230206 (1968).

254 Felten, D. L., Felten, S. Y., Carlson, S. L., Olschowka, J. A. & Livnat, S. Noradrenergic and peptidergic innervation of lymphoid tissue. *J Immunol* 135, 755s-765s (1985).
255 Bjurholm, A., Kreicbergs, A., Brodin, E. & Schultzberg, M. Substance P- and CGRP-immunoreactive nerves in bone. *Peptides* 9, 165-171, doi:10.1016/0196-9781(88)90023-x (1988).
256 Hill, E. L. & Elde, R. Distribution of CGRP-, VIP-, D beta H-, SP-, and NPY-immunoreactive nerves in the periosteum of the rat. *Cell Tissue Res* 264, 469-480, doi:10.1007/BF00319037 (1991).
257 Bellinger, D. L., Lorton, D., Felten, S. Y. & Felten, D. L. Innervation of lymphoid organs and implications in development, aging, and autoimmunity. *Int J Immunopharmacol* 14, 329-344, doi:10.1016/0192-0561(92)90162-e (1992).
258 Hukkanen, M. *et al.* Rapid proliferation of calcitonin gene-related peptide-immunoreactive nerves during healing of rat tibial fracture suggests neural involvement in bone growth and remodelling. *Neuroscience* 54, 969-979, doi:10.1016/0306-4522(93)90588-7 (1993).
259 Tabarowski, Z., Gibson-Berry, K. & Felten, S. Y. Noradrenergic and peptidergic innervation of the mouse femur bone marrow. *Acta Histochem* 98, 453-457, doi:10.1016/S0065-1281(96)80013-4 (1996).
260 Afan, A. M., Broome, C. S., Nicholls, S. E., Whetton, A. D. & Miyan, J. A. Bone marrow innervation regulates cellular retention in the murine haemopoietic system. *Br J Haematol* 98, 569-577, doi:10.1046/j.1365-2141.1997.2733092.x (1997).
261 Artico, M. *et al.* Noradrenergic and cholinergic innervation of the bone marrow. *Int J Mol Med* 10, 77-80 (2002).
262 Bajayo, A. *et al.* Skeletal parasympathetic innervation communicates central IL-1 signals regulating bone mass accrual. *Proc Natl Acad Sci U S A* 109, 15455-15460, doi:10.1073/pnas.1206061109 (2012).
263 Fink, T. & Weihe, E. Multiple neuropeptides in nerves supplying mammalian lymph nodes: messenger candidates for sensory and autonomic neuroimmunomodulation? *Neurosci Lett* 90, 39-44, doi:10.1016/0304-3940(88)90783-5 (1988).
264 Felten, D. L., Felten, S. Y., Bellinger, D. L. & Lorton, D. Noradrenergic and peptidergic innervation of secondary lymphoid organs: role in experimental rheumatoid arthritis. *Eur J Clin Invest* 22 Suppl 1, 37-41 (1992).
265 Lorton, D. *et al.* Local application of capsaicin into the draining lymph nodes attenuates expression of adjuvant-induced arthritis. *Neuroimmunomodulation* 7, 115-125, doi:10.1159/000026429 (2000).
266 Hanes, W. M. *et al.* Neuronal Circuits Modulate Antigen Flow Through Lymph Nodes. *Bioelectron Med* 3, 18-28, doi:10.15424/bioelectronmed.2016.00001 (2016).
267 Huang, S. *et al.* Lymph nodes are innervated by a unique population of sensory neurons with immunomodulatory potential. *Cell* 184, 441-459 e425, doi:10.1016/j.cell.2020.11.028 (2021).
268 Yin, Q. *et al.* Lidocaine Ameliorates Psoriasis by Obstructing Pathogenic CGRP SignalingMediated Sensory NeuronDendritic Cell Communication. *J Invest Dermatol*, doi:10.1016/j.jid.2022.01.002 (2022).

269 Pernow, J. *et al.* Influence of sympathetic discharge pattern on norepinephrine and neuropeptide Y release. *Am J Physiol* 257, H866-872, doi:10.1152/ajpheart.1989.257.3.H866 (1989).
270 Akiyoshi, M., Shimizu, Y. & Saito, M. Interleukin-1 increases norepinephrine turnover in the spleen and lung in rats. *Biochem Biophys Res Commun* 173, 1266-1270, doi:10.1016/s0006-291x(05)80923-4 (1990).
271 Besedovsky, H. O., del Rey, A., Sorkin, E., Da Prada, M. & Keller, H. H. Immunoregulation mediated by the sympathetic nervous system. *Cell Immunol* 48, 346-355, doi:10.1016/0008-8749(79)90129-1 (1979).
272 Bognar, I. T. *et al.* Effects of human recombinant interleukins on stimulation-evoked noradrenaline overflow from the rat perfused spleen. *Naunyn Schmiedebergs Arch Pharmacol* 349, 497-502, doi:10.1007/BF00169139 (1994).
273 Heiffer, M. H., Mundy, R. L. & Mehlman, B. Effect of lethal doses of bacterial endotoxin (E. coli) on sympathetic neurohormones in the rabbit. *Am J Physiol* 198, 1307-1311, doi:10.1152/ajplegacy.1960.198.6.1307 (1960).
274 Kohm, A. P. & Sanders, V. M. Norepinephrine: a messenger from the brain to the immune system. *Immunol Today* 21, 539-542, doi:10.1016/s0167-5699(00)01747-3 (2000).
275 Pardini, B. J., Jones, S. B. & Filkins, J. P. Cardiac and splenic norepinephrine turnovers in endotoxic rats. *Am J Physiol* 245, H276-283, doi:10.1152/ajpheart.1983.245.2.H276 (1983).
276 Ruhl, A., Hurst, S. & Collins, S. M. Synergism between interleukins 1 beta and 6 on noradrenergic nerves in rat myenteric plexus. *Gastroenterology* 107, 993-1001, doi:10.1016/0016-5085(94)90223-2 (1994).
277 Straub, R. H., Westermann, J., Scholmerich, J. & Falk, W. Dialogue between the CNS and the immune system in lymphoid organs. *Immunol Today* 19, 409-413, doi:10.1016/s0167-5699(98)01297-3 (1998).
278 Sanders, V. M. The role of adrenoceptor-mediated signals in the modulation of lymphocyte function. *Adv Neuroimmunol* 5, 283-298, doi:10.1016/0960-5428(95)00019-x (1995).
279 Sanders, V. M. The role of norepinephrine and beta-2-adrenergic receptor stimulation in the modulation of Th1, Th2, and B lymphocyte function. *Adv Exp Med Biol* 437, 269-278, doi:10.1007/978-1-4615-5347-2_30 (1998).
280 Sanders, V. M. *et al.* Differential expression of the beta2-adrenergic receptor by Th1 and Th2 clones: implications for cytokine production and B cell help. *J Immunol* 158, 4200-4210 (1997).
281 Sanders, V. M. & Munson, A. E. Beta adrenoceptor mediation of the enhancing effect of norepinephrine on the murine primary antibody response in vitro. *J Pharmacol Exp Ther* 230, 183-192 (1984).
282 Sanders, V. M. & Munson, A. E. Norepinephrine and the antibody response. *Pharmacol Rev* 37, 229-248 (1985).
283 Sanders, V. M. & Munson, A. E. Role of alpha adrenoceptor activation in modulating the murine primary antibody response in vitro. *J Pharmacol Exp Ther* 232, 395-400 (1985).

284 Sanders, V. M. & Powell-Oliver, F. E. Beta 2-adrenoceptor stimulation increases the number of antigen-specific precursor B lymphocytes that differentiate into IgM-secreting cells without affecting burst size. *J Immunol* 148, 1822-1828 (1992).
285 Abrass, C. K., O'Connor, S. W., Scarpace, P. J. & Abrass, I. B. Characterization of the beta-adrenergic receptor of the rat peritoneal macrophage. *J Immunol* 135, 1338-1341 (1985).
286 Higgins, T. J. & David, J. R. Effect of isoproterernol and aminiphylline on cyclic AMP levels of guinea pig macrophages. *Cell Immunol* 27, 1-10, doi:10.1016/0008-8749(76)90147-7 (1976).
287 Ikegami, K. Modulation of adenosine 3',5'-monophosphate contents of rat peritoneal macrophages mediated by beta2-adrenergic receptors. *Biochem Pharmacol* 26, 1813-1816, doi:10.1016/0006-2952(77)90351-3 (1977).
288 Lavis, V. R., Strada, S. J., Ross, C. P., Hersh, E. M. & Thompson, W. J. Comparison of the responses of freshly isolated and cultured human monocytes and P388D1 cells to agents affecting cyclic AMP metabolism. *J Lab Clin Med* 96, 551-561 (1980).
289 Remold-O'Donnell, E. Stimulation and desensitization of macrophage adenylate cyclase by prostaglandins and catecholamines. *J Biol Chem* 249, 361-321 (1974).
290 Rosati, C., Hannaert, P., Dausse, J. P., Braquet, P. & Garay, R. Stimulation of beta-adrenoceptors inhibits calcium-dependent potassium-channels in mouse macrophages. *J Cell Physiol* 129, 310-314, doi:10.1002/jcp.1041290307 (1986).
291 Verghese, M. W. & Snyderman, R. Hormonal activation of adenylate cyclase in macrophage membranes is regulated by guanine nucleotides. *J Immunol* 130, 869-873 (1983).
292 Bidart, J. M., Motte, P., Assicot, M., Bohuon, C. & Bellet, D. Catechol-O-methyltransferase activity and aminergic binding sites distribution in human peripheral blood lymphocyte subpopulations. *Clin Immunol Immunopathol* 26, 1-9, doi:10.1016/0090-1229(83)90167-8 (1983).
293 Bishopric, N. H., Cohen, H. J. & Lefkowitz, R. J. Beta adrenergic receptors in lymphocyte subpopulations. *J Allergy Clin Immunol* 65, 29-33, doi:10.1016/0091-6749(80)90173-6 (1980).
294 Bourne, H. R. & Melmon, K. L. Adenyl cyclase in human leukocytes: evidence for activation by separate beta adrenergic and prostaglandin receptors. *J Pharmacol Exp Ther* 178, 1-7 (1971).
295 Pochet, R., Delespesse, G., Gausset, P. W. & Collet, H. Distribution of beta-adrenergic receptors on human lymphocyte subpopulations. *Clin Exp Immunol* 38, 578-584 (1979).
296 Smith, J. W., Steiner, A. L. & Parker, C. W. Human lymphocytic metabolism. Effects of cyclic and noncyclic nucleotides on stimulation by phytohemagglutinin. *J Clin Invest* 50, 442-448, doi:10.1172/JCI106511 (1971).
297 Vischer, T. L. The differential effect of cyclic AMP on lymphocyte stimulation by T- or B-cell mitogens. *Immunology* 30, 735-739 (1976).
298 Cremaschi, G. A., Fisher, P. & Boege, F. Beta-adrenoceptor distribution in murine lymphoid cell lines. *Immunopharmacology* 22, 195-206, doi:10.1016/0162-3109(91)90044-y (1991).
299 Fuchs, B. A., Albright, J. W. & Albright, J. F. Beta-adrenergic receptors on murine lymphocytes: density varies with cell maturity and lymphocyte subtype and is decreased

after antigen administration. *Cell Immunol* 114, 231-245, doi:10.1016/0008-8749(88)90318-8 (1988).

300 Kohm, A. P. & Sanders, V. M. Suppression of antigen-specific Th2 cell-dependent IgM and IgG1 production following norepinephrine depletion in vivo. *J Immunol* 162, 5299-5308 (1999).

301 Miles, K., Atweh, S., Otten, G., Arnason, B. G. & Chelmicka-Schorr, E. Beta-adrenergic receptors on splenic lymphocytes from axotomized mice. *Int J Immunopharmacol* 6, 171-177, doi:10.1016/0192-0561(84)90014-6 (1984).

302 Xiao, J. *et al.* Modulation of natural killer cell function by alpha-adrenoreceptor-coupled signalling. *Neuro Endocrinol Lett* 31, 635-644 (2010).

303 Benschop, R. J., Oostveen, F. G., Heijnen, C. J. & Ballieux, R. E. Beta 2-adrenergic stimulation causes detachment of natural killer cells from cultured endothelium. *Eur J Immunol* 23, 3242-3247, doi:10.1002/eji.1830231230 (1993).

304 Berthoud, H. R. & Neuhuber, W. L. Functional and chemical anatomy of the afferent vagal system. *Auton Neurosci* 85, 1-17, doi:10.1016/S1566-0702(00)00215-0 (2000).

305 Groves, D. A. & Brown, V. J. Vagal nerve stimulation: a review of its applications and potential mechanisms that mediate its clinical effects. *Neurosci Biobehav Rev* 29, 493-500, doi:10.1016/j.neubiorev.2005.01.004 (2005).

306 Goehler, L. E. *et al.* Vagal paraganglia bind biotinylated interleukin-1 receptor antagonist: a possible mechanism for immune-to-brain communication. *Brain Res Bull* 43, 357-364, doi:10.1016/s0361-9230(97)00020-8 (1997).

307 Hansen, M. K., O'Connor, K. A., Goehler, L. E., Watkins, L. R. & Maier, S. F. The contribution of the vagus nerve in interleukin-1beta-induced fever is dependent on dose. *Am J Physiol Regul Integr Comp Physiol* 280, R929-934, doi:10.1152/ajpregu.2001.280.4.R929 (2001).

308 Marquette, C. *et al.* IL-1beta, TNFalpha and IL-6 induction in the rat brain after partial-body irradiation: role of vagal afferents. *Int J Radiat Biol* 79, 777-785, doi:10.1080/09553000310001610998 (2003).

309 Buijs, R. M., van der Vliet, J., Garidou, M. L., Huitinga, I. & Escobar, C. Spleen vagal denervation inhibits the production of antibodies to circulating antigens. *PLoS One* 3, e3152, doi:10.1371/journal.pone.0003152 (2008).

310 Chen, X. H., Itoh, M., Sun, W., Miki, T. & Takeuchi, Y. Localization of sympathetic and parasympathetic neurons innervating pancreas and spleen in the cat. *J Auton Nerv Syst* 59, 12-16, doi:10.1016/0165-1838(95)00136-0 (1996).

311 Nance, D. M. & Burns, J. Innervation of the spleen in the rat: evidence for absence of afferent innervation. *Brain Behav Immun* 3, 281-290, doi:10.1016/0889-1591(89)90028-7 (1989).

312 Borovikova, L. V. *et al.* Vagus nerve stimulation attenuates the systemic inflammatory response to endotoxin. *Nature* 405, 458-462, doi:10.1038/35013070 (2000).

313 Bernik, T. R. *et al.* Pharmacological stimulation of the cholinergic antiinflammatory pathway. *J Exp Med* 195, 781-788, doi:10.1084/jem.20011714 (2002).

314 Guarini, S. *et al.* Efferent vagal fibre stimulation blunts nuclear factor-kappaB activation and protects against hypovolemic hemorrhagic shock. *Circulation* 107, 1189-1194, doi:10.1161/01.cir.0000050627.90734.ed (2003).

315 Li, M. *et al.* Vagal nerve stimulation markedly improves long-term survival after chronic heart failure in rats. *Circulation* 109, 120-124, doi:10.1161/01.CIR.0000105721.71640.DA (2004).
316 Ganta, C. K. *et al.* Central angiotensin II-enhanced splenic cytokine gene expression is mediated by the sympathetic nervous system. *Am J Physiol Heart Circ Physiol* 289, H1683-1691, doi:10.1152/ajpheart.00125.2005 (2005).
317 Gaykema, R. P., Goehler, L. E., Hansen, M. K., Maier, S. F. & Watkins, L. R. Subdiaphragmatic vagotomy blocks interleukin-1beta-induced fever but does not reduce IL-1beta levels in the circulation. *Auton Neurosci* 85, 72-77, doi:10.1016/s1566-0702(00)00222-8 (2000).
318 Bartik, M. M., Bauman, G. P., Brooks, W. H. & Roszman, T. L. Costimulatory signals modulate the antiproliferative effects of agents that elevate cAMP in T cells. *Cell Immunol* 158, 116-130, doi:10.1006/cimm.1994.1261 (1994).
319 Goehler, L. E. *et al.* Interleukin-1beta in immune cells of the abdominal vagus nerve: a link between the immune and nervous systems? *J Neurosci* 19, 2799-2806 (1999).
320 Goehler, L. E. *et al.* Activation in vagal afferents and central autonomic pathways: early responses to intestinal infection with Campylobacter jejuni. *Brain Behav Immun* 19, 334-344, doi:10.1016/j.bbi.2004.09.002 (2005).
321 Goldbach, J. M., Roth, J. & Zeisberger, E. Fever suppression by subdiaphragmatic vagotomy in guinea pigs depends on the route of pyrogen administration. *Am J Physiol* 272, R675-681, doi:10.1152/ajpregu.1997.272.2.R675 (1997).
322 Guggilam, A. *et al.* TNF-alpha blockade decreases oxidative stress in the paraventricular nucleus and attenuates sympathoexcitation in heart failure rats. *Am J Physiol Heart Circ Physiol* 293, H599-609, doi:10.1152/ajpheart.00286.2007 (2007).
323 Guggilam, A. *et al.* Cytokine blockade attenuates sympathoexcitation in heart failure: cross-talk between nNOS, AT-1R and cytokines in the hypothalamic paraventricular nucleus. *Eur J Heart Fail* 10, 625-634, doi:10.1016/j.ejheart.2008.05.004 (2008).
324 Haensel, A., Mills, P. J., Nelesen, R. A., Ziegler, M. G. & Dimsdale, J. E. The relationship between heart rate variability and inflammatory markers in cardiovascular diseases. *Psychoneuroendocrinology* 33, 1305-1312, doi:10.1016/j.psyneuen.2008.08.007 (2008).
325 Hamrick, M. W. & Ferrari, S. L. Leptin and the sympathetic connection of fat to bone. *Osteoporos Int* 19, 905-912, doi:10.1007/s00198-007-0487-9 (2008).
326 Hansen, M. K. *et al.* Subdiaphragmatic vagotomy does not block intraperitoneal lipopolysaccharide-induced fever. *Auton Neurosci* 85, 83-87, doi:10.1016/S1566-0702(00)00224-1 (2000).
327 Hansen, M. K. & Krueger, J. M. Subdiaphragmatic vagotomy blocks the sleep- and fever-promoting effects of interleukin-1beta. *Am J Physiol* 273, R1246-1253, doi:10.1152/ajpregu.1997.273.4.R1246 (1997).
328 Holzmann, B. Antiinflammatory activities of CGRP modulating innate immune responses in health and disease. *Curr Protein Pept Sci* 14, 268-274, doi:10.2174/1389203713149990046 (2013).
329 Gao, X. *et al.* Nociceptive nerves regulate haematopoietic stem cell mobilization. *Nature* 589, 591-596, doi:10.1038/s41586-020-03057-y (2021).

330 Lambrecht, B. N. Immunologists getting nervous: neuropeptides, dendritic cells and T cell activation. *Respir Res* 2, 133-138, doi:10.1186/rr49 (2001).
331 Liebig, C. *et al.* Perineural invasion is an independent predictor of outcome in colorectal cancer. *J Clin Oncol* 27, 5131-5137, doi:10.1200/JCO.2009.22.4949 (2009).
332 Huang, D. *et al.* Nerve fibers in breast cancer tissues indicate aggressive tumor progression. *Medicine (Baltimore)* 93, e172, doi:10.1097/MD.0000000000000172 (2014).
333 Hibi, T. *et al.* Synuclein-gamma is closely involved in perineural invasion and distant metastasis in mouse models and is a novel prognostic factor in pancreatic cancer. *Clin Cancer Res* 15, 2864-2871, doi:10.1158/1078-0432.CCR-08-2946 (2009).
334 Horn, L. C., Meinel, A., Fischer, U., Bilek, K. & Hentschel, B. Perineural invasion in carcinoma of the cervix uteri--prognostic impact. *J Cancer Res Clin Oncol* 136, 1557-1562, doi:10.1007/s00432-010-0813-z (2010).
335 Tianhang, L., Guoen, F., Jianwei, B. & Liye, M. The effect of perineural invasion on overall survival in patients with gastric carcinoma. *J Gastrointest Surg* 12, 1263-1267, doi:10.1007/s11605-008-0529-4 (2008).
336 Chen, J. W. *et al.* The prognostic effect of perineural invasion in esophageal squamous cell carcinoma. *BMC Cancer* 14, 313, doi:10.1186/1471-2407-14-313 (2014).
337 Chatterjee, D. *et al.* Perineural and intraneural invasion in posttherapy pancreaticoduodenectomy specimens predicts poor prognosis in patients with pancreatic ductal adenocarcinoma. *Am J Surg Pathol* 36, 409-417, doi:10.1097/PAS.0b013e31824104c5 (2012).
338 Ayala, G. E. *et al.* Cancer-related axonogenesis and neurogenesis in prostate cancer. *Clin Cancer Res* 14, 7593-7603, doi:10.1158/1078-0432.CCR-08-1164 (2008).
339 Bapat, A. A., Hostetter, G., Von Hoff, D. D. & Han, H. Perineural invasion and associated pain in pancreatic cancer. *Nat Rev Cancer* 11, 695-707, doi:10.1038/nrc3131 (2011).
340 Deshmukh, S. D., Willmann, J. K. & Jeffrey, R. B. Pathways of extrapancreatic perineural invasion by pancreatic adenocarcinoma: evaluation with 3D volume-rendered MDCT imaging. *AJR Am J Roentgenol* 194, 668-674, doi:10.2214/AJR.09.3285 (2010).
341 Demir, I. E., Friess, H. & Ceyhan, G. O. Nerve-cancer interactions in the stromal biology of pancreatic cancer. *Front Physiol* 3, 97, doi:10.3389/fphys.2012.00097 (2012).
342 Lei, Y. *et al.* Gold nanoclusters-assisted delivery of NGF siRNA for effective treatment of pancreatic cancer. *Nat Commun* 8, 15130, doi:10.1038/ncomms15130 (2017).
343 Espana-Ferrufino, A., Lino-Silva, L. S. & Salcedo-Hernandez, R. A. Extramural Perineural Invasion in pT3 and pT4 Gastric Carcinomas. *J Pathol Transl Med* 52, 79-84, doi:10.4132/jptm.2017.11.01 (2018).
344 Deng, J. *et al.* Prognostic value of perineural invasion in gastric cancer: a systematic review and meta-analysis. *PLoS One* 9, e88907, doi:10.1371/journal.pone.0088907 (2014).
345 Schmitd, L. B., Scanlon, C. S. & D'Silva, N. J. Perineural Invasion in Head and Neck Cancer. *J Dent Res* 97, 742-750, doi:10.1177/0022034518756297 (2018).
346 Batkin, S., Piette, L. H. & Wildman, E. Effect of muscle denervation on growth of transplanted tumor in mice. *Proc Natl Acad Sci U S A* 67, 1521-1527, doi:10.1073/pnas.67.3.1521 (1970).

347 Kuol, N., Stojanovska, L., Apostolopoulos, V. & Nurgali, K. Role of the Nervous System in Tumor Angiogenesis. *Cancer Microenviron* 11, 1-11, doi:10.1007/s12307-018-0207-3 (2018).
348 Ayala, G. E. *et al.* In vitro dorsal root ganglia and human prostate cell line interaction: redefining perineural invasion in prostate cancer. *Prostate* 49, 213-223, doi:10.1002/pros.1137 (2001).
349 Mauffrey, P. *et al.* Progenitors from the central nervous system drive neurogenesis in cancer. *Nature* 569, 672-678, doi:10.1038/s41586-019-1219-y (2019).
350 Kruttgen, A., Schneider, I. & Weis, J. The dark side of the NGF family: neurotrophins in neoplasias. *Brain Pathol* 16, 304-310, doi:10.1111/j.1750-3639.2006.00037.x (2006).
351 Wang, W. *et al.* Patterns of expression and function of the p75(NGFR) protein in pancreatic cancer cells and tumours. *Eur J Surg Oncol* 35, 826-832, doi:10.1016/j.ejso.2008.10.013 (2009).
352 Dalal, R. & Djakiew, D. Molecular characterization of neurotrophin expression and the corresponding tropomyosin receptor kinases (trks) in epithelial and stromal cells of the human prostate. *Mol Cell Endocrinol* 134, 15-22, doi:10.1016/s0303-7207(97)00165-2 (1997).
353 Montano, X. & Djamgoz, M. B. Epidermal growth factor, neurotrophins and the metastatic cascade in prostate cancer. *FEBS Lett* 571, 1-8, doi:10.1016/j.febslet.2004.06.088 (2004).
354 Satoh, F. *et al.* Autocrine expression of neurotrophins and their receptors in prostate cancer. *Int J Urol* 8, S28-34, doi:10.1046/j.1442-2042.2001.00331.x (2001).
355 Miknyoczki, S. J. *et al.* The neurotrophin-trk receptor axes are critical for the growth and progression of human prostatic carcinoma and pancreatic ductal adenocarcinoma xenografts in nude mice. *Clin Cancer Res* 8, 1924-1931 (2002).
356 Hayakawa, Y. *et al.* Nerve Growth Factor Promotes Gastric Tumorigenesis through Aberrant Cholinergic Signaling. *Cancer Cell* 31, 21-34, doi:10.1016/j.ccell.2016.11.005 (2017).
357 Dolle, L. *et al.* Nerve growth factor receptors and signaling in breast cancer. *Curr Cancer Drug Targets* 4, 463-470, doi:10.2174/1568009043332853 (2004).
358 Marchetti, D. *et al.* Brain-metastatic melanoma: a neurotrophic perspective. *Pathol Oncol Res* 9, 147-158, doi:10.1007/BF03033729 (2003).
359 Schneider, M. B. *et al.* Expression of nerve growth factors in pancreatic neural tissue and pancreatic cancer. *J Histochem Cytochem* 49, 1205-1210, doi:10.1177/002215540104901002 (2001).
360 Renz, B. W. *et al.* beta2 Adrenergic-Neurotrophin Feedforward Loop Promotes Pancreatic Cancer. *Cancer Cell* 33, 75-90 e77, doi:10.1016/j.ccell.2017.11.007 (2018).
361 Lam, C. T. *et al.* Brain-derived neurotrophic factor promotes tumorigenesis via induction of neovascularization: implication in hepatocellular carcinoma. *Clin Cancer Res* 17, 3123-3133, doi:10.1158/1078-0432.CCR-10-2802 (2011).
362 Zeng, Q. *et al.* The relationship between overexpression of glial cell-derived neurotrophic factor and its RET receptor with progression and prognosis of human pancreatic cancer. *J Int Med Res* 36, 656-664, doi:10.1177/147323000803600406 (2008).

363 Cavel, O. *et al.* Endoneurial macrophages induce perineural invasion of pancreatic cancer cells by secretion of GDNF and activation of RET tyrosine kinase receptor. *Cancer Res* 72, 5733-5743, doi:10.1158/0008-5472.CAN-12-0764 (2012).
364 Gil, Z. *et al.* Paracrine regulation of pancreatic cancer cell invasion by peripheral nerves. *J Natl Cancer Inst* 102, 107-118, doi:10.1093/jnci/djp456 (2010).
365 Airaksinen, M. S. & Saarma, M. The GDNF family: signalling, biological functions and therapeutic value. *Nat Rev Neurosci* 3, 383-394, doi:10.1038/nrn812 (2002).
366 Amit, M., Na'ara, S. & Gil, Z. Mechanisms of cancer dissemination along nerves. *Nat Rev Cancer* 16, 399-408, doi:10.1038/nrc.2016.38 (2016).
367 Wang, K. *et al.* The neurotrophic factor neurturin contributes toward an aggressive cancer cell phenotype, neuropathic pain and neuronal plasticity in pancreatic cancer. *Carcinogenesis* 35, 103-113, doi:10.1093/carcin/bgt312 (2014).
368 Gao, L., Bo, H., Wang, Y., Zhang, J. & Zhu, M. Neurotrophic Factor Artemin Promotes Invasiveness and Neurotrophic Function of Pancreatic Adenocarcinoma In Vivo and In Vitro. *Pancreas* 44, 134-143, doi:10.1097/MPA.0000000000000223 (2015).
369 Delloye-Bourgeois, C. *et al.* Netrin-1 acts as a survival factor for aggressive neuroblastoma. *J Exp Med* 206, 833-847, doi:10.1084/jem.20082299 (2009).
370 Fitamant, J. *et al.* Netrin-1 expression confers a selective advantage for tumor cell survival in metastatic breast cancer. *Proc Natl Acad Sci U S A* 105, 4850-4855, doi:10.1073/pnas.0709810105 (2008).
371 Yin, K. *et al.* Netrin-1 promotes cell neural invasion in gastric cancer via its receptor neogenin. *J Cancer* 10, 3197-3207, doi:10.7150/jca.30230 (2019).
372 Gohrig, A. *et al.* Axon guidance factor SLIT2 inhibits neural invasion and metastasis in pancreatic cancer. *Cancer Res* 74, 1529-1540, doi:10.1158/0008-5472.CAN-13-1012 (2014).
373 Li, X. *et al.* Targeting tumor innervation: premises, promises, and challenges. *Cell Death Discov* 8, 131, doi:10.1038/s41420-022-00930-9 (2022).
374 Arese, M., Bussolino, F., Pergolizzi, M., Bizzozero, L. & Pascal, D. Tumor progression: the neuronal input. *Ann Transl Med* 6, 89, doi:10.21037/atm.2018.01.01 (2018).
375 Deborde, S. & Wong, R. J. How Schwann cells facilitate cancer progression in nerves. *Cell Mol Life Sci* 74, 4405-4420, doi:10.1007/s00018-017-2578-x (2017).
376 Mancino, M., Ametller, E., Gascon, P. & Almendro, V. The neuronal influence on tumor progression. *Biochim Biophys Acta* 1816, 105-118, doi:10.1016/j.bbcan.2011.04.005 (2011).
377 Barquilla, A. & Pasquale, E. B. Eph receptors and ephrins: therapeutic opportunities. *Annu Rev Pharmacol Toxicol* 55, 465-487, doi:10.1146/annurev-pharmtox-011112-140226 (2015).
378 Wang, H. *et al.* Role of the nervous system in cancers: a review. *Cell Death Discov* 7, 76, doi:10.1038/s41420-021-00450-y (2021).
379 Madeo, M. *et al.* Cancer exosomes induce tumor innervation. *Nat Commun* 9, 4284, doi:10.1038/s41467-018-06640-0 (2018).
380 Hyenne, V., Labouesse, M. & Goetz, J. G. The Small GTPase Ral orchestrates MVB biogenesis and exosome secretion. *Small GTPases* 9, 445-451, doi:10.1080/21541248.2016.1251378 (2018).

381 Amit, M. *et al.* Loss of p53 drives neuron reprogramming in head and neck cancer. *Nature* 578, 449-454, doi:10.1038/s41586-020-1996-3 (2020).
382 Colombo, M., Raposo, G. & Thery, C. Biogenesis, secretion, and intercellular interactions of exosomes and other extracellular vesicles. *Annu Rev Cell Dev Biol* 30, 255-289, doi:10.1146/annurev-cellbio-101512-122326 (2014).
383 Keskinov, A. A. *et al.* Impact of the Sensory Neurons on Melanoma Growth In Vivo. *PLoS One* 11, e0156095, doi:10.1371/journal.pone.0156095 (2016).
384 Lin, C. *et al.* GDNF secreted by nerves enhances PD-L1 expression via JAK2-STAT1 signaling activation in HNSCC. *Oncoimmunology* 6, e1353860, doi:10.1080/2162402X.2017.1353860 (2017).
385 Kamiya, A. *et al.* Genetic manipulation of autonomic nerve fiber innervation and activity and its effect on breast cancer progression. *Nat Neurosci* 22, 1289-1305, doi:10.1038/s41593-019-0430-3 (2019).
386 McIlvried, L. A., Atherton, M. A., Horan, N. L., Goch, T. N. & Scheff, N. N. Sensory Neurotransmitter Calcitonin Gene-Related Peptide Modulates Tumor Growth and Lymphocyte Infiltration in Oral Squamous Cell Carcinoma. *Adv Biol (Weinh)*, e2200019, doi:10.1002/adbi.202200019 (2022).
387 Thaker, P. H. *et al.* Chronic stress promotes tumor growth and angiogenesis in a mouse model of ovarian carcinoma. *Nat Med* 12, 939-944, doi:10.1038/nm1447 (2006).
388 Kim-Fuchs, C. *et al.* Chronic stress accelerates pancreatic cancer growth and invasion: a critical role for beta-adrenergic signaling in the pancreatic microenvironment. *Brain Behav Immun* 40, 40-47, doi:10.1016/j.bbi.2014.02.019 (2014).
389 Melamed, R. *et al.* Marginating pulmonary-NK activity and resistance to experimental tumor metastasis: suppression by surgery and the prophylactic use of a beta-adrenergic antagonist and a prostaglandin synthesis inhibitor. *Brain Behav Immun* 19, 114-126, doi:10.1016/j.bbi.2004.07.004 (2005).
390 Li, Z. J. & Cho, C. H. Neurotransmitters, more than meets the eye--neurotransmitters and their perspectives in cancer development and therapy. *Eur J Pharmacol* 667, 17-22, doi:10.1016/j.ejphar.2011.05.077 (2011).
391 Lu, R. *et al.* Neurons generated from carcinoma stem cells support cancer progression. *Signal Transduct Target Ther* 2, 16036, doi:10.1038/sigtrans.2016.36 (2017).
392 Chakroborty, D., Sarkar, C., Basu, B., Dasgupta, P. S. & Basu, S. Catecholamines regulate tumor angiogenesis. *Cancer Res* 69, 3727-3730, doi:10.1158/0008-5472.CAN-08-4289 (2009).
393 Madden, K. S., Szpunar, M. J. & Brown, E. B. beta-Adrenergic receptors (beta-AR) regulate VEGF and IL-6 production by divergent pathways in high beta-AR-expressing breast cancer cell lines. *Breast Cancer Res Treat* 130, 747-758, doi:10.1007/s10549-011-1348-y (2011).
394 Xia, Y. *et al.* Catecholamines contribute to the neovascularization of lung cancer via tumor-associated macrophages. *Brain Behav Immun* 81, 111-121, doi:10.1016/j.bbi.2019.06.004 (2019).
395 Basu, S. *et al.* The neurotransmitter dopamine inhibits angiogenesis induced by vascular permeability factor/vascular endothelial growth factor. *Nat Med* 7, 569-574, doi:10.1038/87895 (2001).

396 Moreno-Smith, M. *et al.* Biologic effects of dopamine on tumor vasculature in ovarian carcinoma. *Neoplasia* 15, 502-510, doi:10.1593/neo.121412 (2013).
397 Sternini, C. Organization of the peripheral nervous system: autonomic and sensory ganglia. *J Investig Dermatol Symp Proc* 2, 1-7, doi:10.1038/jidsymp.1997.2 (1997).
398 Erin, N. & Ulusoy, O. Differentiation of neuronal from non-neuronal Substance P. *Regul Pept* 152, 108-113, doi:10.1016/j.regpep.2008.10.006 (2009).
399 Dunn, G. P., Bruce, A. T., Ikeda, H., Old, L. J. & Schreiber, R. D. Cancer immunoediting: from immunosurveillance to tumor escape. *Nat Immunol* 3, 991-998, doi:10.1038/ni1102-991 (2002).
400 Lundberg, J. M., Brodin, E., Hua, X. & Saria, A. Vascular permeability changes and smooth muscle contraction in relation to capsaicin-sensitive substance P afferents in the guinea-pig. *Acta Physiol Scand* 120, 217-227, doi:10.1111/j.1748-1716.1984.tb00127.x (1984).
401 Holzer, P. Role of visceral afferent neurons in mucosal inflammation and defense. *Curr Opin Pharmacol* 7, 563-569, doi:10.1016/j.coph.2007.09.004 (2007).
402 Okajima, K. & Harada, N. Regulation of inflammatory responses by sensory neurons: molecular mechanism(s) and possible therapeutic applications. *Curr Med Chem* 13, 2241-2251, doi:10.2174/092986706777935131 (2006).
403 Goertzen, C. *et al.* Oral inflammation promotes oral squamous cell carcinoma invasion. *Oncotarget* 9, 29047-29063, doi:10.18632/oncotarget.25540 (2018).
404 Lasfar, A., Zloza, A., Silk, A. W., Lee, L. Y. & Cohen-Solal, K. A. Interferon Lambda: Toward a Dual Role in Cancer. *J Interferon Cytokine Res* 39, 22-29, doi:10.1089/jir.2018.0046 (2019).
405 Berger, E. *et al.* Association between low-grade inflammation and Breast cancer and B-cell Myeloma and Non-Hodgkin Lymphoma: findings from two prospective cohorts. *Sci Rep* 8, 10805, doi:10.1038/s41598-018-29041-1 (2018).
406 Praveen, T. K. *et al.* Inflammation targeted nanomedicines: Patents and applications in cancer therapy. *Semin Cancer Biol*, doi:10.1016/j.semcancer.2022.04.004 (2022).
407 Magnon, C. *et al.* Autonomic nerve development contributes to prostate cancer progression. *Science* 341, 1236361, doi:10.1126/science.1236361 (2013).
408 Zhao, C. M. *et al.* Denervation suppresses gastric tumorigenesis. *Sci Transl Med* 6, 250ra115, doi:10.1126/scitranslmed.3009569 (2014).
409 Peterson, S. C. *et al.* Basal cell carcinoma preferentially arises from stem cells within hair follicle and mechanosensory niches. *Cell Stem Cell* 16, 400-412, doi:10.1016/j.stem.2015.02.006 (2015).
410 Horvathova, L. *et al.* Sympathectomy reduces tumor weight and affects expression of tumor-related genes in melanoma tissue in the mouse. *Stress* 19, 528-534, doi:10.1080/10253890.2016.1213808 (2016).
411 Sinha, S. *et al.* PanIN Neuroendocrine Cells Promote Tumorigenesis via Neuronal Cross-talk. *Cancer Res* 77, 1868-1879, doi:10.1158/0008-5472.CAN-16-0899-T (2017).
412 Stopczynski, R. E. *et al.* Neuroplastic changes occur early in the development of pancreatic ductal adenocarcinoma. *Cancer Res* 74, 1718-1727, doi:10.1158/0008-5472.CAN-13-2050 (2014).
413 Erin, N., Shurin, G. V., Baraldi, J. H. & Shurin, M. R. Regulation of Carcinogenesis by Sensory Neurons and Neuromediators. *Cancers (Basel)* 14, doi:10.3390/cancers14092333 (2022).

414 Zahalka, A. H. *et al.* Adrenergic nerves activate an angio-metabolic switch in prostate cancer. *Science* 358, 321-326, doi:10.1126/science.aah5072 (2017).
415 Zahalka, A. H. & Frenette, P. S. Nerves in cancer. *Nat Rev Cancer* 20, 143-157, doi:10.1038/s41568-019-0237-2 (2020).
416 Chambers, C. A., Kuhns, M. S., Egen, J. G. & Allison, J. P. CTLA-4-mediated inhibition in regulation of T cell responses: mechanisms and manipulation in tumor immunotherapy. *Annu Rev Immunol* 19, 565-594, doi:10.1146/annurev.immunol.19.1.565 (2001).
417 Dougan, M. & Dranoff, G. Immune therapy for cancer. *Annu Rev Immunol* 27, 83-117, doi:10.1146/annurev.immunol.021908.132544 (2009).
418 Topalian, S. L. *et al.* Safety, activity, and immune correlates of anti-PD-1 antibody in cancer. *N Engl J Med* 366, 2443-2454, doi:10.1056/NEJMoa1200690 (2012).
419 Baumeister, S. H., Freeman, G. J., Dranoff, G. & Sharpe, A. H. Coinhibitory Pathways in Immunotherapy for Cancer. *Annu Rev Immunol* 34, 539-573, doi:10.1146/annurev-immunol-032414-112049 (2016).
420 Vesely, M. D., Kershaw, M. H., Schreiber, R. D. & Smyth, M. J. Natural innate and adaptive immunity to cancer. *Annu Rev Immunol* 29, 235-271, doi:10.1146/annurev-immunol-031210-101324 (2011).
421 Woo, S. R., Corrales, L. & Gajewski, T. F. Innate immune recognition of cancer. *Annu Rev Immunol* 33, 445-474, doi:10.1146/annurev-immunol-032414-112043 (2015).
422 Anderson, P. & Gonzalez-Rey, E. Vasoactive intestinal peptide induces cell cycle arrest and regulatory functions in human T cells at multiple levels. *Mol Cell Biol* 30, 2537-2551, doi:10.1128/MCB.01282-09 (2010).
423 Chen, G. *et al.* PD-L1 inhibits acute and chronic pain by suppressing nociceptive neuron activity via PD-1. *Nat Neurosci* 20, 917-926, doi:10.1038/nn.4571 (2017).
424 Li, J. M. *et al.* VIPhyb, an antagonist of vasoactive intestinal peptide receptor, enhances cellular antiviral immunity in murine cytomegalovirus infected mice. *PLoS One* 8, e63381, doi:10.1371/journal.pone.0063381 (2013).
425 Li, J. M. *et al.* Modulation of Immune Checkpoints and Graft-versus-Leukemia in Allogeneic Transplants by Antagonizing Vasoactive Intestinal Peptide Signaling. *Cancer Res* 76, 6802-6815, doi:10.1158/0008-5472.CAN-16-0427 (2016).
426 Ondicova, K. & Mravec, B. Role of nervous system in cancer aetiopathogenesis. *Lancet Oncol* 11, 596-601, doi:10.1016/S1470-2045(09)70337-7 (2010).
427 Petersen, C. T., Li, J. M. & Waller, E. K. Administration of a vasoactive intestinal peptide antagonist enhances the autologous anti-leukemia T cell response in murine models of acute leukemia. *Oncoimmunology* 6, e1304336, doi:10.1080/2162402X.2017.1304336 (2017).
428 Pozo, D., Anderson, P. & Gonzalez-Rey, E. Induction of alloantigen-specific human T regulatory cells by vasoactive intestinal peptide. *J Immunol* 183, 4346-4359, doi:10.4049/jimmunol.0900400 (2009).
429 Saloman, J. L. *et al.* Ablation of sensory neurons in a genetic model of pancreatic ductal adenocarcinoma slows initiation and progression of cancer. *Proc Natl Acad Sci U S A* 113, 3078-3083, doi:10.1073/pnas.1512603113 (2016).
430 Talbot, S. *et al.* Silencing Nociceptor Neurons Reduces Allergic Airway Inflammation. *Neuron* 87, 341-354, doi:10.1016/j.neuron.2015.06.007 (2015).

431 Tebas, P. *et al.* Reduction of soluble CD163, substance P, programmed death 1 and inflammatory markers: phase 1B trial of aprepitant in HIV-1-infected adults. *AIDS* 29, 931-939, doi:10.1097/QAD.0000000000000638 (2015).
432 Haqq, C. *et al.* The gene expression signatures of melanoma progression. *Proc Natl Acad Sci U S A* 102, 6092-6097, doi:10.1073/pnas.0501564102 (2005).
433 Harlin, H. *et al.* Chemokine expression in melanoma metastases associated with CD8+ T-cell recruitment. *Cancer Res* 69, 3077-3085, doi:10.1158/0008-5472.CAN-08-2281 (2009).
434 Riker, A. I. *et al.* The gene expression profiles of primary and metastatic melanoma yields a transition point of tumor progression and metastasis. *BMC Med Genomics* 1, 13, doi:10.1186/1755-8794-1-13 (2008).
435 Talantov, D. *et al.* Novel genes associated with malignant melanoma but not benign melanocytic lesions. *Clin Cancer Res* 11, 7234-7242, doi:10.1158/1078-0432.CCR-05-0683 (2005).
436 Renier, N. *et al.* iDISCO: a simple, rapid method to immunolabel large tissue samples for volume imaging. *Cell* 159, 896-910, doi:10.1016/j.cell.2014.10.010 (2014).
437 Hannila, S. S. *et al.* Secretory leukocyte protease inhibitor reverses inhibition by CNS myelin, promotes regeneration in the optic nerve, and suppresses expression of the transforming growth factor-beta signaling protein Smad2. *J Neurosci* 33, 5138-5151, doi:10.1523/JNEUROSCI.5321-12.2013 (2013).
438 Mueller, A. M. *et al.* Novel role for SLPI in MOG-induced EAE revealed by spinal cord expression analysis. *J Neuroinflammation* 5, 20, doi:10.1186/1742-2094-5-20 (2008).
439 Boilly, B., Faulkner, S., Jobling, P. & Hondermarck, H. Nerve Dependence: From Regeneration to Cancer. *Cancer Cell* 31, 342-354, doi:10.1016/j.ccell.2017.02.005 (2017).
440 Larkin, J. *et al.* Five-Year Survival with Combined Nivolumab and Ipilimumab in Advanced Melanoma. *N Engl J Med* 381, 1535-1546, doi:10.1056/NEJMoa1910836 (2019).
441 Long, G. V. *et al.* Nivolumab for Patients With Advanced Melanoma Treated Beyond Progression: Analysis of 2 Phase 3 Clinical Trials. *JAMA Oncol* 3, 1511-1519, doi:10.1001/jamaoncol.2017.1588 (2017).
442 Wolchok, J. D. *et al.* Overall Survival with Combined Nivolumab and Ipilimumab in Advanced Melanoma. *N Engl J Med* 377, 1345-1356, doi:10.1056/NEJMoa1709684 (2017).
443 Wang, J. *et al.* UV-induced somatic mutations elicit a functional T cell response in the YUMMER1.7 mouse melanoma model. *Pigment Cell Melanoma Res* 30, 428-435, doi:10.1111/pcmr.12591 (2017).
444 Meeth, K., Wang, J. X., Micevic, G., Damsky, W. & Bosenberg, M. W. The YUMM lines: a series of congenic mouse melanoma cell lines with defined genetic alterations. *Pigment Cell Melanoma Res* 29, 590-597, doi:10.1111/pcmr.12498 (2016).
445 Cohen, J. A. *et al.* Cutaneous TRPV1(+) Neurons Trigger Protective Innate Type 17 Anticipatory Immunity. *Cell* 178, 919-932 e914, doi:10.1016/j.cell.2019.06.022 (2019).
446 Michoud, F. *et al.* Epineural optogenetic activation of nociceptors initiates and amplifies inflammation. *Nat Biotechnol* 39, 179-185, doi:10.1038/s41587-020-0673-2 (2021).
447 Talbot, S. *et al.* Vagal sensory neurons drive mucous cell metaplasia. *J Allergy Clin Immunol* 145, 1693-1696 e1694, doi:10.1016/j.jaci.2020.01.003 (2020).

448 Pellett, S., Tepp, W. H., Whitemarsh, R. C., Bradshaw, M. & Johnson, E. A. In vivo onset and duration of action varies for botulinum neurotoxin A subtypes 1-5. *Toxicon* 107, 37-42, doi:10.1016/j.toxicon.2015.06.021 (2015).
449 Binshtok, A. M., Bean, B. P. & Woolf, C. J. Inhibition of nociceptors by TRPV1-mediated entry of impermeant sodium channel blockers. *Nature* 449, 607-610, doi:10.1038/nature06191 (2007).
450 Yissachar, N. *et al.* An Intestinal Organ Culture System Uncovers a Role for the Nervous System in Microbe-Immune Crosstalk. *Cell* 168, 1135-1148 e1112, doi:10.1016/j.cell.2017.02.009 (2017).
451 Chiu, I. M. *et al.* Bacteria activate sensory neurons that modulate pain and inflammation. *Nature* 501, 52-57, doi:10.1038/nature12479 (2013).
452 Ding, W., Stohl, L. L., Wagner, J. A. & Granstein, R. D. Calcitonin gene-related peptide biases Langerhans cells toward Th2-type immunity. *J Immunol* 181, 6020-6026, doi:10.4049/jimmunol.181.9.6020 (2008).
453 Kashem, S. W. *et al.* Nociceptive Sensory Fibers Drive Interleukin-23 Production from CD301b+ Dermal Dendritic Cells and Drive Protective Cutaneous Immunity. *Immunity* 43, 515-526, doi:10.1016/j.immuni.2015.08.016 (2015).
454 Cancer Genome Atlas Research, N. *et al.* The Cancer Genome Atlas Pan-Cancer analysis project. *Nat Genet* 45, 1113-1120, doi:10.1038/ng.2764 (2013).
455 Jerby-Arnon, L. *et al.* A Cancer Cell Program Promotes T Cell Exclusion and Resistance to Checkpoint Blockade. *Cell* 175, 984-997 e924, doi:10.1016/j.cell.2018.09.006 (2018).
456 Tirosh, I. *et al.* Dissecting the multicellular ecosystem of metastatic melanoma by single-cell RNA-seq. *Science* 352, 189-196, doi:10.1126/science.aad0501 (2016).
457 Monaco, G. *et al.* RNA-Seq Signatures Normalized by mRNA Abundance Allow Absolute Deconvolution of Human Immune Cell Types. *Cell Rep* 26, 1627-1640 e1627, doi:10.1016/j.celrep.2019.01.041 (2019).
458 Castle, J. C. *et al.* Exploiting the mutanome for tumor vaccination. *Cancer Res* 72, 1081-1091, doi:10.1158/0008-5472.CAN-11-3722 (2012).
459 Heng, T. S., Painter, M. W. & Immunological Genome Project, C. The Immunological Genome Project: networks of gene expression in immune cells. *Nat Immunol* 9, 1091-1094, doi:10.1038/ni1008-1091 (2008).
460 Crosson, T. *et al.* Profiling of how nociceptor neurons detect danger–new and old foes. *Journal of internal medicine* 286, 268-289 (2019).
461 Ray, P. *et al.* Comparative transcriptome profiling of the human and mouse dorsal root ganglia: an RNA-seq-based resource for pain and sensory neuroscience research. *Pain* 159, 1325 (2018).
462 Chiu, I. M. *et al.* Transcriptional profiling at whole population and single cell levels reveals somatosensory neuron molecular diversity. *Elife* 3, e04660 (2014).
463 Usoskin, D. *et al.* Unbiased classification of sensory neuron types by large-scale single-cell RNA sequencing. *Nature neuroscience* 18, 145-153 (2015).
464 Li, C., Wang, S., Chen, Y. & Zhang, X. Somatosensory neuron typing with high-coverage single-cell RNA sequencing and functional analysis. *Neuroscience bulletin* 34, 200-207 (2018).

465 Goswami, S. C. *et al.* Molecular signatures of mouse TRPV1-lineage neurons revealed by RNA-Seq transcriptome analysis. *The Journal of Pain* 15, 1338-1359 (2014).
466 Kupari, J., Häring, M., Agirre, E., Castelo-Branco, G. & Ernfors, P. An atlas of vagal sensory neurons and their molecular specialization. *Cell reports* 27, 2508-2523. e2504 (2019).
467 Hogquist, K. A. *et al.* T cell receptor antagonist peptides induce positive selection. *Cell* 76, 17-27, doi:10.1016/0092-8674(94)90169-4 (1994).
468 Crosson, T. *et al.* FcepsilonR1-expressing nociceptors trigger allergic airway inflammation. *J Allergy Clin Immunol* 147, 2330-2342, doi:10.1016/j.jaci.2020.12.644 (2021).
469 Madisen, L. *et al.* A toolbox of Cre-dependent optogenetic transgenic mice for light-induced activation and silencing. *Nat Neurosci* 15, 793-802, doi:10.1038/nn.3078 (2012).
470 Madisen, L. *et al.* A robust and high-throughput Cre reporting and characterization system for the whole mouse brain. *Nat Neurosci* 13, 133-140, doi:10.1038/nn.2467 (2010).
471 Voehringer, D., Liang, H. E. & Locksley, R. M. Homeostasis and effector function of lymphopenia-induced "memory-like" T cells in constitutively T cell-depleted mice. *J Immunol* 180, 4742-4753, doi:10.4049/jimmunol.180.7.4742 (2008).
472 Lou, S. *et al.* Genetically Targeted All-Optical Electrophysiology with a Transgenic Cre-Dependent Optopatch Mouse. *J Neurosci* 36, 11059-11073, doi:10.1523/JNEUROSCI.1582-16.2016 (2016).
473 Agarwal, N., Offermanns, S. & Kuner, R. Conditional gene deletion in primary nociceptive neurons of trigeminal ganglia and dorsal root ganglia. *Genesis* 38, 122-129, doi:10.1002/gene.20010 (2004).
474 Baral, P. *et al.* Author Correction: Nociceptor sensory neurons suppress neutrophil and gammadelta T cell responses in bacterial lung infections and lethal pneumonia. *Nat Med* 24, 1625-1626, doi:10.1038/s41591-018-0093-8 (2018).
475 Fidler, I. J. Biological behavior of malignant melanoma cells correlated to their survival in vivo. *Cancer Res* 35, 218-224 (1975).
476 Fidler, I. J. & Kripke, M. L. Metastasis results from preexisting variant cells within a malignant tumor. *Science* 197, 893-895, doi:10.1126/science.887927 (1977).
477 Headley, M. B. *et al.* Visualization of immediate immune responses to pioneer metastatic cells in the lung. *Nature* 531, 513-517, doi:10.1038/nature16985 (2016).
478 Twyman-Saint Victor, C. *et al.* Radiation and dual checkpoint blockade activate non-redundant immune mechanisms in cancer. *Nature* 520, 373-377, doi:10.1038/nature14292 (2015).
479 Broz, M. L. *et al.* Dissecting the Tumor Myeloid Compartment Reveals Rare Activating Antigen-Presenting Cells Critical for T Cell Immunity. *Cancer Cell* 26, 938, doi:10.1016/j.ccell.2014.11.010 (2014).
480 Stathopoulou, C. *et al.* PD-1 Inhibitory Receptor Downregulates Asparaginyl Endopeptidase and Maintains Foxp3 Transcription Factor Stability in Induced Regulatory T Cells. *Immunity* 49, 247-263 e247, doi:10.1016/j.immuni.2018.05.006 (2018).
481 Dobin, A. *et al.* STAR: ultrafast universal RNA-seq aligner. *Bioinformatics* 29, 15-21, doi:10.1093/bioinformatics/bts635 (2013).
482 Love, M. I., Huber, W. & Anders, S. Moderated estimation of fold change and dispersion for RNA-seq data with DESeq2. *Genome Biol* 15, 550, doi:10.1186/s13059-014-0550-8 (2014).

483 Barrett, T. *et al.* NCBI GEO: archive for functional genomics data sets--update. *Nucleic Acids Res* 41, D991-995, doi:10.1093/nar/gks1193 (2013).
484 Pool, M., Thiemann, J., Bar-Or, A. & Fournier, A. E. NeuriteTracer: a novel ImageJ plugin for automated quantification of neurite outgrowth. *J Neurosci Methods* 168, 134-139, doi:10.1016/j.jneumeth.2007.08.029 (2008).
485 Garcia-Segura, L. M. & Perez-Marquez, J. A new mathematical function to evaluate neuronal morphology using the Sholl analysis. *J Neurosci Methods* 226, 103-109, doi:10.1016/j.jneumeth.2014.01.016 (2014).
486 Liao, Y., Smyth, G. K. & Shi, W. featureCounts: an efficient general purpose program for assigning sequence reads to genomic features. *Bioinformatics* 30, 923-930, doi:10.1093/bioinformatics/btt656 (2014).
487 Goswami, S. C. *et al.* Molecular signatures of mouse TRPV1-lineage neurons revealed by RNA-Seq transcriptome analysis. *J Pain* 15, 1338-1359, doi:10.1016/j.jpain.2014.09.010 (2014).
488 Kupari, J., Haring, M., Agirre, E., Castelo-Branco, G. & Ernfors, P. An Atlas of Vagal Sensory Neurons and Their Molecular Specialization. *Cell Rep* 27, 2508-2523 e2504, doi:10.1016/j.celrep.2019.04.096 (2019).
489 Usoskin, D. *et al.* Unbiased classification of sensory neuron types by large-scale single-cell RNA sequencing. *Nat Neurosci* 18, 145-153, doi:10.1038/nn.3881 (2015).
490 Li, C., Wang, S., Chen, Y. & Zhang, X. Somatosensory Neuron Typing with High-Coverage Single-Cell RNA Sequencing and Functional Analysis. *Neurosci Bull* 34, 200-207, doi:10.1007/s12264-017-0147-9 (2018).
491 Chiu, I. M. *et al.* Transcriptional profiling at whole population and single cell levels reveals somatosensory neuron molecular diversity. *Elife* 3, doi:10.7554/eLife.04660 (2014).
492 Ray, P. *et al.* Comparative transcriptome profiling of the human and mouse dorsal root ganglia: an RNA-seq-based resource for pain and sensory neuroscience research. *Pain* 159, 1325-1345, doi:10.1097/j.pain.0000000000001217 (2018).
493 Cole, S. W., Nagaraja, A. S., Lutgendorf, S. K., Green, P. A. & Sood, A. K. Sympathetic nervous system regulation of the tumour microenvironment. *Nat Rev Cancer* 15, 563-572, doi:10.1038/nrc3978 (2015).
494 Hanoun, M., Maryanovich, M., Arnal-Estape, A. & Frenette, P. S. Neural regulation of hematopoiesis, inflammation, and cancer. *Neuron* 86, 360-373, doi:10.1016/j.neuron.2015.01.026 (2015).
495 Wang, W. *et al.* Nerves in the Tumor Microenvironment: Origin and Effects. *Front Cell Dev Biol* 8, 601738, doi:10.3389/fcell.2020.601738 (2020).
496 Mitchell, B. S., Schumacher, U., Stauber, V. V. & Kaiserling, E. Are breast tumours innervated? Immunohistological investigations using antibodies against the neuronal marker protein gene product 9.5 (PGP 9.5) in benign and malignant breast lesions. *Eur J Cancer* 30A, 1100-1103, doi:10.1016/0959-8049(94)90465-0 (1994).
497 Zhou, M., Patel, A. & Rubin, M. A. Prevalence and location of peripheral nerve found on prostate needle biopsy. *Am J Clin Pathol* 115, 39-43, doi:10.1309/2APJ-YKBD-97EH-67GW (2001).

498 Tomita, T. Localization of nerve fibers in colonic polyps, adenomas, and adenocarcinomas by immunocytochemical staining for PGP 9.5. *Dig Dis Sci* 57, 364-370, doi:10.1007/s10620-011-1876-7 (2012).
499 van den Beuken-van Everdingen, M. H., Hochstenbach, L. M., Joosten, E. A., Tjan-Heijnen, V. C. & Janssen, D. J. Update on Prevalence of Pain in Patients With Cancer: Systematic Review and Meta-Analysis. *J Pain Symptom Manage* 51, 1070-1090 e1079, doi:10.1016/j.jpainsymman.2015.12.340 (2016).
500 Caraceni, A. & Shkodra, M. Cancer Pain Assessment and Classification. *Cancers (Basel)* 11, doi:10.3390/cancers11040510 (2019).
501 Costigan, M., Scholz, J. & Woolf, C. J. Neuropathic pain: a maladaptive response of the nervous system to damage. *Annu Rev Neurosci* 32, 1-32, doi:10.1146/annurev.neuro.051508.135531 (2009).
502 Peters, C. M. *et al.* Tumor-induced injury of primary afferent sensory nerve fibers in bone cancer pain. *Exp Neurol* 193, 85-100, doi:10.1016/j.expneurol.2004.11.028 (2005).
503 Jimenez-Andrade, J. M., Ghilardi, J. R., Castaneda-Corral, G., Kuskowski, M. A. & Mantyh, P. W. Preventive or late administration of anti-NGF therapy attenuates tumor-induced nerve sprouting, neuroma formation, and cancer pain. *Pain* 152, 2564-2574, doi:10.1016/j.pain.2011.07.020 (2011).
504 Cohnen, J. *et al.* Tumors Provoke Inflammation and Perineural Microlesions at Adjacent Peripheral Nerves. *Cells* 9, doi:10.3390/cells9020320 (2020).
505 Reyes-Gibby, C. C. *et al.* Survival patterns in squamous cell carcinoma of the head and neck: pain as an independent prognostic factor for survival. *J Pain* 15, 1015-1022, doi:10.1016/j.jpain.2014.07.003 (2014).
506 Schmidt, B. L., Hamamoto, D. T., Simone, D. A. & Wilcox, G. L. Mechanism of cancer pain. *Mol Interv* 10, 164-178, doi:10.1124/mi.10.3.7 (2010).
507 Lam, D. K. & Schmidt, B. L. Orofacial pain onset predicts transition to head and neck cancer. *Pain* 152, 1206-1209, doi:10.1016/j.pain.2011.02.009 (2011).
508 Schmidt, B. L. The neurobiology of cancer pain. *Neuroscientist* 20, 546-562, doi:10.1177/1073858414525828 (2014).
509 Oliveira, K. G. *et al.* Relationship of inflammatory markers and pain in patients with head and neck cancer prior to anticancer therapy. *Braz J Med Biol Res* 47, 600-604, doi:10.1590/1414-431x20143599 (2014).
510 Mantyh, P. W. The neurobiology of skeletal pain. *Eur J Neurosci* 39, 508-519, doi:10.1111/ejn.12462 (2014).
511 Mikami, N. *et al.* Calcitonin gene-related peptide is an important regulator of cutaneous immunity: effect on dendritic cell and T cell functions. *J Immunol* 186, 6886-6893, doi:10.4049/jimmunol.1100028 (2011).
512 Fridman, W. H., Pages, F., Sautes-Fridman, C. & Galon, J. The immune contexture in human tumours: impact on clinical outcome. *Nat Rev Cancer* 12, 298-306, doi:10.1038/nrc3245 (2012).
513 Gerber, A. L. *et al.* High expression of FOXP3 in primary melanoma is associated with tumour progression. *Br J Dermatol* 170, 103-109, doi:10.1111/bjd.12641 (2014).

514 Gooden, M. J., de Bock, G. H., Leffers, N., Daemen, T. & Nijman, H. W. The prognostic influence of tumour-infiltrating lymphocytes in cancer: a systematic review with meta-analysis. *Br J Cancer* 105, 93-103, doi:10.1038/bjc.2011.189 (2011).
515 He, W. *et al.* Naturally activated V gamma 4 gamma delta T cells play a protective role in tumor immunity through expression of eomesodermin. *J Immunol* 185, 126-133, doi:10.4049/jimmunol.0903767 (2010).
516 Jacobs, J. F., Nierkens, S., Figdor, C. G., de Vries, I. J. & Adema, G. J. Regulatory T cells in melanoma: the final hurdle towards effective immunotherapy? *Lancet Oncol* 13, e32-42, doi:10.1016/S1470-2045(11)70155-3 (2012).
517 Kobayashi, N. *et al.* FOXP3+ regulatory T cells affect the development and progression of hepatocarcinogenesis. *Clin Cancer Res* 13, 902-911, doi:10.1158/1078-0432.CCR-06-2363 (2007).
518 Rosenberg, S. A. *et al.* Use of tumor-infiltrating lymphocytes and interleukin-2 in the immunotherapy of patients with metastatic melanoma. A preliminary report. *N Engl J Med* 319, 1676-1680, doi:10.1056/NEJM198812223192527 (1988).
519 Sui, P. *et al.* Pulmonary neuroendocrine cells amplify allergic asthma responses. *Science* 360, doi:10.1126/science.aan8546 (2018).
520 Baliu-Pique, M., Jusek, G. & Holzmann, B. Neuroimmunological communication via CGRP promotes the development of a regulatory phenotype in TLR4-stimulated macrophages. *Eur J Immunol* 44, 3708-3716, doi:10.1002/eji.201444553 (2014).
521 Ceyhan, G. O. *et al.* Nerve growth factor and artemin are paracrine mediators of pancreatic neuropathy in pancreatic adenocarcinoma. *Ann Surg* 251, 923-931, doi:10.1097/SLA.0b013e3181d974d4 (2010).
522 Bapat, A. A., Munoz, R. M., Von Hoff, D. D. & Han, H. Blocking Nerve Growth Factor Signaling Reduces the Neural Invasion Potential of Pancreatic Cancer Cells. *PLoS One* 11, e0165586, doi:10.1371/journal.pone.0165586 (2016).
523 Rosso, M., Munoz, M. & Berger, M. The role of neurokinin-1 receptor in the microenvironment of inflammation and cancer. *ScientificWorldJournal* 2012, 381434, doi:10.1100/2012/381434 (2012).
524 Covenas, R. & Munoz, M. Cancer progression and substance P. *Histol Histopathol* 29, 881-890, doi:10.14670/HH-29.881 (2014).
525 Munoz, M. & Covenas, R. Involvement of substance P and the NK-1 receptor in cancer progression. *Peptides* 48, 1-9, doi:10.1016/j.peptides.2013.07.024 (2013).
526 Munoz, M. & Covenas, R. Involvement of substance P and the NK-1 receptor in pancreatic cancer. *World J Gastroenterol* 20, 2321-2334, doi:10.3748/wjg.v20.i9.2321 (2014).
527 Munoz, M. & Covenas, R. Involvement of substance P and the NK-1 receptor in human pathology. *Amino Acids* 46, 1727-1750, doi:10.1007/s00726-014-1736-9 (2014).
528 Li, J. *et al.* Neurokinin-1 receptor mediated breast cancer cell migration by increased expression of MMP-2 and MMP-14. *Eur J Cell Biol* 95, 368-377, doi:10.1016/j.ejcb.2016.07.005 (2016).
529 Reubi, J. C., Gugger, M., Waser, B. & Schaer, J. C. Y(1)-mediated effect of neuropeptide Y in cancer: breast carcinomas as targets. *Cancer Res* 61, 4636-4641 (2001).

530 Gutierrez, S. & Boada, M. D. Neuropeptide-induced modulation of carcinogenesis in a metastatic breast cancer cell line (MDA-MB-231(LUC+)). *Cancer Cell Int* 18, 216, doi:10.1186/s12935-018-0707-8 (2018).
531 Rozengurt, E. Neuropeptides as growth factors for normal and cancerous cells. *Trends Endocrinol Metab* 13, 128-134, doi:10.1016/s1043-2760(01)00544-6 (2002).
532 Levite, M. & Chowers, Y. Nerve-driven immunity: neuropeptides regulate cytokine secretion of T cells and intestinal epithelial cells in a direct, powerful and contextual manner. *Ann Oncol* 12 Suppl 2, S19-25, doi:10.1093/annonc/12.suppl_2.s19 (2001).
533 Levite, M. Dopamine and T cells: dopamine receptors and potent effects on T cells, dopamine production in T cells, and abnormalities in the dopaminergic system in T cells in autoimmune, neurological and psychiatric diseases. *Acta Physiol (Oxf)* 216, 42-89, doi:10.1111/apha.12476 (2016).
534 Kustrimovic, N., Rasini, E., Legnaro, M., Marino, F. & Cosentino, M. Expression of dopaminergic receptors on human CD4+ T lymphocytes: flow cytometric analysis of naive and memory subsets and relevance for the neuroimmunology of neurodegenerative disease. *J Neuroimmune Pharmacol* 9, 302-312, doi:10.1007/s11481-014-9541-5 (2014).
535 McKenna, F. *et al.* Dopamine receptor expression on human T- and B-lymphocytes, monocytes, neutrophils, eosinophils and NK cells: a flow cytometric study. *J Neuroimmunol* 132, 34-40, doi:10.1016/s0165-5728(02)00280-1 (2002).
536 Ganor, Y., Besser, M., Ben-Zakay, N., Unger, T. & Levite, M. Human T cells express a functional ionotropic glutamate receptor GluR3, and glutamate by itself triggers integrin-mediated adhesion to laminin and fibronectin and chemotactic migration. *J Immunol* 170, 4362-4372, doi:10.4049/jimmunol.170.8.4362 (2003).
537 Miglio, G., Dianzani, C., Fallarini, S., Fantozzi, R. & Lombardi, G. Stimulation of N-methyl-D-aspartate receptors modulates Jurkat T cell growth and adhesion to fibronectin. *Biochem Biophys Res Commun* 361, 404-409, doi:10.1016/j.bbrc.2007.07.015 (2007).
538 Pacheco, R. *et al.* Group I metabotropic glutamate receptors mediate a dual role of glutamate in T cell activation. *J Biol Chem* 279, 33352-33358, doi:10.1074/jbc.M401761200 (2004).
539 Poulopoulou, C. & Hatzimanolis, A. Expression of ionotropic glutamate receptor GLUR3 and effects of glutamate on MBP- and MOG-specific lymphocyte activation and chemotactic migration in multiple sclerosis patients. *J Neuroimmunol* 194, 191; author reply 192, doi:10.1016/j.jneuroim.2007.10.005 (2008).
540 Nizri, E. *et al.* Activation of the cholinergic anti-inflammatory system by nicotine attenuates neuroinflammation via suppression of Th1 and Th17 responses. *J Immunol* 183, 6681-6688, doi:10.4049/jimmunol.0902212 (2009).
541 Fujii, T. *et al.* Expression and Function of the Cholinergic System in Immune Cells. *Front Immunol* 8, 1085, doi:10.3389/fimmu.2017.01085 (2017).
542 Mendu, S. K., Bhandage, A., Jin, Z. & Birnir, B. Different subtypes of GABA-A receptors are expressed in human, mouse and rat T lymphocytes. *PLoS One* 7, e42959, doi:10.1371/journal.pone.0042959 (2012).
543 Bhandage, A. K. *et al.* GABA Regulates Release of Inflammatory Cytokines From Peripheral Blood Mononuclear Cells and CD4(+) T Cells and Is Immunosuppressive in Type 1 Diabetes. *EBioMedicine* 30, 283-294, doi:10.1016/j.ebiom.2018.03.019 (2018).

544 Ganea, D., Hooper, K. M. & Kong, W. The neuropeptide vasoactive intestinal peptide: direct effects on immune cells and involvement in inflammatory and autoimmune diseases. *Acta Physiol (Oxf)* 213, 442-452, doi:10.1111/apha.12427 (2015).
545 Levite, M. Nerve-driven immunity. The direct effects of neurotransmitters on T-cell function. *Ann N Y Acad Sci* 917, 307-321, doi:10.1111/j.1749-6632.2000.tb05397.x (2000).
546 Levite, M. Neurotransmitters activate T-cells and elicit crucial functions via neurotransmitter receptors. *Curr Opin Pharmacol* 8, 460-471, doi:10.1016/j.coph.2008.05.001 (2008).
547 Yang, J. C. & Rosenberg, S. A. Adoptive T-Cell Therapy for Cancer. *Adv Immunol* 130, 279-294, doi:10.1016/bs.ai.2015.12.006 (2016).
548 Stroncek, D. F., Reddy, O., Highfill, S. & Panch, S. R. Advances in T-cell Immunotherapies. *Hematol Oncol Clin North Am* 33, 825-837, doi:10.1016/j.hoc.2019.05.006 (2019).
549 Levite, M., Safadi, R., Milgrom, Y., Massarwa, M. & Galun, E. Neurotransmitters and Neuropeptides decrease PD-1 in T cells of healthy subjects and patients with hepatocellular carcinoma (HCC), and increase their proliferation and eradication of HCC cells. *Neuropeptides* 89, 102159, doi:10.1016/j.npep.2021.102159 (2021).
550 Ishihara, K., Kamata, M., Hayashi, I., Yamashina, S. & Majima, M. Roles of bradykinin in vascular permeability and angiogenesis in solid tumor. *Int Immunopharmacol* 2, 499-509, doi:10.1016/s1567-5769(01)00193-x (2002).
551 Toda, M. *et al.* Neuronal system-dependent facilitation of tumor angiogenesis and tumor growth by calcitonin gene-related peptide. *Proc Natl Acad Sci U S A* 105, 13550-13555, doi:10.1073/pnas.0800767105 (2008).
552 Lee, E. W. *et al.* Neuropeptide Y induces ischemic angiogenesis and restores function of ischemic skeletal muscles. *J Clin Invest* 111, 1853-1862, doi:10.1172/JCI16929 (2003).
553 Zhou, N., Li, D., Luo, Y., Li, J. & Wang, Y. Effects of Botulinum Toxin Type A on Microvessels in Hypertrophic Scar Models on Rabbit Ears. *Biomed Res Int* 2020, 2170750, doi:10.1155/2020/2170750 (2020).
554 Dutra, E. H. *et al.* Cellular and Matrix Response of the Mandibular Condylar Cartilage to Botulinum Toxin. *PLoS One* 11, e0164599, doi:10.1371/journal.pone.0164599 (2016).
555 Silva, J. *et al.* Intraprostatic Botulinum Toxin Type A injection in patients with benign prostatic enlargement: duration of the effect of a single treatment. *BMC Urol* 9, 9, doi:10.1186/1471-2490-9-9 (2009).
556 Li, J., Sun, Y., Ding, G. & Jiang, F. Persistent pain accelerates xenograft tumor growth of breast cancer in rat. *Biochem Biophys Res Commun* 495, 2432-2438, doi:10.1016/j.bbrc.2017.12.121 (2018).
557 Garcia-Recio, S. *et al.* Substance P autocrine signaling contributes to persistent HER2 activation that drives malignant progression and drug resistance in breast cancer. *Cancer Res* 73, 6424-6434, doi:10.1158/0008-5472.CAN-12-4573 (2013).
558 Zigmond, R. E. & Echevarria, F. D. Macrophage biology in the peripheral nervous system after injury. *Prog Neurobiol* 173, 102-121, doi:10.1016/j.pneurobio.2018.12.001 (2019).
559 Masuda, K. *et al.* Sema4D stimulates axonal outgrowth of embryonic DRG sensory neurones. *Genes Cells* 9, 821-829, doi:10.1111/j.1365-2443.2004.00766.x (2004).

560 Capparuccia, L. & Tamagnone, L. Semaphorin signaling in cancer cells and in cells of the tumor microenvironment--two sides of a coin. *J Cell Sci* 122, 1723-1736, doi:10.1242/jcs.030197 (2009).